DEVELOPMENT AND ASSESSMENT OF *IN VITRO* SIMULATION APPROACHES TO INTRACEREBRAL HAEMORRHAGE

DOCTOR OF PHILOSOPHY (PhD) THESIS

in NEUROPATHOLOGY

- supported by the Wellcome Trust -

APOSTOLOS ZARROS

UNIVERSITY OF GLASGOW

GLASGOW 2017

DEVELOPMENT AND ASSESSMENT OF *IN VITRO* SIMULATION APPROACHES TO INTRACEREBRAL HAEMORRHAGE

APOSTOLOS ZARROS

physician, MRes, PhD, MAPS, MRSB

submitted in fulfilment of the requirements for the degree of

Doctor of Philosophy (PhD) in Neuropathology

INSTITUTE OF CARDIOVASCULAR AND MEDICAL SCIENCES

COLLEGE OF MEDICAL, VETERINARY AND LIFE SCIENCES

UNIVERSITY OF GLASGOW

APRIL 2017 | GLASGOW

UNITED KINGDOM OF GREAT BRITAIN AND NORTHERN IRELAND

EUROPEAN UNION

Data concerning the current PhD Thesis / author's declaration

Citation of the current PhD Thesis: Zarros A. Development and assessment of *in vitro* simulation approaches to intracerebral haemorrhage. PhD Thesis in Neuropathology. *University of Glasgow*, Glasgow, 2017

Author's name: Dr Apostolos Zarros

Author's declaration: it is hereby declared that, except where explicit reference is made to the contribution of others, this dissertation is the result of my own work and has not been submitted for any other degree at the University of Glasgow or any other institution

Author's signature: _____

Date of author's signature (DD/MM/YYYY): 08/04/2017

Supervisors: Prof. George S. Baillie; Prof. William Cushley

Examiners: Prof. I. Mhairi Macrae; Prof. Maria Mironidou-Tzouveleki

Date of examination (DD/MM/YYYY): 20/12/2016

Date of approval of the final PhD Thesis version (DD/MM/YYYY): 07/04/2017

Sources of author's financial support: Wellcome Trust

Author's conflicts of interest: none declared

Summarized *Curriculum Vitae* of Apostolos Zarros[*]

I was born in Greece (1983) and was raised in a small coastal town by the Corinthian Gulf. Inspired to establish a family tradition, I completed my medical studies at the Medical School of the National and Kapodistrian University of Athens. Throughout my studies I worked as an Undergraduate Research Assistant in the laboratory of Associate Professor Stylianos Tsakiris, where I had the chance to conduct a significant amount of experimental work focussing on rat brain-derived membrane-bound enzyme activities within the context of experimentally-simulated toxic and metabolic encephalopathies. Part of this work has formed the basis for the award of a PhD (by published work / retrospective) by the University of Bolton (supervised by Professors Elias Siores and Martin Grootveld).

In 2011 I was awarded a studentship within the prestigious Wellcome Trust PhD Programme at the University of Glasgow. As part of this Programme, I completed the MRes in Molecular Functions in Disease before proceeding to pursue a PhD in Neuropathology at the Institute of Cardiovascular and Medical Sciences of the University of Glasgow (supervised by Professors George S. Baillie and William Cushley). My PhD Thesis in Neuropathology focused on the development and assessment of *in vitro* simulation approaches to intracerebral haemorrhage, and incorporated the cytomorphological characterization and the real-time cellular response profiling of an immortalized embryonic murine hippocampal cell-line (mHippoE-14).

In 2015 I was appointed as a Research Associate at the Research Department of Pharmaceutics of the University College London (UCL) School of Pharmacy, and participated in an ambitious consortium project aiming to develop antibody-bearing nanoparticles that could be delivered to the brain via the intranasal route. While at this position, I conducted pharmacokinetic studies on the intranasal-to-brain delivery of nanoparticles in rodents, and undertook teaching training through courses offered by the UCL Centre for Advancing Learning and Teaching. After resigning from this appointment (2016), I currently have the honour to serve as a Research Assistant to Professor Tilli Tansey OBE at the History of Modern Biomedicine Research Group of the Queen Mary University of London, and to contribute to the Group's research activities and editorial work on the Wellcome Trust-funded Witness Seminar transcript series entitled "Wellcome Witnesses to Contemporary Medicine".

My primary research focus lies within the field of Experimental Medicine; specifically, on establishing a framework of theoretical principles and technical parameters that could be used

[*] last updated: April 2017.

as a basis for the development and assessment of *in vitro* simulation approaches to brain diseases (with an emphasis on astrocytic tumours, encephalopathies and neurotrauma-associated pathological entities) towards the delivery of more robust drug-screening tools. I recently coined the term "neuropathopoiesis" in order to summarize the priorities and vision of this effort (*NeuroToxicology* 2014; 44: 365).

My research interests also focus on: (i) the coincidental factors that shape pharmaceutical innovation, (ii) the role of sodium / potassium adenosine triphosphatase (Na^+,K^+-ATPase) as a cell type-specific determinant of neuro-pathogenesis, (iii) the molecular mechanisms underlying experimental and human neurocarcinogenesis, and (iv) the prerequisites for a successful implementation of dedicated research within the undergraduate medical curriculum.

My CV includes 66 articles indexed in PubMed and a number of further published works.

I maintain the membership status of the Academy of Pharmaceutical Sciences (MAPS), the British Pharmacological Society, the British Society for the History of Pharmacy, the In Vitro Toxicology Society, and the Royal Society of Biology (MRSB). I also maintain the fellowship status of The Royal Numismatic Society.

Dedicated to the memory of Leonidas El. Gkourvelos
(1925-1995)

ABSTRACT

Development and Assessment of *In Vitro* Simulation Approaches to Intracerebral Haemorrhage

PhD Thesis in Neuropathology by

Apostolos Zarros

University of Glasgow, Glasgow, 2017

This current PhD Thesis in Neuropathology focuses on the development and assessment of *in vitro* simulation approaches to intracerebral haemorrhage. The PhD Thesis provides a clinical and experimental neuropathological overview of intracerebral haemorrhage as well as an account of the *in vitro* simulation approaches to the disease, before proceeding to the presentation of the experimental work designed and performed by the author. The development of the herein presented *in vitro* simulation approaches to intracerebral haemorrhage was based on the use of an immortalized embryonic murine hippocampal cell-line (mHippoE-14) and its response to oligomycin-A and ferrum or haemin under appropriately selected conditions (aiming to simulate the natural history of the disease in a more reliable manner). The PhD Thesis provides a characterization of the mHippoE-14 cell-line (through a real-time cellular response analysis and a cytomorphological characterization), before proceeding to the actual experimental justification of the conditions chosen for the development of the herein presented *in vitro* simulation approaches to intracerebral haemorrhage, and their assessment. The latter was performed through the undertaking of: (a) real-time cellular response analysis, (b) cytomorphological assessment, (c) profiling of neuronal markers' expression, (d) neurochemical assessment, and (e) proteomic profiling. All experiments were performed at the University of Glasgow. The current PhD Thesis also provides a critical appraisal of: (a) the utility, novelty and limitations of the developed *in vitro* simulation approaches, and (b) the positioning of the developed *in vitro* simulation approaches within the neuropathopoietic context.

Keywords: Neuropathology; intracerebral haemorrhage; stroke; intracerebral haematoma; perihaematomal penumbra; *in vitro* simulation approaches; mHippoE-14; embryonic murine hippocampal cell-line; oligomycin-A; ferrum; haemin; characterization; foetal bovine serum-

deprivation; FBS-deprivation; real-time cellular response analysis; xCELLigence technology; high-throughput; parametropoiesis; metaptosis; metaptotic phase; pathopoietic phase; cellular response; CR; normalized cellular response; nCR; metaptotic index; m_i; index of metaptotic adaptability; μ_i; cytomorphology; phase-contrast microscopy; mHippoE-14 classification; mHippoE-14 atlas; development; assessment; neuroprotective drugs; deferoxamine; DFO; cytidine-5'-diphosphocholine; CDP-Ch; neuronal markers' expression; alpha 1 subunit of sodium / potassium adenosine triphosphatase; α1 Na^+,K^+-ATPase; choline acetyltransferase; ChAT; synapsin I; haeme oxygenase 1; HO-1; neurochemical assessment; acetylcholinesterase; AChE; proteomic profiling; cytokine arrays; neuropathopoiesis; drug-screening tools.

PREFACE

Development and Assessment of *In Vitro* Simulation Approaches to Intracerebral Haemorrhage

The research work of Dr Alexios Bimpis (Consultant Neurosurgeon at the Panarcadic General Hospital, Tripoli, Greece) on intracerebral haemorrhage (Bimpis *et al.*, 2012; 2013; 2015) has been an inspiration for the conception and realization of this current PhD Thesis. The countless time we have spent discussing the neuropathology of this complex clinical entity (and its more reliable experimental simulation) has played a major role in the conceptual shaping of the developed and herein presented *in vitro* simulation approaches.

Intracerebral haemorrhage (or cerebral haemorrhage) is classified as an intra-axial intracranial haemorrhage that can occur traumatically or non-traumatically (spontaneously). Its prognosis is defined by a number of factors, including (but not limited to): (a) its cause and potential comorbidities, (b) the anatomical localization of the occurring haematoma and its size, (c) the undertaken medical and / or surgical treatment as well as (d) genetic factors. Despite the recent significant advancements in the field of stroke prevention and treatment (Silver, 2014), a deep controversy over the available options for the treatment of intracerebral haemorrhage is still in place as a result of the disease's complex nature and the variability of its clinical manifestation (Bimpis and Zarros, 2014). Consequently, intracerebral haemorrhage still maintains high incidence (estimated to account for 10-15% of all strokes) and mortality (estimated to be approximately 50%) rates (Broderick *et al.*, 1994; Morgenstern *et al.*, 2015; Rodríguez-Yáñez *et al.*, 2013).

During the last decade, one of the most influential researchers in the field, Professor A. David Mendelow (Professor of Neurosurgery at Newcastle University, Newcastle-upon-Tyne, England, UK), has led a series of studies within the Surgical Trial of IntraCerebral Haemorrhage (STICH; I and II) framework (Mendelow *et al.*, 2005; 2013). These STICH trials have shown that *"patients with spontaneous supratentorial intracerebral haemorrhage in neurosurgical units show no overall benefit from early surgery when compared with initial conservative treatment"* (Mendelow *et al.*, 2005), as well as that *"early surgery does not increase the rate of death or disability at 6 months and might have a small but clinically relevant survival advantage for patients with spontaneous superficial intracerebral haemorrhage without intra-*

ventricular haemorrhage" (Mendelow *et al.*, 2013). These findings: (a) are indicative of the complicated nature of decision-making at the clinical management of intracerebral haemorrhage, (b) underline the need for a more thorough parametropoiesis of the clinical characterization of intracerebral haemorrhage cases, and (c) suggest that the experimental and clinical quest for novel, combinatorial and effective conservative approaches to this disease should by no means be abandoned.

Considering that, to date, no effective non-surgical / pharmacological treatments have been established (Katsuki, 2010), this PhD Thesis provides a small contribution to the development and assessment of novel experimental approaches to intracerebral haemorrhage at the preclinical (*in vitro*) level that would: (a) allow for a more reliable simulation of the disease (or, more realistically, of important aspects of the disease's neuropathology), (b) serve the 3R principles[1], and (c) provide the substrate for high-throughput drug-screening applications. Within this context, this current PhD Thesis provides a clinical and experimental neuropathological overview of intracerebral haemorrhage as well as an account of the so far developed *in vitro* simulation approaches to the disease, before proceeding to the presentation of the experimental work designed and performed by myself.

The development of the herein presented *in vitro* simulation approaches to intracerebral haemorrhage was based on the use of a commercially-available immortalized embryonic murine hippocampal cell-line (mHippoE-14, available from CELLutions Biosystems Inc.) and its response to oligomycin-A and ferrum or haemin under appropriately-selected conditions (aiming to simulate the natural history of the disease in a more reliable manner). Due to the limited data available for the mHippoE-14 cell-line (Gingerich *et al.*, 2010), characterizations of the latter through real-time cellular response analysis (through the xCELLigence Real Time Cell Analysis system, developed by Roche Applied Science in partnership with ACEA Biosciences Inc.) as well as through cytomorphology (through phase-contrast microscopy) have been considered as necessary and have been undertaken prior to the actual experimental justification of the conditions chosen for the development of the herein presented *in vitro* simulation approaches to intracerebral haemorrhage and their assessment. To my belief, the work performed for the purpose of the mHippoE-14 cell-line characterization has the potential of introducing significant technical parameters in the field of "neuropathopoiesis" (Zarros, 2014), and is equally (if not more) important to the task of the actual development and assessment of the *in vitro* simulation approaches that this PhD Thesis presents.

The task of the assessment of the developed *in vitro* simulation approaches to intracerebral haemorrhage was performed through the undertaking of: (a) real-time cellular response analysis, (b) cytomorphological assessment, (c) profiling of selected neuronal mark-

[1] the 3R principles refer to the more ethical use of animals in scientific testing and are summarized by the words "Replacement", "Reduction" and "Refinement" (Bulger, 1987; Richmond, 2002).

ers' expression, (d) neurochemical assessment, and (e) proteomic profiling. Although this assessment is nowhere near of being exhaustive, it is really informative and useful towards a critical appraisal of: (a) the utility, novelty and limitations of the developed *in vitro* simulation approaches, and (b) the positioning of the developed *in vitro* simulation approaches within the neuropathopoietic context.

At this point it is important to note that a major role in the execution of the undertaken and herein presented experiments on the profiling of neuronal markers' expression and the proteomic profiling of the developed *in vitro* simulation approaches to intracerebral haemorrhage (in fact, of a large part of the assessment of these approaches) should be credited to Dr Christina Elliott (Postdoctoral Research Worker at King's College London, London, England, UK; formerly Research Associate at the University of Glasgow); her (theoretical and technical) expertise in basic neuroscientific research has been invaluable.

I am grateful to both my supervisors, Professors George S. Baillie (Professor of Molecular Pharmacology) and William (Bill) Cushley (Professor of Molecular Immunology), for their trust, mentorship and support towards the completion of the work described in this PhD Thesis. All described experiments were performed in the Gardiner Lab located on the fifth floor of the Wolfson Link Building at the Gilmorehill Campus of the University of Glasgow.

Finally, I feel that I should make clear to all readers that I am fully aware that this PhD Thesis contains grammatical and syntactical errors. I am sure that the readers will excuse me for the existence of such errors, since I am not a native speaker of English. I also feel that I should apologize for the fact that the output of the work presented in the current PhD Thesis will include only a selection of the herein presented findings as well as a different approach to their presentation and interpretation. Although this is an expected and unavoidable "transformation" required for the availability of these data to a wider scientific audience (through peer-reviewed journal articles, book chapters and proceeding abstracts), readers should still consider this PhD Thesis as a reference source for a number of useful technical details, findings and comments.

Glasgow, April 2017

AZ

ACKNOWLEDGMENTS

Development and Assessment of *In Vitro* Simulation Approaches to Intracerebral Haemorrhage

This PhD Thesis in Neuropathology could not have been realized without the support of the University of Glasgow through its prestigious Wellcome Trust 4-year PhD Programme entitled "Molecular Functions in Disease". The encouragement, continuous support and mentorship of the PhD Programme's Director (Professor Darren Monckton) and Deputy Director (Dr Olwyn Byron) are gratefully acknowledged. Moreover, the author's sincere respect and gratitude are extended to his supervisors, Professors George S. Baillie and William Cushley, for their unconditional support towards the undertaking of the work described in this PhD Thesis. The completion of the latter has also been facilitated by the intellectual input of the below-listed (in alphabetical order) colleagues and external collaborators:

Dr Alexios Bimpis | *Panarcadic General Hospital*

Dr Christina Elliott | *King's College London; University of Glasgow (formerly)*

Dr Apostolos Papalois | *Experimental - Research Center, ELPEN Pharmaceuticals*

Dr Stylianos Tsakiris | *National and Kapodistrian University of Athens*

Dr Konstantinos Voumvourakis | *National and Kapodistrian University of Athens*

as well as by the technical contribution and assistance of the below-mentioned (in alphabetical order) colleagues, technicians, students or co-workers, being (at some point during the undertaking of the herein described experimental work) members of the Gardiner Lab (the well-equipped laboratory of Professor Baillie, located on the fifth floor of the Wolfson Link Building at the Gilmorehill Campus of the University of Glasgow):

Ashleigh-Maria Byrne, Ryan T. Cameron, Nicola M. Devine, Jane E. Findlay, Vasiliki Gkanti, Connie A. Mackenzie-Gray Scott, Ruth MacLeod, Rebecca B. Roscoe, Ivona Ruseva, Aislynn Taggart, Dimitrios Tsallos.

Additionally, the administrative support of Mrs Linda Atkinson and Mrs Joyce Smith has been invaluable, and so has been the support and guidance received from the members of the University of Glasgow Postgraduate Research Progress Review Panel (Professors Muriel Caslake, Kennedy Lees and Chris Packard) throughout the academic years 2012-2015.

CONTENTS

Development and Assessment of *In Vitro* Simulation Approaches to Intracerebral Haemorrhage

(Front cover / binding cover) ..... (unnumbered)
(Cover / inner first page) 1
(Data concerning the current PhD Thesis / author's declaration) 2
(Summarized *Curriculum Vitae* of Apostolos Zarros) 3
(Dedication) 5
Abstract 6
Preface 8
Acknowledgments 11
Contents 12
List of Tables 17
List of Figures 21

PART A 25
Intracerebral haemorrhage and its *in vitro* simulation approaches

Chapter I 26
Intracerebral haemorrhage: a clinical and experimental neuropathological overview
I.1. Defining intracerebral haemorrhage 27
I.2. Epidemiological and aetiological overview of intracerebral haemorrhage 28
I.3. Clinical presentation of intracerebral haemorrhage 30
I.4. Diagnostic investigation of intracerebral haemorrhage 31
I.5. Surgical management of intracerebral haemorrhage 32
I.6. Non-surgical management of intracerebral haemorrhage 33
I.7. Prognosis of intracerebral haemorrhage 35
I.8. Neuropathological overview of intracerebral haemorrhage 36
I.9. Clinical neuropathology of intracerebral haemorrhage 39
I.10. Experimental neuropathology of intracerebral haemorrhage 40
I.11. Potential neuropharmacological approaches to intracerebral haemorrhage 42
I.12. Momentum of the experimental research on intracerebral haemorrhage 43

Table A.1 45
Table A.2 46
Table A.3 47
Table A.4 48
Table A.5 49
Table A.6 50
Table A.7 51
Table A.8 52
Figure A.1 53
Figure A.2 54
Figure A.3 55
Figure A.4 56
Figure A.5 58
Chapter II 59
Overview of *in vitro* simulation approaches to intracerebral haemorrhage
II.1. Simulation of intracerebral haemorrhage under *in vitro* conditions 59
II.2. Selection of the *in vitro* conditions simulating intracerebral haemorrhage 61
II.3. Markers of *in vitro* injury associated with intracerebral haemorrhage 62
II.4. Challenges of the *in vitro* simulation of intracerebral haemorrhage 63
II.5. Aims of the current PhD Thesis 63
Table A.9 65

PART B 66
Characterization of the embryonic murine hippocampal cell-line mHippoE-14

Chapter III 67
The commercially-available embryonic hippocampal cell-line mHippoE-14
III.1. Development of the mHippoE-14 and associated cell-lines 67
III.2. Characterization of the mHippoE-14 and associated cell-lines 69
Table B.1 71
Table B.2 72
Figure B.1 73
Figure B.2 74
Chapter IV 75
Real-time cellular response analysis of the mHippoE-14 cell-line
IV.1. The xCELLigence system and its applications 75
IV.2. Technical restrictions, archiving, analysis and statistical evaluation 76
IV.3. Characterization of the mHippoE-14 cell-line response patterns 77

IV.4. Pathopoietic transformation of the mHippoE-14 cell-line 78
IV.5. Metaptosis of the mHippoE-14 cell-line and its parametropoiesis 78
Table B.3 80
Table B.4 81
Table B.5 82
Table B.6 83
Figure B.3 84
Figure B.4 86
Figure B.5 87
Figure B.6 89
Chapter V 91
Cytomorphological characterization of the mHippoE-14 cell-line
V.1. Established cytomorphological characterization of hippocampal neurons 91
V.2. Preliminary assessment of the cytomorphology of the mHippoE-14 cell-line 92
V.3. Atlas of the mHippoE-14 cellular morphology 92
V.4. Parametropoiesis of the mHippoE-14 cellular morphology assessment 93
V.5. Cytomorphological assessment of the mHippoE-14 cell-line 93
Table B.7 95
Table B.8 96
Figure B.7 97
Figure B.8 98
Figure B.9 99
Figure B.10 100
PART C 102
mHippoE-14-utilizing *in vitro* simulation approaches to intracerebral haemorrhage
Chapter VI 103
Development of *in vitro* simulation approaches to intracerebral haemorrhage
VI.1. Preliminary attempts 103
VI.2. Determination of appropriately-toxic concentrations of haemin and ferrum 104
VI.3. Use of oligomycin-A as an approach to ischaemia-related phenomena 106
VI.4. Development of two distinct and dynamic *in vitro* experimental settings 107
Table C.1 109
Table C.2 110
Figure C.1 111
Figure C.2 112
Figure C.3 113

Figure C.4 114
Figure C.5 115
Figure C.6 116
Figure C.7 117
Chapter VII 119
Assessment of *in vitro* simulation approaches to intracerebral haemorrhage
VII.1. Real-time cellular response analysis 119
VII.2. Cytomorphological assessment 121
VII.3. Profiling of neuronal markers' expression 121
VII.4. Neurochemical assessment 124
VII.5. Proteomic profiling 125
Table C.3 129
Table C.4 130
Table C.5 131
Table C.6 134
Figure C.8 135
Figure C.9 136
Figure C.10 138
Figure C.11 140
Figure C.12 142
Figure C.13 143
Figure C.14 144
Figure C.15 145
Figure C.16 146
Figure C.17 147
Figure C.18 148
Figure C.19 149
Figure C.20 150
Figure C.21 151

PART D 152
Critical appraisal

Chapter VIII 153
Utility, novelty and limitations of the developed *in vitro* simulation approaches
VIII.1. Utility of the developed *in vitro* simulation approaches 153
VIII.2. Novelty of the developed *in vitro* simulation approaches 154
VIII.3. Limitations of the developed *in vitro* simulation approaches 155

Table D.1 ... 157
Table D.2 ... 158
Figure D.1 ... 159
Chapter IX ... 160
The developed *in vitro* simulation approaches within the neuropathopoietic context
IX.1. Neuropathopoiesis ... 160
IX.2. Suggested theoretical and technical parametropoiesis ... 161
IX.3. Assessment and perspective of the developed *in vitro* simulation approaches ... 161
Table D.3 ... 163
Table D.4 ... 164
Figure D.2 ... 165

References ... 166

Appendix A ... 209
List of biomedical abbreviations and symbolography used

Appendix B ... 215
Notes related to the current PhD Thesis
Table APP.1 ... 216
Table APP.2 ... 217
Table APP.3 ... 218
Table APP.4 ... 219
Figure APP.1 ... 220
Figure APP.2 ... 221

(Copy and owner details / last page) ... 222

LIST OF TABLES

Development and Assessment of *In Vitro* Simulation Approaches to Intracerebral Haemorrhage

PART A 25

Intracerebral haemorrhage and its *in vitro* simulation approaches

Table A.1 45

Aetiological overview of intracerebral haemorrhage: common clinical conditions, incidents and lifestyle options related to the development of primary and secondary intracerebral haemorrhage

Table A.2 46

Overview of clinical symptoms accompanying intracerebral haemorrhage, based on the neuroanatomical localization (and size) of the haematoma

Table A.3 47

Clinical grading scale for intracerebral haemorrhage: determination and prognostic interpretation according to Hemphill *et al*. (2001)

Table A.4 48

Overview of the indications, advantages and limitations of the surgical approaches to the treatment of intracerebral haemorrhage

Table A.5 49

Overview of the most frequently-employed medical (non-surgical; pharmacological; conservative) approaches to the treatment of intracerebral haemorrhage

Table A.6 50

Major experimental techniques employed toward the *in vivo* simulation of intracerebral haemorrhage

Table A.7 51

Selection of compounds suggested to exert neuroprotection against intracerebral haemorrhage, based on experimental data

Table A.8 52

Research priorities toward an effective treatment of intracerebral haemorrhage

Table A.9 65

Assessment parameters (markers) used within the *in vitro* context of intracerebral haemorrhage simulation, in order to study the induced cellular injury and / or the po-

tential neuroprotective effects of drugs

PART B 66

Characterization of the embryonic murine hippocampal cell-line mHippoE-14

Table B.1 71

Immortalized hippocampal (and hippocampal-like) cell-lines developed and studied prior to the development of the mHippoE series of cell-lines: a summarized view of their origin and their main limitation

Table B.2 72

Overview of a RT-PCR screening of the mHippoE-type cell-lines available by CELLutions Biosystems Inc.

Table B.3 80

Proposed nomenclature for the description of standardized real-time cellular response profiles through the use of the xCELLigence technology

Table B.4 81

Proposed symbolography for the mapping of real-time cellular responses through the use of the xCELLigence technology

Table B.5 82

Established and proposed parameters for a more thorough analysis of real-time cellular responses through the use of the xCELLigence technology

Table B.6 83

Effects of FBS-deprivation on selected proposed cellular response parameters of the mHippoE-14 cell-line

Table B.7 95

Algorithm for the proposed cytomorphological classification of mHippoE-14 cells: a software-friendly presentation, as compared to the stage classification of Dotti *et al*. (1988)

Table B.8 96

Cytomorphological parameters employed in the mHippoE-14 cell cultures' phase-contrast microscopy imaging assessment

PART C 102

mHippoE-14-utilizing *in vitro* simulation approaches to intracerebral haemorrhage

Table C.1 109

Preliminary assessment of the cellular response of mHippoE-14 to various concentrations of haemin or ferrum, in the presence or absence of oligomycin

Table C.2 110

Practical advantages of the conditions chosen to be included in the developed *in vitro* simulation approaches to intracerebral haemorrhage

Table C.3 129

Assessment of the nCR values of mHippoE-14 within the developed *in vitro* simulation approaches to intracerebral haemorrhage: a sample

Table C.4 130

List of antibodies used for the performance of Western blotting toward the profiling of neuronal markers' expression in mHippoE-14 cells under the developed intracerebral haemorrhage-simulating *in vitro* conditions

Table C.5 131

Designation of analytes upon each cytokine array slide used for the proteomic profiling of the cell-culture medium, as provided in the Proteome Profiler Array - Mouse XL Cytokine Array Kit (product ARY028; R&D Systems Inc.)

Table C.6 134

Synopsis of the statistically significant analyte changes detected by the proteomic profiling of the developed *in vitro* simulation approaches to intracerebral haemorrhage

PART D 152

Critical appraisal

Table D.1 157

Synopsis of the novelty of the developed *in vitro* simulation approaches to intracerebral haemorrhage

Table D.2 158

Synopsis of the limitations of the developed *in vitro* simulation approaches to intracerebral haemorrhage

Table D.3 163

The proposed NAS: an overview of the TPE_i and its calculation as part of the TPE assessment procedure

Table D.4 164

The proposed NAS: an overview of the TMES and its calculation as part of the TME assessment procedure

APPENDIX B 215

Notes related to the current PhD Thesis

Table APP.1 216

Cellular responses to inflammation, cell injury and malignant transformation: an interpretation of the cytopathological perspective (based on Buckner *et al.*, 1992)

Table APP.2 217

Cellular responses to therapy and typical or atypical repair: an interpretation of the cytopathological perspective (based on Buckner *et al.*, 1992)

Table APP.3 218

Inter- and intra-variance of independent experiments conducted for the cytomorpholog-

ical analysis of the mHippoE-14 cells' confluency in response to FBS-deprivation

Table APP.4 219

Z-factors for the mHippoE-14 cellular status under the major conditions chosen for the developed *in vitro* simulation approaches to intracerebral haemorrhage

LIST OF FIGURES

Development and Assessment of *In Vitro* Simulation Approaches to Intracerebral Haemorrhage

PART A 25

Intracerebral haemorrhage and its *in vitro* simulation approaches

Figure A.1 53
Basic presentation of the phases of intracerebral haemorrhage development

Figure A.2 54
Neuropathological processes associated with the lysis of the haematoma's erythrocytes in intracerebral haemorrhage: a simplified schematic overview

Figure A.3 55
Schematic summary of the mechanistic pathways leading to neuronal loss in intracerebral haemorrhage

Figure A.4 56
Simplified schematic overview of the role of microglia / macrophages and activated astrocytes in the neuropathology of intracerebral haemorrhage

Figure A.5 58
Chemical structures of selected compounds that have been suggested to exert neuroprotection against intracerebral haemorrhage, based on experimental data

PART B 66

Characterization of the embryonic murine hippocampal cell-line mHippoE-14

Figure B.1 73
Schematic representation of the procedure followed for the generation of the immortalized hippocampal mHippoE-14 cells, as described by Gingerich *et al*. (2010)

Figure B.2 74
Representative phase-contrast microscopy captions of the mHippoE-14 cells

Figure B.3 84
Representative screen captions from the xCELLigence RTCA SP analysis software

Figure B.4 86
Changes in the mHippoE-14 cellular response profiling due to FBS-deprivation

Figure B.5 87
Mapping the real-time cellular response of mHippoE-14 cells to FBS-deprivation
Figure B.6 89
Mapping the metaptosis of the mHippoE-14 cells
Figure B.7 97
Algorithm for the proposed cytomorphological classification of mHippoE-14 cells
Figure B.8 98
Atlas of the mHippoE-14 cell-line
Figure B.9 99
Representative phase-contrast microscopy captions of live mHippoE-14 cells under optimal (growth) and FBS-deprived conditions
Figure B.10 100
Cytomorphological analysis of the mHippoE-14 response to FBS-deprivation

PART C 102
mHippoE-14-utilizing *in vitro* simulation approaches to intracerebral haemorrhage

Figure C.1 111
Preliminary assessment of the toxicity of ferrum or haemin on mHippoE-14 cells: MTT reduction activity after a 24 h exposure in the presence of FBS
Figure C.2 112
Preliminary assessment of the toxicity of ferrum or haemin on mHippoE-14 cells: MTT reduction activity after a 24 h exposure in the absence of FBS
Figure C.3 113
Preliminary assessment of the toxicity of ferrum or haemin on mHippoE-14 cells: MTT reduction activity after a 48 h exposure in the presence of FBS
Figure C.4 114
Preliminary assessment of the toxicity of ferrum or haemin on mHippoE-14 cells: MTT reduction activity after a 48 h exposure in the absence of FBS
Figure C.5 115
Oligomycin-A as an *in vitro* tool for the simulation of aspects of ischaemic or metabolic penumbra
Figure C.6 116
Preliminary assessment of the toxicity of oligomycin and / or ferrum or haemin on mHippoE-14 cells: MTT reduction and released LDH activity after a 24 h exposure in the absence of FBS
Figure C.7 117
Preliminary assessment of the cellular response of mHippoE-14 to various concentrations of haemin or ferrum, in the presence or absence of oligomycin
Figure C.8 135

Graphic summary of the assessed *in vitro* simulation approaches to intracerebral haemorrhage, based on the exposure of mHippoE-14 cells to FBS-deprivation and followed by exposure to oligomycin-A and, finally, to ferrum or haemin (at a concentration of 500 μM)
Figure C.9 136
Real-time cellular response profile of the developed *in vitro* simulation approaches to intracerebral haemorrhage
Figure C.10 138
Real-time cellular response analysis of the effect of CDP-Ch (100 μM) on the developed *in vitro* simulation approaches to intracerebral haemorrhage
Figure C.11 140
Real-time cellular response analysis of the effect of DFO (100 μM) on the developed *in vitro* simulation approaches to intracerebral haemorrhage
Figure C.12 142
Representative phase-contrast microscopy captions of live mHippoE-14 cells under the developed intracerebral haemorrhage-simulating conditions
Figure C.13 143
Cytomorphological analysis of the mHippoE-14 response to developed intracerebral haemorrhage-simulating conditions
Figure C.14 144
Profiling of neuronal markers' expression in mHippoE-14 cells: comparing the expression in the presence and absence of FBS
Figure C.15 145
Profiling of neuronal markers' expression in mHippoE-14 cells: early effects of oligomycin's addition to FBS-deprived cultures
Figure C.16 146
Profiling of neuronal markers' expression in mHippoE-14 cells under the developed intracerebral haemorrhage-simulating *in vitro* conditions
Figure C.17 147
Activity of mHippoE-14 cells' AChE under the developed intracerebral haemorrhage-simulating *in vitro* conditions (a), and of *Electrophorus electricus* pure AChE following incubation with media deriving from mHippoE-14 cell cultures under the same intracerebral haemorrhage-simulating *in vitro* conditions (b)
Figure C.18 148
Overview of the proteomic profiling methodology and the arrays produced
Figure C.19 149
Volcano plot of the proteomic profiling of the O_{48} treatment group as compared to that of the control (C_{48})
Figure C.20 150

Volcano plot of the proteomic profiling of the OH_{48} treatment group as compared to that of the control (C_{48})

Figure C.21 151

Volcano plot of the proteomic profiling of the OF_{48} treatment group as compared to that of the control (C_{48})

PART D 152

Critical appraisal

Figure D.1 159

Synopsis of the developed *in vitro* simulation approaches to intracerebral haemorrhage

Figure D.2 165

Temporary simplified schematic outline of the proposed NAF for *in vitro* simulation approaches to diseases, and its functions

APPENDIX B 215

Notes related to the current PhD Thesis

Figure APP.1 220

Real-time cellular response of the mHippoE-14 cells after exposure to oligomycin and / or haemin or ferrum (at various concentrations), within metaptosis

Figure APP.2 221

Representative captions of mHippoE-14 cells after attempts to remove haemin- or ferrum-induced debris through washing with PBS

PART A

Intracerebral haemorrhage and its *in vitro* simulation approaches

CHAPTER I

Intracerebral haemorrhage: a clinical and experimental neuropathological overview

One of the finest summaries of the way the pre-Galenic world identified stroke is written by Anonymi Medici in the manuscript "De Morbis Acutis et Chroniis". The manuscript provides an overview of the cause of each disease (as suggested by earlier authors), before proceeding to the description of their symptomatology and suggestive treatment (Nutton, 1998), and includes an interesting excerpt on "apoplexy" ("Περὶ ἀποπληξίας"):

> "… Πραξαγόρας καὶ Διοκλῆς περὶ τὴν παχεῖαν ἀρτηρίαν γίνεσθαί φασι τὸ πάθος ὑπὸ φλέγματος [δὲ] ψυχροῦ καὶ παχέος ὡς μηδ' ἐν αὐτῇ οὐχ ὅτι πνεῦμα παραπνεῖσθαι δύνασθαι· καὶ οὕτω κινδυνεύειν τὸ πᾶν ἐγκαταπνιγῆναι. Ἱπποκράτης δὲ καὶ Ἐρασίστρατός φασι περὶ τὸν ἐγκέφαλον φλέγματος ψυχροῦ καὶ παγετώδους γίνεσθαι σύστασιν, ὑφ' οὗ καὶ τὰ ἀπὸ τούτου πεφυκότα νεῦρα πληρούμενα μὴ παραδέχεσθαι τὸ ψυχικὸν πνεῦμα, ἀλλ' ἐγκαταπνιγόμενον τοῦτο κινδυνεύειν ἀποσβησθῆναι",

which has been translated as follows (Garofalo, 1997):

> "… Praxagoras and Diocles say that the affection arises in the thick artery from cold and thick phlegm, in such a way that pneuma in it cannot transpire at all and thus risks being choked off. Hippocrates and Erasistratus say that cold, frozen phlegm forms in the brain: the nerves that arise from the brain, filled by this phlegm, do not receive the psychic pneuma, and this, being choked off, risks being extinguished".

Furthermore, the same manuscript provides an account of the signs of apoplexy:

> "… τοῖς δὲ ἀποπληκτικοῖς παρέπεται ἀφωνί(αν καὶ) ἀναισθησίαν γίνεσθαι μετὰ ἀτενισμοῦ, ὥσπερ ἀκινησίας τῶν ὀμμάτων, ὥστε δοκεῖν λελιθῶσθαι, καὶ οἷον ἀποπεπηγῆναι· ὅθεν δὴ καὶ τοὔνομα κέκτηται τὸ πάθος. καὶ οἱ μέν περὶ τὴν πρώτην ἢ δευτέραν ἢ τρίτην ἡμέραν ἢ ἔτι μακροτέραν ἀπαυδῶσιν, ἢ ἐσώθησαν μέν, παρελύθησαν δέ τι τοῦ σώματος· οἱ δὲ κοιλίας αὐτομάτου ὑπελθούσης ἀπηλλάγησαν τοῦ πάθους",

which has been translated as follows (Garofalo, 1997):

> "… symptoms of apoplexy are: sudden loss of voice (and) insensibility with fixed gaze, such as immobility of the eyes, so that they look rigid like stones, frozen: from this the affection has acquired its name. Some give in about the first, second or third day; others escape, but with a part of the body paralyzed; others are freed from the affection by a spontaneous evacuation of the bowels",

before proceeding to a prognostic account of the disease:

> "… ἡ δὲ ἀποπληξία σπανίως μὲν λυομένη, ταχέως δ'ἀναιροῦσα, ἔχουσα δὲ καὶ τὴν λύσιν χαλεπωτέραν τῶν ἄλλων παθῶν. τὰ πολλὰ γὰρ μετὰ τὸ παραλῦσαί τι μέρος ἀπαλλάττεται",

which has been translated as follows (Garofalo, 1997):

> "… apoplexy seldom clears up and it kills rapidly, and is more difficult to resolve than the older affections. In fact it often goes way after paralysing some part".

This very interesting account of "apoplexy" (literally meaning "being struck down")[1] (Gerber, 2003) does not identify its cause into any vascular aetiology, but is representative of what became a "remarkable longevity" for the term (Storey and Pols, 2010). The introduction of the term "stroke" is placed in 1599 (Schiller, 1970), while the identification of a cerebrovascular pathology behind "apoplexy" is a result of the work of William Harvey (1578-1657), Johann Jakob Wepfer (1620-1695) and Thomas Willis (1621-1675) (Gerber, 2003; Storey and Pols, 2010). A few decades later, Giovanni Battista Morgagni (1682-1771) provides the first classification of "apoplexy" into "sanguineous apoplexy", "serous apoplexy" and "neither serous nor sanguineous apoplexy" (Gerber, 2003; Heros and Morcos, 2000); a development that opens the way to a more accurate nosological characterization of the disease.

I.1. Defining intracerebral haemorrhage

Intracerebral haemorrhage (or cerebral haemorrhage) is an intra-axial[2] intracranial haemorrhage that can occur traumatically or non-traumatically (spontaneously). The term describes a number of conditions with different underlying causes (Al-Shahi Salman *et al.*, 2009; Steiner *et al.*, 2011) that will be analytically presented further below, and its classification is primarily aetiological and anatomical. Spontaneous[3] intracerebral haemorrhage is the type of haemorrhagic stroke that occurs within the brain parenchyma due to a cause that cannot be de-

[1] it should be noted that, in more recent years, the word "apoplexy" lost its initial meaning of stroke and has been (primarily) used for the description of any sudden death that began with a sudden loss of consciousness; nowadays, the word "apoplexy" is sometimes used for the description of acute haemorrhagic incidents in specified organs (e.g. ovarian apoplexy, pituitary apoplexy).

[2] the term "intra-axial" denotes lesions that develop / exist within the brain parenchyma, in contrast to the term "extra-axial" which describes lesions that develop / exist outside the brain.

[3] it is important to clarify that all spontaneous intracerebral haemorrhage cases fall within the non-traumatic aetiological category of the disease, but not all non-traumatic cases of intracerebral haemorrhage can be characterized as "spontaneous", although occurring spontaneously.

tected with the available diagnostic approaches (cryptogenic) or due to a cause that is unknown (idiopathic) (Steiner *et al.*, 2011). Intracerebral haemorrhage should not be confused with intraventricular haemorrhage (which is a different type of intra-axial intracranial haemorrhage) or with the clinical entities that fall under the extra-axial intracranial haemorrhages' category (such as the subarachnoid, subdural or epidural haemorrhage).

I.2. Epidemiological and aetiological overview of intracerebral haemorrhage

Intracerebral haemorrhage is the second most commonly occurring type of stroke (accounting for approximately 10% to 15% of new cases of stroke on an annual basis) (Manno, 2012; Rincon and Mayer, 2013; Roger *et al.*, 2012; Thrift *et al.*, 1995), and is characterized by an early (21-day to 30-day) case fatality of 25% to 35% in high-income countries (Feigin *et al.*, 2009) and of 30% to 48% in low- to middle-income countries (Feigin *et al.*, 2009). Despite the fact that the age-adjusted stroke incidence in high-income countries has decreased by 42% in the last 40 years (Feigin *et al.*, 2009; van Asch *et al.*, 2010), this reduction primarily reflects the lowering in the incidence of ischaemic stroke rather than that of intracerebral haemorrhage. The latter demonstrates relatively stable morbidity and mortality rates over the past decades (Manno, 2012; van Asch *et al.*, 2010), with only 20% of patients with intracerebral haemorrhage being able to regain functional independence at 6 months (Counsell *et al.*, 1995; Manno, 2012). The estimated mortality rate of intracerebral haemorrhage is approximately 50% (Broderick *et al.*, 1994; Morgenstern *et al.*, 2015; Rodríguez-Yáñez *et al.*, 2013), although this rate largely depends on the nature of the intracerebral haemorrhage as well as on the treatment it receives. Moreover, the incidence rate of intracerebral haemorrhage in Europe is estimated to account for approximately 15 cases for every 100,000 inhabitants (Giroud *et al.*, 1991), and it varies by country, age, race and sex (Appelros *et al.*, 2009; Feigin *et al.*, 2009; James and Gokhale, 2014; Rodríguez-Yáñez *et al.*, 2013; van Asch *et al.*, 2010).

The aetiology of intracerebral haemorrhage can be attributed to a number of factors that are synopsized in Table A.1. The two major causes of primary intracerebral haemorrhage are considered to be hypertension (Hassan *et al.*, 2010; Sessa, 2008; Thrift *et al.*, 1999b) and cerebral amyloid angiopathy (Bornebroek *et al.*, 1996; Chaudhary *et al.*, 2014; Greenberg, 2010; Maat-Schieman *et al.*, 1996; Pezzini and Padovani, 2008; Samarasekera *et al.*, 2012), although other unknown causes should be considered as well (Ferro, 2006). More than a decade ago, Mead *et al.* (2002) have also suggested the consideration of some cases of haemorrhagic transformation of cerebral infarcts as a potential cause of primary intracerebral haemorrhage; a suggestion that remains to be clarified.

On the other hand, secondary intracerebral haemorrhage could occur due to a large variety of causes (Table A.1), including: (a) prior traumatic brain injury (in which intracere-

bral haemorrhage develops either immediately or at a later time-point) (Kurland *et al.*, 2012; Ozgun and Castillo, 1995; Squier, 2011; Zahari *et al.*, 1996), (b) rupture of aneurysms or other vascular malformations (Abbed and Ogilvy, 2003; Detwiler *et al.*, 1997; Jensen *et al.*, 2009; Sandin *et al.*, 1999; Stapf and Mohr, 2010), (c) bleeding due to neoplasms and / or their treatment (de San Pedro *et al.*, 2010; Feldman *et al.*, 1991; Hottinger and DeAngelis, 2010; Kondziolka *et al.*, 1987; McDonald *et al.*, 1997; Nutt and Patchell, 1992; Park *et al.*, 2007; Rapanà *et al.*, 1998; Salmaggi *et al.*, 2008), (d) coagulopathies (Huttner and Steiner, 2010; Lilleyman, 1997; Quinones-Hinojosa *et al.*, 2003), (e) cerebral venous thrombosis (Crassard and Bousser, 2010; Kalita *et al.*, 2008), (f) vasculitides (Chiaretti *et al.*, 2002; Mencacci *et al.*, 2011), (g) vasculopathies (including the moyamoya syndrome)[4] (Kobayashi *et al.*, 2000; Kuroda and Houkin, 2008), (h) iatrogenic causes (particularly due to surgical procedures or other therapeutic interventions) (Asgari *et al.*, 2003; Brisman *et al.*, 1996; Cheng *et al.*, 2001; Friedman *et al.*, 2002; Gibbons *et al.*, 1992; Halliday *et al.*, 2014; Hassler and Hejazi, 1998; Mansoor *et al.*, 1996; Missori *et al.*, 2002; Russell and Gough, 2004; Seifman *et al.*, 2011), (i) anticoagulant and thrombolytic medication (Babikian *et al.*, 1989; Cavallini *et al.*, 2008; Cervera *et al.*, 2012; Da Silva and Bormanis, 1992; Derex and Nighoghossian, 2008; Flaherty, 2010; Lovelock *et al.*, 2010; Steiner *et al.*, 2006), (j) antiplatelet medication (Govaert *et al.*, 1995; Thoonsen *et al.*, 2010), (k) heavy ethanol consumption (Ariesen *et al.*, 2003; Thrift *et al.*, 1999a), (l) use of sympathomimetic and illicit drugs (Aggarwal *et al.*, 1996; Chaudhuri and Salahudeen, 1999; Forman *et al.*, 1989; McGee *et al.*, 2004; Pozzi *et al.*, 2008), (m) honeybee stings (Remes-Troche *et al.*, 2003), (n) snake bites (Mosquera *et al.*, 2003; Pinho and Burdmann, 2001), and (o) other causes (Argyriou *et al.*, 2006; Gironell *et al.*, 1995; Kumar *et al.*, 2009; Senanayake and Román, 1992; Viola *et al.*, 2011).

In a systematic review undertaken by Ariesen *et al*. (2003), the authors concluded that age, male sex, hypertension, as well as a high intake of alcohol, are risk factors for intracerebral haemorrhage. On the other hand, the same study suggested that smoking, diabetes mellitus and hypercholesterolaemia should not be considered as risk factors for the development of intracerebral haemorrhage (Ariesen *et al.*, 2003). In fact, hypercholesterolaemia seems to lower the risk of intracerebral haemorrhage (Ariesen *et al.*, 2003), despite it being a proven risk factor for ischaemic stroke (Goldstein *et al.*, 2001)[5]. A medical history of cerebral infarction seems to also be associated with an increased chances of developing intracerebral haem-

[4] the most common medical conditions that associate with the moyamoya angiographic pattern are neurofibromatosis, sickle cell disease, and previous cranial irradiation; however, there is a significant number of other disorders linked to this pattern, namely pyogenic meningitis, tuberculosis, leptospirosis, Fanconi anaemia, Marfan syndrome, pseudoxanthoma elasticum (Grönblad-Strandberg syndrome), Apert syndrome, glycogen storage disease and connective tissue defects (Riela and Roach, 1993).

[5] thankfully, low serum cholesterol levels (due to intensive statin treatment) are not associated with an increased risk of intracerebral haemorrhage, with the exception of cases with a medical history of intracerebral haemorrhage (Athyros *et al.*, 2010).

orrhage (Flaherty *et al.*, 2010; Woo *et al.*, 2002), while the use of medication such as anticoagulants, thrombolytics and antiplatelet drugs, also seems to bear a small (but debatable) risk of developing intracerebral haemorrhage (Brass *et al.*, 2000; Flaherty *et al.*, 2010; Gebel *et al.*, 1998; Gorelick and Weisman, 2005; Gurwitz *et al.*, 1998; Hart *et al.*, 1995; Själander *et al.*, 2003; Thrift *et al.*, 1999c). Finally, there seems to be a small heritability component to the risk of developing intracerebral haemorrhage, which is, so far, mainly highlighted on the role of specific apolipoprotein E genotypes and their particular association with lobar[6] intracerebral haemorrhage (Flaherty *et al.*, 2010; O'Donnell *et al.*, 2000; Woo *et al.*, 2002; 2005).

I.3. Clinical presentation of intracerebral haemorrhage

More than half of the patients with intracerebral haemorrhage will report a progressive onset of clinical symptoms over minutes to hours (Hänggi and Steiger, 2008); these symptoms depend largely on the location and the size of the occurring haematoma. A non-exhaustive overview of clinical symptoms accompanying different types of intracerebral haematomas, based on the neuroanatomical localization (and size) of the latter, is provided in Table A.2.

Lobar intracerebral haemorrhage appears in most cases with headache (Arboix *et al.*, 2006; Massaro *et al.*, 1991; Ohtani *et al.*, 2003; Ropper and Davis, 1980); an onset symptom accompanied some times by vomiting (Caplan, 1993; Kase, 2010) or, more rarely, by seizures (Cervoni *et al.*, 1994; De Reuck *et al.*, 2007; Passero *et al.*, 2002). Depending on the location of the haematoma, symptomatology varies significantly amongst the frontal, parietal, temporal and occipital haemorrhages: impaired consciousness, hemiparesis, sensory loss, hemianopia, aphasia and constructional apraxia are amongst the main symptoms associated with lobar intracerebral haemorrhage (Caplan, 1993; Kase, 2010; Lunardi, 2012; Thrift *et al.*, 1995).

The symptomatology of the deep-seated intracerebral haemorrhage is systematically distinguished into that of the putaminal (small or large, depending on the haematoma's size), caudate and thalamic haemorrhages. Large putaminal haemorrhages could even lead to coma (Hier *et al.*, 1977), and are likely to expand intraventricularly (Stein *et al.*, 1983). On the other hand, small putaminal haemorrhages can still produce motor and sensory deficits (Table A.2), but not to the severity or with the certainty of the large putaminal ones (Caplan, 1993). Putaminal haemorrhages are mainly associated with hypertension (Weisberg *et al.*, 1990), have a mortality rate of approximately 20% (Thrift *et al.*, 1995), and present with a variety of clinical syndromes, depending on the exact neuroanatomical location and size of the haematoma (Ghetti, 2012; Kase, 2010).

[6] a number of studies tends to classify intracerebral haemorrhage according to the anatomical position of the haematoma, as "lobar", "deep-seated", "cerebellar" or "pontine"; this classification could, to an extent, considered to be suggestive of the aetiology of intracerebral haemorrhage (e.g. white matter and cortical haematomas are more likely to occur due to cerebral amyloid angiopathy, compared to anatomically deeper-seated haematomas) (Sutherland and Auer, 2006).

The caudate haemorrhages are rare, small haematomas that could present with headache, vomiting or decreased alertness (Caplan, 1993; Stein *et al.*, 1984), and that could easily discharge intraventricularly (Liliang *et al.*, 2001); in fact, an haemorrhage at the caudate nucleus could clinically resemble a subarachnoid one (Kase, 2010; Pellizzaro Venti *et al.*, 2012). States of confusion and disorientation could also occur in patients with caudate haematomas, but sensory deficits are, in most cases, absent (Caplan, 1993).

A different case are the thalamic haemorrhages, that are presented with contralateral hemiparesis, hemisensory syndrome, and severe ophthalmological signs (Chung *et al.*, 1996; Fisher, 1959). Their prognosis is worse than that of putaminal or caudate haematomas of equal volumes (Caplan, 1993; Thrift *et al.*, 1995), and, in some cases, thalamic haemorrhages can trigger memory disturbances and behavioural abnormalities (Caplan, 1993; Kase, 2010).

Cerebellar intracerebral haemorrhage is rarely characterized by hemiplegia (a major exclusion criterion for its diagnosis), but it is most commonly presented as a sudden onset of lack of balance, along with vomiting, dizziness and headache (Caplan, 1993; Heros, 1982; Ott *et al.*, 1974). Ataxia and facial palsy are common clinical signs of cerebellar haemorrhage, and so is the development of dysarthria (Kase, 2010) and oculomotor deficits (Bosch *et al.*, 1975).

The last major type of intracerebral haemorrhage to be mentioned within this short summarization of the clinical presentation of the disease, the pontine haemorrhage, is characterized by a wide clinical spectrum and poor prognosis (Wessels *et al.*, 2004); large pontine haematomas will cause quadriplegia, oculomotor deficits, hyperventilation, or even coma (Caplan, 1993), while smaller haematomas are more likely to be non-life-threatening, and to produce mild neurological deficits (Kase, 2010; Moncayo, 2012b; Wessels *et al.*, 2004).

A thorough clinical evaluation of the patient with intracerebral haemorrhage is a major part of the diagnostic investigation, and a monitor of the disease's progression. Over recent years, a number of clinical grading scales has been developed (Hwang *et al.*, 2010) in order to address the need for more accurate management protocols and less varied approaches to the design / execution of clinical trials, as well as in order to serve as prediction tools (a side of which will be briefly discussed in subchapter I.7). Table A.3 provides a synopsis of the first clinical grading scale for intracerebral haemorrhage as developed by Hemphill *et al*. (2001): the parameters considered for its determination, and its score's prognostic interpretation according to the "outcome measure" chosen (30-day mortality).

I.4. Diagnostic investigation of intracerebral haemorrhage

Upon admission, a patient suspected to suffer from an intracerebral haemorrhage should undergo a diagnostic investigation that consists of three elements: (a) the acquisition of his history (e.g. age, hypertension, cognitive decline, trauma, use of anticoagulants, co-morbidities,

use of drugs), (b) the undertaking of a clinical examination (e.g. blood pressure measurement, scoring according to the available clinical grading scales, identification of signs of trauma, bleeding and / or drug abuse), and (c) the immediate performance of a neuroradiological examination of the patient's head and neck region, through either a computed tomography (CT) or a magnetic resonance imaging (MRI) scan (as an approach to the identification of the location, size and nature of the haematoma and its associated lesions) (Allen, 1984; Anzalone *et al.*, 2004; Chen and Caplan, 2010; Linn and Brückmann, 2009). These three elements are usually sufficient in order to lead to the diagnosis of a primary hypertensive intracerebral haemorrhage, but might not be enough in order to define the cause of a secondary intracerebral haemorrhage or even set a diagnostic label for a primary intracerebral haemorrhage due to cerebral amyloid angiopathy (Chen and Caplan, 2010); diagnostic tests that might be needed in order to secure a diagnosis (and be able to effectively manage) such cases of intracerebral haemorrhages, are routine laboratory tests[7], coagulation studies, blood cultures, toxicological or more specific biochemical[8] studies, cerebrospinal fluid (CSF) analyses, and the undertaking of further neuroradiological tests (e.g. MRI, CT angiography, cerebral catheter angiography) (Butcher and Davis, 2010; Chen and Caplan, 2010; Chewning and Murphy, 2010a; 2010b; Kernagis and Laskowitz, 2012; Parizel *et al.*, 2001; Schellinger and Fiebach, 2004; Wong *et al.*, 2012; Xavier *et al.*, 2003). In some difficult cases (e.g. suspicion of vasculitis or of a tumour as a cause of the haematoma), the pathognomonic acquisition of brain biopsies might also be necessary (Chen and Caplan, 2010).

At this point, it might be worth mentioning that according to a recent systematic review by Hasan *et al*. (2012) on a total of 136 molecular variables measured and analysed with regards to their association with stroke, only 4 were found to be of able to reliably serve as diagnostic biomarkers for stroke; of these, it is only the glial fibrillary acidic protein (GFAP)[9] that has been shown to be a reliable indicator of a haemorrhagic stroke (as opposed to an ischaemic one) (Foerch *et al.*, 2006; Zhang *et al.*, 2013).

I.5. Surgical management of intracerebral haemorrhage

The controversy over the surgical or conservative management of an intracerebral haemorrhage patient has already been briefly highlighted in the Preface of the current PhD Thesis, with a particular mention on the STICH trials' results (Mendelow *et al.*, 2005; 2013); this con-

[7] such as an electrocardiogram (ECG), a chest X-ray, a full blood count, liver function tests, the assessment of markers of inflammation, as well as the measurement of electrolytes, urea and creatinine (Josephson *et al.*, 2010).
[8] such as the measurement of human chorionic gonadotrophin in the case of pregnant women.
[9] the release of GFAP into the bloodstream is believed to be solely brain-derived, pathognomonic within specific timeframes following the onset of clinical symptomatology, and associated with blood-brain barrier (BBB) injury (Schiff *et al.*, 2012).

troversy lies at the heart of the problem with regards to the urgent need of novel treatment approaches for this devastating disease (Josephson *et al.*, 2010; Wang and Talkad, 2009). One must recognise that the removal of the haematoma is expected to reduce the mechanical compression caused by it over the perihaematomal region, and to prevent the subsequent haematoma-induced neurotoxic effects (Mendelow, 2010; Minematsu, 2003). However, such an intervention might evolve risks that might outweigh the potential benefits from it (Hankey, 2003; Rodríguez-Yáñez *et al.*, 2013), and should be considered on a case-by-case level, based on the patient's clinical grading (Rodríguez-Yáñez *et al.*, 2013), the specifics of the clinical presentation of the disease (Chen *et al.*, 2014; Mendelow and Unterberg, 2007) as well as the most recent clinical guidelines (Steiner *et al.*, 2014).

The most commonly-employed surgical treatment approaches to intracerebral haemorrhage (Fiorella *et al.*, 2015; Mendelow, 2010; Wang and Talkad, 2009) are synoptically presented in Table A.4 and include: (a) decompressive craniotomy or craniectomy followed by open surgery, (b) stereotactic aspiration[10], and (c) endoscopic aspiration. Further supplementary to the decompressive craniotomy or craniectomy techniques, such as the ventricular external drainage for cases of intracerebral haemorrhage with hydrocephalus and intraventricular bleeding, can also been undertaken (Dey *et al.*, 2012; Ferro, 2006).

Donnan and Davis (2003) have attributed the ineffectiveness of the surgical treatment of intracerebral haemorrhage to the lack of evidence with regards to the disease's neuropathology, as well as to the very small number of patients included in the - by the time - published clinical trials. The STICH trials' results[11] that followed, underlined the need for a more thorough parametropoiesis of the clinical characterization of intracerebral haemorrhage cases; a dimension of the problem that is now recognised (Bimpis and Zarros, 2014; Kirkman *et al.*, 2011b).

I.6. Non-surgical management of intracerebral haemorrhage

The non-surgical (conservative; medical) management of intracerebral haemorrhage is more dependent on the early identification of the triggering cause of the disease than the surgical approach. A brief overview of what such a management could involve is provided herein (Table A.5), but one should bear in mind that aspects of the non-surgical management could still be essential parts of the surgical management, if such was to take place within the treatment approach to intracerebral haemorrhage.

[10] usually combined with local thrombolysis (Thiex, 2011), the technique is considered as a minimally-invasive surgical approach to the treatment of intracerebral haemorrhage (Nyquist *et al.*, 2010); a very informative review article on the history of the development of stereotactic fibrinolytic evacuation as a treatment option for intracerebral haemorrhage is that of Samadani and Rohde (2009).

[11] in particular, STICH II is claimed to be the 15th randomized trial aiming to assess the surgical management of intracerebral haemorrhage as compared to a non-surgical one (Starke *et al.*, 2014).

Intracerebral haemorrhage is a medical emergency and, as such, any delay in its treatment is unfavourable in terms of outcome (Elliott and Smith, 2010; Marietta *et al.*, 2007). Upon admission, an intracerebral haemorrhage patient should be stabilized in terms of adequacy of airway, breathing and circulation[12], particularly in cases where a rapid neurological decline and low levels of consciousness are evident (Elliott and Smith, 2010; Mayer and Rincon, 2005; Naval *et al.*, 2010; Sacco *et al.*, 2004). Immediate endotracheal intubation, mechanical ventilation and correction of hypertension should be undertaken in order to: (a) secure an adequate cerebral perfusion pressure[13] and (b) eliminate the potential for a further haematoma expansion[14], the development of cerebral oedema[15] and / or hydrocephalus (Anderson, 2009; Elliott and Smith, 2010; Mayer and Rincon, 2005). The management of hypertension (a common feature of patients with intracerebral haemorrhage at the time of admission) should be addressed preferably with labetalol (a mixed alpha/beta adrenergic receptor antagonist), esmolol (a beta-1 adrenergic receptor antagonist) or nicardipine (an L-type calcium channel blocker) (Asdaghi *et al.*, 2007; Elliott and Smith, 2010; Mocco *et al.*, 2006; Naval *et al.*, 2010). Moreover, the non-surgical management of an increased ICP should also be considered; head elevation (Rincon and Mayer, 2008), short-term hyperventilation (Badjatia and Rosand, 2005; Rincon and Mayer, 2008), osmotherapy (primarily through mannitol administration) (Asdaghi *et al.*, 2007; Kalita *et al.*, 2003; Rincon and Mayer, 2008; Sacco *et al.*, 2004), pentobarbital-induced cerebral hypometabolism (Rincon and Mayer, 2008) and hypothermia induction (Rincon and Mayer, 2008), are some of the options for the achievement of control on ICP within an intensive care unit.

One of the first steps that a non-surgical approach should also include is the immediate stop and, if possible, reversal of any oral anticoagulant treatment (Flower and Smith, 2011; Goldstein *et al.*, 2008); the immediate administration of vitamin K and the clotting factor replacement with fresh-frozen plasma or prothrombin complex concentrate, are recommended options for the immediate reversal of the effects of warfarin[16] (Masotti *et al.*, 2011). On the other hand, heparin can be inactivated by protamine sulphate administration (Badjatia and Rosand, 2005), while the transfusion of platelets and the administration of desmopressin acetate could offer some coverage for patients previously on antiplatelet medication (Badjatia and Rosand, 2005).

[12] also known as the ABCs.
[13] the cerebral perfusion pressure is defined as the difference between the mean arterial pressure and the intracranial pressure (ICP).
[14] there have been reports challenging the belief that the early intensive (aggressive) lowering of blood pressure can beneficially affect the outcome of intracerebral haemorrhage (Worster *et al.*, 2009).
[15] interestingly, again, McCourt *et al*. (2014) have recently provided evidence that cerebral perfusion and blood pressure do not affect perihaematomal oedema growth in acute intracerebral haemorrhage.
[16] the administration of recombinant factor VIIIa is not recommended for the reversal of warfarin in intracerebral haemorrhage (Aiyagari and Testai, 2009; Anderson, 2009; Flower and Smith, 2011).

It is also worth noting that efficient glycaemic control, venous thrombosis prophylaxis, nutrition and temperature control, are vital aspects of the acute management of intracerebral haemorrhage patients (Aguilar and Freeman, 2010; Balami and Buchan, 2012; Flower and Smith, 2011; Mayer and Rincon, 2005; Nyquist, 2010; Rincon and Mayer, 2008; Rincon *et al.*, 2014; Rodríguez-Yáñez *et al.*, 2013). For the management of intracerebral haemorrhage-induced seizures, acute administration of lorazepam (followed by phenytoin, fosphenytoin, valproic acid or phenobarbital) is required (Mayer and Rincon, 2005), and an 8 to 12-week prophylactic anticonvulsant therapy has also been considered, particularly in the case of lobar haematomas (Asdaghi *et al.*, 2007); the latter is not a universally encouraged option (Flower and Smith, 2011). Finally, the role for corticosteroids in the treatment of intracerebral haemorrhage has been a matter of debate (Elliott and Smith, 2010; Sacco *et al.*, 2004).

In recent decades, the identification of the limited efficacy of both the surgical and the non-surgical treatment approaches to intracerebral haemorrhage has led to the undertaking of a number of experimental and clinical trials on the identification of compounds that could exert neuroprotection on the perihaematomal regions. Some of these (promising) treatment options have been tightly linked to the contemporary understanding of the neuropathology of the disease and, thus, will be appropriately discussed further below.

I.7. Prognosis of intracerebral haemorrhage

Intracerebral haemorrhage is characterized by high rates of morbidity and mortality (Hanel *et al.*, 2002). Although the 30-day mortality rates in a population study conducted by Broderick *et al*. (1994) appear to be different between the surgically- (25%) and the conservatively-managed patients (46%), the overall morbidity and mortality for these two management approaches were not statistically, significantly different. Amongst the most frequently assessed clinical and radiologic predictors of survival and functional outcome in intracerebral haemorrhage, one should consider: (a) the patient's age, (b) the patient's gender, (c) the patient's initial level of consciousness, (d) the anatomical location of the haematoma, (e) the existence of intraventricular haemorrhagic spread, (f) the development of hydrocephalus, (g) the development of a midline shift or mass effect, (h) the progression of the bleeding, and (i) the patient's blood pressure (Diamond *et al.*, 2003). Diabetes has not been associated with a worsening of the outcome prognosis for spontaneous intracerebral haemorrhage (Wang *et al.*, 2015), but the use of antiplatelet therapy at the time of incident has been suggested to increase mortality (Thompson *et al.*, 2010).

A number of mathematical models of outcomes in intracerebral haemorrhage has been developed over the years (Tuhrim, 2010); these approaches have: (a) fostered the development of predictive algorithms that can inform prognosis (with an emphasis on the likelihood

of survival and recovery), and (b) identified a number of clinical and laboratory parameters that have contributed immensely to the improvement of the design of clinical trials in the field. Apart from the prognostic interpretation of the first clinical grading scale for intracerebral haemorrhage developed by Hemphill *et al*. (2001) that has already been presented in this Thesis (Table A.3) and that has provided the basis for the development of a number of further clinical grading scores (Hwang *et al*., 2010), the recently developed prediction score for haematoma expansion in patients with primary intracerebral haemorrhage (Brouwers *et al.*, 2014) is also worth mentioning.

I.8. Neuropathological overview of intracerebral haemorrhage

The development of intracerebral haemorrhage could be considered to be taking place in at least five phases (Figure A.1; phases I-V): a very brief phase in which the vascular rupture occurs (1-10 sec; phase I), a second phase in which the haematoma is formed (<1 h; phase II), a third phase in which the haematoma is expanding (1-6 h; phase III), a fourth phase in which the perihaematomal oedema is established (24-72 h; phase IV), and a final phase of undefined duration, in which late injury is exerted (phase V). This ideographic perception of the development of intracerebral haemorrhage is, of course, simplistic; reality is far more complicated and largely-dependent on the neuroanatomical and aetiological aspects of the bleeding. It is, however, very helpful in understanding the sequence of events that take place in the development of this disease, particularly in view of its dynamic nature.

Once the vascular rupture occurs (phase I) - irrespectively of its aetiology - the speed of the haematoma formation (phase II) as well as the volume it will reach (phase III) will be dictated by the patient's blood pressure, the existence of any coagulation abnormalities, the local neuroanatomical environment and the extent of the simultaneously developing perihaematomal injury (Figure A.1). Within these crucial first hours, the haematoma leads to the establishment of perihaematomal oedema (phase IV); the end-stage of what is known as "primary" injury. The "secondary" injury is introduced sometime between phases III and IV, and is attributed to certain products of coagulation, the breakdown of the entrapped (in the haematoma's clot) erythrocytes, and the microglial activation; this secondary injury could be taking place for many days after the haemorrhagic incident (phase V; Figure A.1). Oedema plays a crucial part within this secondary injury.

In more detail, phases I, II and III seem to provoke a mechanical disruption and deformation of the local brain parenchyma (Qureshi *et al.*, 2001b; 2009); a direct injurious process for the local neuronal and glial cell populations, and a basis for the establishment of oligae-

mia, metabolic suppression or even ischaemia[17] (Qureshi *et al.*, 2009). During these pathophysiological events, the perihaematomal tissue's cells seem to be releasing excitotoxic levels of glutamate (due to the mechanical stretch they endure), and to suffer severe mitochondrial dysfunction, membrane depolarization and calcium influx; as a result, the development of oxidative stress, sodium accumulation, cellular swelling (cytotoxic oedema)[18] and necrosis, follow (Lo *et al.*, 2005; Qureshi *et al.*, 2003a; 2009). Glial activation occurs (Karwacki *et al.*, 2006), and a cascade of cellular interactions seems to be triggered *via* the activation of nuclear factor kappa B (NF-κB)[19] and the secretion of pro-inflammatory cytokines such as tumour necrosis factor alpha (TNF-α), interleukin 1 beta (IL-1β) and interleukin 6 (IL-6) (Karwacki *et al.*, 2006; Wagner, 2007; Wang, 2014; Zarros *et al.*, 2014). The glial activation aims to form a glial scar (gliosis) in order to make up for the generated space due to the neuronal loss (Figure A.2); meanwhile, the secreted TNF-α and IL-1β exacerbate this loss (Katsuki, 2010; Wang and Doré, 2007; Zarros *et al.*, 2014). This situation is soon becoming more complicated, as the blood degradation and the induction of cellular and humoral toxicity enhance the development of vasogenic oedema in the perihaematomal region (Figure A.2).

The degradation of the erythrocytes that are entrapped in the haematoma is facilitated by the complement cascade (Ducruet *et al.*, 2009) and leads to the release of haemoglobin (Figure A.2). Haemoglobin causes inflammation, oxidative stress and activates matrix metalloproteinase-9 (MMP-9) (Katsu *et al.*, 2010); a major member of the matrix metalloproteinase (MMP) family[20] that is associated to microglial activation, can enhance the release thrombin from the haematoma as well as cause a further disruption of the BBB[21] (Keep *et al.*, 2008; Rodríguez-Yáñez *et al.*, 2010; Rosell *et al.*, 2008). Haemoglobin is metabolized by microglia and macrophages and produces haeme (Aronowski and Zhao, 2011), which then is either re-

[17] the "ischaemic" brain injury associated with intracerebral haemorrhage has been a matter of extensive but inconclusive debate, particularly with regards to its nature and causes (Gass, 2007; Herweh *et al.*, 2007; Josephson *et al.*, 2010; Kirkman, 2011; Mackenzie and Clayton, 1999; Mitchell and Gregson, 2011; Prabhakaran and Naidech, 2012; Thanvi *et al.*, 2012; Vespa, 2009); it is neither clear whether this persisting "ischaemia" is also a result of a perihaematomal hypoperfusion due to the haematoma products' toxicity-induced hypometabolism, or even a result of the aggressive antihypertensive therapy that is usually adopted (Prabhakaran and Naidech, 2012; Qureshi *et al.*, 2009; Thiex and Tsirka, 2007). The issue of whether we are talking about an "ischaemic" or a "metabolic" penumbra complicated by the presence of oedema in intracerebral haemorrhage, is elegantly discussed by Thiex and Tsirka (2007).

[18] the development of cytotoxic oedema is due to insufficient adenosine triphosphate (ATP) availability, leading to a failure of the sodium / potassium adenosine triphosphatase (Na^+,K^+-ATPase) function, and causing cellular swelling (Rodríguez-Yáñez *et al.*, 2010); it should not be confused with the oedema characterizing phase IV of the development of intracerebral haemorrhage (Figure A.1), which is far more extensive and vasogenic (due to the breakdown of the BBB) (Thiex and Tsirka, 2007).

[19] oxidative stress is also an activator of NF-κB (Aronowski and Zhao, 2011; Zarros *et al.*, 2014), while NF-κB is also responsible for the upregulation of the expression of the inducible nitric oxide synthase (iNOS) (Zhao *et al.*, 2007b); a potential contributor to the oedema formation observed in intracerebral haemorrhage (Kim *et al.*, 2009).

[20] a very informative review article on the role of MMPs in the neuropathology of intracerebral haemorrhage, has been written by Xue and Yong (2008).

[21] the BBB disruption facilitates the local neutrophil infiltration (Wang, 2014).

leased as toxic haemin[22] (Babu *et al.*, 2012) or further metabolized by haeme oxygenases (HOs)[23] into biliverdin, ferrous iron[24] and carbon monoxide (CO) (Aronowski and Zhao, 2011; Wagner *et al.*, 2003) (Figure A.2). Biliverdin will be further converted by biliverdin reductase into bilirubin; the latter being an oxidant on its own right (Karwacki *et al.*, 2006; Lakovic *et al.*, 2014). The released iron will play a major role in enhancing oxidative reactions, promoting oedema formation and being neurotoxic (Hua *et al.*, 2007; Huang *et al.*, 2002; Karwacki *et al.*, 2006; Lou *et al.*, 2009; Wagner *et al.*, 2003) (Figure A.2). At the same time, as already mentioned, thrombin is also released from the haematoma (Figure A.2) and, like haemoglobin, triggers microglial activation by stimulating them to release TNF-α and IL-1β (Wu *et al.*, 2008). Thrombin is also known to activate the complement cascade, promote neuroinflammation and exacerbate the iron-induced neurotoxicity (Babu *et al.*, 2012; Hua *et al.*, 2007; Liu *et al.*, 2014; Xi *et al.*, 2006; 2010).

It is without doubt that neuronal loss is the major determinant of the clinical outcome in patients suffering from intracerebral haemorrhage. Figure A.3 summarizes the three pathways through which neuronal loss is believed to take place in intracerebral haemorrhage. Necrosis, as a consequence of cytotoxic oedema, is the result of the primary injury (Qureshi *et al.*, 2001b; Xi *et al.*, 2006). A prominent mode of neuronal loss is apoptosis (Qureshi *et al.*, 2003b; Xi *et al.*, 2006); this is mainly the result of caspase activation (Wu *et al.*, 2006; Xi *et al.*, 2006) due to the toxic effects of the erythrocyte lysis products (particularly of haeme and iron) and the neuroinflammation[25] generated within the secondary injury (Figure A.3). Neuronal loss due to autophagy remains elusive[26], and its involvement in the intracerebral haemorrhage-induced neuronal loss is suggested only by experimental findings (Hu *et al.*, 2011; Shen *et al.*, 2016).

On the other hand, the key players in this complex cascade of pathophysiological interactions are the activated (reactive) astrocytes and the microglia / macrophages (Figure A.4). The role of the reactive astrocytes in the intracerebral haemorrhage-induced secondary injury has been more or less already highlighted, and it mainly involves the secretion of cytokines (particularly of TNF-α and IL-1β) (Karwacki *et al.*, 2006). Microglia and macrophages are a

[22] haemin is the oxidative form of haeme (Babu *et al.*, 2012); it exerts its neurotoxicity be releasing excessive iron, depleting glutathione and inducing oxidative stress (Wagner *et al.*, 2003; Wang, 2014).
[23] there are two HO isoforms implicated in the neuropathology of intracerebral haemorrhage: haeme oxygenase 1 (HO-1) and 2 (HO-2) (Maines, 1997); the latter is thought to be the major HO expressed in neurons and in the brain under normal conditions (Maines, 1997; Wang and Doré, 2008; Wang *et al.*, 2006), while HO-1 is predominantly induced in non-neural cells (microglia / macrophages and endothelial cells) (Wang, 2014).
[24] "ferrous" indicates a divalent iron compound (+2 oxidation state; Fe^{2+}), as opposed to "ferric" which indicates a trivalent iron compound (+3 oxidation state; Fe^{3+}).
[25] a very recent and well-written review article on neuroinflammation in intracerebral haemorrhage is written by Askenase and Sansing (2016).
[26] autophagy has been associated with the neurotoxic effects of iron (He *et al.*, 2008b).

more complex case; their ability to phagocytose haeme[27] / haemin, haemoglobin[28] or even whole erythrocytes[29], designates them as key regulators of extracellular iron concentrations (Aronowski and Zhao, 2011). On the other hand, their inability to cope with excessive concentrations of iron promotes oxidative stress[30] (through the iron-induced generation of ROS; reactive oxygen species) (Aronowski and Zhao, 2011; Duan *et al.*, 2016). The latter further exacerbates the BBB disruption and facilitates the subsequent formation and exacerbation of the perihaematomal oedema (Duan *et al.*, 2016; Rodríguez-Yáñez *et al.*, 2010) (Figure A.4).

With regards to the genetic background of intracerebral haemorrhage, little is known (Xi *et al.*, 2006). A number of studies has suggested that the ε4 and ε2 alleles of the apolipoprotein E (ApoE) gene (*APOE*) are linked to a predisposition to intracerebral haemorrhage (Greenberg *et al.*, 1995; Martínez-González and Sudlow, 2006; Maxwell *et al.*, 2011; McCarron *et al.*, 1999), while other studies have revealed an association of this disease with polymorphisms in the genes encoding the angiotensin-converting enzyme (ACE) (Slowik *et al.*, 2004), the methylenetetrahydrofolate reductase (Fang *et al.*, 2005), the alpha-1 antichymotrypsin (Obach *et al.*, 2001), and others (Jensson *et al.*, 1989; Liu *et al.*, 2012; Lu *et al.*, 2006).

I.9. Clinical neuropathology of intracerebral haemorrhage

In clinical practice, the neuropathologist will aim, primarily, at identifying the site, the size and the aetiology of intracerebral haemorrhage (Dye *et al.*, 2014; Sutherland and Auer, 2006); the first two within an autopsy procedure, and the third either through a biopsy, a haematoma evacuation sampling or an autopsy. Macroscopically, intracerebral haemorrhage causes a destruction of the local parenchyma and provokes oedema of the surrounding (perihaematomal) parenchyma; the necrotic brain tissue is replaced by gliosis and sometimes contains cystic elements that appear to be yellow-brown (Chandrasoma and Taylor, 1995; Govan *et al.*, 1995). The immediately-attached to the haematoma perihaematomal tissue will also have a brown appearance; a characteristic of the thereby attracted haemosiderin-laden macrophages (Chandrasoma and Taylor, 1995). The existence of multiple microaneurysms (particularly

[27] toxic free haeme is neutralized by haemopexin (Figure A.4), and they both form a complex that can be subject to phagocytosis *via* CD91 (Aronowski and Zhao, 2011; Wang, 2014).
[28] haemoglobin binds to haptoglobin (a blood- and oligodendrocyte-deriving protein), forming a complex that is then endocytosed by microglia / macrophages *via* CD163; the expression of haptoglobin is regulated by the nuclear factor (erythroid-derived 2)-like 2 (Nrf2) (Aronowski and Zhao, 2011; Wang, 2014; Zhao *et al.*, 2009) (Figure A.4). Interestingly, Nrf2 also induces the expression of HO-1 (Aronowski and Zhao, 2011; Kensler *et al.*, 2007) (Figure A.4).
[29] the peroxisome proliferator-activated receptor gamma (PPAR-γ) regulates the transcription of CD36 (Figure A.4); the latter facilitates the phagocytosis of erythrocytes (Aronowski and Zhao, 2011; Wang, 2014; Zarros *et al.*, 2014; Zhao *et al.*, 2007a).
[30] oxidative stress is partially managed by the local antioxidant defences, the expression of major enzymes in which are known to be also regulated by PPAR-γ and Nrf2 (Aronowski and Zhao, 2011; Kensler *et al.*, 2007; Zhao *et al.*, 2006; 2007a) (Figure A.4).

in the very small cerebral arteries[31]) could be a finding suggesting that the rupture of one of these could have led to the examined haemorrhage (Govan *et al.*, 1995). Apart from aneurysms[32] and vascular malformations, other findings sought after by the neuropathologist are the presence of characteristics of cerebral amyloid angiopathy[33], neuropathological findings suggesting chronic hypertension, primary or secondary tumours, haemorrhagic infarcts, and other factors of aetiological significance (Crassard and Bousser, 2010; Dye *et al.*, 2014; Esiri, 1996; Greenberg, 2010; Hamann *et al.*, 1999; Hassan *et al.*, 2010; Hottinger and DeAngelis, 2010; Huttner and Steiner, 2010; Stapf and Mohr, 2010; Sutherland and Auer, 2006).

I.10. Experimental neuropathology of intracerebral haemorrhage

Throughout the last 60 years, a number of experimental simulation approaches to intracerebral haemorrhage have been developed (Andaluz *et al.*, 2002; James *et al.*, 2008; Krafft *et al.*, 2012a; Ma *et al.*, 2011; Manaenko *et al.*, 2011; Strbian *et al.*, 2008; Wagner and Zuccarello, 2010). The most characteristic *in vivo* simulation approaches to intracerebral haemorrhage are synopsized in Table A.6 (along with representative references), while the *in vitro* ones will be discussed in Chapter II. One must admit that these experimental tools have allowed us to gain more knowledge about the neuropathology of intracerebral haemorrhage than clinical studies have, but - as with all experimental approaches aiming to simulate clinical reality - these tools also suffer from a number of limitations.

The setting up and execution of an *in vivo* experimental procedure aiming to simulate an aspect of intracerebral haemorrhage is undoubtedly time-consuming, expensive, subject to regulation by strict legislation, requiring the sacrifice of a significant number of animals and, unfortunately, is bearing a number of potential pitfalls with regards to its translational interpretation (Barratt *et al.*, 2014; Kirkman *et al.*, 2011a; Leonardo *et al.*, 2012; MacLellan *et al.*, 2010; Nabika *et al.*, 2004). However, it is to these same experimental procedures that we owe the majority of our current understanding of intracerebral haemorrhage's neuropathology (Aronowski and Hall, 2005; Yan *et al.*, 2015; Wang, 2010). And it is these same experimental procedures that we employ every time we aim to test the efficacy and safety of potential new drugs for the non-surgical management of this devastating disease (Aronowski and Hall, 2005; Kathirvelu and Carmichael, 2015; Kellner and Connolly, 2010; Xi *et al.*, 2014). This sub-

[31] small penetrating arteries or arterioles, with a diameter of 50 to 200 μm (Hänggi and Steiger, 2008).
[32] it might be worth noting that the most common site of spontaneous intracerebral haemorrhage is the lentiform nucleus; an area where the branching of the lateral striate group of arteries (that supply the putamen) is considered very vulnerable to intravascular stress (Esiri, 1996).
[33] with regards to cerebral amyloid angiopathy, the undertaking of immunohistochemistry for amyloid beta (Aβ) has been suggested as being a more sensitive marker than Congo red staining (Dye *et al.*, 2014); cerebral amyloid angiopathy is a result of the deposition of insoluble Aβ in the *tunica media* and *tunica adventitia* of cortical, subcortical and leptomeningeal blood vessels, leading the latter to become more vulnerable to intravascular pressure or trauma (Chaudhary *et al.*, 2014; Greenberg, 2010; Sutherland and Auer, 2006).

chapter does not focus on providing an analytical presentation of these procedures, as such does not fall within the scope of this PhD Thesis. Instead, readers might find useful to go through a few examples of important and recent experimental findings with regards to the neuropathology and potential treatment of intracerebral haemorrhage; a "potpourri" of experimental findings and their translational interpretation.

A very first example can be a study that is now considered of paramount importance for our understanding of the role of thrombin in intracerebral haemorrhage in which Lee *et al*. (1997) have undertaken *in vivo* and *in vitro* experiments that have suggested that the cell toxicity and the BBB disruption induced by thrombin are triggering mechanisms for the oedema formation that follows intracerebral hemorrhage. Their *in vivo* experiments involved the stereotactic infusion of solutions of thrombin into the right basal ganglia of rats and the measurement of their cerebral blood flow and BBB permeability, while in some of their *in vitro* experiments, thrombin was superfused on cortical brain slices and a monitoring of the slices' microvessels' diameter *via* videomicroscopy was performed (Lee *et al.*, 1997).

On a more recent example, Chen-Roetling *et al*. (2015) have shown that in a murine simulation approach to intracerebral haemorrhage through striatal injections of autologous blood, the selective (GFAP-driven) HO-1 overexpression in astrocytes reduces the mortality and the neurological deficits in the mice, as well as the extent of the occurring BBB disruption[34] and perihaematomal cell injury; a finding of great importance both in terms of neuropathological significance as well as in terms of revealing a new pharmacological target.

Of course, one should admit that in some cases, results from *in vitro* and *in vivo* experiments are not always in agreement. For example, recent *in vitro* studies have shown that bilirubin, through its toxicity-exerting products (bilirubin oxidative products; BOXes), can cause both structural and functional damage on myelinated neuraxons in murine brain slices, but not on unmyelinated neuraxons (Lakovic *et al.*, 2014); interestingly, *in vivo* studies are not in agreement with this finding, as unmyelinated neuraxons have been reported to be more susceptible to an intracerebral bilirubin-injection (Lakovic *et al.*, 2014).

Finally, in view of the major role of neuronal loss in determining the clinical outcome of intracerebral haemorrhage, and with regards to the pathophysiological mechanisms underlying neuronal apoptosis in this context, recent *in vivo* experiments (Ni *et al.*, 2016) have suggested, for example, that an upregulation of the haematoma-adjacent rat neuronal prostaglandin E2 receptor subtype 3 (EP3) is accompanied by an increased expression of the active caspase-3, and of the pro-apoptotic B cell lymphoma-2 (Bcl-2)-associated X protein (Bax), as well as by a decreased expression of the anti-apoptotic Bcl-2. These findings provide us with confidence on the belief that apoptosis plays a prominent role in the intracerebral haemor-

[34] assessed through a BBB permeability assay with the use of Evans blue dye (Uyama *et al.*, 1988).

rhage-induced neuronal loss, and confirm the validity of a number of previous experimental studies. Another recent example of how experimentation can shed more light on the neuropathology of intracerebral haemorrhage is the recent study of Shen *et al*. (2016). This study has used an *in vivo* experimental approach to intracerebral haemorrhage by infusing collagenase type IV into the brain of mice (Shen *et al.*, 2016); a popular and well-established approach to this disease (Clark *et al.*, 1998; James *et al.*, 2008; Kirkman *et al.*, 2011a; Ma *et al.*, 2011; MacLellan *et al.*, 2010; Manaenko *et al.*, 2011). Their data suggest that enhanced autophagy may exacerbate the perihaematomal oedema and promote neuronal death, as well as that autophagy in intracerebral haemorrhage could be regulated by the NF-κB pathway, and thus be tightly related to the induction of inflammation and apoptosis (Shen *et al.*, 2016); a suggestion that is novel and of paramount importance, but certainly requires further research. This suggestion adds to the data acquired by experiments on Sprague-Dawley rats that included the infusion of autologous whole blood or ferrous iron into their basal ganglia, and that have suggested an increase in the microtubule-associated protein light chain-3 (LC3) conversion (from LC3-I to LC3-II; a biomarker of autophagosome), and in cathepsin D (a known mediator of autophagy and a lysosomal marker) levels, as well as high levels of vacuole formation in the hemisphere ipsilateral to the infusion parenchymal area (He *et al.*, 2008b). These same experiments have suggested a major role of iron in triggering this type of cell death (He *et al.*, 2008b).

I.11. Potential neuropharmacological approaches to intracerebral haemorrhage

A selection of important agents that have been tested with regards to their suitability within a neuroprotective approach to intracerebral haemorrhage is presented in Table A.7 and Figure A.5; these include the iron-chelator deferoxamine (DFO)[35] (Cui *et al.*, 2015; Nakamura *et al.*, 2004a; Ni *et al.*, 2015; Okauchi *et al.*, 2009; Selim, 2009; Staykov *et al.*, 2010), minocycline[36] (Wasserman and Schlichter, 2007a; 2007b; Wu *et al.*, 2010; Yenari *et al.*, 2006), atorvastatin (Jung *et al.*, 2004; Karki *et al.*, 2009; Seyfried *et al.*, 2004), simvastatin (Karki *et al.*, 2009), celecoxib (Park *et al.*, 2009; Sinn *et al.*, 2007), rosiglitazone (Wu *et al.*, 2015), citicoline (cytidine-5'-diphosphocholine; CDP-Ch) (Clark *et al.*, 1998; Iranmanesh and Vakilian, 2008), MK-801[37] (Kane *et al.*, 1994; Thiex *et al.*, 2007) and U-74389G (Bimpis *et al.*, 2012; 2013; 2015). Notable tested compounds have also been: the thrombin inhibitor argatroban, the MMP in-

[35] DFO has been shown to reduce the extent of the intracerebral haemorrhage-induced autophagy in Sprague-Dawley rats infused with autologous whole blood or ferrous iron into their basal ganglia (He *et al.*, 2008b).
[36] minocycline has been reported to suppress monocytoid cell activation, downregulate matrix metalloproteinase 12 (MMP-12) expression, reduce marked glial activation and apoptosis, as well as to improve neurobehavioral outcomes in *in vivo* and *in vitro* experiments conducted by Power *et al.* (2003).
[37] also known as dizocilpine.

hibitors BB-1101 and GM6001, clioquinol, erythropoietin, dexamethasone, the brain-derived neurotrophic factor (BDNF), cystamine, telmisartan, tin-mesoporphyrin (SnMP)[38], valproic acid and other agents (Guan *et al.*, 2015; Hwang *et al.*, 2011; Katsuki, 2010; Kwon *et al.*, 2013; Zhou *et al.*, 2014). The majority of these compounds are characterized by non-specific anti-inflammatory and / or antioxidant properties, and are experimentally shown to be neuroprotective in intracerebral haemorrhage by targeting iron, MMP-9, COX-2, TNF-α (Hwang *et al.*, 2011; Katsuki, 2010). Other recently highlighted potential targets are the sphingosine-1-phosphate receptor 2 (S1PR2) (Kim *et al.*, 2015)[39] and EP3 (Ni *et al.*, 2016). Moreover, as already mentioned above, the experimental data of Chen-Roetling *et al*. (2015) have suggested that the genetic or pharmacological therapies that could enhance HO-1 expression in astrocytes could also be of benefit.

One also needs to mention that through a less conventional mode, Lee *et al*. (2007) have reported that the transplantation of F3 human neural stem cells over-expressing vascular endothelial growth factor (VEGF) near the (intrastriatal) collagenase-induced lesion sites of mice, not only has provided differentiation and survival of the grafted human neural stem cells, but also managed to renew angiogenesis of the host murine brain and trigger significant functional recovery in these mice. More recently, Lee *et al.* (2015) have reported that when Wharton's jelly-derived mesenchymal stromal / stem cells primed with fasudil (10 mM, exposure for 6 h) were transplanted into Sprague-Dawley rats with a collagenase type IV-induced intracerebral haemorrhage - 1 week after injury, when hypoxia inducible factor 1 alpha (HIF-1α) upregulation occurs - the animals' functional outcome was significantly improved. Stem cell-based therapies hold high potential in providing solutions to the treatment puzzle of intracerebral haemorrhage, but a significant number of issues must be addressed prior to their translation into clinical practice (Andres *et al.*, 2008; Ma *et al.*, 2015).

I.12. Momentum of the experimental research on intracerebral haemorrhage

Until the introduction of CT in clinical practice (around 1973), very little was known about intracerebral haemorrhage, and very little could be done for it at the clinical level (Fiorella *et al.*, 2015). Today, 43 years later, both clinical and preclinical research have delivered an impressive and constantly increasing amount of outputs that, however, have neither addressed major questions with regards to the exact neuropathology of intracerebral haemorrhage, nor have indicated an effective therapeutic treatment for it. Eminent researchers in the field (Le-

[38] SnMP is a considered to be a competitive inhibitor of the HOs (Reddy *et al.*, 2003); it has been suggested to exert a neuroprotective role by reducing both the haematoma and the perihaematomal oedema volumes in an experimental approach to intracerebral haemorrhage using pigs injected with autologous blood into their frontal white matter (Wagner *et al.*, 2000).

[39] inhibition of S1PR2 results in decreased MMP-9 activity, as suggested by *in vivo* experiments (Kim *et al.*, 2015).

onardo *et al.*, 2012; NINDS ICH Workshop Participants, 2005; Steiner *et al.*, 2011; Xi *et al.*, 2014) have indicated that certain priorities should be adopted in order to overcome this stagnation; an interpretation of these priorities is summarized in Table A.8.

This current PhD project has aimed in serving the development of more sophisticated *in vitro* simulation approaches to intracerebral haemorrhage (priority 6; Table A.8).

>> Table A.1: page 45
>> Table A.2: page 46
>> Table A.3: page 47
>> Table A.4: page 48
>> Table A.5: page 49
>> Table A.6: page 50
>> Table A.7: page 51
>> Table A.8: page 52
>> Figure A.1: page 53
>> Figure A.2: page 54
>> Figure A.3: page 55
>> Figure A.4: page 56
>> Figure A.5: page 58

Table A.1: Aetiological overview of intracerebral haemorrhage: common clinical conditions, incidents and lifestyle options related to the development of primary and secondary intracerebral haemorrhage.

Main causes of intracerebral haemorrhage
PRIMARY intracerebral haemorrhage
– hypertension
– cerebral amyloid angiopathy
– other unknown causes
– (haemorrhagic transformation of infarct)
SECONDARY intracerebral haemorrhage
– prior traumatic brain injury (immediate or delayed)
– aneurysms and vascular malformations
– neoplasms and / or their treatment
– coagulopathies
– cerebral venous thrombosis
– vasculitides
– vasculopathies (including the Moya-Moya syndrome)
– iatrogenic; due to surgical procedures or other therapeutic interventions
– anticoagulant and thrombolytic medication
– antiplatelet medication
– heavy ethanol consumption
– use of sympathomimetic and illicit drugs
– honeybee stings
– snake bites
– other causes

Note: the current overview is in no case exhaustive, nor considers in depth the aetiological basis of intracerebral haemorrhage in paediatric populations; for the latter, the readers are referred to the work of Riela and Roach (1993). The structure of the current overview is based on the work of Ferro (2006), with additions and significant modifications.

Table A.2: Overview of clinical symptoms accompanying intracerebral haemorrhage, based on the neuroanatomical localization (and size) of the haematoma.

Clinical sign	**Expression in lobar intracerebral haemorrhage**
motor weakness	hemiparesis (frontal; parietal), mild hemiparesis (occipital)
sensory loss	yes (parietal), no / transient (occipital), no (frontal; temporal)
hemianopia	yes (occipital; parietal; temporal), no (frontal)
pupils	normal
eye movement	unaffected
other	abulia (frontal, rarely), aphasia (parietal; temporal), apraxia (parietal)
Clinical sign	**Expression in deep-seated intracerebral haemorrhage**
motor weakness	hemiparesis (putaminal; caudate; thalamic)
sensory loss	yes (large putaminal; thalamic), some (small putaminal), no (caudate)
hemianopia	yes (large putaminal), no (small putaminal; caudate)
pupils	small and nonreactive (thalamic), dilated (large putaminal, lesion's side)
eye movement	affected (with the exception of small putaminal cases)
other	confusion (caudate; thalamic), aphasia (left large putaminal; left thalamic)
Clinical sign	**Expression in cerebellar intracerebral haemorrhage**
motor weakness	none
sensory loss	no
hemianopia	no
pupils	slightly constricted on side of lesion
eye movement	affected
other	ipsilateral limb ataxia, dizziness, dysarthria
Clinical sign	**Expression in pontine intracerebral haemorrhage**
motor weakness	quadriplegia
sensory loss	contralateral hemisensory (lateral tegmental)
hemianopia	no
pupils	constricted and reactive
eye movement	affected
other	hyperventilation, limb ataxia, facial numbness and weakness

Note: the current overview does not include symptoms such as headaches, vomiting, seizures or coma, as these are appropriately discussed in the text; for the latter as well as for more details on the expression patterns and neuroanatomical correlations of the herein presented symptoms, the readers are advised to consult the excellent works of Caplan (1993) and Kase (2010). It should also be noted that in this overview, the clinical symptoms of midbrain (Moncayo, 2012a) and medullary (Balucani and Barlinn, 2012) haemorrhages are not presented due to their rarity. Moreover, variations in the herein presented symptomatology patterns do exist.

Table A.3: Clinical grading scale for intracerebral haemorrhage: determination and prognostic interpretation according to Hemphill *et al*. (2001).

Component of the clinical grading scale	**Component's specifics**	**Points**
Glasgow Coma Scale (GCS) score (on initial presentation)	3-4	2
	5-12	1
	13-15	0
volume of the haematoma (on initial CT scan)	≥ 30 cm^3	1
	< 30 cm^3	0
presence of intraventricular haemorrhage	yes	1
	no	0
infratentorial origin of intracerebral haemorrhage	yes	1
	no	0
patient's age	≥ 80 years	1
	< 80 years	0
Prognostic parameter	**Mortality** (30-day)	**Score**
30-day mortality as assessed by Hemphill *et al*. (2001)	0%	0
	13%	1
	26%	2
	72%	3
	97%	4
	100%	5
	not determined (100%)	6

Note: the review article by Hwang *et al*. (2010) provides a critical overview of the clinical grading scales developed based on the "ICH score" of Hemphill *et al*. (2001), and those developed independently of it since then. In some of these scales, the presence of intraventricular haemorrhage is determined according to the Graeb scale (Godoy *et al.*, 2006), while in others the GCS score is replaced by the ischaemic stroke-relevant National Institute of Health Stroke Scale (NIHSS), with or without a consideration of the NIHSS level of consciousness (Cheung and Zou, 2003; Weimar *et al.*, 2006). Although a thorough description of these clinical grading scales is not within the scope of this PhD Thesis, it might be useful to note that, amongst the components of some scales, one can spot parameters such as "temperature", "glucose levels", "dialysis dependency", and others (Cheung and Zou, 2003; Chuang *et al.*, 2009), as well as the adoption of a variation of the Hemphill *et al*. (2001) component specifics (Cho *et al.*, 2008; Godoy *et al.*, 2006; Rost *et al.*, 2008; Ruiz-Sandoval *et al.*, 2007). This plethora of clinical grading scales has arisen from the understanding that the different types of intracerebral haemorrhage require distinct methods of assessment, could be subject to type-specific management approaches, and bear different prognosis.

CT: computed tomography; ICH: intracerebral haemorrhage (abbreviation not in use throughout the Thesis)

Table A.4: Overview of the indications, advantages and limitations of the surgical approaches to the treatment of intracerebral haemorrhage.

Surgical approaches and their main characteristics (indication; advantage; limitation)
MAIN approaches
– decompressive craniotomy or craniectomy followed by open surgery
– *indication:* approach of choice for emergent decompression and non-deep-seated haematomas
– *advantage:* better access to the haematoma; allows for intraoperative (and post-operative, when craniectomy is applied) cerebral decompression from the oedema; well-documented procedure
– *limitation:* demands large craniotomy and corticectomy in order to gain access to the haematoma; could end with removed craniotomy bone flap (craniectomy); extensive surgical trauma; not beneficial for patients who do not require emergent life-saving decompression
– stereotactic aspiration combined with local thrombolysis
– *indication:* suitable for the evacuation of large deep-seated haematomas
– *advantage:* minimally-invasive approach; promising results from its application
– *limitation:* demands small craniotomy
– endoscopic aspiration
– *indication:* suitable for the evacuation of large deep-seated haematomas
– *advantage:* minimally-invasive approach
– *limitation:* limited data on the technique; not as widely-employed as the stereotactic aspiration; demands small craniotomy
OTHER approaches
– ventricular drainage
– *indication:* ventricular external drainage for cases of intracerebral haemorrhage with hydrocephalus and intraventricular bleeding
– *advantage:* efficient management of high ICP
– *limitation:* still an invasive procedure with potential complications

Note: the current overview is based on data from Dey *et al*. (2012), Ferro (2006), Fiorella *et al*. (2015), Mendelow (2010), and Wang and Talkad (2009).

ICP: intracranial pressure

Table A.5: Overview of the most frequently-employed medical (non-surgical; pharmacological; conservative) approaches to the treatment of intracerebral haemorrhage.

Non-surgical approaches
– patient's stabilization in terms of adequacy of airway, breathing and circulation
– management of hypertension
– non-surgical management of increased ICP
– stop / reversal of any oral anticoagulant therapy (if patient was receiving such)
– inactivation of heparin (if patient was receiving such)
– coverage against previous antiplatelet medication (if patient was receiving such)
– efficient glycaemic control
– venous thrombosis prophylaxis
– nutrition
– temperature control
– management of seizures and / or prophylactic anticonvulsant therapy
– corticosteroids' administration (under debate)
– administration of other neuroprotective agents
– management of complications

Note: for more details, see subchapter I.6.

ICP: intracranial pressure

Table A.6: Major experimental techniques employed toward the *in vivo* simulation of intracerebral haemorrhage.

Experimental techniques and representative references
– autologous blood injection – Belayev *et al.*, 2003; Bimpis *et al.*, 2012; Bullock *et al.*, 1984; 1988; Deinsberger *et al.*, 1996; Kaufman *et al.*, 1985; Koeppen *et al.*, 1995; Krafft *et al.*, 2012b; Küker *et al.*, 2000; Lee *et al.*, 1999; Liu *et al.*, 2015; Marinkovic *et al.*, 2014; Nakamura *et al.*, 2004b; Qureshi *et al.*, 1999; 2001a; Ropper and Zervas, 1982; Rynkowski *et al.*, 2008; Wagner *et al.*, 1996; Yang *et al.*, 1994; Zhou *et al.*, 2014
– bacterial collagenase injection – Choudhri *et al.*, 1997; Clark *et al.*, 1998; Krafft *et al.*, 2012b; Mun-Bryce *et al.*, 2001; Rosenberg *et al.*, 1990
– microballoon insertion technique – Lopez Valdes *et al.*, 2000; Shi *et al.*, 2010; Sinar *et al.*, 1987; Takasugi *et al.*, 1985
– cerebral blood vessel avulsion – Funnell *et al.*, 1990; Xue and Del Bigio, 2003
– hypertensive background / stroke-prone animals – Iida *et al.*, 2005; Okamoto *et al.*, 1975; Randell and Daneshtalab, 2016; Wu *et al.*, 2011
– other techniques and backgrounds – Christie *et al.*, 2001; Fryer *et al.*, 2003; Herzig *et al.*, 2004; Hook *et al.*, 1962; Johnson and Narayan, 1974; Jung *et al.*, 2016

Note: the herein presented references are representative of the most frequently employed experimental techniques toward the *in vivo* simulation of intracerebral haemorrhage; an effort has been made in order to cite modified methods and / or techniques on different animal species. The Takasugi *et al.* (1985) technique is a modified version of the microballoon insertion technique that could also fall under the "autologous blood injection" technique category.

Table A.7: Selection of compounds suggested to exert neuroprotection against intracerebral haemorrhage, based on experimental data.

Compound	Characteristics
DFO	iron chelator; restricts oedema formation; antioxidant; increases HIF-1α
minocycline	microglia deactivator; iron chelator; reduces TNF-α and MMP-12
atorvastatin	statin; enhances cell-survival; blocks neuronal apoptosis; decreases MMP-9
simvastatin	statin; enhances cell-survival; protects BBB integrity
celecoxib	COX-2 inhibitor; anti-inflammatory; restricts oedema formation
rosiglitazone	PPAR-γ agonist; downregulates MMP-9 expression
CDP-Ch	cell membrane stabilizer; antioxidant; improves neuronal survival
MK-801	NMDA receptor antagonist
U-74389G	lazaroid; antioxidant

Note: for more details, see subchapter I.11 and Figure A.5.

BBB: blood-brain barrier; CDP-Ch: cytidine-5'-diphosphocholine; COX-2: cyclooxygenase 2; DFO: deferoxamine; HIF-1α: hypoxia inducible factor 1 alpha; MMP-9: matrix metalloproteinase 9; MMP-12: matrix metalloproteinase 12; NMDA: *N*-methyl-D-aspartate; PPAR-γ: peroxisome proliferator-activated receptor gamma; TNF-α: tumour necrosis factor alpha

Table A.8: Research priorities toward an effective treatment of intracerebral haemorrhage.

1. Adoption of rigorous methodological practices in *in vitro* and *in vivo* preclinical research
2. Better representation of comorbidities and of clinical variability within the experimental simulation approaches employed
3. Effectiveness of potential treatment approaches should be studied under a number of injury-related levels, over a number of *in vitro* and *in vivo* approaches
4. Adoption of more behavioural batteries / endpoints within the assessment protocols of *in vivo* experimental approaches to intracerebral haemorrhage
5. Adoption of the benefits of enhanced image technologies for live (*in vivo*) brain imaging
6. Development of more sophisticated *in vitro* simulation approaches
7. More transparent reporting of experimental failures; need for the encouragement of negative data to be published
8. Establishment of academic networks with a focus on the improvement of translational intracerebral haemorrhage research

Note: these priorities refer to the experimental research on intracerebral haemorrhage.

Figure A.1: Basic presentation of the phases of intracerebral haemorrhage development.

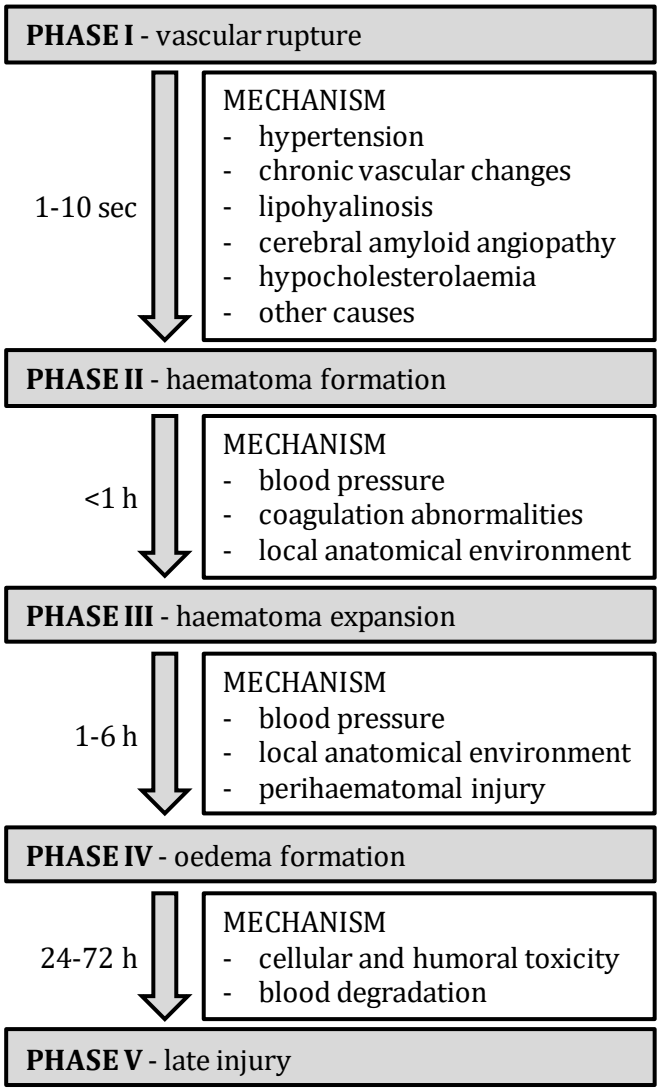

Note: this is a modified and enriched version of the pathophysiological phases of intracerebral haemorrhage development proposed by Rincon and Mayer (2004); phase V was not originally suggested, and neither were some of the presented pathophysiological mechanisms. For more details, see subchapter I.8.

Figure A.2: Neuropathological processes associated with the lysis of the haematoma's erythrocytes in intracerebral haemorrhage: a simplified schematic overview.

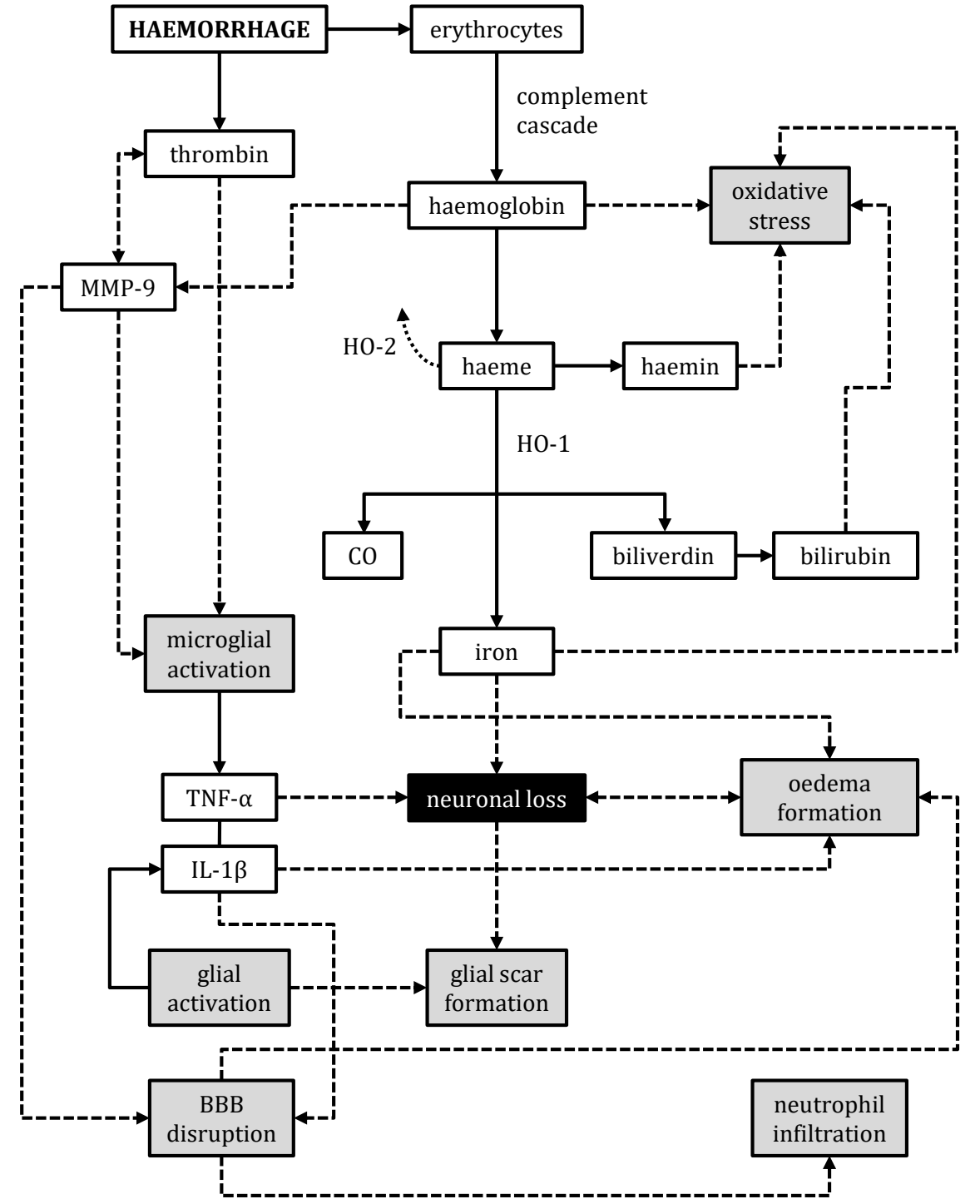

Note: for more details, see subchapter I.8.

BBB: blood-brain barrier; CO: carbon monoxide; HO-1: haeme oxygenase 1; HO-2: haeme oxygenase 2; IL-1β: interleukin 1 beta; MMP-9: matrix metalloproteinase 9; TNF-α: tumour necrosis factor alpha

Figure A.3: Schematic summary of the mechanistic pathways leading to neuronal loss in intracerebral haemorrhage.

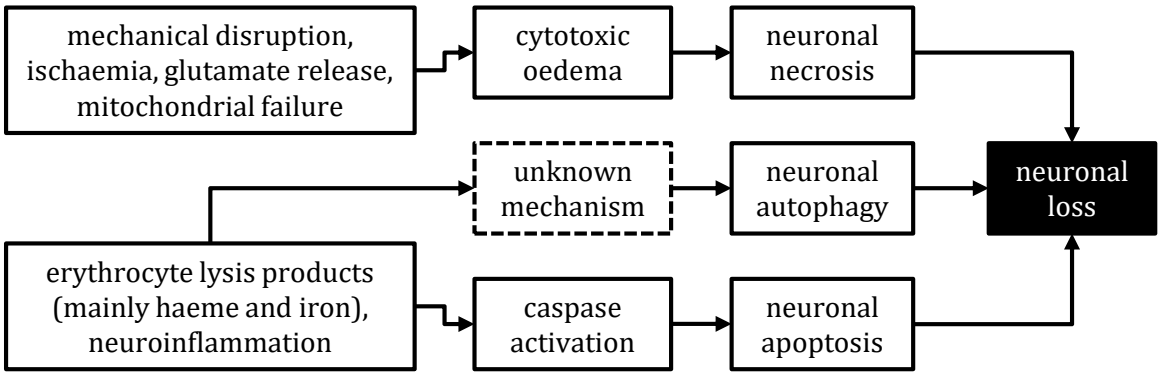

Note: apoptosis is a prominent mode of neuronal loss in intracerebral haemorrhage (Qureshi *et al.*, 2003b). The role of autophagy in intracerebral haemorrhage remains elusive; the majority of the findings with regards to its implication in neuronal loss are a result of very recent *in vivo* and *in vitro* experimental studies (He *et al.*, 2008a; 2008b; Hu *et al.*, 2011; Shen *et al.*, 2016).

Figure A.4: Simplified schematic overview of the role of microglia / macrophages and activated astrocytes in the neuropathology of intracerebral haemorrhage.

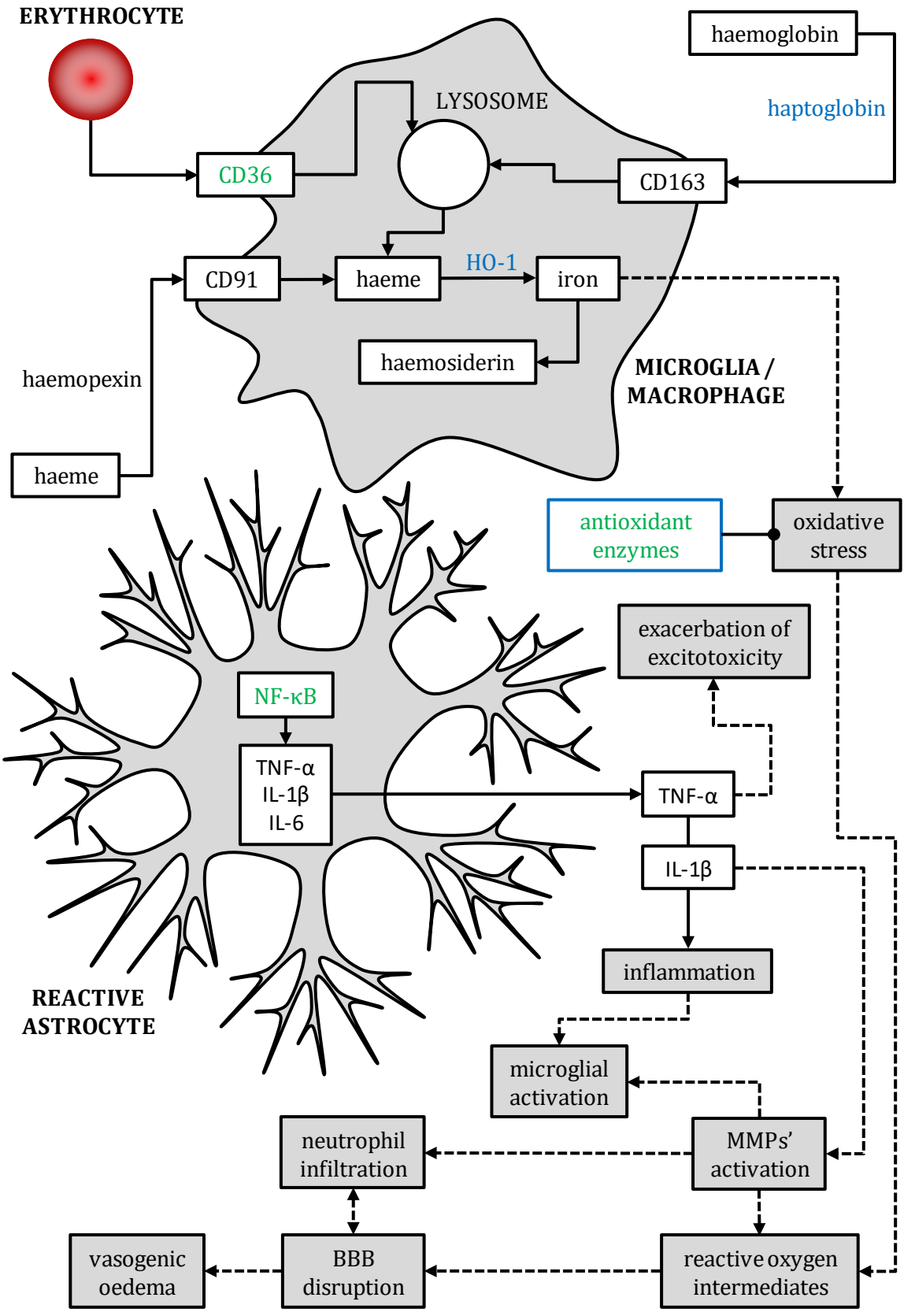

Note: the expression of elements / proteins highlighted in green font is regulated by PPAR-γ, while the expression of elements / proteins highlighted in blue font / boxes is regulated by Nrf2. For more details, see subchapter I.8.

BBB: blood-brain barrier; HO-1: haeme oxygenase 1; IL-1β: interleukin 1 beta; IL-6: interleukin 6; MMPs: matrix metalloproteinases; NF-κB: nuclear factor kappa B (kappa-light-chain-enhancer of activated B cells); Nrf2: nuclear factor (erythroid-derived 2)-like 2; PPAR-γ: peroxisome proliferator-activated receptor gamma; TNF-α: tumour necrosis factor alpha

Figure A.5: Chemical structures of selected compounds that have been suggested to exert neuroprotection against intracerebral haemorrhage, based on experimental data.

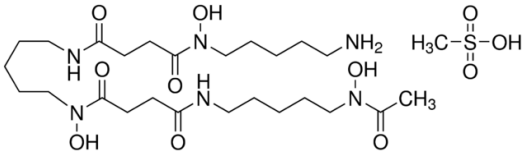

DFO (mesylate)

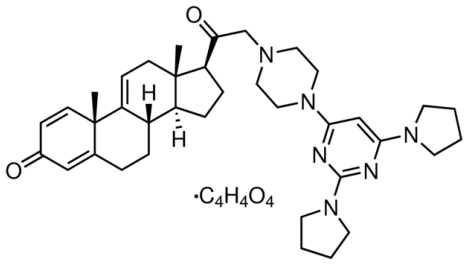

U-74389G

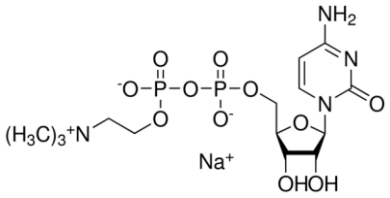

CDP-Ch (sodium salt)

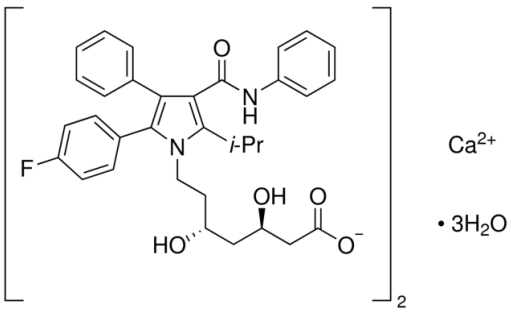

atorvastatin (calcium salt trihydrate)

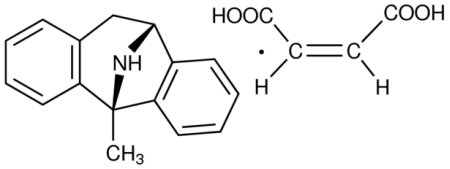

(+)-MK-801 (hydrogen maleate)

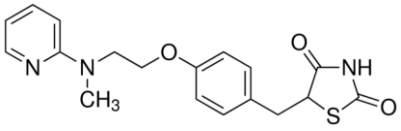

rosiglitazone

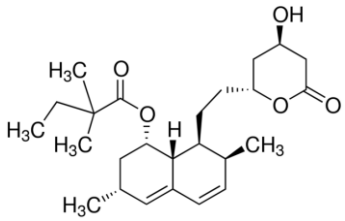

simvastatin

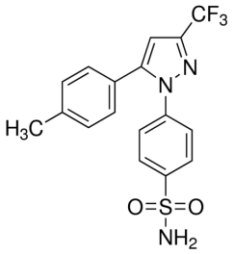

celecoxib

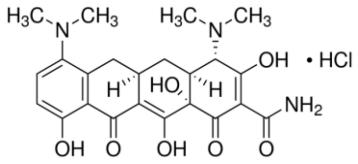

minocycline (hydrochloride)

Note: for more details, see subchapter I.11 and Table A.7.

CDP-Ch: cytidine-5'-diphosphocholine; DFO: deferoxamine

CHAPTER II

Overview of *in vitro* simulation approaches to intracerebral haemorrhage

The *in vitro* simulation of intracerebral haemorrhage has not been as popular as the *in vitro* simulation of ischaemic stroke; a main reason for this should be attributed to the comparatively more complex neuropathology of the first. This chapter provides an overview of the *in vitro* simulation approaches to intracerebral haemorrhage reported in the literature, with a focus on: (a) the "cellular substrates" commonly used for the development of such[1], (b) the specific pathology-simulating *in vitro* conditions chosen, and (c) common assessment parameters (markers) of *in vitro* injury and / or responsiveness to treatment. This overview is not exhaustive, but is certainly representative of the current practice / options in the field.

II.1. Simulation of intracerebral haemorrhage under *in vitro* conditions

The choice of a suitable "cellular substrate" for the *in vitro* simulation of intracerebral haemorrhage is not a specific feature of this neuropathological entity, as - in most cases - it mimics the choices offered for a wide variety of other entities, primarily for ischaemic stroke. The use of brain slices (Khama-Murad *et al.*, 2008) for such *in vitro* simulation approaches seems a reasonable option, and such slices could be of murine origin (Lakovic *et al.*, 2014) or could refer to rat cortical brain (Ciuffi *et al.*, 1996; Lee *et al.*, 1997) or olfactory cortex slices (Khama-Murad *et al.*, 2009). In fact, in a series of rarely-encountered experiments that do feature an intracerebral haemorrhage-specific logic in their choice of "cellular substrates", brain slices (Khama-Murad, 2011b) and olfactory cortex slices of spontaneously hypertensive rats (Khama-Murad, 2009; 2011a; 2011c; Khama-Murad *et al.*, 2011; Mokrushin and Pavlinova, 2012; 2013; Mokrushin *et al.*, 2008) were used. It is without doubt that brain slices introduce the highest possible neuroanatomical simulation of the complexity of an *in vivo* situation (Cho *et al.*, 2007; Humpel, 2015); an advantage that is, however, overshadowed by: (a) the need for

[1] *in vitro* approaches aiming to simulate only the ischaemic element of stroke (Woodruff *et al.*, 2011) are not included in this chapter, and neither are *in vitro* approaches using clots (see, for example, Wagner *et al.*, 2000) or brain microvascular endothelial cells (see a thorough review by Camós and Mallolas, 2010) as "substrates"; as an exception to his, the study of Neuhaus *et al.* (2014) will be discussed due to its relevance to the haemorrhagic transformation aspect of ischaemic stroke.

a significant number of experimental animals to be sacrificed for their obtaining, (b) their demanding technical handling, and (c) their genetic background variation (that, in some cases, could introduce reproducibility issues). A similar, technically-demanding option is the use of primary cortical neurons of embryonic murine (Chang *et al.*, 2011; Shen *et al.*, 2016) or rat (Bao *et al.*, 2015; Kwon *et al.*, 2013) origin or of mixed cortical cell cultures from, say, embryonic day 14 to 16 (E14-E16) mice (Chen-Roetling *et al.*, 2008; 2011; Regan and Panter, 1993); these cell populations could be handled in a more flexible manner than brain slices, but their systematic use is still demanding in terms of animal sacrifices, and the cells themselves are characterized by neurodevelopmental (dynamic) features and frequently give rise to reproducibility issues. An example of the flexible handling of such primary cell cultures is showcased by Schlichter *et al.* (2010), who in order to study an aspect of microglia-induced neurotoxicity within the context of intracerebral haemorrhage-simulation, have isolated microglia from 1 or 2-day-old rats as well as mixed cortical cell cultures from embryonic day 18 (E18) rat embryos, have grew them separately, and then have co-cultured them in a Transwell™ system that allowed chemical communication between the two cell populations.

Particular mention should be made to the project report of Patel (2015) of the Syracuse University: the project aimed at examining the roles of microglia in the context of an *in vitro* simulation approach to the use of intracerebral haemorrhage. Patel (2015) has used co-cultures of microglia, astrocytes, and granule neurons, prepared from neonatal rat cerebellar cortex, and grown in standard medium containing foetal bovine serum (FBS) or a serum-free chemically defined medium. Patel (2015) used the aforementioned co-cultures (grown for 7 to 8 days *in vitro*) that were challenged with two different concentrations of haemin (20 and 100 μM), supposedly *"corresponding to a mild versus a severe brain bleed"*.

The use of the rat pheochromocytoma PC12 cells (Levy *et al.*, 2002; Ni *et al.*, 2016; Sun *et al.*, 2013) has recently been an option for the development of an *in vitro* simulation approach to neuropathological aspects of intracerebral haemorrhage[2]; the adoption of such "immortal" cell-lines as "cellular substrates" restricts the cellular representation of the nervous system in the developed *in vitro* simulation approaches, but also restricts the possibility of the occurrence of reproducibility issues. Such lines are easy to maintain, and can provide ideal bases for high-throughput applications. Other cell-lines of this nature that have been used as "cellular substrates" towards the *in vitro* simulation of intracerebral haemorrhage include the C6 glioma cells (Lee *et al.*, 1997; Morita *et al.*, 2009), the widely-used SH-SY5Y cells (Hahl *et al.*, 2013; Levy *et al.*, 2002), the human neuroblastoma cell-line SK-N-MC (Chang

[2] of particular interest is the "prognostic" experimental set-up suggested by Ballesteros *et al*. (2007), where PC12 cells (differentiated into neurons) are incubated with 10% of heat-inactivated patient's sera, and their apoptotic rate is determined by flow cytometry.

et al., 2011) as well as the U937 human monocytoid cells[3] (Power *et al.*, 2003). Very recently, a BBB-mimicking cellular transwell arrangement using the murine cell-line cerebEND[4] as well as the rat glioma cell-line C6 has also been used (Neuhaus *et al.*, 2014).

II.2. Selection of the *in vitro* conditions simulating intracerebral haemorrhage

The conditions applied on the "cellular substrates" toward the *in vitro* simulation of intracerebral haemorrhage, have been primarily aiming to simulate the so-called "late" injury[5] (Figure A.1; phase V). These conditions primarily involve the exposure of the more complex "cellular substrates" (such as brain slices) to autologous blood (Khama-Murad, 2009; 2011a; 2011b; 2011c; Khama-Murad *et al.*, 2008; 2009; 2011; Mokrushin and Pavlinova, 2012; 2013; Mokrushin *et al.*, 2008), and the exposure of the less complex ones (such as primary cultures and other of the aforementioned cell-lines) to erythrocyte-degradation elements such as haemoglobin (usually 3 or 10 μM in serum-free media; rarely higher concentrations)[6] (Chen-Roetling *et al.*, 2008; 2011; Levy *et al.*, 2002; Regan and Panter, 1993), haemin (in various concentrations ranging from 5 to 100 μM) (Chang *et al.*, 2011; Kwon *et al.*, 2013; Levy *et al.*, 2002; Morita *et al.*, 2009; Ni *et al.*, 2016; Patel, 2015; Shen *et al.*, 2016; Sun *et al.*, 2013) and bilirubin (100 or 500 μM) (Lakovic *et al.*, 2014). In some cases, the exposure to the haemorrhage-deriving thrombin (Bao *et al.*, 2015; Lee *et al.*, 1997; Power *et al.*, 2003) has been employed, while Hahl *et al.* (2013) have exposed their SH-SY5Y cells to haeme-haemopexin complexes (15 and 25 μM). Rare but notable are the cases of Schlichter *et al.* (2010) that stimulated their microglia with lipopolysaccharide (LPS; for 24 h)[7] prior to exerting their neurotoxic effects on mixed cortical cultures in their Transwell™ system, and of Neuhaus *et al.* (2014) that have employed the standard oxygen / glucose deprivation (OGD)[8] conditions in their aforementioned BBB-mimicking approach; both groups have chosen to develop *in vitro* approaches that aim at simulating earlier phases of the intracerebral haemorrhage neuropathology.

---

[3] the U937 cell-line is a neoplastic, histiocytic cell-line (Sundström and Nilsson, 1976), that upon stimulation, can adopt the morphology and characteristics of mature macrophages (Sharp, 2013).

[4] the cerebEND cell-line is produced from isolated brain endothelial cells of the cerebellum of neonatal 129Sv mice (Silwedel and Förster, 2006).

[5] the *in vitro* simulation approaches to intracerebral haemorrhage through the employment of conditions based solely on the exposure to ferrous iron are few (Cui *et al.*, 2016; He *et al.*, 2008a; Levy *et al.*, 2002), and are not discussed herein.

[6] haemoglobin (10^{-9} to 10^{-5} M) has also been used on rat cortical brain slices (Ciuffi *et al.*, 1996).

[7] a similar approach has been adopted by Cai *et al*. (2011) on microglia, prior to exposure to haemin.

[8] the OGD technique is widely used as an *in vitro* simulation approach to ischaemic cerebral stroke; in this technique, cells or tissue cultures are incubated in a glucose-free medium under a deoxygenated atmosphere (e.g. in a hypoxic chamber) (Singh *et al.*, 2009; Tasca *et al.*, 2015). A variation of this technique is the OGD-reoxygenation technique (see, for example, Alluri *et al.*, 2015). Alternatively, hypoxia can also be induced chemically, by treatment with cyanide (either as sodium cyanide or potassium cyanide; NaCN or KCN) (Woodruff *et al.*, 2011).

II.3. Markers of *in vitro* injury associated with intracerebral haemorrhage

Similarly to the conditions chosen for the *in vitro* simulation of intracerebral haemorrhage, their assessment parameters (markers of injury) are also chosen based, largely, on their "cellular substrates"; brain slices exposed to intracerebral haemorrhage-simulating conditions are ideal for the undertaking of electrophysiological studies (Khama-Murad, 2009; 2011a; 2011b; 2011c; Khama-Murad *et al.*, 2008; 2011; Lakovic *et al.*, 2014; Mokrushin and Pavlinova, 2012; 2013; Mokrushin *et al.*, 2008), the assessment of swelling (oedema) *via* weighting the slices on a torsion balance (Khama-Murad, 2011a; 2011c) and the assessment of vasoreactivity (by monitoring microvessel diameter with videomicroscopy) (Lee *et al.*, 1997). In terms of morphometry, the employment of basic phase-contract microscopy (Chen-Roetling *et al.*, 2011; Regan and Panter, 1993) as well as the assessment of the neuraxonal density and mitochondrial appearance through transmission electron microscopy (Lakovic *et al.*, 2014) can offer critical information on cell type-specific cellular responses within these systems. Equally useful has been the performance of iron staining (Chen-Roetling *et al.*, 2011; Patel, 2015).

Two major and frequently-encountered assays used for the assessment of *in vitro* simulation approaches to intracerebral haemorrhage are, as in the case of most *in vitro* simulation approaches to any entity of neuropathological interest, the lactate dehydrogenase (LDH) release assay (Bao *et al.*, 2015; Chen-Roetling *et al.*, 2008; 2011; Lee *et al.*, 1997; Ni *et al.*, 2016; Patel, 2015; Regan and Panter, 1993)[9] and the 3-(4,5-dimethylthiazol-2-yl)-2,5-diphenyltetrazolium bromide (MTT) reduction assay (Chang *et al.*, 2011; Kwon *et al.*, 2013)[10]. Other "cell viability" assays have also been employed (Levy *et al.*, 2002; Schlichter *et al.*, 2010), and so have been the neutral red uptake assay (Morita *et al.*, 2009)[11], the fluorescent staining of live / dead cells (Patel, 2015; Shen *et al.*, 2016), the measurement of the intracellular levels of ROS (Kwon *et al.*, 2013) as well as assays for the assessment of phagocytosis (Chen-Roetling *et al.*, 2011; Patel, 2015) and the activity of caspase (Schlichter *et al.*, 2010) or HO (Chen-Roetling *et al.*, 2008; Kwon *et al.*, 2013).

---

[9] the LDH release assay is often presented as a "cell death" assay (see, for example, Patel, 2015); this misinterpretation can be a basis of drawing unjustified conclusions by both authors and readers. The LDH release assays are colorimetric assays that quantitatively measure the activity of the LDH released into the cell culture media, through a coupled enzymatic reaction. Moreover, LDH is a cytosolic enzyme that can act as an indicator of cellular toxicity or cell membrane lysis or membrane injury, under a number of conditions, such as the assumption that the different contents of the media do not affect the cytosolic LDH levels, the LDH to formazan conversion reactions (either by binding to the substrates or the enzymes involved) or the actual colorimetric measurement. To my opinion, on its own, the *in vitro* LDH release assay should only be considered as an indicator of membrane injury.

[10] the MTT reduction assay is widely-known as the "cell viability" assay that, actually, is a tetrazolium reduction assay; the MTT tetrazolium dye is reduced by NAD(P)H-dependent cellular oxidoreductases to insoluble formazan; a reaction presumably considered to be proportional to the number of viable cells.

[11] for more details, see Repetto *et al*. (2008).

Of particular interest are the molecular targets aimed within such *in vitro* simulation approaches, either through immunocytochemistry, Western blotting, reverse transcriptase polymerase chain reaction (RT-PCR) or other techniques: HO-1, HO-2, ferritin, TfR1, neuronal nuclei antigen (NeuN), microtubule-associated protein 2 (MAP2), caspase-3, caspase-9, Bcl-2, LC3, beclin-1, p62, TNF-α, NF-κB, COX-2, iNOS, MMPs and others (Bao *et al.*, 2015; Chang *et al.*, 2011; Chen-Roetling *et al.*, 2011; Ciuffi *et al.*, 1996; Hahl *et al.*, 2013; Kwon et al., 2013; Levy *et al.*, 2002; Morita *et al.*, 2009; Neuhaus *et al.*, 2014; Patel, 2015; Power *et al.*, 2003; Schlichter *et al.*, 2010; Shen *et al.*, 2016; Sun *et al.*, 2013). Table A.9 provides a synopsis of the above.

II.4. Challenges of the *in vitro* simulation of intracerebral haemorrhage

The challenges presented in the development of an *in vitro* simulation approach to intracerebral haemorrhage have primarily to do with the complexity that the disease represents; it is, thus, impossible to reliably and holistically simulate a disease, the pathophysiology of which we can only partially understand. One must consider that the development of such an *in vitro* approach should: (a) identify and attempt to simulate critical aspects of the disease's pathophysiology (preferably, aspects that appear to be promising for the development of potential therapeutic interventions), (b) be suitable for use in high-throughput contexts, and (c) serve the 3R principles. In the case of intracerebral haemorrhage, one can clearly realize that an unmet challenge of the aforementioned approaches has been the development of an *in vitro* experimental protocol that would simulate the natural history of the disease: e.g. that of the continuity between the mechanic / ischaemic phenomena occurring in the perihaematomal region (Figure A.1; phases III and IV) and the blood degradation (Figure A.1; phase V).

A less obvious, but equally critical challenge is the adoption of appropriate assessment criteria: what are the "markers" that will assess the success of the developed *in vitro* simulation approach to intracerebral haemorrhage? How relevant are they be to the simulated neuropathology or the "cellular substrate" itself? Will one be able to develop the assessment of these "markers" into a high-throughput assay?

II.5. Aims of the current PhD Thesis

The aim of this PhD Thesis was to provide a small contribution to the development and assessment of novel experimental approaches to intracerebral haemorrhage at the preclinical (*in vitro*) level that would: (a) allow for a more reliable simulation of the disease (or, more realistically, of important aspects of the disease's neuropathology), (b) serve the 3R principles, and (c) provide the substrate for high-throughput drug-screening applications. In order to achieve this, we hypothesized that the use of immortalized cell-lines that maintains func-

tional properties and phenotypes of crucial central nervous system cell populations could provide a more consistent, realistic and low-cost way to simulate a complex disease such as intracerebral haemorrhage, *in vitro*. We have also considered that the set-up of such *in vitro* approaches should particularly aim in simulating aspects of the secondary injury associated with the cytotoxicity produced by haematoma degradation, not as a stand-alone context, but as a continuity to a hypoxic preconditioning, and - if possible - in parallel to the latter.

As expected, the implementation of novel immortalized cell-lines requires a systematic study of their neuropathological and neurochemical responses to such *in vitro* conditions. Whilst designing this project, our anticipation was that: (a) these responses would bear neuropathological similarities to the ones observed in clinical practice or following *in vivo* experiments, and (b) the development of reliable and consistent *in vitro* approaches to intracerebral haemorrhage would be a significant contribution to the field and might be able to act as "models" for pre-clinical drug screening as well as for the undertaking of further pathophysiological research.

Parts B and C of this PhD Thesis describe the procedure followed toward the materialization of these aims; they provide the details of our hypotheses, our experimental efforts and our findings. Part D of this PhD Thesis provides a critical appraisal of this contribution.

>> Table A.9: page 65

Table A.9: Assessment parameters (markers) used within the *in vitro* context of intracerebral haemorrhage simulation, in order to study the induced cellular injury and / or the potential neuroprotective effects of drugs.

***In vitro* assessment parameters (markers) of injury and / or neuroprotection**
CYTOMORPHOLOGICAL markers
– undertaking of phase-contrast microscopy
– assessment of neuraxonal density (transmission electron microscopy)
– assessment of mitochondrial appearance (transmission electron microscopy)
– assessment of vasoreactivity (videomicroscopy; applied for studies on brain tissue slices)
NON-SPECIFIC CELL VIABILITY, INJURY AND METABOLISM markers
– performance of the LDH release assay
– performance of the MTT reduction assay
– performance of the neutral red uptake assay
– undertaking of fluorescent staining of live / dead cells
– measurement of the intracellular levels of ROS
– performance of other "cell viability" assays
NEUROBIOLOGICAL markers
– assessment of HO activity and of haemotoxicity-induced markers' expression
– assessment of the expression of neuronal markers
– assessment of caspase activity and of cell death-related markers' expression
– assessment of the expression of inflammation-related markers
– assessment of the expression of other markers
OTHER parameters / markers
– undertaking of electrophysiological studies
– assessment of swelling (oedema) *via* weighting (applied for studies on brain tissue slices)
– assessment of phagocytosis

Note: this overview is not an indirect suggestion of other parameters that could have been assessed; it just organizes the markers discussed within the text of Chapter II, and is neither exhaustive nor useful for any further interpretation, other than to provide the reader with the general framework in which the *in vitro* simulation attempts to intracerebral haemorrhage have been undertaken so far.

HO: haeme oxygenase; LDH: lactate dehydrogenase; MTT: 3-(4,5-dimethylthiazol-2-yl)-2,5-diphenyltetrazolium bromide; ROS: reactive oxygen species

PART B

Characterization of the embryonic murine hippocampal cell line mHippoE-14

CHAPTER III

The commercially-available embryonic hippocampal cell-line mHippoE-14

In order to address the need for the development of novel *in vitro* simulation approaches to intracerebral haemorrhage, we decided to use the commercially-available immortalized embryonic murine hippocampal cell-line mHippoE-14 (catalogue number: CLU198; CELLutions Biosystems Inc., Ontario, Canada) on the promise that they are *"easy to culture, have efficient transfection rates and have robust gene and protein expression"*, as well as that they *"enable accurate in vitro assays for use in the discovery, development and validation of new therapeutics targeted to central nervous system diseases and disorders, including obesity, stress, reproduction and metabolic disorders, amongst others"*. The mHippoE-14 cell-line is part of a group of 4 commercially-available embryonic murine hippocampal cell-lines developed by the same research group (Gingerich *et al*., 2010), each of which seems to bear a distinct phenotype and gene expression profile. However, all 4 cell-lines are reported to exhibit neuronal cytomorphologies and neuronal markers' expression (Gingerich *et al*., 2010); a major advantage of the specific cell-lines over other commercially-available ones (see Chapter II). A brief account of the methodology followed for the generation of the mHippoE-14 and the other 3 associated immortalized cell-lines will be provided in the next few pages, along with an overview of the data referring to their characterization attempts. This account is also necessary for the justification of the selection of the specific cell-line over the others.

III.1. Development of the mHippoE-14 and associated cell-lines

The development of the mHippoE series of cell-lines served both the need for distinct immortalized neuronal cell-lines as *in vitro* "models"[1] for the simulation and study of hippocampal cell function (Gingerich *et al.*, 2010), as well as the fact that non-transformed primary hippocampal cell-lines are heterogeneous, difficult to maintain and, by nature, cytologically- and genetically-inconsistent. There have been reports of a few immortalized hippocampal (and

[1] with very few exceptions, I tend not to adopt the use of the word "model" in this PhD Thesis, as its careless use in the literature over the last decades has rendered it meaningless; Part D of this current Thesis provides a number of further reasons for this choice.

hippocampal-like) cell-lines in the literature (Davis and Maher, 1994; Eves *et al.*, 1992; Hoshimaru *et al.*, 1996; Lee *et al.*, 1990; Morimoto and Koshland, 1990a; 1990b; Renfranz *et al.*, 1991; Whittemore *et al.*, 1991), all prior to the development of those of the mHippoE series (Table B.1). Most of these cell-lines have not been well-characterized over the last 20 years, and those who have been more widely used / studied (H19-7, HiB5, HT-22) are barely representative of the hippocampal neuronal heterogeneity.

Gingerich *et al.* (2010) generated the cell-lines of the mHippoE series by following the same methodology to that used for the generation of immortalized embryonic murine hypothalamic cell-lines (Belsham *et al.*, 2004). The methodology is synopsized in Figure B.1 and consists of the following 6 steps: (a) the use of pregnant Swiss Webster mice (anaesthetized on E18)[2] as a source of foetal hippocampi, (b) the appropriate handling / processing of the foetal hippocampi and their plating (as cell suspensions) in culture dishes coated with poly-L-lysine and incubated for 7 days (37°C, 5% carbon dioxide; CO_2) with primary culture medium consisting of Dulbecco's modified Eagle's medium (DMEM) containing 10% heat-inactivated FBS, 10% heat-inactivated horse serum, 1% penicillin - streptomycin and 20 mM D-glucose, (c) the transfection[3] (48 h) of the cell cultures with a recombinant murine retrovirus harbouring simian virus (SV40) T-antigen and the neomycin resistance gene from the pZIPNeo SV(X) 1 vector, (d) the treatment of the cells with geneticin[4] (G418; 400 μg/mL every 3 days for 2 weeks, followed by 250 μg/mL for further 2-3 weeks), (e) the selective expansion[5] of the resistant cell colonies (through the use of cloning cylinders), and (f) the subcloning of the mixed populations of the embryonic hippocampal cells through successive dilutions into 96-well plates (coated with poly-L-lysine) where optimal dilution allowed for 1-2 cells per well (ratio 1:1 of conditioned medium and fresh DMEM with 15% FBS), prior to their growth and cryopreservation. As a result of this approach, Gingerich *et al.* (2010) isolated and characterized 4 clonal cell-lines: mHippoE-2, mHippoE-5, mHippoE-14[6] and mHippoE-18.

---

[2] neurogenesis is peaking in the murine hippocampal CA1 and CA2 regions on E15 (Finlay and Darlington, 1995), a phenomenon that extends into early postnatal life.

[3] it is worth noticing that the immortalization process is believed to arrest the transfected cells at the respective specific developmental stage, and to prevent them from differentiating any further (Ryder *et al.*, 1990); the immortalizing of embryonic hippocampal cells should, at least to an extent, arrest several functional properties expected to accompany the dynamic processes characterizing hippocampal neurogenesis.

[4] geneticin is a neomycin analogue that, once added to the medium, allows only for the successfully-transfected (immortalized) cells to survive (Lendahl and McKay, 1990).

[5] this is a step of great importance, as Gingerich *et al.* (2010) have undertaken this selective expansion based on whether the cells demonstrated a *"predominant neuronal morphology"*; although the authors do not provide more details on how exactly this morphology is assessed, their previous study (Belsham *et al.*, 2004) claims this selection step to be based on whether the cells demonstrate *"small, rounded, or ovoid perikarya and long neuritic processes"*.

[6] optimal (growth) cell-culture conditions for the mHippoE-14 cells are: DMEM (with 4500 mg/L glucose, L-glutamine and sodium bicarbonate, without sodium pyruvate, liquid, sterile-filtered, suitable for cell culture; Sigma product code: D5796) supplemented with 10% FBS and 1% penicillin - streptomycin; cells must be cultured in a humidified, 5% CO_2, 37°C incubator.

Upon development, Gingerich *et al*. (2010) have submitted the mHippoE cell-lines into a characterization through a well-selected RT-PCR screening (Table B.2), as well as through a number of experiments aiming to assess their responsiveness to glutamate-induced neurotoxicity and oestrogen-induced neuroprotection. However, Gingerich *et al*. (2010) have made no attempts in order to provide a cytomorphological characterization of theses cell-lines under either optimal (normal) or neurotoxic *in vitro* conditions. Figure B.2 provides some representative phase-contrast microscopy captions of the mHippoE-14 cells, as cultured in the Gardiner lab.

III.2. Characterization of the mHippoE-14 and associated cell-lines

Gingerich *et al*. (2010) have provided us with a semi-quantitative RT-PCR profiling of the 4 mHippoE cell-lines over a total of 19 markers (Table B.2). Of these, notable are GFAP (the absence of the expression of which indicates that none of the cell-lines are of astrocytic or ependymal nature), and the neuronal markers MAP2 and neuron specific enolase (NSE; whose levels of gene expression suggest a neuronal profile for the cell-lines in question). All mHippoE cell-lines seem to share a common profile with regards to a total of 10 of the studied markers, while the authors attribute the fact that the mHippoE-14 cells are negative for the spermiogenesis specific transcript on the Y 1 (SSTY1) mRNA to the belief that they originate from female embryos (Gingerich *et al.*, 2010).

Although far from being exhaustive, the RT-PCR profiling (Table B.2) as well as the experimental assessment of the mHippoE cell-lines performed by Gingerich *et al*. (2010) have provided us with a number of reasons on why the mHippoE-14 cell-line is the best choice for the development of novel *in vitro* simulation approaches to intracerebral haemorrhage. Apart from the fact that the mHippoE-14 cell-line seems to be an equivalently (to the rest of the mHippoE series cell-lines) potent expresser of major neuronal markers (MAP2 and NSE), the mHippoE-14 cells express the tropomyosin receptor kinase A (TrkA) mRNA stronger than the other cell-lines (Table B.2); TrkA is the high-affinity nerve growth factor (NGF) receptor and as such, a major regulator of neuronal differentiation and a major blocker of programmed cell death (Culmsee *et al.*, 2002; Marlin and Li, 2015). Moreover, mHippoE-14 seems to be the only cell-line of the mHippoE series expressing the tropomyosin receptor kinase B (TrkB)[7] mRNA; an important finding if one considers the importance of the TrkB / BDNF pathway as a regulator of neuronal growth (Gonzalez *et al.*, 2016) and the memory processes (Yamada and Nabeshima, 2003). The moderate expression of the glutamate receptor subtype 4 (GluR4) mRNA is another unique feature of the mHippoE-14 cell-line, that along with the

[7] TrkB is activated primarily by BDNF and neurotrophin-4, and to a lesser extent by neurotrophin-3 (Barbacid, 1994; Squinto *et al.*, 1991).

strongest expression of the growth hormone secretagogue receptor (GHSR) mRNA (the mRNA of the only molecularly identified receptor for ghrelin), classify this cell-line as an ideal representative of the hippocampal neuronal population. The latter is due to the fact that GluR4 is known to be highly-expressed in the hippocampus during neurodevelopment (Gomes *et al.*, 2007), while GHSR is recently reported to be enriched in the neurogenic niche of the hippocampal dentate gyrus (Hornsby *et al.*, 2016), as well as a mediator of a dopaminergic initiation of hippocampal synaptic plasticity through the dopamine receptor 1 (Kern *et al.*, 2015).

The conducted experiments on the responsiveness of the mHippoE cell-lines to glutamate-induced neurotoxicity and oestrogen-induced neuroprotection have also revealed that the mHippoE-14 did not differ from the mHippoE-18 in terms of susceptibility to glutamate-induced neurotoxicity (expressed as % viability and assessed *via* MTT assays), but required much higher levels of the tested oestrogen (17β-oestradiol) in order to exhibit a significant level of neuroprotection; a finding attributed to the fact that the mHippoE-14 express lower mRNA levels of the oestrogen receptor alpha (ERα) compared to that of the mHippoE-18 ones (Gingerich *et al.*, 2010). Finally, the mHippoE-14 cells were also shown to possess a unique neuron-like property: as a response to acute treatment with 20% FBS, they express c-Fos mRNA (Gingerich *et al.*, 2010), which is a response suggestive of neuronal activation (Bullitt, 1990).

To date, interestingly, it is only the mHippoE-18 cell-line that has been cited in the literature as a cellular substrate for the undertaking of *in vitro* nanoneurotoxicity assessments (Janaszewska *et al.*, 2013; 2015; Lazniewska *et al.*, 2013a; 2013b; Milowska *et al.*, 2014; 2015; Nawrotek *et al.*, 2016a; 2016b; Zarros *et al.*, 2015), and more recently as a cell-line of choice for the characterization of the endogenous G protein-coupled receptor 30 (GPR30) signalling (Evans *et al.*, 2016).

>> Table B.1: page 71
>> Table B.2: page 72
>> Figure B.1: page 73
>> Figure B.2: page 74

Table B.1: Immortalized hippocampal (and hippocampal-like) cell-lines developed and studied prior to the development of the mHippoE series of cell-lines: a summarized view of their origin and their main limitation.

Cell-line	Origin	Main limitation
H19-5	E17 Holtzman rat hippocampi	glial lineage
H19-7	E17 Holtzman rat hippocampi	neuronal markers expressed only after induction
H583-5	E17 Holtzman rat hippocampi	bipotential in lineage
HC2S2	adult rat hippocampi	immortalized neuronal progenitor cells
HiB5	E16 Sprague-Dawley rat hippocampi	morphology subject to conditions
HN9e	C57BL/6 E18 mouse hippocampi	immortalized *via* fusion with N18TG2
HT-4	murine neuronal cell-line	origin is not clearly defined
HT-22	sub-line of HT-4	particularly sensitive to glutamate

Note: the herein presented list of cell-lines is not exhaustive. Eves *et al.* (1992) provide more details on the H19-5, H19-7 and H583-5 cell-lines, as well as on another 10 immortalized embryonic cell-lines of hippocampal origin. Hoshimaru *et al*. (1996) describe the use of the immortalized adult rat hippocampal cell-line HC2S2 as a valuable tool for the study of neuronal differentiation, while Lee *et al*. (1990) have characterized a total of 5 hybrid cell-lines by fusing E18 and P21 hippocampal cells to N18TG2 neuroblastoma cells; of these, HN9e is the most notable as it has been reported to possess neuritic processes and excitable membrane. The HiB5 cells are considered to be hippocampal progenitor cells, whose morphological characteristics are dependent upon their *in vitro* culturing or *in vivo* implanting conditions (for more details, see Renfranz *et al.*, 1991). Finally, the HT-4 cell-line is considered by several authors to be a neuronal cell-line of murine origin (Morimoto and Koshland, 1990a; 1990b), for which very little is known, apart from the fact that HT-4 cells can take on properties of differentiated neurons when cultured at nonpermissive temperatures (39^{o}C); in fact, Whittemore *et al*. (1991) report HT-4 to be an immortalized mouse neuroblastoma cell-line (without any mention of its hippocampal origin). The HT-22 cell-line is a popular subclone of the aforementioned HT-4 cells (Davis and Maher, 1994); its hippocampal origin is highly-cited in the literature, but should be received with reservation. Bearing hippocampal-like cellular properties and being of hippocampal origin are two distinct qualities for a given immortalized cell-line; qualities that might have been mixed up by several researchers / authors over the last decades.

Ex: embryonic day x (x: day number); P21: postnatal day 21

Table B.2: Overview of a RT-PCR screening of the mHippoE-type cell-lines available by CELLutions Biosystems Inc.

Marker for which gene expression was tested	mHippoE-2	mHippoE-5	mHippoE-14	mHippoE-18
androgen receptor; AR	-	-	++	-
brain-derived neurotrophic factor; BDNF	+++	+++	+++	+++
glial fibrillary acidic protein; GFAP	-	-	-	-
glutamate receptor subtype 3; GluR3	+++	+++	+++	+++
glutamate receptor subtype 4; GluR4	-	-	++	-
G protein-coupled receptor 30; GPR30	++	-	+++	+++
growth hormone secretagogue receptor; GHSR	+	++	+++	+
insulin receptor; IR	+++	+++	+++	+++
leptin receptor; OB-R	+	+	+	+
N-methyl-D-aspartate receptor 1; NMDA-R1	++	++	++	++
microtubule-associated protein 2; MAP2	++	++	++	++
neuron specific enolase; NSE	+++	+++	+++	+++
neuropeptide Y; NPY	++	+++	+++	++
oestrogen receptor alpha; ERα	++	++	++	++
oestrogen receptor beta; ERβ	++	++	++	++
proglucagon; PG	+++	+++	-	+++
spermiogenesis specific transcript on the Y 1; SSTY1	++	++	-	++
tropomyosin receptor kinase A; TrkA	++	++	+++	++
tropomyosin receptor kinase B; TrkB	-	-	+	-

Note: data acquired from Gingerich *et al.* (2010) and presented with aesthetic modifications; gene expression levels were analyzed by semi-quantitative RT-PCR and were classified as strong (+++), moderate (++), weak (+) or negative (-) when compared to the strong expression of each gene in murine hypothalamus-derived positive controls.

RT-PCR: reverse transcriptase polymerase chain reaction

Figure B.1: Schematic representation of the procedure followed for the generation of the immortalized hippocampal mHippoE-14 cells, as described by Gingerich *et al*. (2010).

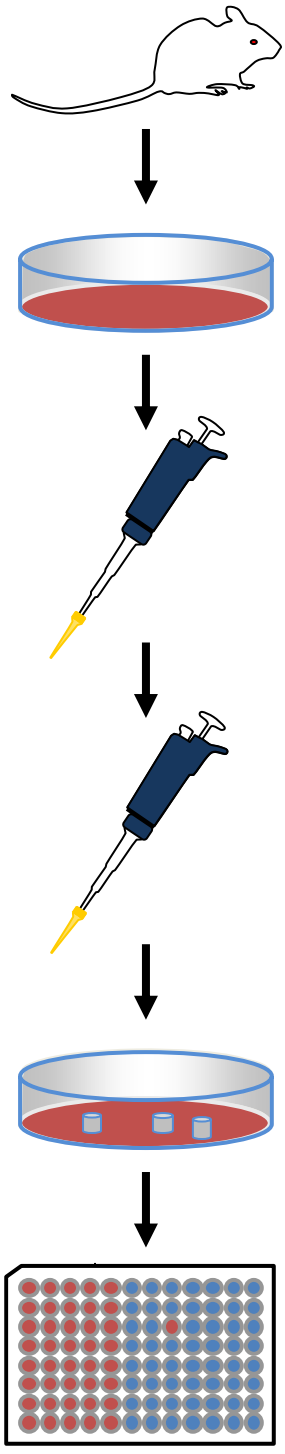

pregnant Swiss Webster mice were deeply anaesthetised with isoflurane on E18

foetal hippocampi were dissected, pooled together, triturated and plated on a 60 mm^2 culture dish (coated with poly-L-lysine) and left to be incubated (37°C, 5% CO_2) for 7 days in DMEM containing 10% heat-inactivated defined FBS, 10% heat-inactivated horse serum, 1% penicillin/streptomycin and 20 mM D-glucose

cultures were immortalized by transfection with recombinant murine retrovirus harbouring simian virus (SV40) T-antigen and neomycin-resistance gene from the pZIPNeo SV(X) 1 vector and left for 48 h

cultures were treated with G418 (400 μg/mL) every 3 days over a period of 2 weeks, prior to a further 2-3 week (maintenance) treatment with a lower concentration of G418 (250 μg/mL)

resistant cell colonies were selected using cloning cylinders and allowed to expand; of these, further selection allowed only for those clones demonstrating predominant neuronal morphology to expand

mixed cell populations were further subcloned through successive dilutions into 96-well plates (coated with poly-L-lysine; optimal dilution allowed for 1-2 cells per well; ratio 1:1 of conditioned medium and fresh DMEM with 15% FBS), and were then grown and cryopreserved

Note: the procedure is very similar to the one followed by Belsham *et al*. (2004) for the generation of immortalized hypothalamic neuronal cell-lines (N-1, N-2, N-3, N-4, N-6, N-7, N-8, N-11, N-19, N-20, N-22, N-25, N-29, N-36, N-37 and N-38) from mice. It should be noted that some of the latter cell-lines are also commercially-available by the same company as mHippoE-14, CELLutions Biosystems Inc.

DMEM: Dulbecco's modified Eagle's medium; E18: embryonic day 18; FBS: foetal bovine serum; G418: geneticin

Figure B.2: Representative phase-contrast microscopy captions of the mHippoE-14 cells.

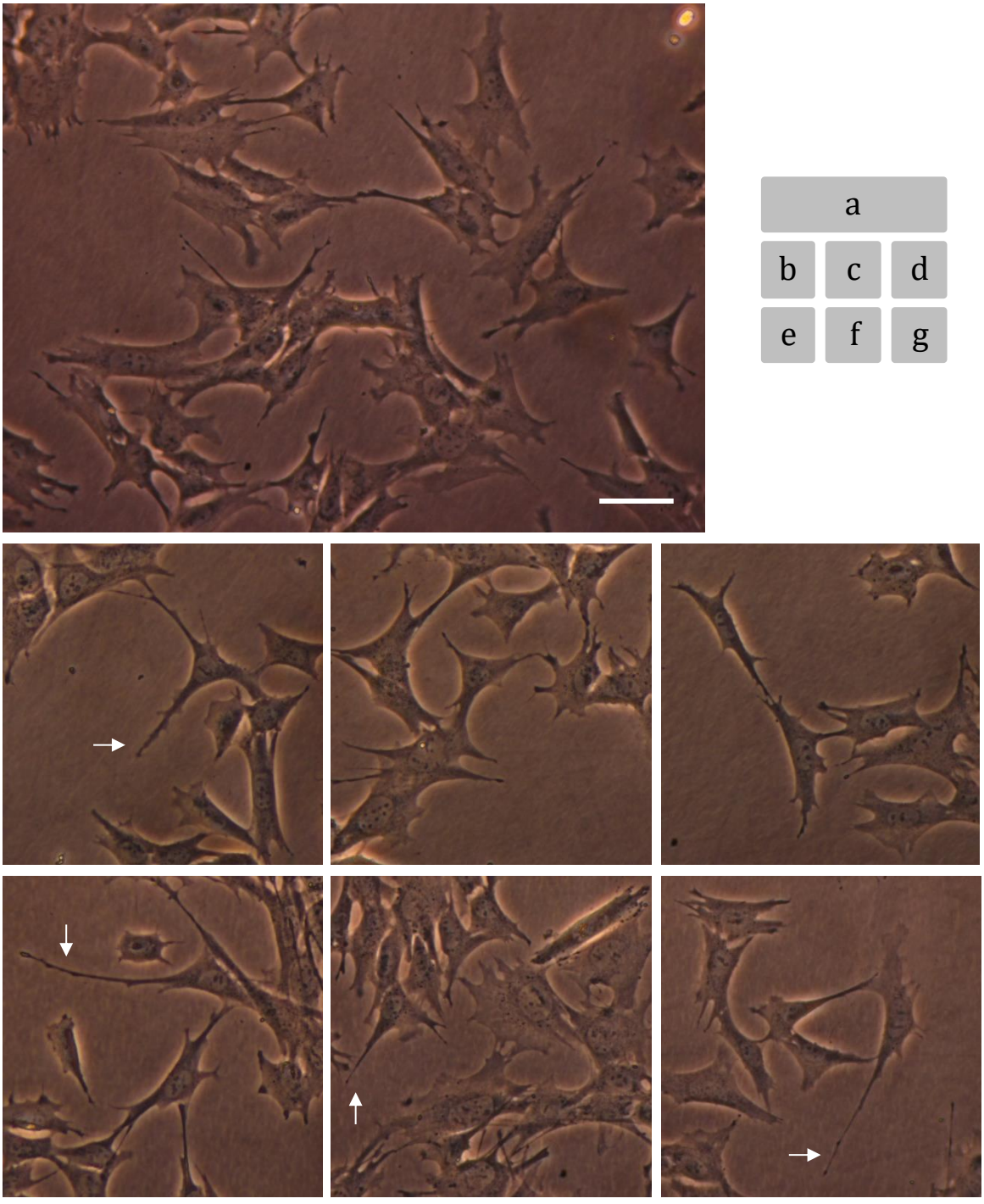

Note: all panels (a-g) accommodate phase-contrast microscopy captions of mHippoE-14 cells in the presence of an optimal (FBS-supplemented) medium (scale bar: 50 μm). White arrows (panels b, e, f and g) demonstrate unmet (expanding and / or free-standing) cellular protrusions suggestive of a neuronal phenotype.

FBS: foetal bovine serum

CHAPTER IV

Real-time cellular response analysis of the mHippoE-14 cell-line

A major tool employed for the development and assessment of the herein presented *in vitro* simulation approaches to intracerebral haemorrhage has been the undertaking of real-time cellular response analysis through the xCELLigence[1] Real Time Cell Analysis system (xCELLigence RTCA system; developed by Roche Applied Science in partnership with ACEA Biosciences Inc., and being available at the Gardiner Laboratory of the University of Glasgow). The xCELLigence technology is not by definition a "high-throughput" platform, but has the potential to act as one if appropriate apparatuses are used[2] or if multiple of the currently available apparatuses are simultaneously employed under appropriate conditions, towards the same drug-screening purpose. This chapter provides an overview of the xCELLigence technology and its applications, a summary of the work performed in order to characterize the cellular response patterns of the mHippoE-14 cells under optimal (growth-stimulating) and FBS-deprivation (growth-altering) conditions, and a presentation of novel concepts related to the necessary parametropoiesis of the outputs of this technology toward the optimization of its applicability in the development and assessment of *in vitro* simulation approaches with the use of the mHippoE-14 cell-line.

IV.1. The xCELLigence system and its applications

The xCELLigence technology monitors dynamic cellular events / cellular phenotypic changes under *in vitro* conditions, in real-time, without the incorporation of labels (label-free technology), by measuring electrical impedance across interdigitated micro-electrodes integrated on the bottom of the wells of tissue culture plates (E-Plates[3]) (Guan *et al.*, 2013; Ke *et al.*, 2011; Roshan Moniri *et al.*, 2015; Scrace *et al.*, 2013). The dimensions of an E-Plate 96 are 12.77 x 8.55 x 1.75 cm (width x depth x height); it accommodates 96 wells, with a well volume capaci-

[1] xCELLigence®.
[2] the xCELLigence RTCA HT device can perform label-free, real-time cell analysis in a 384-well format.
[3] E-Plate®.

ty of 243 ± 5 μL and a well bottom diameter of 5.00 ± 0.05 mm each[4]. The E-Plate 96 is made of biocompatible materials, is sterile, and its electrical interface is compatible with the RTCA SP station[5]. The E-Plate-hosting unit of the apparatus is placed in a standard cell culture incubator and interfaces *via* a cable with the analysis and control unit of the apparatus; the latter is housed outside the incubator.

The readings of the xCELLigence system are a complex mathematical algorithm interpretation of the electrical impedance across the aforementioned interdigitated microelectrodes, that are expressed and plotted over time as cell index (CI) values. Representative screen captions of how these readings are presented by the xCELLigence RTCA SP analysis software, are provided in Figure B.3. This technology can have multiple applications in the performance of growth / proliferation assays (Roshan Moniri *et al.*, 2015; Witzel *et al.*, 2015), the assessment of cell viability (Ke *et al.*, 2011; Limame *et al.*, 2012; Roshan Moniri *et al.*, 2015), the monitoring of cellular differentiation (Kramer *et al.*, 2014), the monitoring of cell migration / invasion (Limame *et al.*, 2012; Roshan Moniri *et al.*, 2015), the molecular profiling of cell-lines (Ke *et al.*, 2015), the undertaking of pathophysiological mechanisms' exploring experiments (Marinova *et al.*, 2013; Moodley *et al.*, 2011; van Kralingen *et al.*, 2013), the detection of neuronal death (Diemert *et al.*, 2012), the undertaking and optimization of cytotoxicity assays (Meindl *et al.*, 2013; Pan *et al.*, 2013a; 2013b; Ramis *et al.*, 2013), and the performance of drug-screening and drug-safety tests (Cruceru *et al.*, 2013; Hou *et al.*, 2014; Kho *et al.*, 2015; Kustermann *et al.*, 2013).

IV.2. Technical restrictions, archiving, analysis and statistical evaluation

A major technical restriction of the xCELLigence system (at least of the xCELLigence RTCA SP apparatus used) is that it is not fully automated: it does require human interference in changing the media, adding compounds or modifying *in vitro* conditions. This means that the system's inter-assay repeatability is largely dependent upon the user being consistent in these interferences. Moreover, the system is not capable of accommodating conditions that require exposure of some treatment groups to different temperature and / or different atmospheric composition, on the same E-Plate; a restriction that implies that *in vitro* simulating attempts incorporating oxygen-deprivation (e.g. *in vitro* OGD set-ups) cannot be simultaneously hosted along with appropriate controls on the same E-Plate. A third worth-mentioning restriction of the xCELLigence technology is that its application as an analytical and / or high-throughput screening tool should be preceded by an evaluation of its suitability to reliably represent the

[4] this means that the well bottom surface area of the wells of an E-Plate 96 are smaller (approximately -39%) than that of the wells of a standard 96-well microplate.
[5] the RTCA SP apparatus (that has been used for all the herein presented work) can only host one E-Plate 96 at a time (SP: single plate).

cellular events / cellular phenotypic changes in question; a comparative evaluation of the system's output against traditional assays (Limame *et al.*, 2012; Vistejnova *et al.*, 2009) and analytical cytomorphology (Vistejnova *et al.*, 2009).

The xCELLigence output is provided as ".plt" files with an automatically-generated ID for each experiment; these files are operational through the (in our case) xCELLigence RTCA SP analysis software (Figure B.3). Data can be easily extracted from these .plt files, and can be archived and further analysed through Microsoft Excel and / or other software. The analysis of these data can be subject to extensive customization, depending on the experiment's specifics and the assessment endpoints chosen. Statistical evaluation of these data can be performed through appropriate tests; in general, data of well-performed experiments tend to have low inter- and intra-assay variations, and values tend to be provided within normal distribution patterns.

IV.3. Characterization of the mHippoE-14 cell-line response patterns

In order to characterize the mHippoE-14 cell-line response patterns in a real-time manner, we decided to undertake a basic experiment: to map the growth of mHippoE-14 cells under optimal (FBS-supplemented) cell-culture conditions (as described in Chapter III) as well as to characterize the cellular response of these cells to FBS-deprivation (an interference expected to exert a cytostatic or cellular response-modifying effect). For this purpose, mHippoE-14 cells were seeded (at a density of 7,500 cells/well) into E-Plates, and were monitored while left to grow in FBS-supplemented medium (growth medium) for 24 h, prior to them being washed twice and having their medium replaced by a non-FBS-containing one; treatment group "FBS(+/-)" (Figure B.4). The monitoring of the mHippoE-14 cellular response was performed for further 36 h (to a total of 60 h) (Figure B.4). As a control, mHippoE-14 cells that were not subject to any change of their medium were used; treatment group "FBS(+)". Both treatment groups were subject to the same time (and subsequent cellular stress) outside the incubator (37^{o}C, 5% CO_2), but the FBS(+/-) cells were also subject to the washing and medium-renewing procedure.

The average cellular response profiling obtained from this experiment (performed in triplicate) has revealed a cellular response-modifying effect of FBS-deprivation, that after a few hours seems to be holding the affected mHippoE-14 FBS(+/-) cells in a "cytostatic" / non-proliferating / cytokinetically-stable status (Figure B.4). A closer look on this status (as compared to the profiling of the FBS(+) treatment group) has allowed us to distinguish the mHippoE-14 cellular response patterns into phases (Table B.3; Figures B.5.a and B.5.b). Of these phases, of particular interest are the "metaptotic" and the "pathopoietic" phases (Table B.3).

Moreover, based on these findings, the adoption of novel symbolography for the mapping of real-time cellular responses (Table B.4) has been considered and set into effect for the purpose of the herein presented studies. This adoption facilitates a more thorough analysis of the observed cellular response profiles, and enables a wider, specialized and more accurate analysis of the obtained data through established and novel (proposed) parameters (Table B.5). An example of this analysis is provided in Table B.6 and in Figures B.5.c, B.5.d, B.5.e and in Figure B.6.

IV.4. Pathopoietic transformation of the mHippoE-14 cell-line

The deprivation of FBS from the medium in which mHippoE-14 cells grow, leads, eventually, to the establishment of a "pathopoietic phase" (Table B.3; Figures B.4, B.5.a and B.5.b). The normalized cellular response (nCR) of the FBS-deprived mHippoE-14 cells within this phase is statistically significantly lower than those continuing on the dynamic phase (Table B.6; Figure B.5.e). In fact, the mean nCR values of the mHippoE-14 cells within the metaptosis' recovery point (R_m) and the evaluation endpoints at 36, 48 or 60 h (E_{36}, E_{48} or E_{60}, respectively) are not statistically significantly different from 0 (the FBS(+/-) mean nCR values ± standard deviations are presented in Table B.6; significance analysis towards 0 is not presented).

The pathopoietic transformation of the mHippoE-14 cells through FBS-deprivation is a great property of the specific cell-line, and allows for a more reliable simulation of neuronal entities *in vivo*, where neurons are expected to be cytostatic / non-proliferating. This pathopoietic transformation ought to be, of course, further characterized and adopted, as it has the potential to provide an ideal cellular substrate basis for the development of *in vitro* human brain disease-simulating conditions.

IV.5. Metaptosis of the mHippoE-14 cell-line and its parametropoiesis

Apart from the pathopoietic transformation of the mHippoE-14 cells, the xCELLigence technology has also revealed a phase of rapid cellular response transitions (metaptotic phase; Table B.3; Figures B.5.a, B.5.b and B.6). This phase is of particular interest for a very specific reason: it reveals a grey zone of cellular instability due to FBS-deprivation and / or handling of the cells in a non-regulated (in terms of temperature and atmosphere composition) environment. The cells need time to recover from this phase, which is significantly lower in the FBS(+)- than in the FBS(+/-)-treated cells (approximately 2 *versus* 6 h, respectively, $p<0.01$; Figure B.6.b)[6]. The cells also undertake metaptosis with patterns (Figure B.6.a) and nCR val-

[6] the majority of the published *in vitro* studies ignore this phase and present toxicity or drug efficiency assessments within a few hours or even minutes after the FBS-deprivation; this practice is wrong. The addition of a toxic compound or a drug under FBS-deprived conditions - in fact, any further interven-

ues (Table B.6) that are in all cases statistically significantly different amongst the studied treatment groups. The adoption of the proposed symbolography with regards to major mapping points within metaptosis (I_m, metaptosis' initiation point; Z_m, metaptosis' zenith point; N_m, metaptosis' nadir point; R_m; Table B.4) is, in my opinion, a major prerequisite for a more accurate study of this phase (Table B.6; Figures B.6.c, B.6.d and B.6.e), as well as for its further parametropoiesis towards the establishment of intra- and inter-assay standards; see, in particular, the proposed metaptotic index (m_i) and the index of metaptotic adaptability (μ_i) in Table B.5.

>> Table B.3: page 80
>> Table B.4: page 81
>> Table B.5: page 82
>> Table B.6: page 83
>> Figure B.3: page 84
>> Figure B.4: page 86
>> Figure B.5: page 87
>> Figure B.6: page 89

tion after FBS-deprivation - should be done at a time point where evidence suggests that for the specific cellular substrate, under the specific *in vitro* conditions, a recovery from metaptosis has occurred.

Table B.3: Proposed nomenclature for the description of standardized real-time cellular response profiles through the use of the xCELLigence technology.

Phase	Description and potential
initial	phase describing the "S"-shaped short-lasting cellular profile recorded from the moment of cell-seeding until their entry into the next phase; represents the recordings matching to the attachment of the cells to the bottom of the wells
dynamic	phase describing the cellular profile in which the growth / multiplying of the recently-seeded / attached cells occurs (under appropriate conditions); it is characterized by a cell growth rate (cellular response) that tends to be stable
metaptotic	phase describing the cellular profile recorded right after a media-renewing (>10% of the volume of the well's medium) or long-lasting stressful (due to a change in the environmental conditions; e.g. temperature, levels of CO_2, *etc.*) interruption of a recording, until the re-establishment of a cellular response that tends to be stable (recovery); this phase's duration, nature and intensity depend on the duration, nature and intensity of the inducing interruption
pathopoietic	phase describing the cellular profile in which the cellular status of the studied cell-line is constant; this phase is particularly relevant to cases where the studied "cellular substrate" is not supposed to be mimicking a dynamic cell population or a condition where cell proliferation should not occur

Note: the herein presented phase definitions are subject to improvement prior and / or after publication, and have been defined with the perspective of being applicable in the case of the studied mHippoE-14 cell-line. For a visualized presentation of these phases, see Figure B.5.

CO_2: carbon dioxide

Table B.4: Proposed symbolography for the mapping of real-time cellular responses through the use of the xCELLigence technology.

Symbol	Meaning(s)
$\mathbf{I_o}$	recording's initiation point
$\mathbf{I_e}$	experiment's initiation point
$\mathbf{I_m}$	metaptosis' initiation point
$\mathbf{I_t}$	treatment's initiation point
$\mathbf{S_e}$	stabilization point (point of transition from initial to dynamic phase)
$\mathbf{R_m}$	metaptosis' recovery point
$\mathbf{R_t}$	recovery point after a treatment intervention
$\mathbf{Z_m}$	metaptosis' zenith point
$\mathbf{Z_t}$	zenith point after treatment
$\mathbf{N_m}$	metaptosis' nadir point
$\mathbf{N_t}$	nadir point after treatment
E	endpoint, any; see for subtypes below
$\mathbf{E_d}$	endpoint within the dynamic phase
$\mathbf{E_p}$	endpoint within the pathopoietic phase
$\mathbf{E_t}$	endpoint after a treatment intervention
$\mathbf{E_x}$	evaluation endpoint at a time point of choice; 'x' can be replaced by number / letter
$\mathbf{E_e}$	end of the experiment (endpoint)

Note: all hereby presented symbols might be subject to revision prior to further publication. The R_m is manually defined within a dataset of the xCELLigence technology as the earliest point after Z_m in which the cellular response profiling curve adopts a stable response over time. Obviously, the recording time-intervals are a major parameter defining the accuracy with which one can identify this point. For further details on the calculation of "cellular response" and the uses of R_m, see Table B.5.

Table B.5: Established and proposed parameters for a more thorough analysis of real-time cellular responses through the use of the xCELLigence technology.

Parameter	Symbol	Meaning and calculation
cell index	**CI**	major unit of measurement for the xCELLigence technology; it reflects the cell number, adhesion and/or morphology
cellular response	**CR**	measured in CI/h; the response of a given cellular group over a given time; for two given time points (α and β, where α < β), the CR would be presented as $CR_{(\alpha,\beta)}$ and would be calculated as: $CR_{(\alpha,\beta)} = \Delta CI_{(\alpha,\beta)} / \Delta t_{(\alpha,\beta)}$
normalized cell index	**nCI**	a CI normalized to that of a control time point; in the case of the experiments described in this Thesis, normalization is usually performed toward the CI values of the last endpoint within the dynamic phase (E_d) recording
normalized cellular response	**nCR**	measured in nCI/h; for the same given time points as above (α and β, where α < β), the nCR would be presented as $nCR_{(\alpha,\beta)}$ and would be calculated as: $nCR_{(\alpha,\beta)} = \Delta nCI_{(\alpha,\beta)} / \Delta t_{(\alpha,\beta)}$
metaptotic index	$\mathbf{m_i}$	a number; for a given cell-line, the m_i is the result of the ratio between the nCI at the recovery point of metaptosis (R_m) for the group of cells undergoing FBS-deprivation and the nCI at the respective R_m point for the group of cells that is not subject to any media change or addition: $m_i = nCI_{(Rm;FBS\text{-}deprived)} / nCI_{(Rm;control)}$ provided that normalization occurs towards the CI value of the same group at the I_m time point
index of metaptotic adaptability	$\mathbf{\mu_i}$	measured in h^{-2}; for a given group of cells, the μ_i reflects the intensity with which the specific group undergoes metaptosis; would be calculated as: $\mu_i = nCR_{(Zm,Nm)} / (\Delta nCI_{(Im,Rm)} * \Delta t_{(Im,Rm)})$ provided that normalization occurs towards the CI value of the same group at the I_m time point

Note: all hereby presented parameters might be subject to revision prior to further publication, with the exception of cell index (CI) and normalized cell index (nCI) that are established parameters. For more details on the symbols used within the third column, see Table B.4.

Δ: difference (operator); FBS: foetal bovine serum; t: time

Table B.6: Effects of FBS-deprivation on selected proposed cellular response parameters of the mHippoE-14 cell-line.

Parameter (unit)	**FBS(+)**	**FBS(+/-)**	**Significance**
$\mathbf{nCR_{(Se,E24)}}$ (nCI/h)	0.037 ± 0.003	0.037 ± 0.003	---
$\mathbf{nCR_{(E24,Zm)}}$ (nCI/h)	0.511 ± 0.113	-0.319 ± 0.294	$p<0.05$
$\mathbf{nCR_{(E24,Nm)}}$ (nCI/h)	0.063 ± 0.011	-0.507 ± 0.076	$p<0.001$
$\mathbf{nCR_{(E24,Rm)}}$ (nCI/h)	0.045 ± 0.002	-0.025 ± 0.027	$p<0.05$
$\mathbf{nCR_{(Zm,Nm)}}$ (nCI/h)	-0.204 ± 0.059	-0.558 ± 0.100	$p<0.01$
$\mathbf{nCR_{(Nm,Rm)}}$ (nCI/h)	0.023 ± 0.016	0.067 ± 0.021	$p<0.05$
$\mathbf{nCR_{(Rm,E36)}}$ (nCI/h)	0.078 ± 0.008	0.016 ± 0.030	$p<0.05$
$\mathbf{nCR_{(Rm,E48)}}$ (nCI/h)	0.085 ± 0.007	0.014 ± 0.020	$p<0.01$
$\mathbf{nCR_{(Rm,E60)}}$ (nCI/h)	0.085 ± 0.008	0.006 ± 0.014	$p<0.01$
$\boldsymbol{\mu_i}$ (h^{-2})	-1.206 ± 0.455	1.154 ± 0.822	$p<0.05$
$\mathbf{m_i}$ (-)	0.786 ± 0.134		n/a

Note: data are presented as mean ± standard deviation of three independent experiments (n=3; IDs: 1407101722, 1407130859, 1408040936), and statistical analysis has been performed through the use of Student's *t*-test. Only statistically significant differences ($p<0.05$) are annotated. For all experiments, normalization has been performed at the I_m time point. For more details on the symbols used within the first column, see Table B.4. For more details on the experimental protocol followed for the performance of these experiments as well as for a visualization of the average real-time cellular response profiling of the mHippoE-14 cells under these conditions, see Figure B.4.

n/a: not applicable; FBS: foetal bovine serum

Figure B.3: Representative screen captions from the xCELLigence RTCA SP analysis software.

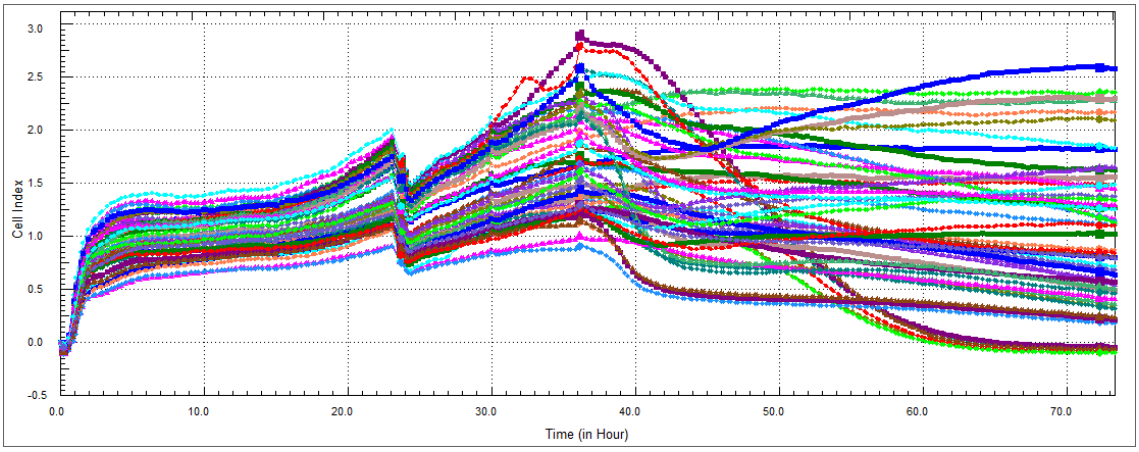

setting A: CI per well
54 wells included

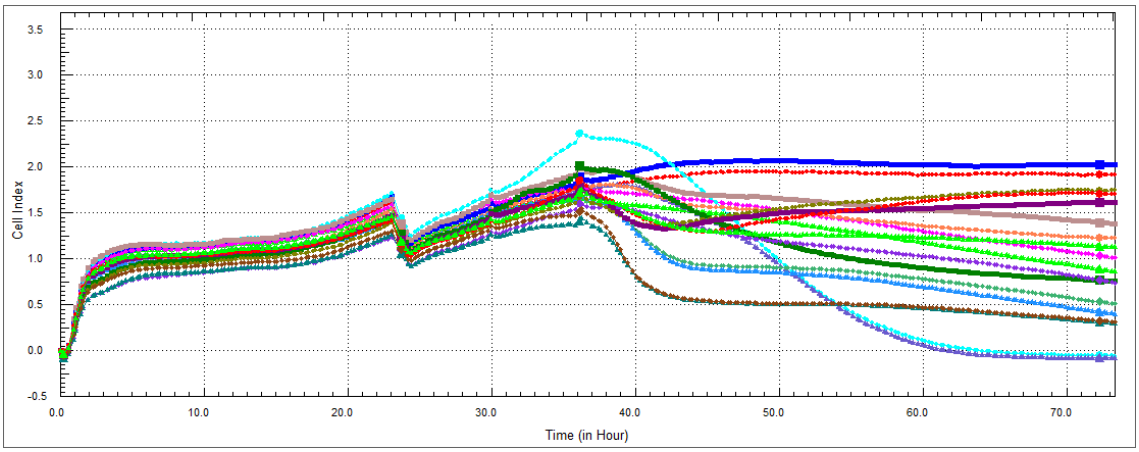

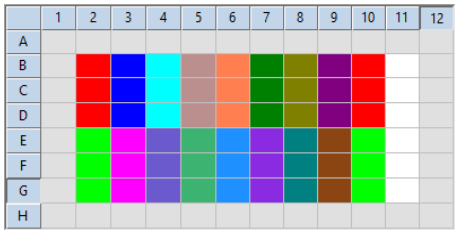

setting B: average CI per group
18 well groups included

(continues on next page)

(continues from previous page)

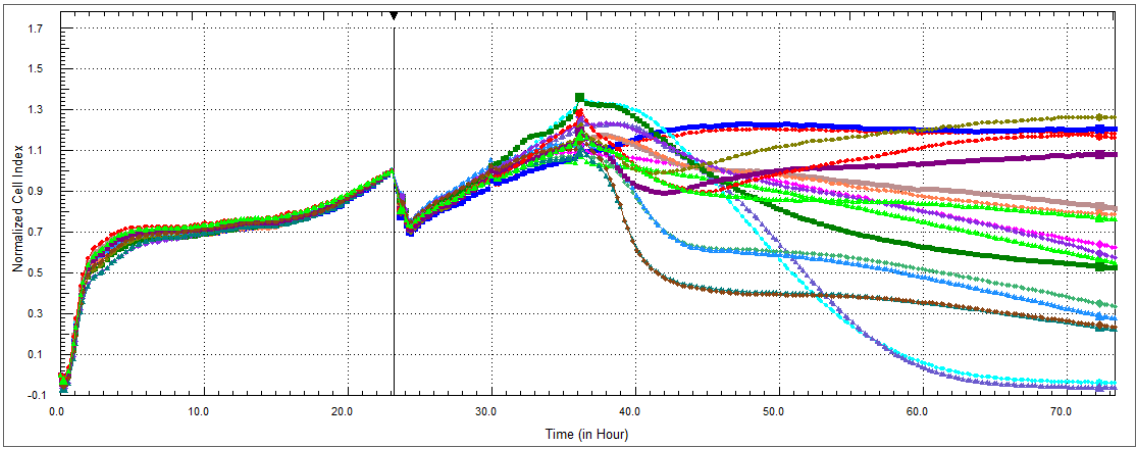

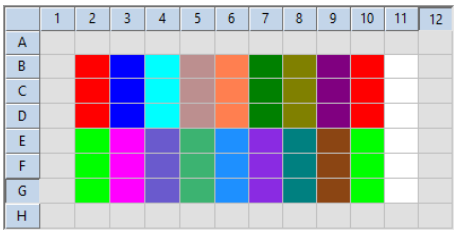

setting C: average nCI per group
normalization at 23:15:55
18 well groups included

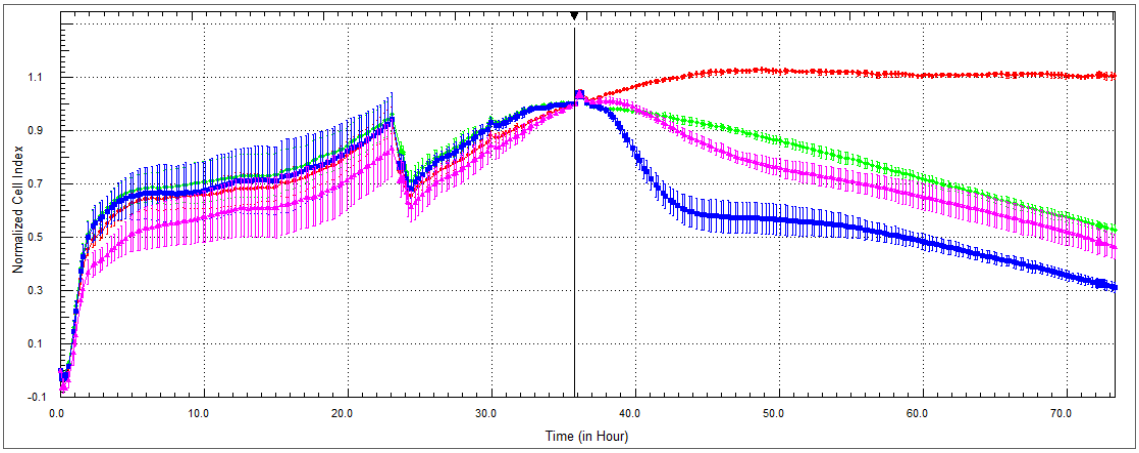

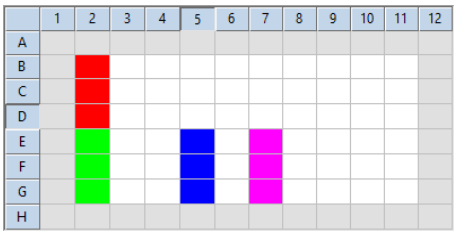

setting D: average nCI per group
standard deviation presented
normalization at 35:48:33
4 well groups included

Note: the screen captions presented are indicative of the potential of the xCELLigence RTCA SP analysis software: *setting A* presents the real-time cellular responses (as "cell index", CI) of a selection of 54 individual wells within a given E-Plate 96, with each well being annotated with a different colour; *setting B* provides a more tidy version of *setting A*, in which the averages (mean values) of the CI of the wells that belong to the same treatment group are presented with different colours; *setting C* provides the same information as *setting A*, with the difference that this time a normalization upon the CI values has occurred towards those of a specific time point (e.g. 23:15:55; "normalized cell index"; nCI); *setting D* presents the average nCI values of 4 well groups, with the additional presentation of their standard deviations. For all performed experiments, recordings were set to be obtained an a 1 per 10 min frequency, while for the analysis of the experiments presented in this PhD Thesis, the xCELLigence RTCA SP analysis software (version 2.0) was used.

CI: cell index; nCI: normalized cell index

Figure B.4: Changes in the mHippoE-14 cellular response profiling due to FBS-deprivation.

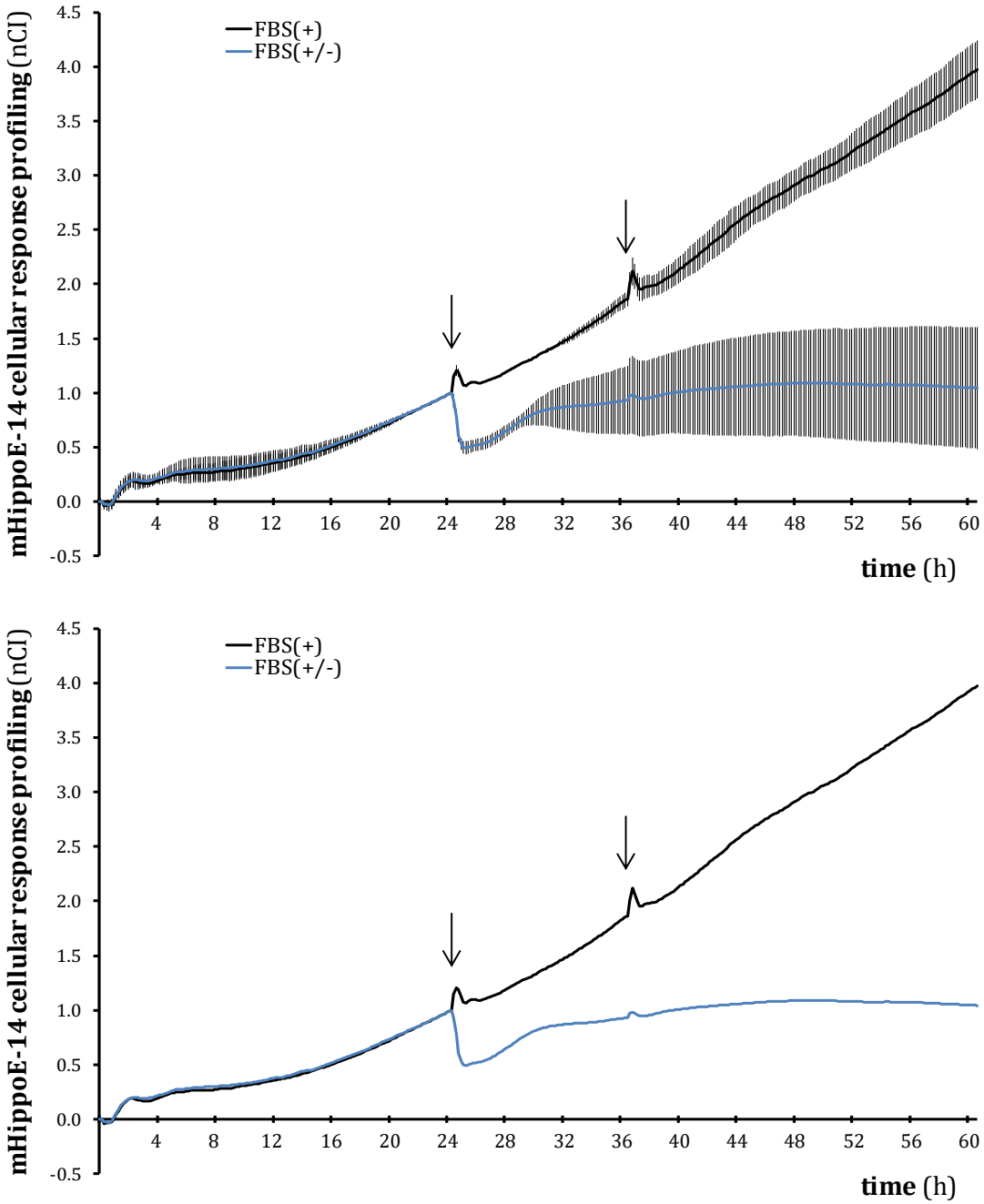

Note: data are presented as mean ± standard deviation (top diagram) or mean (bottom diagram) of three independent experiments (n=3; IDs: 1407101722, 1407130859, 1408040936). For all experiments, normalization has been performed at the I_m time point (approximately 24 h post-seeding of the mHippoE-14 cells into the wells of an E-Plate 96; seeding density: 7,500 cells/well). In brief, mHippoE-14 cells were seeded and left to grow in FBS-supplemented medium (growth medium) for 24 h, prior to them being washed twice and having their medium replaced by a non-FBS-containing one; treatment group "FBS(+/-)". As a control, mHippoE-14 cells that were not subject to any change of their medium were used; treatment group "FBS(+)". Both treatment groups were subject to the same time (and subsequent cellular stress) outside the incubator, but the FBS(+/-) cells were also subject to the washing and medium-renewing procedure. Arrows indicate the medium renewal (FBS-deprivation) time point (approximately 24 h post-seeding) and a later time point where a 10% medium renewal took place (approximately 36 h post-seeding); the latter was a simulation of a drug- or toxic compound-adding interference.

FBS: foetal bovine serum; I_m: metaptosis' initiation point; nCI: normalized cell index

Figure B.5: Mapping the real-time cellular response of mHippoE-14 cells to FBS-deprivation.

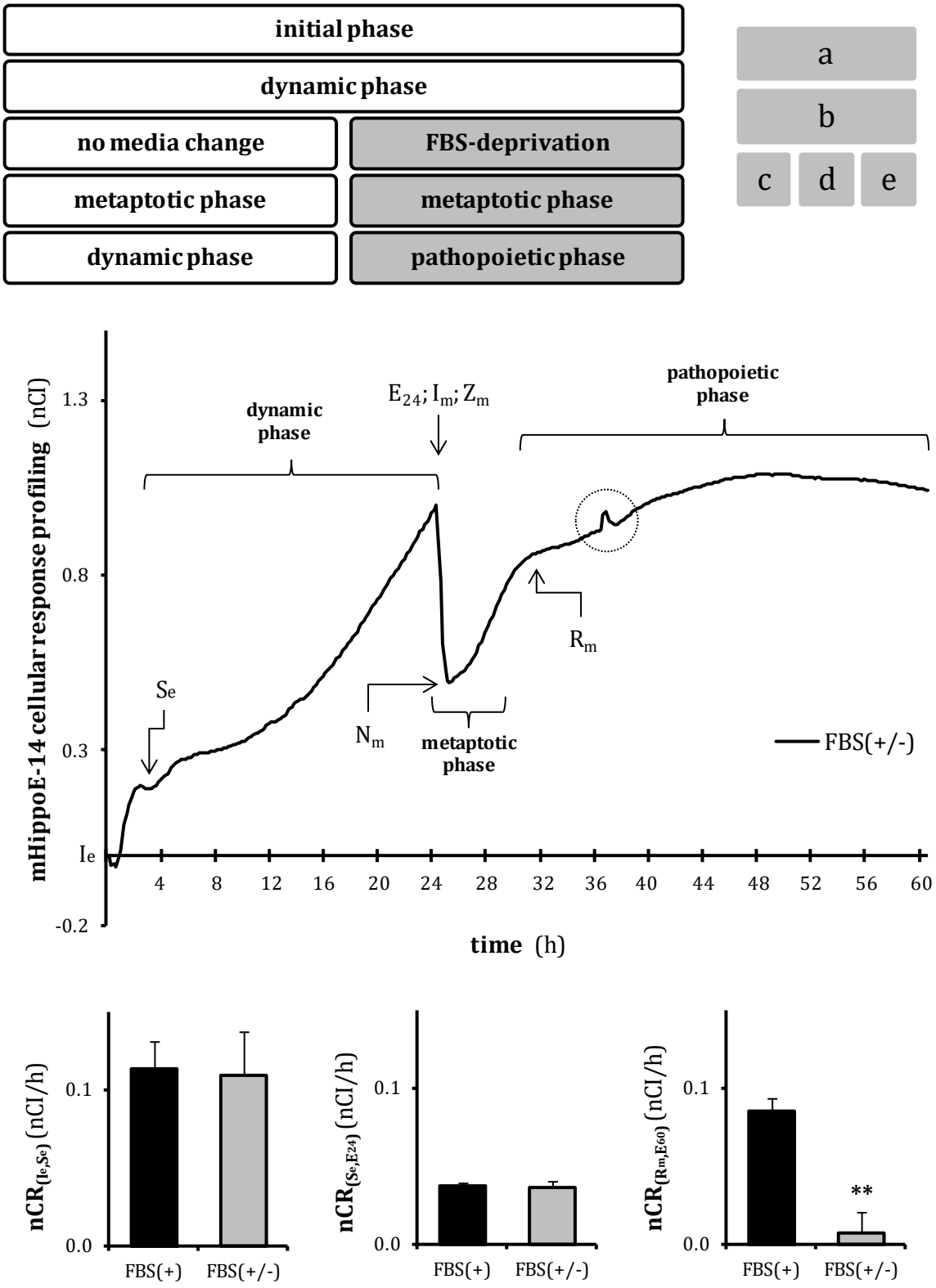

Note: Figure B.5.a is an ideographic representation of the effects of FBS-deprivation on the phase succession occurring in terms of the real-time cellular response of mHippoE-14 cells under conditions similar to the ones presented in Figure B.4. Figure B.5.b provides a visualization of the aforementioned phases in the case of the FBS(+/-) treatment group (see note of Figure B.4 for protocol's details); of interest are the S_e time point (see Table B.4) as well as the circled area that represents an non-metaptotic interruption within the pathopoietic phase (in which a

10% volume renewal of the media has taken place; simulation of a drug- or toxic compound-adding interference). Finally, the data on Figures B.5.c, B.5.d and B.5.e are presented as mean ± standard deviation of three independent experiments (n=3; IDs: 1407101722, 1407130859, 1408040936). Statistical analysis has been performed through the use of Student's *t*-test, and only statistically significant differences ($p<0.05$) are annotated. For all experiments, normalization has been performed at the I_m time point (approximately 24 h post-seeding of the mHippoE-14 cells into the wells of an E-Plate 96; seeding density: 7,500 cells/well). For more details on these experiments, consult note of Figure B.4. For more details on the time points and the parameters presented, consult Tables B.4 and B.5, respectively.

**: $p<0.01$; E_{24}: evaluation endpoint at 24 h; E_{60}: evaluation endpoint at 60 h; FBS: foetal bovine serum; I_e: experiment's initiation point; I_m: metaptosis' initiation point; nCI: normalized cell index; nCR: normalized cellular response; R_m: metaptosis' recovery point; S_e: stabilization point

Figure B.6: Mapping the metaptosis of the mHippoE-14 cells.

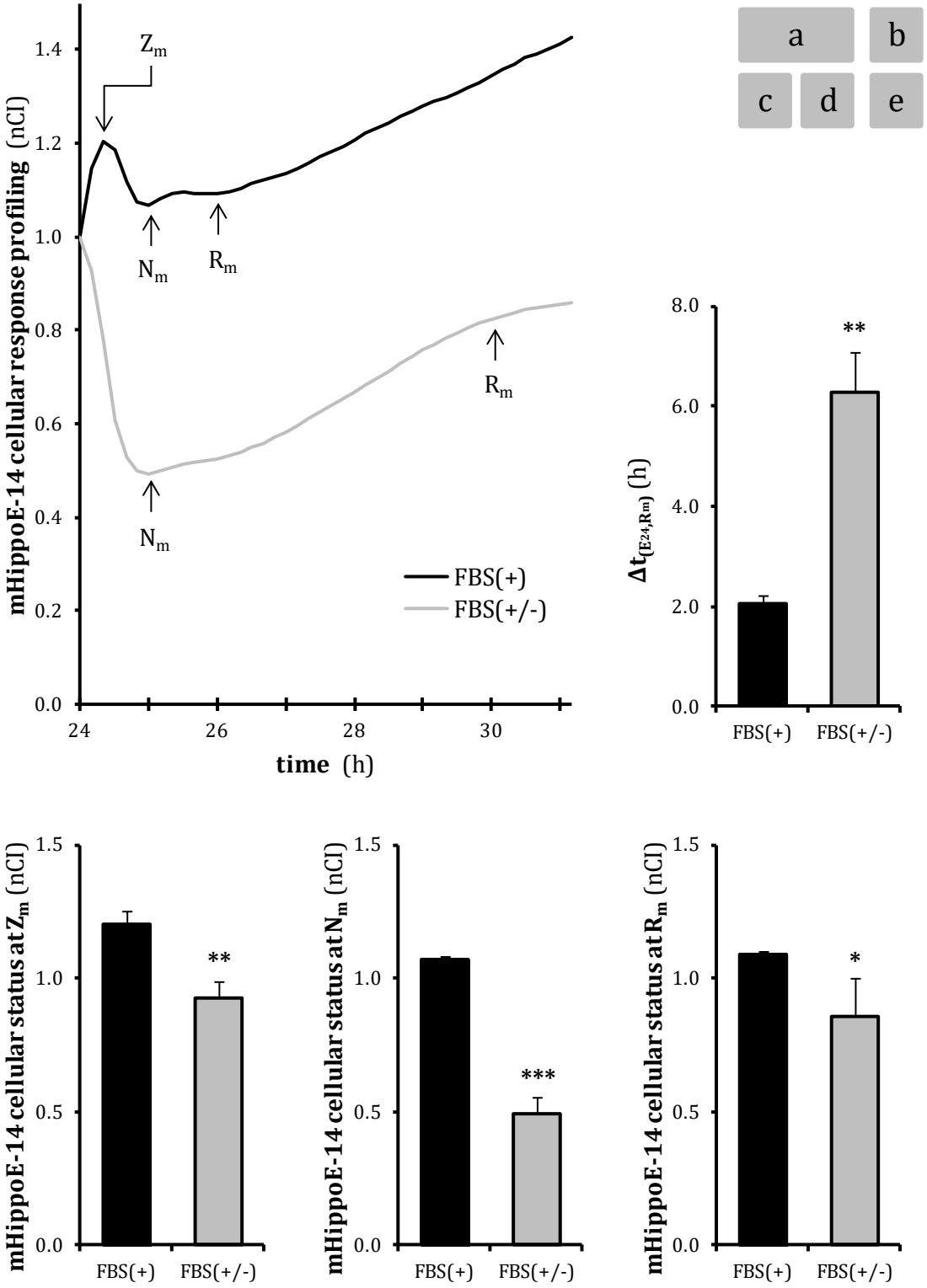

Note: Figure B.6.a provides a visualization of the metaptotic phase for both the FBS(+) and the FBS(+/-) treatment groups (see note of Figure B.4 for protocol's details); of interest are the Z_m, N_m and R_m time points of metaptosis (see Table B.4) as well as the time it takes for each group to recover (Figure B.6.b). Finally, the data on Figures B.6.b, B.6.c, B.6.d and B.6.e are presented as mean ± standard deviation of three independent experiments (n=3; IDs: 1407101722, 1407130859, 1408040936), and statistical analysis has been performed through the use of Stu-

dent's *t*-test. For all experiments, normalization has been performed at the I_m time point (approximately 24 h post-seeding of the mHippoE-14 cells into the wells of an E-Plate 96; seeding density: 7,500 cells/well). For more details on these experiments, consult note of Figure B.4. For more details on the time points presented, consult Table B.4.

*: $p<0.05$; **: $p<0.01$; ***: $p<0.001$; Δ: difference (operator); E_{24}: evaluation endpoint at 24 h; FBS: foetal bovine serum; I_m: metaptosis' initiation point; nCI: normalized cell index; N_m: metaptosis' nadir point; R_m: metaptosis' recovery point; t: time; Z_m: metaptosis zenith point

CHAPTER V

Cytomorphological characterization of the mHippoE-14 cell-line

As with the real-time cellular response analysis characterization of the mHippoE-14 cell-line presented in Chapter IV, the cytomorphological characterization of this novel, commercially-available, immortalized cell-line has been considered and undertaken for two reasons: (a) out of genuine interest in the cell-line's cytomorphology and the desire to explore its phenotypic transformations under the experimental conditions we were aiming to employ, and (b) as a prerequisite for the validation of the phenomena observed through the xCELLigence technology - particularly those occurring following an FBS-deprivation of these cells.

V.1. Established cytomorphological characterization of hippocampal neurons

The cytomorphological characteristics of hippocampal cells that grow / survive under *in vitro* conditions, have been the subject of extensive neuroscientific interest and thorough study throughout the recent decades (Barnes and Polleux, 2009; Beaudoin *et al.*, 2012; Bradke and Dotti, 2000; Del Turco and Deller 2007; Kaech and Banker, 2006; Majd *et al.*, 2008; Peacock *et al.*, 1979; Tseng *et al.*, 2006; Xie *et al.*, 2000). Of this wealth of information, the study of Dotti *et al*. (1988) on the establishment of polarity by hippocampal neurons *in vitro*, has been of great importance for the development and introduction of a multi-stage scale for the classification of these neurons, based on phase-contrast microscopy of live cells (Table B.7). Dotti *et al*. (1988) have studied the development of neurons obtained from the embryonic hippocampi of rats, and have suggested that these neurons: (a) should *"reproducibly display a characteristic shape"*[1], (b) should develop a distinguishable major process within the first 24 h post-seeding, and (c) should become polarized within the first 48 h. They also suggested that in order to achieve polarity, hippocampal neurons will go through 3 stages: the formation of lamelipodia (stage 1), the outgrowth of processes that are more than 10 μm in length (stage 2), and the development of an axon (stage 3; development of polarization) (Dotti *et al.*, 1988). These stages were suggested to be followed by dendritic growth (stage 4) and the establish-

[1] which they then clarified as *"a single long axon of relatively uniform diameter, and several shorter, tapering dendrites (Bartlett and Banker, 1984)"* (Dotti *et al.*, 1988).

ment of neuronal "maturity" (stage 5) (Dotti *et al.*, 1988) (Table B.7), and their use has been even extended to the study of cortical neurons, after minor modifications (Davis *et al.*, 2013).

V.2. Preliminary assessment of the cytomorphology of the mHippoE-14 cell-line

In order to assess the suitability of the Dotti *et al*. (1988) stage scale for the cytomorphological classification of the mHippoE-14 cells, we designed and undertook four independent experiments (n=4) in which the cells were cultured in 35 mm Corning[2] Dishes and their growth was followed *via* live cell phase-contrast microscopy at 6, 12, 18, 24, 30, 36 and 48 h post-seeding (at a seeding density of 211,000 cells/dish)[3]. The protocol also included the induction of FBS-deprivation (see FBS(+/-) from Chapter IV) at 24 h, and its parallel assessment to the FBS(+) (control) condition (see Chapter IV) at 30, 36 and 48 h; in other words, the protocol aimed to simulate the experiments summarized in Figure B.4 and discussed in Chapter IV, but on a 35 mm dish. As a result, 880 captions[4] were generated through a Carl Zeiss Axiovert 40 C inverted phase-contrast microscope (Ph1 condenser annulus; x10 and x20 magnification objective; blue filter) and an attached photo camera (Canon PowerShot A650 IS digital camera). Image analysis was performed through the ImageJ (1.48v) software. A preliminary assessment of these captions have made us realize that the Dotti *et al*. (1988) could not be practically applicable in the case of the mHippoE-14 cells, at least under the attempted experimental conditions, as after 12 h in culture the cells tend to form aggregates, and as time passes, these aggregates make it hard to identify cytomorphological features of individual cells. As a result, two new challenges arose: (a) the classification of mHippoE-14 cell-line, and (b) the identification of cytomorphological assessment parameters that could provide a basic but comparable means to validate the data acquired from the xCELLigence technology.

V.3. Atlas of the mHippoE-14 cellular morphology

The first challenge was addressed with the attempt to generate an algorithm (Table B.7; Figure B.7) and an atlas of the mHippoE-14 cell-line (Figure B.8). The proposed cytomorphological classification is based on whether the cells maintain shape regularity[5], protoplasmic pro-

[2] Corning®.
[3] this seeding density was adopted in order to simulate the cell density achieved when seeding 7,500 cells in a 96-well plate well, and to make results from different methods "comparable".
[4] for each experiment (out of 4), 10 different "states" (unique time point / treatment conditions) were captioned; for every state, 7 captions of x10 and 15 captions of x20 magnification were produced.
[5] shape regularity is associated with the minimum prerequisites set by Dotti *et al*. (1988) for the classification of a hippocampal neuron as "polarized" (stage 3; see Table B.7), and one must not forget that the monolayer monoculture of the mHippoE-14 cells cannot possibly be expected to adopt a 3-dimentional shape regularity observed *in vivo* or in organotypic cultures; within this PhD Thesis, an mHippoE-14 cell is considered to be characterized by shape regularity if it appears polarized, and has at least one process longer than 10 μm.

trusions[6] longer than 10 μm, met protrusional outreach and episomatic[7] attachment (to other cells), and it can classify the mHippoE-14 cells into ten types: type Ia, Ib, IIa, IIb, IIIa, IIIb, IVa, IVb, Va and Vb (Table B.7; Figures B.7 and B.8). Those cells belonging to a Va type at any given assessment endpoint are ideal candidates for the cytomorphological assessment of these cells; unfortunately, Va mHippoE-14 cells were rarely observed under the attempted *in vitro* conditions. However, the value of the proposed classification lies in its potential utilization within integrated (Migliore and Shepherd, 2005), multi-parametric (Chen *et al.*, 2012; Santana *et al.*, 2013) and / or automated (Chan *et al.*, 2015; Leach *et al.*, 2011) cytomorphology assays, and the identification of patterns for a cytopathological assessment based on parameters currently employed by clinical cytopathologists (see Tables APP.1 and APP.2; Buckner *et al.*, 1992).

V.4. Parametropoiesis of the mHippoE-14 cellular morphology assessment

The second challenge was addressed with the adjustment and adoption of the following 4 cellular morphology assessment parameters: (a) the confluency score (Table B.8), (b) the aggregation score[8] (Table B.8), (c) the background score[9] (Table B.8), and (d) the measurement of floating debris particles (per optical field)[10]. The first three of these parameters are semi-quantitative (see Table B.8), and require a non-automated, "blind" assessment by a user who has been familiar with the cellular response of these cells to various insults. This has been feasible due to a number of preliminary data (on neurotoxic settings) acquired in parallel to this PhD project.

V.5. Cytomorphological assessment of the mHippoE-14 cell-line

The representative phase-contrast microscopy captions of live mHippoE-14 cells under optimal (growth) and FBS-deprived conditions presented in Figure B.9, demonstrate the gradual increase in confluency that the FBS(+) cultures go through as time passes (captions B.9.a to B9.g), as opposed to the FBS(+/-) treatment group (captions B.9.h to B.9.j) that seems to be facing a halt of its cells' proliferation and a time-dependent increase in the number of floating debris particles. When quantifying these captions, one is relieved to realize that the pattern with which confluency develops over time (Figure B.10.a) is resembling the pattern with

[6] the words "neuraxons", "dendrites", "neurites" are avoided; to prove the existence of those, neuronal cytoskeletal protein immunocytochemistry must be applied.
[7] soma-to-soma cytoplasmic attachment.
[8] the aggregation score could be refined based on the data presented in Tables APP.1 and APP.2.
[9] the background score is very similar to what the cytopathologists assess as "diathesis" in tumour biopsy samples.
[10] in this particular case, image analysis and image element counting tools available through the ImageJ (1.48v) software were also employed as appropriate.

which the cellular statuses of the respective treatment groups has been recorded to develop through real-time cellular response analysis (Chapter IV). Moreover, as time passes the aggregation score increases in the FBS(+) treatment group, but this is not the case for the FBS-deprived cell cultures in which it actually becomes statistically significantly (p<0.001) lower than that of the FBS(+) cell cultures only at 48 h (see Figure B.10.b). Interestingly, the number of floating debris particles per caption in the FBS(+) treatment group is maintained constant throughout the 48 h of the experiment, while the induction of FBS-deprivation causes a rapid and statistically significant increase of this number as compared to that of the FBS(+) equivalent (at 48 h, this is +373%, p<0.001; Figure B.10.e). The latter increase is also accompanied by a statistically significant increase in the background score (at 36 h and 48 h: p<0.05 and p<0.001, respectively; results not shown)[11].

These findings suggest that the pathopoietic phase is not genuinely cytostatic, but an actively injurious process for the mHippoE-14 cells; a suggestion that requires further study.

>> Table B.7: page 95
>> Table B.8: page 96
>> Figure B.7: page 97
>> Figure B.8: page 98
>> Figure B.9: page 99
>> Figure B.10: page 100

[11] note that the method is semi-quantitative and that despite the statistically significant increase, the background score was still very low by the end of this set of experiments (at 48 h, the FBS-deprived treatment group has a median background score of 1).

Table B.7: Algorithm for the proposed cytomorphological classification of mHippoE-14 cells: a software-friendly presentation, as compared to the stage classification of Dotti *et al*. (1988).

Type	Shape regularity	Protoplasmic protrusions	Met protrusional outreach	Episomatic attachment	Notes
Type Ia	0	0	0	0	see Figure B.8.a
Type Ib	0	0	0	1	see Figure B.8.b
Type IIa	0	1	0	0	see Figure B.8.c
Type IIb	0	1	0	1	see Figure B.8.d
Type IIIa	0	1	1	0	see Figure B.8.e
Type IIIb	0	1	1	1	see Figure B.8.f
Type IVa	1	1	0	0	see Figure B.8.g
Type IVb	1	1	0	1	see Figure B.8.h
Type Va	1	1	1	0	see Figure B.8.i; ideal type
Type Vb	1	1	1	1	see Figure B.8.j

Stage	Lamelipodia present	Process >10 μm	Axonal growth / polarization	Dendrites' growth	Notes
Stage 0	0	0	0	0	not originally suggested
Stage 1	1	0	0	0	expected by 0.25 days in culture
Stage 2	1	1	0	0	expected by 0.5 days in culture
Stage 3	1	1	1	0	expected by 1.5 days in culture
Stage 4	1	1	0 or 1	1	expected by 4 days in culture
Stage 5	maturity stage				expected >7 days in culture

Note: "0" stand for "no" and "1" stand for "yes". The proposed mHippoE-14 cells' cytomorphological classification is based on the assumption that: (a) a hippocampal cell that does not have protoplasmic protrusions, cannot have any sort of protrusional outreach to be met, and (b) a hippocampal cell that is characterized by shape regularity, has, *de facto*, protoplasmic protrusions. The herein presented cytomorphological classification of the mHippoE-14 cells (types Ia and Ib to Va and Vb) resulted for a series of four independent experiments (n=4) in which the cells were cultured in 35 mm Corning Dishes and their growth was followed *via* live cell phase-contrast microscopy at 6, 12, 18, 24, 30, 36 and 48 h post-seeding (at a density of 211,000 cells/dish). The protocol also included the induction of FBS-deprivation (see FBS(+/-) from Chapter IV) at 24 h, and its parallel assessment to the FBS(+) (control) condition (see Chapter IV) at 30, 36 and 48 h. In total, 600 captions were generated through a Carl Zeiss Axiovert 40 C inverted phase-contrast microscope (Ph1 condenser annulus; x20 magnification objective; blue filter) and an attached digital photo camera. These captions were studied toward the generation of this algorithm (Figure B.7) as well as of an atlas of the mHippoE-14 cells (Figure B.8). The stage classification of hippocampal neurons growing *in vitro*, developed by Dotti *et al*. (1988), did not originally have a stage 0, and its algorithmic interpretation is performed for the purpose of this chapter. What I perceive as "shape regularity" is the equivalent of what Dotti *et al*. (1988) defined as a "stage 3" phenotype.

FBS: foetal bovine serum

Table B.8: Cytomorphological parameters employed in the mHippoE-14 cell cultures' phase-contrast microscopy imaging assessment.

Parameter	Scale	Meaning
Confluency score	0	exactly 0% confluency; no live cells
	1	0-10% confluency
	2	10-20% confluency
	3	20-30% confluency
	4	30-40% confluency
	5	40-50% confluency
	6	50-60% confluency
	7	60-70% confluency
	8	70-80% confluency
	9	80-90% confluency
	10	90-100% confluency
Aggregation score	0; -	no aggregation exists
	1; -/+	episomatic attachments; not aggregation
	2; +	aggregates exist, but is mild
	3; ++	aggregates exist
	4; +++	extensive presence of aggregates
	5; ++++	aggregates are the dominant form of cell arrangement
Background score	0; -	no sign of debris
	1; -/+	some small defined debris on dish's bottom
	2; +	debris evident, but limited in number
	3; ++	debris evident, including undefined debris
	4; +++	extensive presence of debris
	5; ++++	debris are dominant background feature

Note: the use of the herein presented semi-quantitative parameters in the assessment of mHippoE-14 cell-line's cytomorphology has been performed on low magnification (x10) phase-contrast microscopy captions. The assessment of these parameters was not done automatically, but manually, in a "blind" to the sample identity manner. Moreover, for the assessment of these three parameters, the user's estimation of the scoring was primarily employed (exercised through previous experience on mHippoE-14 cytomorphology evaluation under different experimental conditions), while statistical analysis treated these scores as non-continuous (discrete) parameters.

Figure B.7: Algorithm for the proposed cytomorphological classification of mHippoE-14 cells.

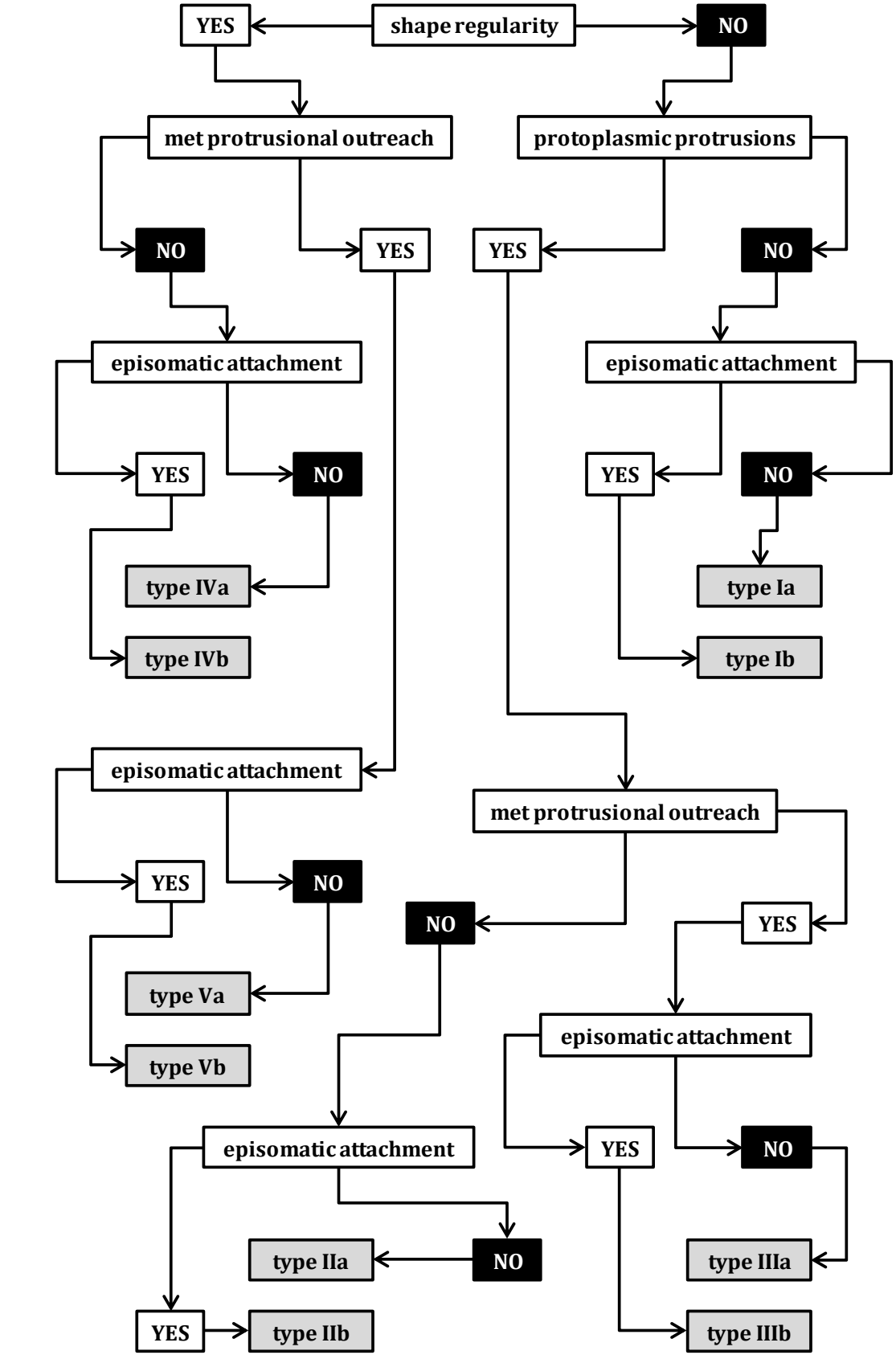

Note: for more details, see Table B.7.

Figure B.8: Atlas of the mHippoE-14 cell-line.

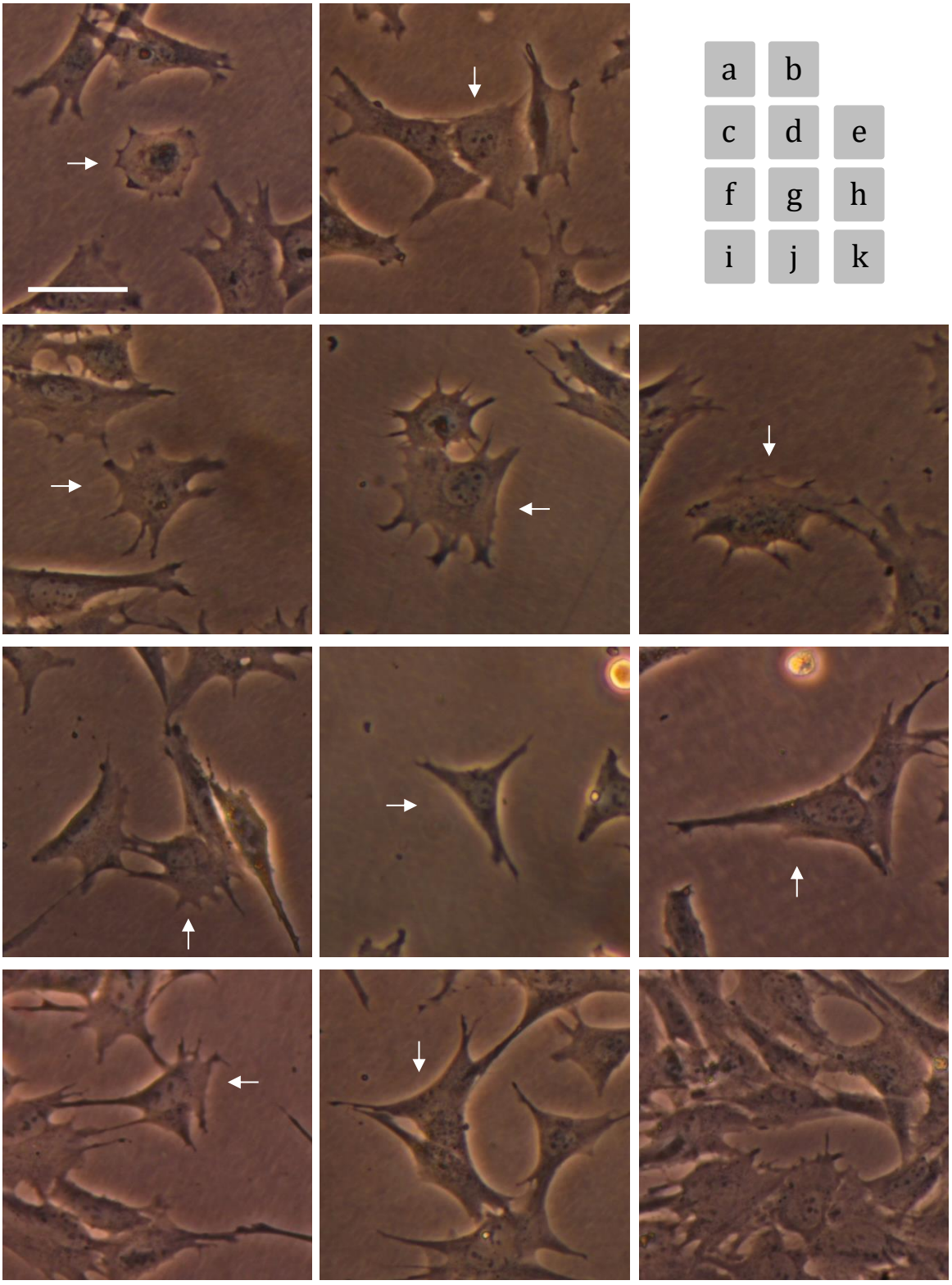

Note: the current mHippoE-14 cell-line atlas was generated as described in the note of Table B.7, and reflects the proposed cytomorphological classification types (see white arrows): type Ia (Figure B.8.a), type Ib (B.8.b), type IIa (B.8.c), type IIb (B.8.d), type IIIa (B.8.e), type IIIb (B.8.f), type IVa (B.8.g), type IVb (B.8.h), type Va (B.8.i) and type Vb (B.8.j). Figure B.8.k depicts an aggregation of mHippoE-14 cells, which is, unfortunately, an unavoidable effect of the attempted seeding cell-density. White bar equals to 50 μm.

Figure B.9: Representative phase-contrast microscopy captions of live mHippoE-14 cells under optimal (growth) and FBS-deprived conditions.

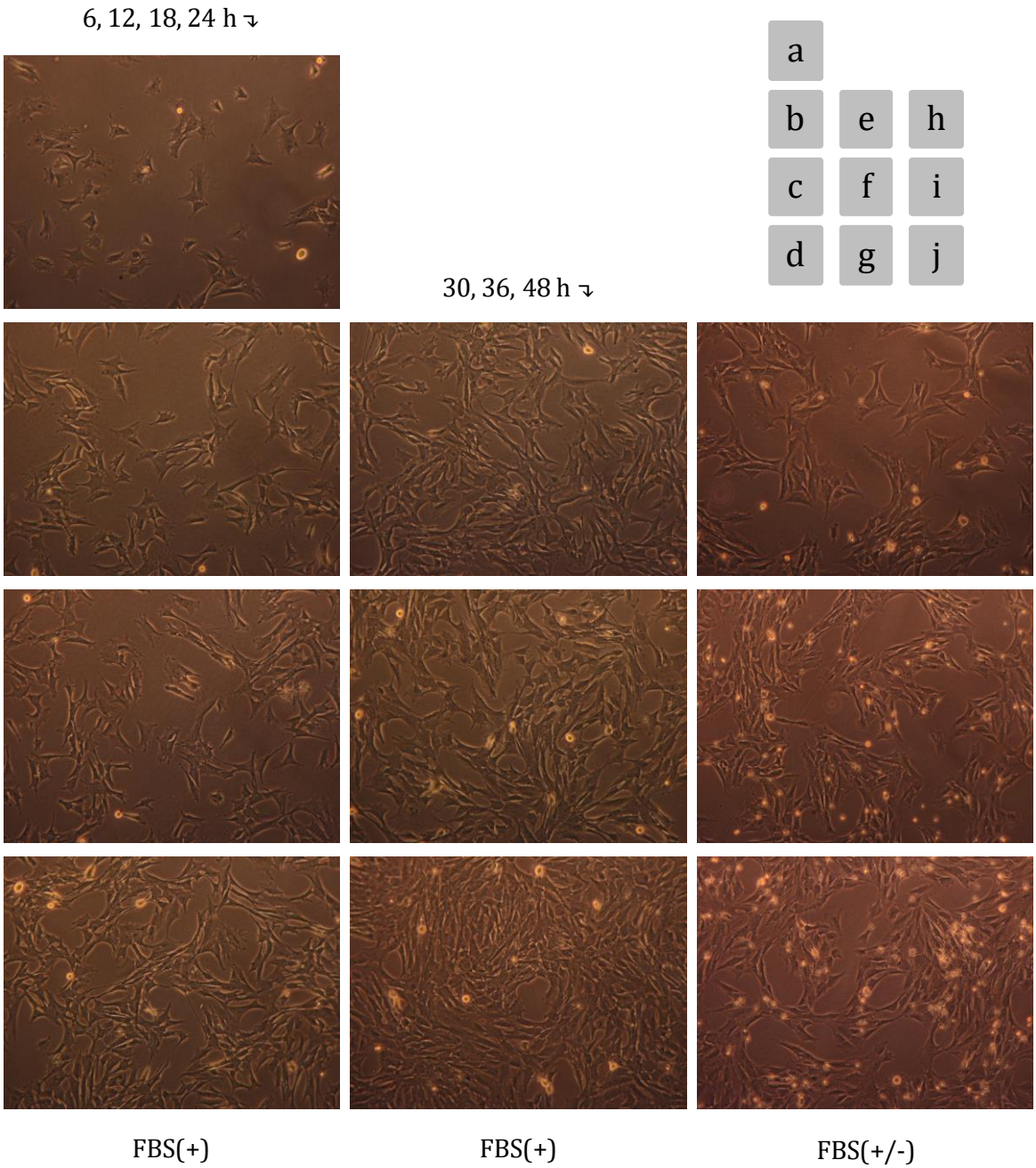

Note: the presented phase-contrast microscopy captions of the mHippoE-14 cell-line are representative captions from a series of four independent experiments (n=4) in which the cells were cultured in 35 mm Corning Dishes and their growth was followed at 6, 12, 18, 24, 30, 36 and 48 h post-seeding (at a density of 211,000 cells/dish). The protocol also included the induction of FBS-deprivation (see FBS(+/-) from Chapter IV) at 24 h, and its parallel assessment to the FBS(+) (control) condition (see Chapter IV) at 30, 36 and 48 h. In total, 280 captions were generated through a Carl Zeiss Axiovert 40 C inverted phase-contrast microscope (Ph1 condenser annulus; x10 magnification objective; blue filter) and an attached digital photo camera. Captions B.9.a to B.9.g represent the FBS(+) treatment group and demonstrate the gradual increase in confluency that these cultures go through as time passes. Captions B.9.h to B.9.j represent the FBS(+/-) treatment group and demonstrate a halt of their proliferation and a time-dependent increase in the number of floating debris particles. For more details, see Figure B.10.

FBS: foetal bovine serum

Figure B.10: Cytomorphological analysis of the mHippoE-14 response to FBS-deprivation.

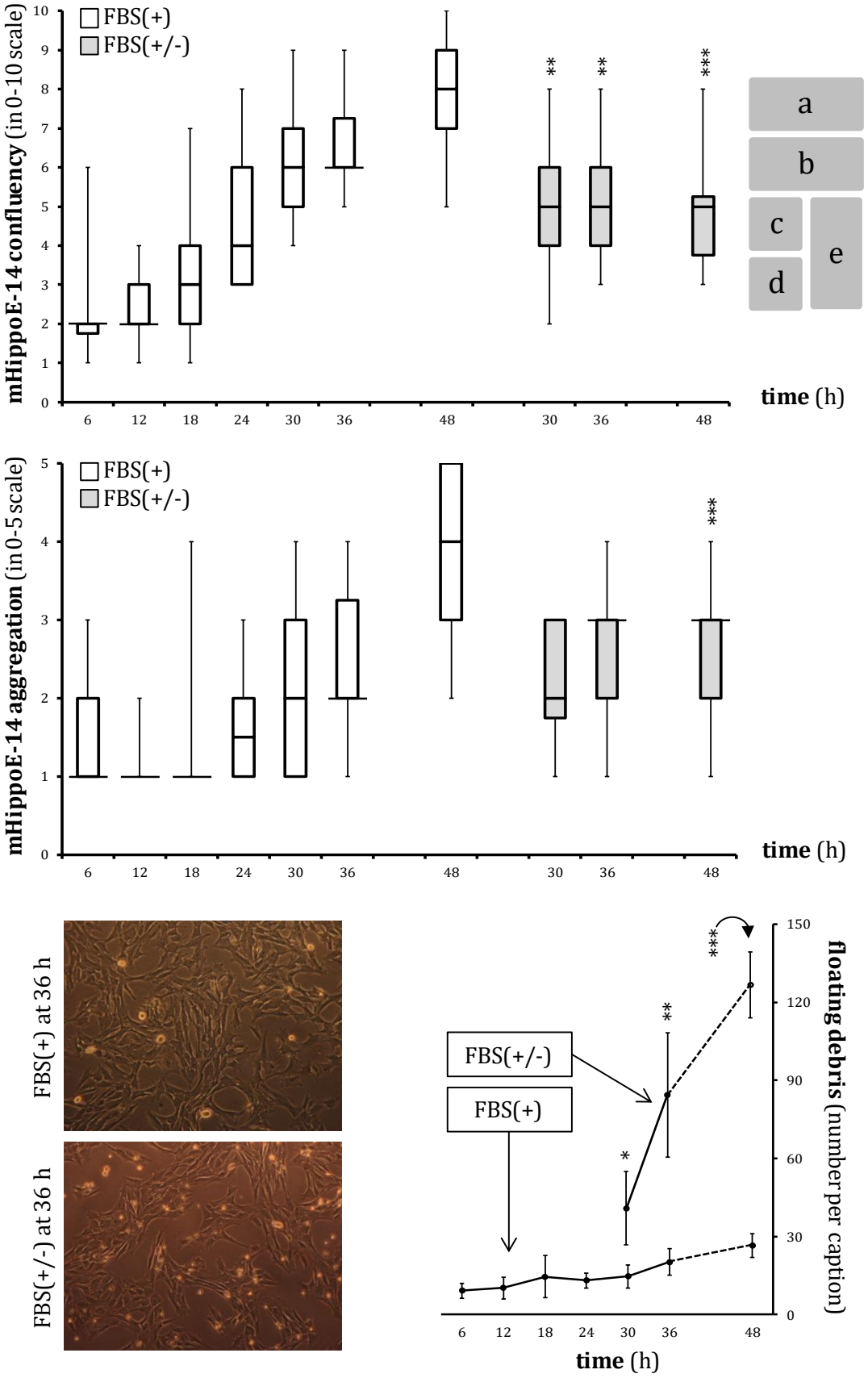

Note: the floating debris are assessed as number of particles per x10 magnification caption. Data on Figures B.10.a and B.10.b are presented as median and interquartile range (IQR) in a box-and-whisker plot (pooled caption scoring of four independent experiments; n=28), and statistical analysis has been performed through the use of a Mann-Whitney U test. Table APP.3 provides more details on the variability of the confluency scoring data within and between the experiments conducted. The data on Figure B.10.e are presented as mean ± standard deviation of four independent experiments (n=4), and statistical analysis has been performed through the use of one-way ANOVA followed by *post hoc* Tukey's range test. Only statistically significant differences ($p<0.05$) are annotated. For more details on the parameters assessed and the experimental protocol followed, consult Table B.8 and the note of Figure B.9, respectively.

*: $p<0.05$; **: $p<0.01$; ***: $p<0.001$; ANOVA: analysis of variance; FBS: foetal bovine serum; IQR: interquartile range

PART C

mHippoE-14-utilizing *in vitro* simulation approaches to intracerebral haemorrhage

CHAPTER VI

Development of *in vitro* simulation approaches to intracerebral haemorrhage

The real-time cellular response analysis of the mHippoE-14 cell-line presented in Chapter IV and the cytomorphological characterization of this cell-line presented in Chapter V, have allowed us to gain valuable insight with regards to the potential and the (technical) limitations of FBS-deprivation within the development of *in vitro* simulation approaches to intracerebral haemorrhage. The next step was to conduct a number of preliminary experiments in order to define the specific conditions that would allow for the simulation of one or more aspects of the disease's neuropathology on the mHippoE-14 cells; a task that would allow us to develop our simulation approaches upon evidence.

VI.1. Preliminary attempts

Our first attempt was to examine the effect of various concentrations of iron[1] and of haemin[2] on the mHippoE-14 cells through the "popular" MTT reduction assay (see Chapter II). For this purpose, mHippoE-14 cells were seeded into 96-well plates at densities of 7,500 and 15,000 cells/well, and were grown in DMEM supplemented with 10% FBS and 1% penicillin - streptomycin (as described in Chapter III). After 24 h, the cells were exposed to the following concentrations of ferrum or haemin: 0, 5, 10, 25, 50, 75, 100, 150, 200 and 500 μM[3]. The assessment of their MTT reduction activity[4], 24 h later (Figure C.1), has revealed no evidence of toxicity by the aforementioned compounds at the chosen concentrations. As a result, a new experiment was performed in the absence of FBS (Figure C.2): at 24 h the FBS was removed and the mHippoE-14 cells were immediately exposed to either ferrum or haemin, resulting into

[1] exposure to iron, in all the experiments of this PhD Thesis, was performed as $FeCl_2$; iron will be hereafter referred to as "ferrum". The choice of Fe^{2+} over Fe^{3+} is based on the ability of the first to act as an electron donor (and thus, as a contributor to oxidative stress), as well as on previous practice evident in the literature (see, for example, Levy *et al.*, 2002).

[2] haemin was dissolved into sodium hydroxide (NaOH, 0.1 M; final concentration 0.05%) prior to its addition to the medium; this NaOH addition was appropriately simulated at control treatments, and had no effect whatsoever on the parameters examined in this phase. Haemin is a ferric protoporphyrin.

[3] higher concentrations of haemin were attempted, but not tested due to solubility problems.

[4] the herein described MTT reduction assays were performed in accordance to the Promega CellTiter 96® non-radioactive cell proliferation assay (product number: G4000) instructions. For a more details, see also Riss and Moravec (2006).

some positive results (24 h later) by the treatment groups exposed to 500 μM of ferrum and to concentrations of haemin higher than 50 μM; both belonging to the low (7,500 cells/well) seeding density treatment groups. Further experiments of similar nature were performed, but this time on a prolonged exposure timeframe: the mHippoE-14 cells were exposed to ferrum or haemin in the presence or in the absence of FBS, and the MTT activity assessment took place 48 h later (Figures C.3 and C.4, respectively). These experiments confirmed the necessity for the adoption of FBS-deprivation as a facilitating factor for the exertion of ferrum- and haemin-induced toxicity, and suggested the suitability of the low (7,500 cells/well) seeding density in the undertaking of further experiments. However, they have also indicated that haemin is far more toxic than ferrum under the examined FBS-deprivation conditions (particularly at the highest tested concentration; 500 μM), and that exposure to ferrum could even be advantageous to the mHippoE-14 MTT reduction activity at low concentrations (5 μM; Figure C.4.d).

VI.2. Determination of appropriately-toxic concentrations of haemin and ferrum

A major concern has been the relatively high toxicity-exerting concentrations of haemin required within these settings; most *in vitro* simulation approaches to intracerebral haemorrhage have used lower concentrations of haemin (5 to 100 μM; see Chapter II). Both these concentrations and ours (500 μM) are still within acceptable ranges, as the blood is known to contain approximately 2.5 mM of haemoglobin that can subsequently give rise (through haemolysis) to up to 10 mM of haemin (Robinson *et al.*, 2009). In other words, the 500 μM concentration of haemin is still one twentieth of what can be found to interact with the brain parenchyma cells in reality.

A second interesting finding has been the role of FBS-deprivation in enhancing the exertion of haemin-induced neurotoxicity on the mHippoE-14 cells. While elucidating this finding, it might be a fine opportunity to discuss a bit about the role, the properties and the origin of FBS; the widely used cell culture growth supplement cocktail that is believed to contain - similarly to the human serum - around 1,800 proteins and more than 4,000 metabolites (Anderson *et al.*, 2004; Gstraunthaler *et al.*, 2013; Psychogios *et al.*, 2011). This by-product of the food industry is a poorly-defined cocktail that happens to contain necessary factors for the attachment and growth (including the stimulation of the "mitogenic effect"; proliferation)[5] of the majority of mammalian cells *in vitro*, but also happens to be characterized by significant batch-to-batch variation and major ethical concerns with regards to its sourcing (Gstraun-

[5] including hormones, growth factors, various binding and transport proteins, protease inhibitors, fatty acids, lipids, amino acids, vitamins and trace elements (Gstraunthaler, 2003; van der Valk *et al.*, 2010).

thaler *et al.*, 2013). As an alternative to the use of FBS, the use of serum-free[6] (Brunner *et al.*, 2010; Gstraunthaler, 2003), chemically-defined (Brunner *et al.*, 2010; van der Valk *et al.*, 2010), and animal-derived component-free[7] (Brunner *et al.*, 2010) media have been proposed and studied, revealing a number of additional properties and advantages towards the adoption of techniques / experimental approaches that would contribute to the restriction of the need for FBS in contemporary cell culture practice. We now know, for example, that the use of serum-free media can facilitate the longer maintenance of aggregating brain cell cultures (Honegger and Schilter, 1995) as well as that defined (serum-free) media cause changes in the appearance of glial-derived cells (as compared to serum-supplemented conditions)[8] (Michler-Stuke and Bottenstein, 1982). We also know that the adaptation of the C6 glioma cell-line to FBS-free conditions has been reported to significantly alter their morphological phenotype, and to enhance their neurite-promoting capacity (Coyle, 1995). Moreover, FBS-deprivation has been shown to trigger neuronal apoptosis in rat primary cortical cultures (Terro *et al.*, 2000) and hippocampal organotypic cultures (Rivera *et al.*, 1998), and to modify the proliferation rates (Fan and Uzman, 1977) and the neurochemical sensitivity (Dibner and Insel, 1981a; 1981b) of C6 glioma cells.

A very interesting study has been conducted by Brenner *et al*. (2010) and has revealed that the preceding culture conditions (e.g. the presence of FBS or not) can define the peroxide-induced oxidative damage on C6 glioma cells; a property attributed to the supply (or not) of the cells with FBS-deriving antioxidants (Brenner *et al.*, 2010). Moreover, the binding of FBS proteins (such as albumin) to neurotoxic compounds has been recently reported as a major implication for the reliable undertaking of MTT reduction assays on the C6 glioma cell-line (Bilmin *et al.*, 2013). These findings could justify the fact that FBS-deprivation was a prerequisite for the enhanced exertion of haemin-induced neurotoxicity on the mHippoE-14 cells (Figures C.2.c, C.2.e, C.4.c, C.4.e as opposed to C.1.c, C.1.e, C.3.c, C.3.e, respectively), and are in agreement with the comparative study of Chow *et al*. (2008) on the cytotoxic effect of haemin on glioblastoma cell-lines in the presence and absence of FBS.

Finally, with regards to the observation that low concentrations of ferrum can even be beneficial for the mHippoE-14 cells' MTT reduction activity (Figure C.4.d), one must consider the possibility of these cells being inducible by iron under FBS-deprivation in ways similar to those suggested by Basset *et al*. (1985) in the case of C6 glioma cells and L_{1210} leukaemic cells.

[6] for a very interesting resource on the development and optimization of serum-free media, see Jayme and Gruber (2006).
[7] types of cell culture media that do not contain any components of animal or human origin; this definition doesn't necessarily make them "chemically-defined" ones.
[8] in fact, cells were reported to adopt a less flattened and more spherical cytoplasmic phenotype in defined media (Michler-Stuke and Bottenstein, 1982).

On the other hand, the comparatively lower toxicity of ferrum as compared to equimolar concentrations of haemin is supported by findings on PC12 and SH-SY5Y cells (Levy *et al.*, 2002).

VI.3. Use of oligomycin-A as an approach to ischaemia-related phenomena

Our second attempt was to introduce the use of oligomycin-A[9] into our *in vitro* simulation approaches to intracerebral haemorrhage. Oligomycin is a macrolide and an inhibitor of the mitochondrial F_0F_1 ATP synthase; an enzyme necessary for the conduction of oxidative phosphorylation toward the production of ATP (Brand and Nicholls, 2011). Along with OGD, glucose-deprivation and excitotoxicity-triggering NMDA administration, the use of mitochondrial inhibitors (such as oligomycin or NaCN) are thought to be useful techniques for the *in vitro* simulation of neuronal death within an ischaemic penumbra (Taoufic and Probert, 2008). In view of this property of oligomycin, and being aware of a recent study in which oligomycin has been employed as an inducer of autophagy within the context of an *"in vitro mimic of the ischaemic penumbra"* (Pamenter *et al.*, 2012), we decided to consider oligomycin as a condition suitable for the (additional) *in vitro* simulation of the primary injury induced by intracerebral haemorrhage (see subchapter I.8). This decision was also justified by the ongoing controversy over the nature of the perihaematomal penumbra (briefly mentioned in subchapter I.8; Thiex and Tsirka, 2007) and the suggestion of the latter being primarily "metabolic"[10] rather than "ischaemic" (Vespa, 2009); a dilemma that would ideally be represented by the use of oligomycin in this context (Figure C.5).

As a consequence of this decision, we undertook a preliminary assessment of the neurotoxicity of oligomycin (tested at a final concentration of 1 μg/mL; Dayan *et al.*, 2009) and / or of ferrum or haemin (at various concentrations: 0, 5, 50, 100 and 500 μM) on mHippoE-14 cells, through MTT reduction and released LDH[11] activity assays after a 24 h exposure in the absence of FBS (Figure C.6). The results obtained were not consistent with regards to statistical significance of the oligomycin-induced effects amongst the conducted experiments, but suggested an oligomycin-induced decreased MTT reduction activity (Figures C.6.b and C.6.c) and an oligomycin-induced increased released LDH activity (Figures C.6.d and C.6.e). Moreover, the same experiments have suggested that the co-exposure of the mHippoE-14 cells to haemin and oligomycin could exacerbate the oligomycin-induced neurotoxicity, particularly when the first is administered at a concentration of 500 μM (Figures C.6.c and C.6.e).

---

[9] hereafter simply referred to as "oligomycin", in most cases.

[10] it has been reported, for example, that the immediately-attached to the intracerebral haematoma perihaematomal brain region displays a reduction of its oxidative metabolism with very low rates of oxygen use, due to hypoperfusion rather than ischaemia (Zazulia *et al.*, 2001).

[11] the herein described released LDH assays were performed in accordance to the *In Vitro* Toxicology Assay Kit, Lactic Dehydrogenase based (catalog number: TOX7; Sigma-Aldrich) instructions.

In order to shed more light on these findings, we subsequently undertook a real-time cellular response analysis of the mHippoE-14 cell-line under the same *in vitro* conditions (see Figure APP.1), and realized that: (a) oligomycin is the leading cause for the reduction of nCI in mHippoE-14 cells, (b) ferrum or haemin exert their highest toxicity at 500 μM (irrespectively of the presence of oligomycin), and (c) the addition of these compounds within the metaptotic phase modifies the mHippoE-14 metaptotic response and, thus, should be avoided. These findings have prompted us to undertake a final experiment within this set of preliminary experimental attempts, in which the exposure of the mHippoE-14 cells to oligomycin was simultaneous to the FBS-deprivation, but both the additions of ferrum and haemin to the media (at various concentrations) were performed significantly later (12 h after the induction of metaptosis) (Figure C.7); an experimental design closer to the neuropathological reality of intracerebral haemorrhage, where the primary injury precedes the secondary one. This final experiment has produced encouraging results with regards to the adoption of oligomycin as a suitable option for the exertion of a slowly-progressing metabolic penumbra-mimicking "injury" on the mHippoE-14 cells, and to its further complication with the addition of either haemin or ferrum at the highest tested concentration (500 μM) (Table C.1).

VI.4. Development of two distinct and dynamic *in vitro* experimental settings

The aforementioned preliminary experiments have indicated that the use of FBS-deprivation along with the exposure of the mHippoE-14 cells to oligomycin (1 μg/mL) and, later on, to haemin or ferrum (500 μM), could define two[12] novel *in vitro* experimental settings that could be of considerable value for the simulation of intracerebral haemorrhage. If these conditions were combined in a protocol that would allow for an undisturbed metaptosis, the two novel *in vitro* simulation approaches to intracerebral haemorrhage would have the potential to form reliable, distinct and dynamic experimental settings that would: (a) be 3R-friendly (due to the use of the chosen cell-line), (b) be relatively easy to set up and perform experiments on, (c) be employing acceptable (and stoichiometrically-matching) haemin and ferrum concentrations, (d) be introducing the simulation of multiple aspects of the disease's pathophysiology, (e) be limiting the use of FBS, (f) be providing detectable toxicity / injury by both conventional and novel (e.g. the xCELLigence technology) approaches, and (g) be promising of high-throughput applicability (Table C.2).

>> Table C.1: page 109

>> Table C.2: page 110

>> Figure C.1: page 111

[12] one considering the toxicity of haemin as a final simulation endpoint of the "secondary injury", and the other one considering that of ferrum; both after an oligomycin-induced simulation of the "primary injury" of intracerebral haemorrhage.

>> Figure C.2: page 112
>> Figure C.3: page 113
>> Figure C.4: page 114
>> Figure C.5: page 115
>> Figure C.6: page 116
>> Figure C.7: page 117

Table C.1: Preliminary assessment of the cellular response of mHippoE-14 to various concentrations of haemin or ferrum, in the presence or absence of oligomycin.

Treatment	**nCR$_{(Rt,Ee)}$** (nCI/h)	**nCI$_{(E48)}$** (nCI)	**nCI$_{(Ee)}$** (nCI)
control	-0.005	0.811 ± 0.030	0.763 ± 0.031
haemin (5 μM)	-0.005	0.847 ± 0.017	0.802 ± 0.010
haemin (50 μM)	-0.006	0.822 ± 0.024	0.774 ± 0.027
haemin (100 μM)	-0.010	0.782 ± 0.066	0.682 ± 0.070
haemin (500 μM)	-0.014	0.672 ± 0.048	0.544 ± 0.069
oligomycin	-0.019	0.494 ± 0.020	0.307 ± 0.020
oligomycin + haemin (5 μM)	-0.018	0.502 ± 0.036	0.310 ± 0.037
oligomycin + haemin (50 μM)	-0.018	0.495 ± 0.014	0.310 ± 0.009
oligomycin + haemin (100 μM)	-0.020	0.494 ± 0.038	0.290 ± 0.031
oligomycin + haemin (500 μM)	-0.023	0.425 ± 0.029	0.196 ± 0.024
control	-0.005	0.840 ± 0.026	0.812 ± 0.030
ferrum (5 μM)	-0.006	0.802 ± 0.037	0.742 ± 0.022
ferrum (50 μM)	-0.009	0.768 ± 0.041	0.675 ± 0.060
ferrum (100 μM)	-0.010	0.716 ± 0.032	0.604 ± 0.031
ferrum (500 μM)	-0.018	0.659 ± 0.052	0.484 ± 0.046
oligomycin	-0.017	0.527 ± 0.027	0.358 ± 0.054
oligomycin + ferrum (5 μM)	-0.018	0.495 ± 0.053	0.307 ± 0.049
oligomycin + ferrum (50 μM)	-0.018	0.487 ± 0.022	0.292 ± 0.018
oligomycin + ferrum (100 μM)	-0.019	0.481 ± 0.010	0.285 ± 0.010
oligomycin + ferrum (500 μM)	-0.024	0.425 ± 0.010	0.208 ± 0.010

Note: results based on a single experiment (ID: 1210132003), where the addition of oligomycin (1 μg/mL) into the E-Plate 96 wells was performed along with FBS-deprivation (metaptosis), and the addition of ferrum or haemin followed after approximately 12 h. The nCR$_{(Rt,Ee)}$ values are expressed as mean, and the nCI$_{(E48)}$ and nCI$_{(Ee)}$ values are expressed as mean ± standard deviation of intra-assay triplicates; normalization occurs at 24:36:46, R_t is considered at 37:04:50 and E_e is at 60:55:00. For a visualization of this experiment, see Figure C.7.

E_{48}: evaluation endpoint at 48 h; E_e: end of the experiment; FBS: foetal bovine serum; nCI: normalized cell index; nCR: normalized cellular response; R_t: recovery point after a treatment intervention

Table C.2: Practical advantages of the conditions chosen to be included in the developed *in vitro* simulation approaches to intracerebral haemorrhage.

Practical advantages of the developed *in vitro* simulation approaches' conditions
– are 3R-friendly (due to the use of an immortalized cell-line)
– are easy to perform
– use acceptable (and matching) haemin and ferrum concentrations
– introduce the simulation of multiple aspects of the disease's pathophysiology
– are limiting the use of FBS
– provide detectable toxicity / injury by both conventional and novel approaches
– are promising of high-throughput applicability

Note: this basic account of practical advantages is based on the data obtained through the preliminary assessment of the conditions chosen for the development of the *in vitro* simulation approaches to intracerebral haemorrhage; not on data deriving for their assessment (Chapter VII).

FBS: foetal bovine serum

Figure C.1: Preliminary assessment of the toxicity of ferrum or haemin on mHippoE-14 cells: MTT reduction activity after a 24 h exposure in the presence of FBS.

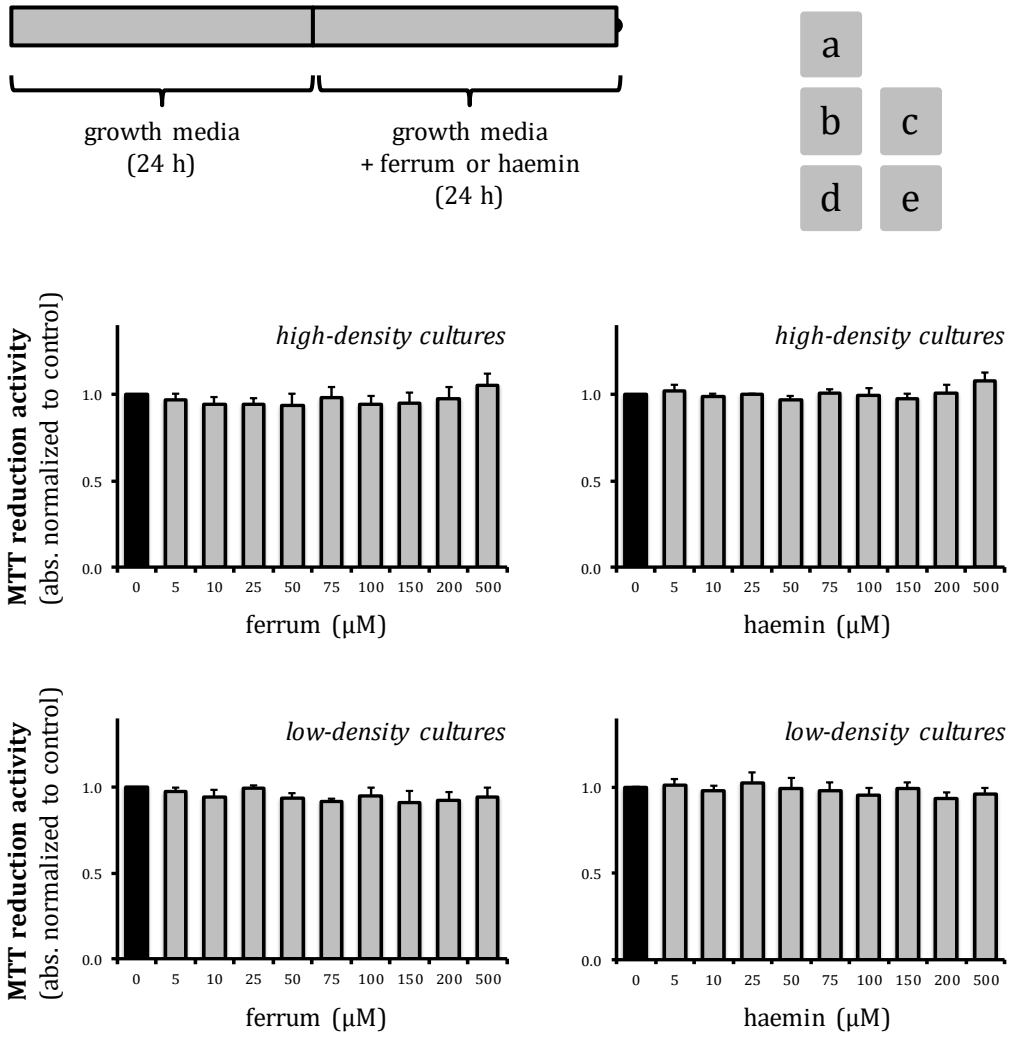

Note: the presented data refer to a single preliminary experiment in which every treatment group was assessed in triplicate (intra-assay's n=3); all data of Figures C.1.b to C.1.e are presented as normalized mean ± standard error. For more details on the experiment's protocol, see subchapter VI.1.

FBS: foetal bovine serum; MTT: 3-(4,5-dimethylthiazol-2-yl)-2,5-diphenyltetrazolium bromide

Figure C.2: Preliminary assessment of the toxicity of ferrum or haemin on mHippoE-14 cells: MTT reduction activity after a 24 h exposure in the absence of FBS.

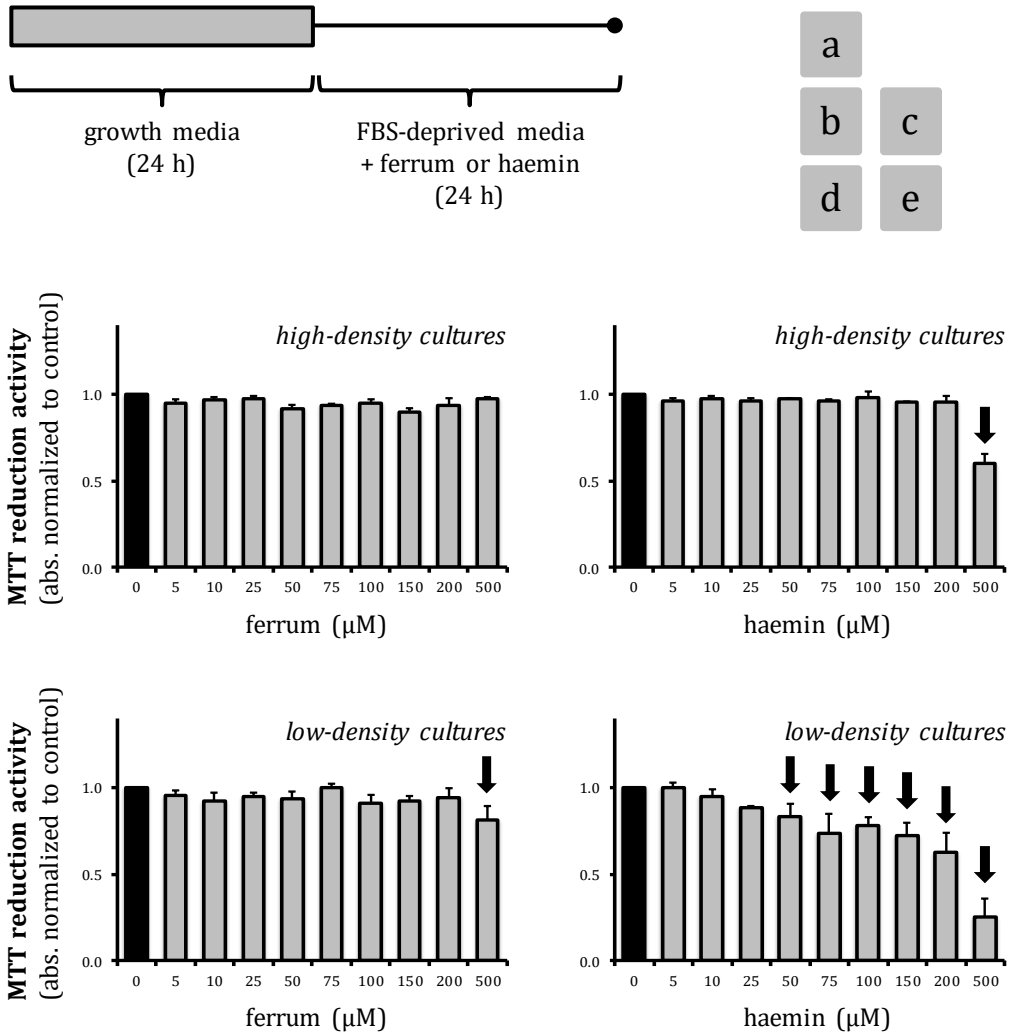

Note: the presented data refer to a single preliminary experiment in which every treatment group was assessed in triplicate (intra-assay's n=3); all data of Figures C.2.b to C.2.e are presented as normalized mean ± standard error. Arrows indicate normalized mean differences higher than 15% as compared to control (black columns). For more details on the experiment's protocol, see subchapter VI.1.

FBS: foetal bovine serum; MTT: 3-(4,5-dimethylthiazol-2-yl)-2,5-diphenyltetrazolium bromide

Figure C.3: Preliminary assessment of the toxicity of ferrum or haemin on mHippoE-14 cells: MTT reduction activity after a 48 h exposure in the presence of FBS.

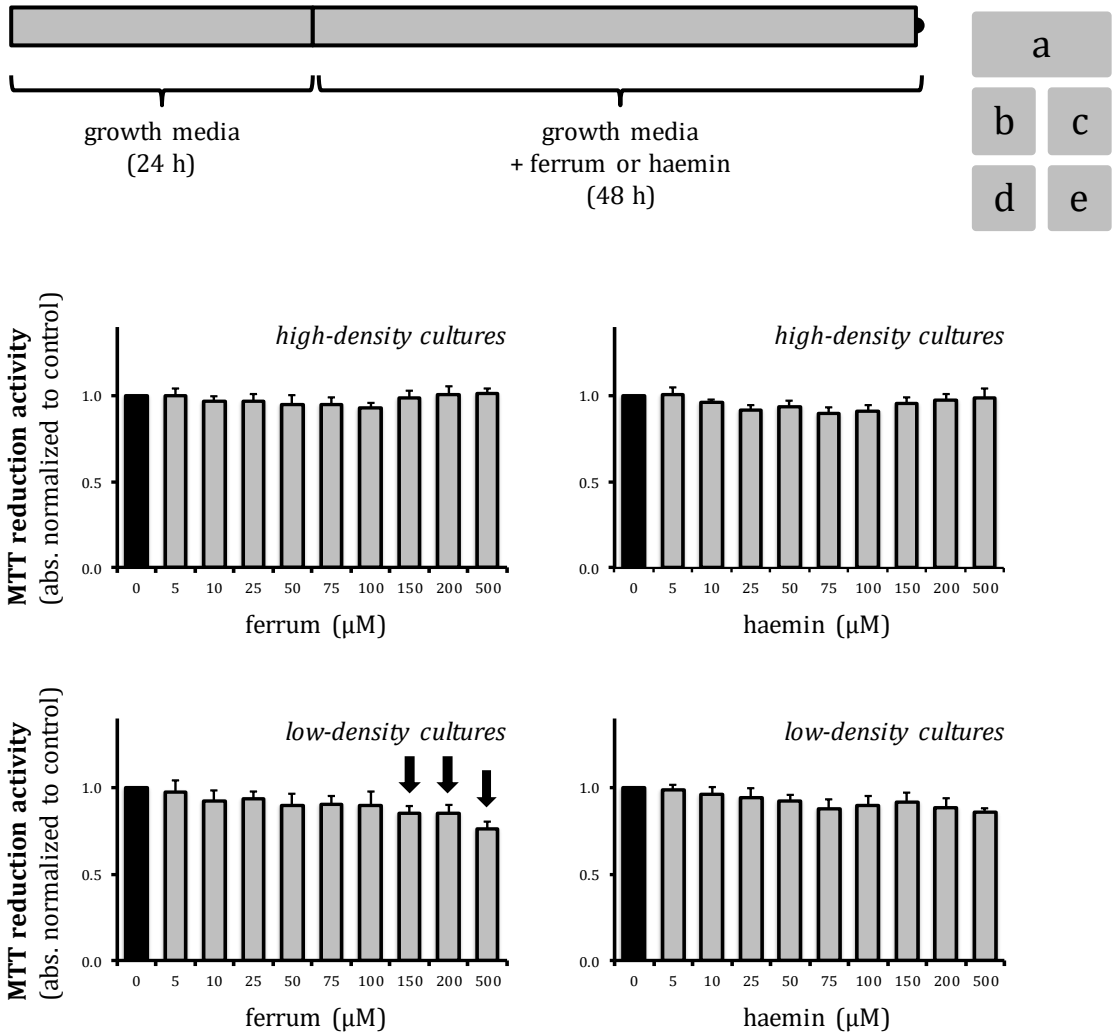

Note: the presented data refer to a single preliminary experiment in which every treatment group was assessed in triplicate (intra-assay's n=3); all data of Figures C.3.b to C.3.e are presented as normalized mean ± standard error. Arrows indicate normalized mean differences higher than 15% as compared to control (black columns). For more details on the experiment's protocol, see subchapter VI.1.

FBS: foetal bovine serum; MTT: 3-(4,5-dimethylthiazol-2-yl)-2,5-diphenyltetrazolium bromide

Figure C.4: Preliminary assessment of the toxicity of ferrum or haemin on mHippoE-14 cells: MTT reduction activity after a 48 h exposure in the absence of FBS.

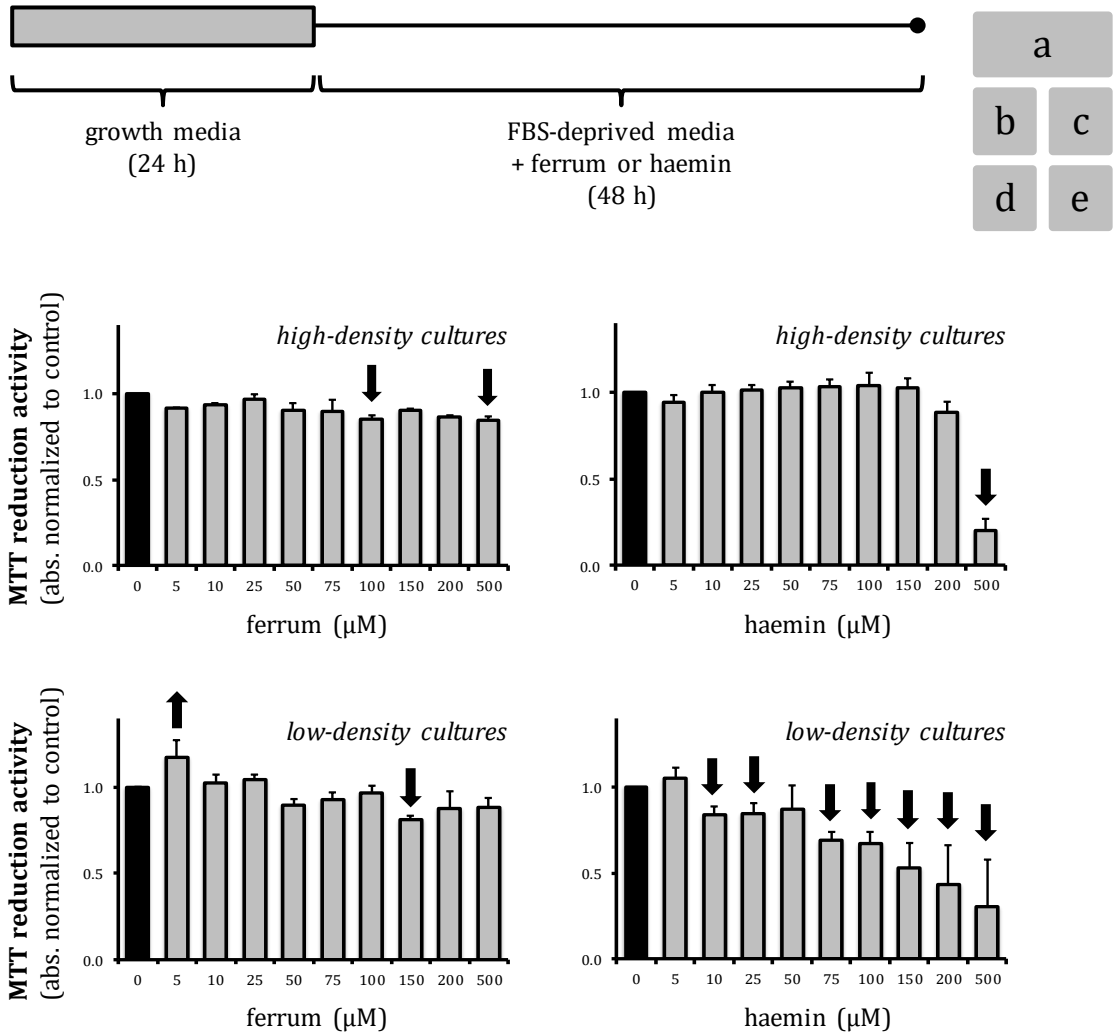

Note: the presented data refer to a single preliminary experiment in which every treatment group was assessed in triplicate (intra-assay's n=3); all data of Figures C.4.b to C.4.e are presented as normalized mean ± standard error. Arrows indicate normalized mean differences higher than 15% as compared to control (black columns). For more details on the experiment's protocol, see subchapter VI.1.

FBS: foetal bovine serum; MTT: 3-(4,5-dimethylthiazol-2-yl)-2,5-diphenyltetrazolium bromide

Figure C.5: Oligomycin-A as an *in vitro* tool for the simulation of aspects of ischaemic or metabolic penumbra.

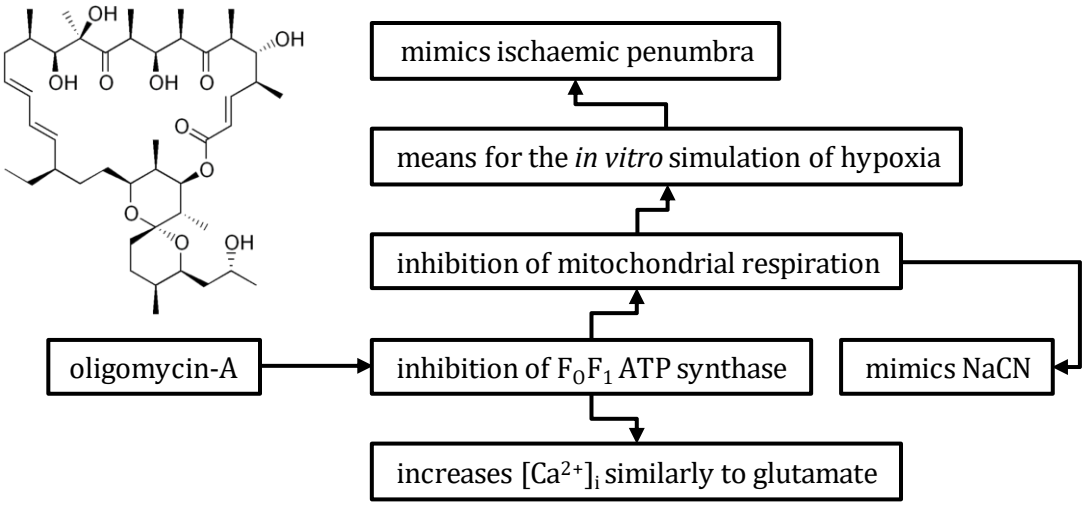

Note: oligomycin blocks the F_0 subunit of the F_0F_1 ATP synthase and, as a result, inhibits ATP synthesis. The presented functions of oligomycin are based on data from Dubinsky and Rothman (1991) and Pamenter *et al*. (2012).

$[Ca^{2+}]_i$: intracellular calcium concentration; ATP: adenosine triphosphate; NaCN: sodium cyanide

Figure C.6: Preliminary assessment of the toxicity of oligomycin and / or ferrum or haemin on mHippoE-14 cells: MTT reduction and released LDH activity after a 24 h exposure in the absence of FBS.

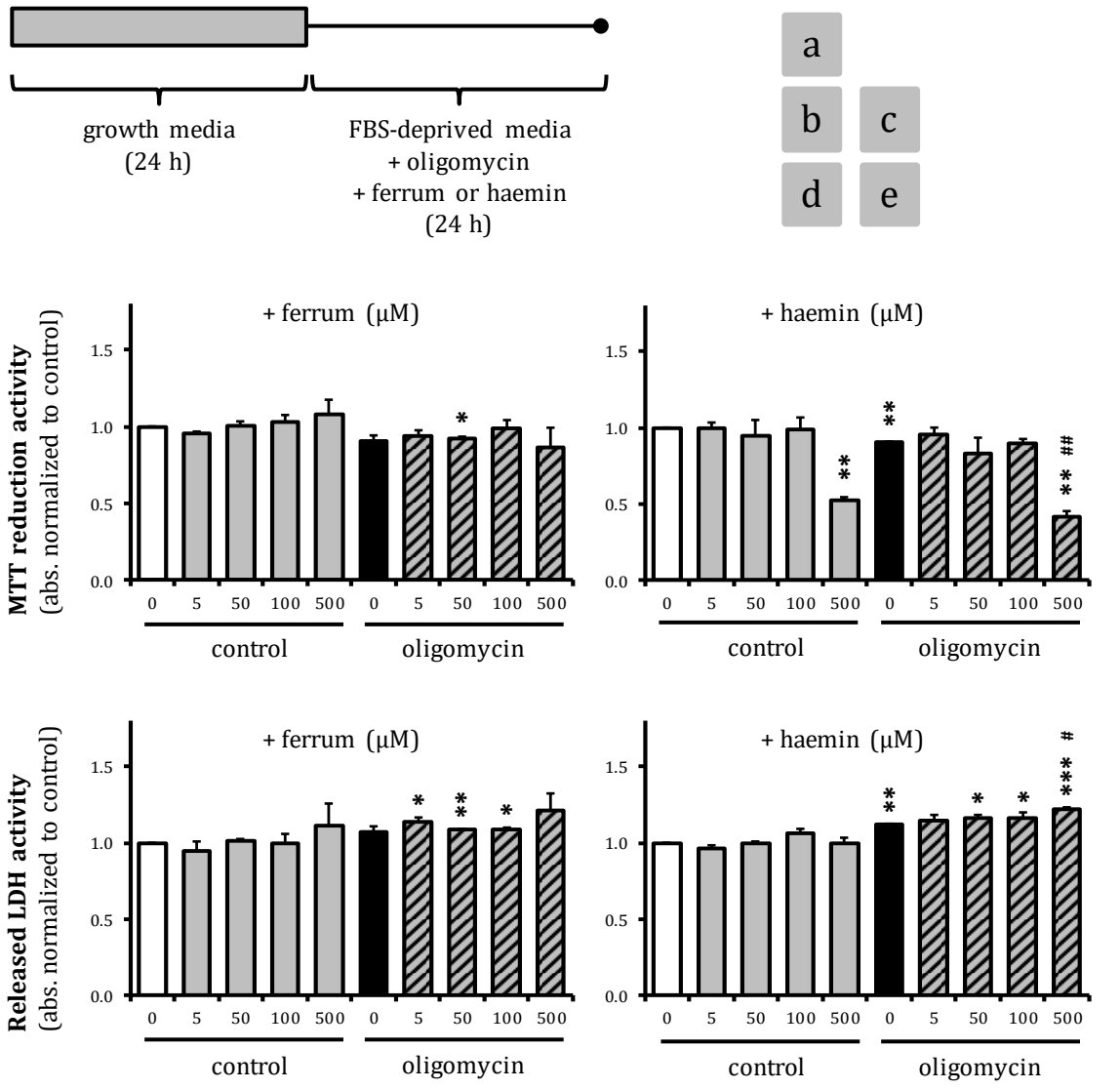

Note: the presented data refer to only two independent preliminary experiments (n=2) in which every treatment group was assessed in triplicate; all data of Figures C.6.b to C.6.e are presented as normalized mean ± standard error, and statistical analysis has been performed through the use of one-way ANOVA followed by *post hoc* Tukey's range test. Only statistically significant differences ($p<0.05$) are annotated. For more details on the experiments' protocol, see subchapter VI.3.

***: $p<0.001$ (as compared to control; white column); **: $p<0.01$ (as compared to control; white column); *: $p<0.05$ (as compared to control; white column); ##: $p<0.01$ (as compared to oligomycin; black column); #: $p<0.05$ (as compared to oligomycin; black column); ANOVA: analysis of variance; FBS: foetal bovine serum; LDH: lactate dehydrogenase; MTT: 3-(4,5-dimethylthiazol-2-yl)-2,5-diphenyltetrazolium bromide

Figure C.7: Preliminary assessment of the cellular response of mHippoE-14 to various concentrations of haemin or ferrum, in the presence or absence of oligomycin.

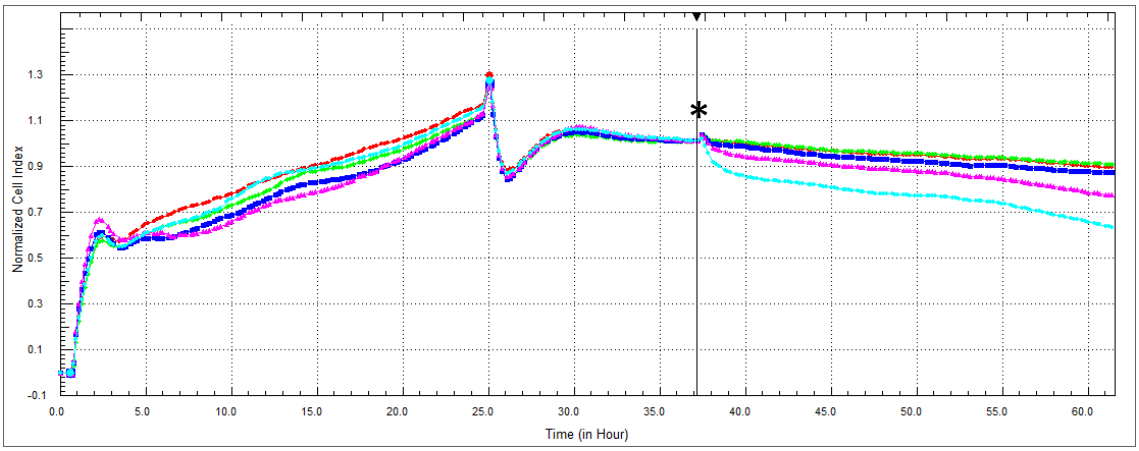

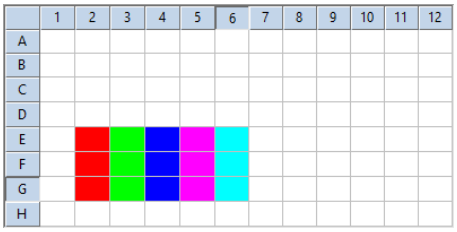

setting A: average nCI per group
normalization at 36:51:17
haemin at 0, 5, 50, 100, 500 μM
*: addition of haemin

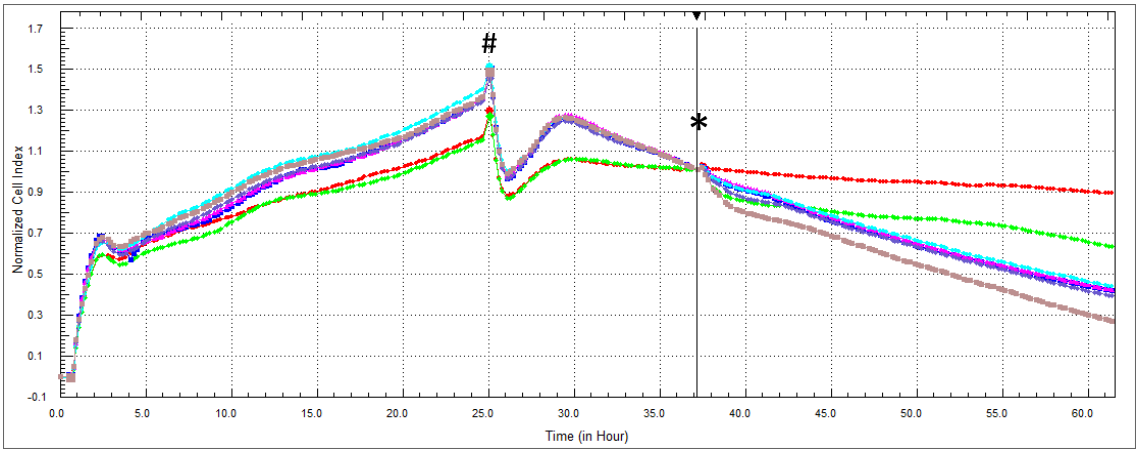

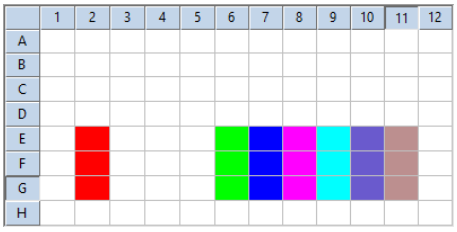

setting B: average nCI per group
haemin at 0 and 500 μM, as above
oligomycin at 1 μg/mL + haemin at 0, 50, 100, 500 μM
#: addition of oligomycin
*: addition of haemin

(continues on next page)

(continues from previous page)

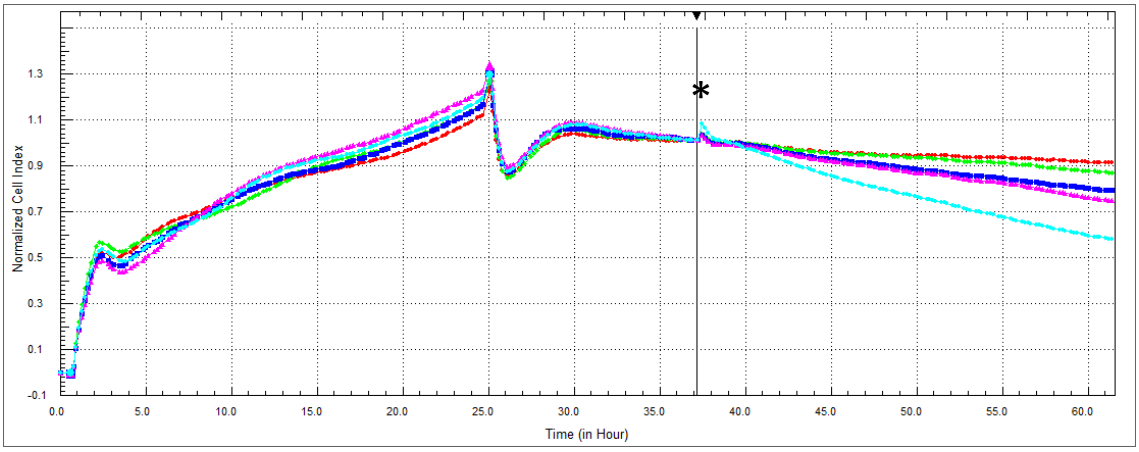

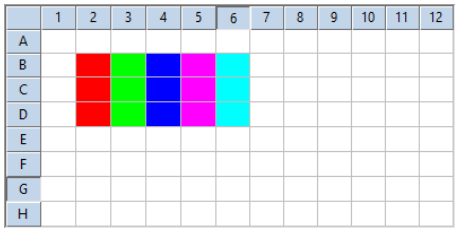

setting C: average nCI per group
normalization at 36:51:17
ferrum at 0, 5, 50, 100, 500 μM
*: addition of ferrum

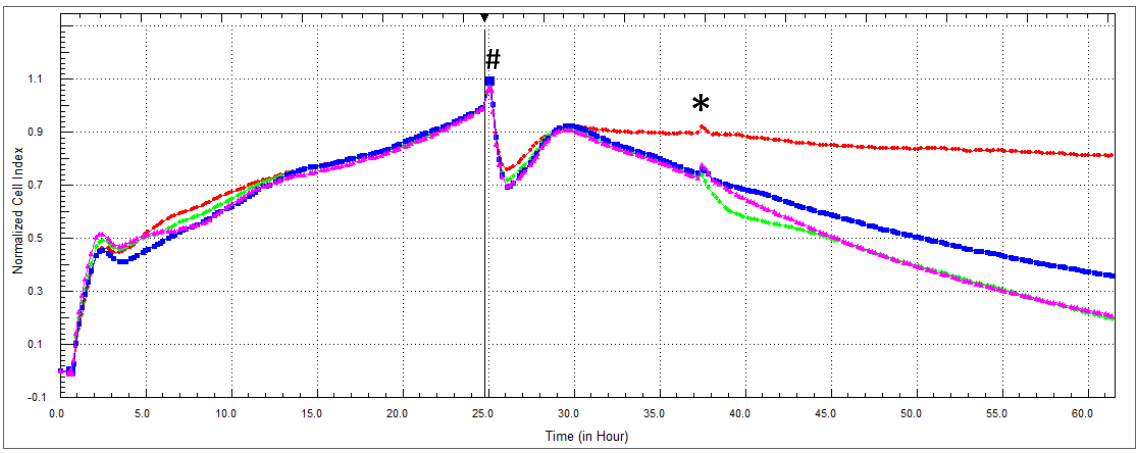

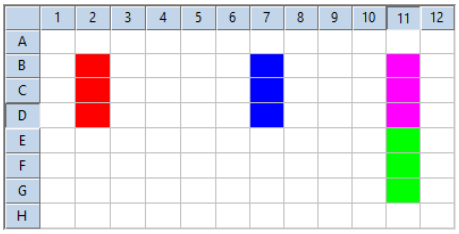

setting D: average nCI per group
normalization at 24:36:46
control
oligomycin
oligomycin + ferrum at 500 μM
oligomycin + haemin at 500 μM
#: addition of oligomycin
*: addition of haemin or ferrum

Note: representative and annotated screen captions from the xCELLigence RTCA SP analysis software (plots and well selection maps) from a single experiment (ID: 1210132003); the addition of oligomycin (1 μg/mL) into the E-Plate 96 wells was performed along with FBS-deprivation (metaptosis), and the addition of ferrum or haemin followed after approximately 12 h. For all settings (A-D), the following key applies: control (B2, C2, D2), ferrum [5 μM] (B3, C3, D3), ferrum [50 μM] (B4, C4, D4), ferrum [100 μM] (B5, C5, D5), ferrum [500 μM] (B6, C6, D6), oligomycin (B7, C7, D7), oligomycin + ferrum [5 μM] (B8, C8, D8), oligomycin + ferrum [50 μM] (B9, C9, D9), oligomycin + ferrum [100 μM] (B10, C10, D10), oligomycin + ferrum [500 μM] (B11, C11, D11), control (E2, F2, G2), haemin [5 μM] (E3, F3, G3), haemin [50 μM] (E4, F4, G4), haemin [100 μM] (E5, F5, G5), haemin [500 μM] (E6, F6, G6), oligomycin (E7, F7, G7), oligomycin + haemin [5 μM] (E8, F8, G8), oligomycin + haemin [50 μM] (E9, F9, G9), oligomycin + haemin [100 μM] (E10, F10, G10), oligomycin + haemin [500 μM] (E11, F11, G11). Data from this experiment are presented in Table C.1.

FBS: foetal bovine serum; nCI: normalized cell index

CHAPTER VII

Assessment of *in vitro* simulation approaches to intracerebral haemorrhage

In a 96-well plate, the seeding of mHippoE-14 cells at a density of 7,500 cells/well and their growth in optimal (growth, FBS-supplemented) medium for 24 h, has been considered as a necessary and adequate step towards the acquisition of a sufficient cell number for the execution of the neuropathopoietic steps to follow, in a manner that: (a) would allow for enough time in order to study (and / or attempt to rescue) the neurotoxic responses of these cells to oligomycin and haemin or ferrum (Chapter VI), and, at the same time, (b) provide a reasonably good confluency of the optical fields[1], that would allow for enough cells to survive metaptosis (Chapter V) and to be subject to some basic cytomorphological assessment of their undergoing cellular responses to the aforementioned insults. At this cell density, our experiments have shown that the subsequent FBS-deprivation of these cells would require approximately 6 h in order to allow for a recovery from metaptosis (Chapter IV); a period of time that we decided to adopt in our *in vitro* simulation approaches to intracerebral haemorrhage, prior to the mHippoE-14 exposure to oligomycin and a subsequent (6 h later) exposure to the chosen products of haemolysis (Figure C.8). For the assessment of the developed *in vitro* simulation approaches to intracerebral haemorrhage that is presented in the current chapter, we undertook: (a) real-time cellular response analysis, (b) phase-contrast microscopy-assisted live-cell cytomorphological assessment, (c) a profiling of selected neuronal markers' expression, (d) some basic neurochemical assessment, and (e) a (cytokine-focused) proteomic profiling of representative treatment states of the mHippoE-14 cells.

VII.1. Real-time cellular response analysis

The undertaking of the assessment of the real-time cellular response of the mHippoE-14 cells under the aforementioned protocol was performed in quadruplicate (n=4), by employing the xCELLigence technology as previously described (Chapter IV). Figure C.9.a summarizes the timeline of interventions monitored, where particular emphasis should be given on the fact that apart from the profiling of the real-time cellular response of the mHippoE-14 cells under

[1] when the protocol would be simulated in 35 mm Corning Dishes (see Chapter V).

the developed *in vitro* simulating conditions, and in parallel or simultaneously to the addition of oligomycin, two drugs were also added and monitored: CDP-Ch and DFO, both at a concentration of 100 μM. Figure C.9.b provides what probably is the most important illustration of this PhD Thesis: the mHippoE-14 cellular response profiling under the four major of the developed *in vitro* conditions (control, oligomycin, oligomycin + haemin, oligomycin + ferrum). The profiling is normalized at the R_m time point and presents a clear but mild decline of the oligomycin-treated mHippoE-14 cells' nCI over time, and a more pronounced decrease of the nCI in the mHippoE-14 treatment groups that were additionally exposed (at 36 h) to haemin or ferrum. A statistically-analysed snapshot of the cellular status of the mHippoE-14 cells at 48, 60 and 72 h is provided in Figures C.9.c, C.9.d and C.9.e, respectively. The latter demonstrates that 36 h after the addition of haemin or ferrum in the oligomycin-containing media (OH_{72} or OF_{72}), the nCI values of the mHippoE-14 cells are -73% (p<0.001) or -71% (p<0.001) as compared to the control (C_{72}), and -44% (p<0.01) or -38% (p<0.01) as compared to oligomycin treatment group (O_{72}), respectively.

An estimation of the statistical effect size through the Z-factor[2], where the mHippoE-14 O, OH and OF cellular status values (as nCI) were considered as samples and the respective C values as the control, was attempted for the means and standard deviations of each of the conducted four aforementioned experiments, at 48, 60 and 72 h (Table APP.4). In the majority of the cases, the Z-factors were higher than 0.5 and lower than 1, indicating that the real-time cellular response profiling of the mHippoE-14 cells at the given time points, under the examined conditions, can be classified an "excellent assay" for the high-throughput screening of potential neuroprotective drugs, but could also be subject to further optimization (Zhang *et al.*, 1999).

As a sample of how such potentially-neuroprotective drugs could modify the cellular status of the chosen conditions, the membrane stabilizer CDP-Ch (Hurtado *et al.*, 2005; Matyja *et al.*, 2008) and the iron-chelator DFO (Braughler *et al.*, 1988; Hua *et al.*, 2008) were tested. The first was found, in most cases, to exert no statistically significant effects on the *in vitro* simulating approaches to intracerebral haemorrhage (Figure C.10), while DFO (at the tested concentration; 100 μM) was found to be extremely toxic for the control and oligomycin-treated mHippoE-14 cells and (statistically significantly) beneficial for the haemin- and the ferrum-treated ones that have previously been exposed to oligomycin (Figure C.11). The latter could imply an iron-dependent mechanism of survival for the mHippoE-14 cells, while it is likely that the DFO concentration tested in our experiments was very high (Chen-Roetling *et al.*, 2001).

[2] the Z-factor is used for the categorization of the quality of a screening assay as well as its optimization; for Z-factor values higher than 0.5, one can characterize an assay as "excellent", while for values lower than 0, one must interpret that the screening is "impossible" (Zhang *et al.*, 1999).

Finally, the nCR values of the mHippoE-14 within the developed *in vitro* simulation approaches to intracerebral haemorrhage, focused on the time between 48 and 60 h, are provided in Table C.3. These data confirm a particularly neuroprotective effect of DFO in the case of the OH (oligomycin + haemin) treatment group, where the mHippoE-14 cells tend to maintain their nCR values close to 0 / control levels (Table C.3).

VII.2. Cytomorphological assessment

Representative captions and the findings of the phase-contrast microscopy-assisted live-cell cytomorphological assessment performed on the developed *in vitro* simulation approaches to intracerebral haemorrhage, are presented in Figures C.12 and C.13, respectively. The addition of oligomycin to the media exerts no statistically significant effects on the mHippoE-14 confluency at 36 h (at least as assessed; see Table B.8 and Figure C.13.a), but does cause a statistically significant decrease at 48 and 72 h ($p<0.05$ and $p<0.01$, respectively). The addition of oligomycin also causes a significant decrease of the mHippoE-14 aggregation at 72 h ($p<0.01$; Figure C.13.b), but causes no significant change on the cell cultures' background score (results not shown). Moreover, the oligomycin-treated cellular groups that get exposed to haemin or ferrum present with a statistically significantly decreased confluency scores (Figure C.13.a), as well as with statistically significantly decreased aggregation scores ($p<0.001$ in all cases; Figure C.13.b), and increased background scores ($p<0.001$ at both 48 and 72 h when compared to respective control cultures; results not shown); the latter are even reaching as high as level 4 (in the 0 to 5 scale; see Table B.8) in the case of the OF_{48} and OF_{72} treatment groups, indicating the extensive presence of debris in these conditions (Figure C.12).

It is the author's estimation (through observation) that a small shrinkage of the cytoplasm of the mHippoE-14 cells occurs due to oligomycin[3], and that this shrinkage is further exacerbated by haemin or ferrum, along with the induction of cell death; all compatible with the findings of the real-time cellular response profiling of these conditions. However, the debris accumulating due to the addition of ferrum (and to a lesser extent of haemin) into the media, make the cytomorphological assessment a hard task for one to perform, as floating debris (as number per caption) is a parameter impossible to assess, and the washing of cells with phosphate-buffered saline (PBS) prior to captioning could not resolve the problem (Figure APP.2).

VII.3. Profiling of neuronal markers' expression

The third step in the assessment of the developed *in vitro* simulation approaches to intracerebral haemorrhage has been the profiling of the expression of a number of neuronal markers

[3] ischaemic neuronal injury is a well-known cause of cytoplasmic shrinkage (Mena *et al.*, 2004).

at cell lysates obtained at 30, 36 and 48 h (Figure C.8). In brief, cell lysates were generated by scraping cells into ice-cold lysis buffer[4] and incubating on ice for 30 min, with vortexing at 10 min intervals. Lysates were then cleared by centrifugation at 14,000 rpm, for 10 min, at 4^{o}C, and their protein concentrations were determined according to the method of Lowry *et al.* (1951). Prior to loading for sodium dodecyl sulfate polyacrylamide gel electrophoresis (SDS-PAGE), the mHippoE-14 lysates were boiled for 2 min in 2x Laemmli sample buffer[5] at 95^{o}C. Subsequently, Western blotting was performed using the Novex[6] NuPAGE[7] SDS-PAGE Gel System (Thermo Fisher Scientific Inc.) following manufacturer's guidelines. The produced membranes were then blocked in 5% skimmed milk in Tris-buffered saline - Tween 20 (TBS-T)[8] for 1 h, at room temperature, prior to being exposed (overnight, at 4^{o}C) to the primary antibodies (Table C.4) that were diluted in 1% milk in TBS-T. The blots were then washed 3 times in TBS-T, and were incubated with fluorophore-conjugated secondary antibodies[9] (LI-COR Inc.; diluted in 1% milk in TBS-T; 1:10,000) for 1 h, at room temperature, followed by 3 TBS-T washes. Finally, the blots were visualized and their signal densitometry values were obtained using the Odyssey Classic imaging system and software (LI-COR Inc.).

Of the 9 neuronal markers sought after, 5 could not be detected at the attempted primary antibody dilutions (Table C.4): the calcium-binding proteins calbindin (CB), calretinin (CAL2) and parvalbumin (PV), the immature neurons' marker doublecortin (DCX), and the popular 200 kDa + 160 kDa neurofilament (SMI-310). Of the neuronal markers that were detected, FBS-deprivation was found to particularly decrease the expression of synapsin I in mHippoE-14 cells at the R_m time point (p<0.001, as compared to non-FBS-deprived control at 30 h; Figure C.14), while treatment with oligomycin (as assessed at 36 h; O_{36}) was found to cause a statistically-significantly decrease of the alpha 1 subunit of Na^+,K^+-ATPase (α1 Na^+,K^+-ATPase; p<0.01), the choline acetyltransferase (ChAT; p<0.01) and the synapsin I (p<0.001) expression levels (as compared to C_{36}; Figure C.15). When assessed at 48 h, the only treatment group that produced statistically-significant changes in its neuronal markers' expression (as compared to C_{48}) has been the OH_{48} treatment group, with a 7-fold increase in the mHippoE-14 expression of HO-1 (p<0.05; Figure C.16) and a decrease in the expression of the α1 Na^+,K^+-ATPase (p<0.01; Figure C.16).

[4] purchased by Sigma-Aldrich (product number: R0278).
[5] purchased by Sigma-Aldrich (product number: S3401).
[6] Novex®.
[7] NuPAGE®.
[8] TBS-T consists of 50 mM tris(hydroxymethyl)aminomethane (Tris), 150 mM sodium chloride (NaCl), and 0.05% Tween 20; all adjusted to pH 7.6.
[9] the following secondary antibodies were used: IRDye 800CW donkey anti-rabbit IgG (H+L), (product number: 925-32213), IRDye 800CW donkey anti-goat IgG (H+L) (product number: 925-32214), IRDye 800CW donkey anti-mouse IgG (H+L) (product number: 925-32212), IRDye 680RD donkey anti-mouse IgG (H+L), (product number: 925-68072), IRDye 680RD donkey anti-rabbit IgG (H+L) (product number: 925-68073); all purchased from LI-COR Inc.

Synapsin I is a synaptic vesicle protein that ties the vehicle to the neuronal cytoskeleton (Jovanovic *et al.*, 2000), characterizes functional neurons (Guan *et al.*, 2016) and is a key-modulator of neuroplasticity (Okabe *et al.*, 1998; Ploughman *et al.*, 2005). Its decreased expression due to both FBS-deprivation ($p<0.001$; Figure C.14) and oligomycin ($p<0.001$; Figure C.15) could indicate synaptic loss due to injury and / or loss of the mHippoE-14 functionality.

Na^+,K^+-ATPase is a major consumer of ATP in neurons (Erecińska and Silver, 1994) and (amongst others) the enzyme responsible for the maintenance of neuronal excitability (Sastry and Phillis, 1977). The decrease in the expression of its α1 subunit in O_{36} cells ($p<0.01$, as compared to C_{36} cells; Figure C.15) comes as no surprise, as oligomycin should restrict ATP availability and thus, cause a downregulation of the Na^+,K^+-ATPase subunits' synthesis. Moreover, the blocking or the decline in Na^+,K^+-ATPase functionality has also been considered as an apoptotic mechanism (Wang *et al.*, 2003), while one must not exclude the possibility of a direct role[10] of oligomycin in the observed phenomena (Arato-Oshima *et al.*, 1996). It should be noted, however, that although hippocampal neurons express the α1 subunit of Na^+,K^+-ATPase in the membranes of both axons and dendrites (Pietrini *et al.*, 1992), the same subunit isoform is not a hippocampal neuron-specific marker as it can also be found expressed in glial cells (Cameron *et al.*, 1994; Kwon *et al.*, 2003). Moreover, in a recent *in vivo* study of ours (Bimpis *et al.*, 2013), Na^+,K^+-ATPase activity was found unaltered when compared amongst the perihaematomal and the neuroanatomically-matching (control) region of swines, 4 and 24 h following autologous blood infusion.

The cholinergic marker ChAT was found to be expressed by O_{36} mHippoE-14 cells, but at statistically significantly lower levels than the respective control ones ($p<0.01$ as compared to C_{36}; Figure C.15); a trend that was confirmed 12 h later at a non-statistically significant level ($p>0.05$; Figure C.16). Knowing that ChAT is the enzyme responsible for the synthesis of acetylcholine (ACh) and a marker of cholinergic neurons (Shi *et al.*, 2012), the finding might imply a downregulation of the cholinergic function / ACh-synthesizing capacity of the oligomycin-treated cells due to the metabolic stress implemented by oligomycin; a suggestion that would have been in agreement with previous studies on other cytotoxic conditions (Barald, 1989; Osborne *et al.*, 1995), but wouldn't have managed to explain the reason the OF_{48} or the OH_{48}[11] cells do not follow this pattern (Figure C.16).

Finally, the induction of HO-1 expression due to haemin ($p<0.05$, in OH_{48} as compared to C_{48} levels; Figure C.16) is a particularly welcome finding, in view of its role in degrading haemin and acting as a marker of oxidative stress related to cellular injury (Chow *et al.*, 2008; Sharp, 1995; Wagner *et al.*, 2003). Although the induction of HO-1 in the context of intracere-

[10] oligomycin is known to interact with the sodium ion (Na^+) occlusion site on the extracellular side of Na^+,K^+-ATPase and, as a result, delay the release of Na^+ (Arato-Oshima *et al.*, 1996).

[11] in fact, the OH_{48} cells are characterized by an increased expression of ChAT ($p>0.05$, as compared to C_{48}; Figure C.16) under the experimental conditions studied.

bral haemorrhage is induced primarily by non-neural cells *in vivo* (Wang, 2014), neurons are also known to express HO-1 in ischaemic brain regions (Geddes *et al.*, 1996; Nimura *et al.*, 1996; Wagner *et al.*, 2003), sometimes in a transient way (Matsuoka *et al.*, 1998; Takeda *et al.*, 1996; Wagner *et al.*, 2003), and more likely as a neuroprotective response (Hua *et al.*, 2007; Wagner *et al.*, 2003). However, Suttner and Dennery (1999) have suggested that a marked overexpression of HO-1 could also result to cell death due to iron accumulation; a claim that might explain the fate of the mHippoE-14 cells in the OH_{48} treatment group, and be considered to be confirmed by the recent study of Kwon *et al*. (2013) where valproic acid was suggested to exert neuroprotection in intracerebral haemorrhage-related experimental contexts through the decrease of HO-1 expression, both *in vivo* and *in vitro*.

VII.4. Neurochemical assessment

The neurochemical assessment of the mHippoE-14 cells under the developed intracerebral haemorrhage-simulating *in vitro* conditions has been limited to the undertaking of acetylcholinesterase (AChE) activity assays. Two sets of experiments were conducted: (a) the assessment of the AChE activity of mHippoE-14 cells at 48 h under the developed intracerebral haemorrhage-simulating *in vitro* conditions (conditions C_{48}, O_{48}, OH_{48} and OF_{48}), and (b) the assessment of the effects of media deriving from these same *in vitro* conditions on *Electrophorus electricus* (electric eel) pure AChE activity, following an 1 h incubation. A third set of experiments assessing the effects of media deriving from earlier *in vitro* conditions on *Electrophorus electricus* (electric eel) pure AChE activity was unsuccessful, due to the very high values recorded in the presence of FBS-supplemented media[12].

For the first set of experiments, mHippoE-14 cells at 48 h (that have been grown in 6-well plates; conditions C_{48}, O_{48}, OH_{48} and OF_{48}) were washed twice with ice cold (0-4^{o}C) PBS prior to being treated with an ice-cold (0-4^{o}C) buffer containing 50 mM Tris-hydrochloride (Tris-HCl), pH 7.4, and 300 mM sucrose, and being mechanically scrapped from their wells. Subsequently, the lysates were centrifuged at 1,000 × g for 10 min in order to remove nuclei and debris, and in the resulting supernatants, the protein content was determined according to the method of Lowry *et al*. (1951), and the activity of AChE was determined by recording the hydrolysis rate of acetylthiocholine (at 37^{o}C) according to the method of Ellman *et al*. (1961), following the exact procedure described in detail by Tsakiris (2001). The AChE assay incubation mixture (1 mL) contained 50 mM Tris-HCl, pH 8, 240 mM sucrose, and 120 mM NaCl. The protein concentration of the incubation mixture was 1-3 μg/mL. The reaction was initiated after addition of 0.03 mL of 5,5'-dithionitrobenzoic acid (DTNB), and 0.05 mL of acetylthiocholine iodide, which was used as a substrate. The final concentration of DTNB and

[12] it is known that FBS contains AChE in it (Chatonnet and Lockridge, 1989; Ralston *et al.*, 1985).

substrate were 0.125 and 0.5 mM, respectively. The reaction was followed spectrophotometrically[13] over a period of 120 sec, by the increase of absorbance (ΔOD) at 412 nm, where ΔOD accounts for the mean of the difference in the optical density measured.

For the second set of experiments, media from the mHippoE-14 cell cultures at 48 h (*in vitro* conditions same as for the first set) were obtained and centrifuged at 1,000 x g for 10 min in order to remove nuclei and debris. The commercially-available pure enzyme (product C3389, Sigma-Aldrich; electric eel AChE) was incubated for 1 h (37^{o}C) at a concentration of 0.120 μg/mL in a reaction mixture (1 mL) that contained 50 mM Tris-HCl, pH 8, 240 mM sucrose, 120 mM NaCl and 50 μL of media, prior to the addition of DTNB and acetylthiocholine iodide, and the determination of AChE activity as described above.

Figure C.17 presents our findings with regards to the activity of the mHippoE-14 cells' AChE under the developed intracerebral haemorrhage-simulating *in vitro* conditions (Figure C.17.a), and of *Electrophorus electricus* pure AChE following incubation with media deriving from mHippoE-14 cell cultures under the same *in vitro* conditions (Figure C.17.b). Unfortunately, none of the conducted experiments produced any statistically significant findings, either due to the very low AChE activity levels detected or the very low expression of this enzyme by the mHippoE-14 cells under FBS-deprivation. This was a rather disappointing outcome in view of our interest in studying the mHippoE-14 cellular response to the developed *in vitro* simulation approaches to intracerebral haemorrhage through the assessment of the activity of this crucial cholinergic marker[14], but, on the other side, the findings did fit well (if to be considered as sufficiently reliable[15]) to our recent *in vivo* work on swines (Bimpis *et al.*, 2012) that has found no differences between the affected and the non-affected (but neuroanatomically-matching) brain regions' AChE activity, 4 and 24 h following autologous blood infusion.

VII.5. Proteomic profiling

Detection of the expression of 111 soluble cytokines, chemokines, and growth factors (Table C.5) in the media of mHippoE-14 cell cultures of the developed *in vitro* simulation approaches to intracerebral haemorrhage, was performed with the commercially-available Proteome Profiler Mouse XL Cytokine Array Kit (R&D Systems, product number: ARY028), which is a membrane-based sandwich immunoassay. Experiments were conducted on the 4 basic developed *in vitro* conditions, at 48 h (C_{48}, O_{48}, OH_{48} and OF_{48}), following the manufacturer's instructions (Figure C.18), while analysis of the array captions was performed through the Im-

[13] a Cole-Parmer S2100 Spectrophotometer (Cole-Parmer Instrument Co. Ltd) was used.
[14] one must note that Lee *et al*. (2010) have suggested the existence of a cholinergic anti-inflammatory pathway that regulates inflammation within the context of intracerebral haemorrhage, based on experimental data.
[15] technically speaking; see subchapter VIII.3.

ageJ (1.48v) software. The findings of these arrays are visualized in Figures C.19, C.20 and C.21, and their most notable "hits" are presented in Table C.6.

Although the proteomic profiling performed is extensive (in terms of analyte content), it is still a collection of arrays whose hits need to be further validated (through Western blotting), on a case-by-case basis. Of the statistically-significant analyte changes presented in Table C.6, one should consider, in future experimental attempts, the elucidation of the following analytes:

- *angiopoietin 1 and angiopoietin 2 (ANGPT1 and ANGPT2):* ANGPT1 levels were found to be very high in the O_{48} and OH_{48} treatment groups (17.5x and 27.7x, respectively, as compared to C_{48}), while ANGPT2 was found increased in the OF_{48} treatment group; both vascular growth factors must be considered as oligomycin-triggered cytokines, and should be further studied in view of their association to BBB permeability (de)regulation within brain injury related contexts (Chittiboina *et al.*, 2013),
- *haemolytic complement (C5):* C5 levels were found to be very high in both the OH_{48} and OF_{48} treatment groups (5.0x and 11.2x, respectively, as compared to C_{48}); a positive cellular response for these particular conditions,
- *chemokine (C-X-C motif) ligand 11 (CXCL11):* as with C5, CXCL11 levels were found to be very high in both the OH_{48} and OF_{48} treatment groups (20.9x and 31.8x, respectively, as compared to C_{48}); a cellular response that could not be correlated with interferon gamma (IFN-γ; the usual inducer of CXCL11) changes under the examined conditions,
- *fibroblast growth factor 21 (FGF-21):* FGF-21 levels were found to be very high in the O_{48} and OH_{48} treatment groups (as compared to C_{48}, where these were non-existent); interestingly, FGF-21 is an endogenous regulator of glucose and lipid metabolism, that once expressed by neurons, might exert neuroprotection (Leng *et al.*, 2015),
- *FMS-like tyrosine kinase 3 ligand (Flt3l):* the levels of Flt3l were found to be high in the OF_{48} treatment group only (6.0x, as compared to C_{48}); Flt3l is a blood cell progenitor-stimulating cytokine, and its role in the current context is unknown,
- *interleukin 1 alpha (IL-1α) and IL-1β:* IL-1α levels have been found increased in all examined oligomycin-treated mHippoE-14 groups (2.4x, 3.9x and 4.2x, in O_{48}, OH_{48} and OF_{48}, respectively, as compared to C_{48}), while IL-1β levels were found to be extremely high only in the OF_{48} treatment group (12.0x, as compared to C_{48}); although the upregulation of IL-1β in perihaematomal neurons due to an *in vivo* simulation of intracerebral haemorrhage is a recently confirmed process (Bimpis *et al.*, 2015; Zarros *et al.*, 2014), the potential role of IL-1α as a (neuronal-specific) response to the intracerebral haemorrhage-induced injury could be an interesting matter for further study,
- *interleukin 1 receptor antagonist (IL-1ra):* IL-1ra levels were found to be high in both the OH_{48} and OF_{48} treatment groups (2.8x and 2.4x, respectively, as compared to C_{48}); a

cellular response that could be an attempt of the mHippoE-14 cells to block the IL-1-driven cell death (Greenhalgh *et al.*, 2012),

- *leptin (OB):* like in the case of FGF-21, OB levels were found to be very high in the O_{48} and OH_{48} treatment groups (as compared to C_{48}, where these were non-existent); OB is a well-characterized mediator of inflammation within the secondary injury of intracerebral haemorrhage (Kim *et al.*, 2013), and its receptor (OB-R) is known to be (weakly) expressed by mHippoE-14 cells (see Table B.2),
- *matrix metallopeptidase 2 (MMP-2):* MMP-2 levels were found to be high in both the OH_{48} and OF_{48} treatment groups (5.7x and 3.0x, respectively, as compared to C_{48}); a finding probably related to the occurring neuronal apoptosis (Koutroulis *et al.*, 2008),
- *serine (or cysteine) peptidase inhibitor, clade F, member 1 (SERPINF1)*[16]*:* SERPINF1 levels were found to be extremely high in the OH_{48} and high in the OF_{48} treatment groups (109.6x and 4.7x, respectively, as compared to C_{48}); SERPINF1 might be (in this particular contexts) acting as an activator of the NF-κB pathway (Tombran-Tink and Barnstable, 2003) and / or of PPAR-γ expression (Ho *et al.*, 2007),
- *TNF-α:* finally, TNF-α expression was found increased in the O_{48} treatment group (as compared to C_{48}, where its expression was non-existent); interestingly, TNF-α was not detected at statistically significant levels in either of the other two conditions (OH_{48} or OF_{48}).

Such an elucidation should not only focus on the comparative analysis of the herein presented developed *in vitro* simulation approaches to intracerebral haemorrhage, but might also be worth attempting on neuronal populations of the perihaematomal brain regions in *in vivo* experimental settings.

>> Table C.3: page 129
>> Table C.4: page 130
>> Table C.5: page 131
>> Table C.6: page 134
>> Figure C.8: page 135
>> Figure C.9: page 136
>> Figure C.10: page 138
>> Figure C.11: page 140
>> Figure C.12: page 142
>> Figure C.13: page 143
>> Figure C.14: page 144
>> Figure C.15: page 145
>> Figure C.16: page 146
>> Figure C.17: page 147

[16] also known as pigment epithelium-derived factor (PEDF).

>> Figure C.18: page 148
>> Figure C.19: page 149
>> Figure C.20: page 150
>> Figure C.21: page 151

Table C.3: Assessment of the nCR values of mHippoE-14 within the developed *in vitro* simulation approaches to intracerebral haemorrhage: a sample.

Treatment (abbreviation)	**nCR$_{(E48,E60)}$** (nCI/h)	**Significance *vs* 0**
control (C)	0.001 ± 0.003	---
CDP-Ch (CDP-Ch)	0.000 ± 0.003	---
DFO (DFO)	-0.058 ± 0.004	$p<0.001$
haemin (H)	0.006 ± 0.004	$p<0.05$
ferrum (F)	-0.008 ± 0.001	$p<0.001$
CDP-Ch + haemin (CDP-Ch+H)	0.002 ± 0.003	---
CDP-Ch + ferrum (CDP-Ch+F)	-0.011 ± 0.001	$p<0.001$
DFO + haemin (DFO+H)	0.007 ± 0.009	---
DFO + ferrum (DFO+F)	-0.016 ± 0.007	$p<0.01$
oligomycin (O)	-0.014 ± 0.002	$p<0.001$
CDP-Ch + oligomycin (CDP-Ch+O)	-0.015 ± 0.003	$p<0.001$
DFO + oligomycin (DFO+O)	-0.059 ± 0.006	$p<0.001$
oligomycin + haemin (OH)	-0.005 ± 0.001	$p<0.001$
oligomycin + ferrum (OF)	-0.011 ± 0.002	$p<0.001$
CDP-Ch + oligomycin + haemin (CDP-Ch+OH)	-0.005 ± 0.001	$p<0.001$
CDP-Ch + oligomycin + ferrum (CDP-Ch+OF)	-0.013 ± 0.002	$p<0.001$
DFO + oligomycin + haemin (DFO+OH)	-0.003 ± 0.003	---
DFO + oligomycin + ferrum (DFO+OF)	-0.011 ± 0.002	$p<0.001$

Note: data are presented as mean ± standard deviation of four independent experiments (n=4; IDs: 1410161436, 1410202228, 1410251044, 1410251218); normalization occurs at the R_m time point of each experiment (approximately 6 h after FBS-deprivation and 30 h after cells' seeding). Statistical analysis has been performed through the use of Student's *t*-test. Only statistically significant differences ($p<0.05$) are annotated. For more details and further findings of these experiments, see Figures C.9, C.10 and C.11.

CDP-Ch: cytidine-5'-diphosphocholine; DFO: deferoxamine; E_{48}: evaluation endpoint at 48 h; E_{60}: evaluation endpoint at 60 h; FBS: foetal bovine serum; nCI: normalized cell index; nCR: normalized cellular response; R_m: recovery point after metaptosis

Table C.4: List of antibodies used for the performance of Western blotting toward the profiling of neuronal markers' expression in mHippoE-14 cells under the developed intracerebral haemorrhage-simulating *in vitro* conditions.

Antibody	Host	Clonality	Dilution	Provider	Product
Anti-α-tubulin	mouse	mono (IgG1)	1:10,000	Abcam PLC	ab7291
Anti-α1 Na^+,K^+-ATPase	mouse	mono (IgG1)	1:1,000	Abcam PLC	ab7671
Anti-CAL2	rabbit	mono (IgG)	1:1,000	Abcam PLC	ab133316
Anti-CB	rabbit	poly (IgG)	1:10,000	Abcam PLC	ab11426
Anti-ChAT	rabbit	poly (IgG)	1:100	Abcam PLC	ab68779
Anti-DCX	rabbit	poly (IgG)	1:1,000	Abcam PLC	ab18723
Anti-GAPDH	mouse	mono (IgG1)	1:10,000	Abcam PLC	ab8245
Anti-HO-1	goat	poly (IgG)	1:100	R&D Systems Inc.	967381
Anti-PV	rabbit	poly (IgG)	1:10,000	Abcam PLC	ab11427
Anti-SMI-310	mouse	mono (IgG1)	1:1,000	Abcam PLC	ab24570
Anti-synapsin I	rabbit	poly (IgG)	1:1,000	Abcam PLC	ab64581

Note: antibodies presented in alphabetical order. With the exception of the anti-HO-1 antibody that was part of a solid phase sandwich ELISA kit (human / mouse total HO-1 / HMOX1 cell-based ELISA kit; product KCB3776; R&D Systems Inc.), the rest of the antibodies used were purchased from Abcam PLC.

a-tubulin: alpha-tubulin; α1 Na^+,K^+-ATPase: alpha 1 subunit of sodium / potassium adenosine triphosphatase; CAL2: calretinin; CB: calbindin; ChAT: choline acetyltransferase; DCX: doublecortin; ELISA: enzyme-linked immunosorbent assay; GAPDH: glyceraldehyde-3-phosphate dehydrogenase; HMOX-1: human haeme oxygenase 1; HO-1: haeme oxygenase 1; IgG: immunoglobulin G; IgG1: immunoglobulin G1; mono: monoclonal; poly: polyclonal; PV: parvalbumin; SMI-310: 200 kDa + 160 kDa neurofilament

Table C.5: Designation of analytes upon each cytokine array slide used for the proteomic profiling of the cell-culture medium, as provided in the Proteome Profiler Array - Mouse XL Cytokine Array Kit (product ARY028; R&D Systems Inc.).

Coordinates	Analyte; abbreviation; NCBI Gene ID(s)
A1, A2	reference; N/A; N/A
A3, A4	adiponectin, C1Q and collagen domain containing; AdipoQ; 11450
A5, A6	amphiregulin; AR; 11839
A7, A8	angiopoietin 1; ANGPT1; 11600
A9, A10	angiopoietin 2; ANGPT2; 11601
A11, A12	angiopoietin-like 3; ANGPT-L3; 30924
A13, A14	tumour necrosis factor (ligand) superfamily, member 13b; BAFF; 24099
A15, A16	CD93 antigen; CD93; 17064
A17, A18	chemokine (C-C motif) ligand 2; CCL2; 20296
A19, A20	chemokine (C-C motif) ligand 3/4; CCL3/CCL4; 20302; 20303
A21, A22	chemokine (C-C motif) ligand 5; CCL5; 20304
A23, A24	reference; N/A; N/A
B3, B4	chemokine (C-C motif) ligand 6; CCL6; 20305
B5, B6	chemokine (C-C motif) ligand 11; CCL11; 20292
B7, B8	chemokine (C-C motif) ligand 12; CCL12; 20293
B9, B10	chemokine (C-C motif) ligand 17; CCL17; 20295
B11, B12	chemokine (C-C motif) ligand 19; CCL19; 24047
B13, B14	chemokine (C-C motif) ligand 20; CCL20; 20297
B15, B16	chemokine (C-C motif) ligand 21A (serine); CCL21; 18829
B17, B18	chemokine (C-C motif) ligand 22; CCL22; 20299
B19, B20	CD14 antigen; CD14; 12475
B21, B22	CD40 antigen; CD40; 21939
C3, C4	CD160 antigen; CD160; 54215
C5, C6	retinoic acid receptor responder (tazarotene-induced) 2; RARRES2; 71660
C7, C8	chitinase 3-like 1; CHI3L1; 12654
C9, C10	coagulation factor III; TF; 14066
C11, C12	haemolytic complement; C5; 15139
C13, C14	complement factor D (adipsin); CFD; 11537
C15, C16	C-reactive protein, pentraxin-related; CRP; 12944
C17, C18	chemokine (C-X3-C motif) ligand 1; CX3CL1; 20312
C19, C20	chemokine (C-X-C motif) ligand 1; CXCL1; 14825
C21, C22	chemokine (C-X-C motif) ligand 2; CXCL2; 20310
D1, D2	chemokine (C-X-C motif) ligand 9; CXCL9; 17329
D3, D4	chemokine (C-X-C motif) ligand 10; CXCL10; 15945
D5, D6	chemokine (C-X-C motif) ligand 11; CXCL11; 56066
D7, D8	chemokine (C-X-C motif) ligand 13; CXCL13; 55985
D9, D10	chemokine (C-X-C motif) ligand 16; CXCL16; 66102
D11, D12	cystatin C; CST3; 13010
D13, D14	dickkopf homolog 1 (*Xenopus laevis*); DKK-1; 13380
D15, D16	dipeptidylpeptidase 4; DPP4; 13482
D17, D18	epidermal growth factor; EGF; 13645
D19, D20	endoglin; ENG; 13805
D21, D22	collagen, type XVIII, alpha 1; Col18α1; 12822
D23, D24	alpha-2-HS-glycoprotein; AHSG; 11625

(continues on next page)

Coordinates	Analyte; abbreviation; NCBI Gene ID(s)
E1, E2	fibroblast growth factor 1; FGF-1; 14164
E3, E4	fibroblast growth factor 21; FGF-21; 56636
E5, E6	FMS-like tyrosine kinase 3 ligand; Flt3l; 14256
E7, E8	growth arrest specific 6; Gas6; 14456
E9, E10	colony stimulating factor 3 (granulocyte); G-CSF; 12985
E11, E12	growth differentiation factor 15; GDF-15; 23886
E13, E14	colony stimulating factor 2 (granulocyte-macrophage); GM-CSF; 12981
E15, E16	hepatocyte growth factor; HGF; 15234
E17, E18	intercellular adhesion molecule 1; ICAM-1; 15894
E19, E20	interferon-gamma; IFN-γ; 15978
E21, E22	insulin-like growth factor binding protein 1; IGFBP-1; 16006
E23, E24	insulin-like growth factor binding protein 2; IGFBP-2; 16008
F1, F2	insulin-like growth factor binding protein 3; IGFBP-3; 16009
F3, F4	insulin-like growth factor binding protein 5; IGFBP-5; 16011
F5, F6	insulin-like growth factor binding protein 6; IGFBP-6; 16012
F7, F8	interleukin 1 alpha; IL-1α; 16175
F9, F10	interleukin 1 beta; IL-1β; 16176
F11, F12	interleukin 1 receptor antagonist; IL-1ra; 16181
F13, F14	interleukin 2; IL-2; 16183
F15, F16	interleukin 3; IL-3; 16187
F17, F18	interleukin 4; IL-4; 16189
F19, F20	interleukin 5; IL-5; 16191
F21, F22	interleukin 6; IL-6; 16193
F23, F24	interleukin 7; IL-7; 16196
G1, G2	interleukin 10; IL-10; 16153
G3, G4	interleukin 11; IL-11; 16156
G5, G6	interleukin 12 beta subunit p40; IL-12 p40; 16160
G7, G8	interleukin 13; IL-13; 16163
G9, G10	interleukin 15; IL-15; 16168
G11, G12	interleukin 17A; IL-17A; 16171
G13, G14	interleukin 22; IL-22; 50929
G15, G16	interleukin 23, alpha subunit p19; IL-23 p19; 83430
G17, G18	interleukin 27, alpha subunit p28; IL-27 p28; 246779
G19, G20	interferon lambda 2/3; IL-28A/B; 330496, 338374
G21, G22	interleukin 33; IL-33; 77125
G23, G24	low-density lipoprotein receptor; LDL-R; 16835
H1, H2	leptin; OB; 16846
H3, H4	leukemia inhibitory factor; LIF; 16878
H5, H6	lipocalin 2; NGAL; 16819
H7, H8	chemokine (C-X-C motif) ligand 5; CXCL5; 20311
H9, H10	colony stimulating factor 1 (macrophage); M-CSF; 12977
H11, H12	matrix metallopeptidase 2; MMP-2; 17390
H13, H14	matrix metallopeptidase 3; MMP-3; 17392
H15, H16	matrix metallopeptidase 9; MMP-9; 17395
H17, H18	myeloperoxidase; MPO; 17523
H19, H20	secreted phosphoprotein 1; SPP1; 20750
H21, H22	osteoprotegerin; OPG; 18383
H23, H24	thymidine phosphorylase; TP; 72962
I1, I2	platelet derived growth factor, B polypeptide; PDGF-BB; 18591

(continues on next page)

Coordinates	Analyte; abbreviation; NCBI Gene ID(s)
I3, I4	serum amyloid P-component; SAP; 20219
I5, I6	pentraxin-related protein 3; PTX3; 19288
I7, I8	periostin, osteoblast specific factor; POSTN; 50706
I9, I10	delta-like 1 homolog (*Drosophila*); DLK-1; 13386
I11, I12	prolactin family 2, subfamily c, member 2 (proliferin); PLF; 18811
I13, I14	proprotein convertase subtilisin/kexin type 9; PCSK9; 100102
I15, I16	advanced glycosylation end product-specific receptor; RAGE; 11596
I17, I18	retinol binding protein 4, plasma; RBP4; 19662
I19, I20	regenerating islet-derived 3 gamma; REG-3γ; 19695
I21, I22	resistin (adipose tissue-specific secretory factor); ADSF; 57264
J1, J2	reference; N/A; N/A
J3, J4	selectin, endothelial cell; CD62E; 20339
J5, J6	selectin, platelet; CD62P; 20344
J7, J8	serine (or cysteine) peptidase inhibitor, clade E, member 1; SERPINE1; 18787
J9, J10	serine (or cysteine) peptidase inhibitor, clade F, member 1; SERPINF1; 20317
J11, J12	thrombopoietin; THPO; 21832
J13, J14	hepatitis A virus cellular receptor 1; HAVcR-1; 171283
J15, J16	tumour necrosis factor alpha; TNF-α; 21926
J17, J18	vascular cell adhesion molecule 1; VCAM-1; 22329
J19, J20	vascular endothelial growth factor A; VEGF-A; 22339
J21, J22	WNT1 inducible signalling pathway protein 1; WISP-1; 22402
J23, J24	negative control; N/A; N/A

Note: the herein presented analyte abbreviations are not included in Appendix A, unless they happen to be mentioned or discussed elsewhere in this PhD Thesis. For more details on the proteomic profiling performed, see protocol's description in Figure C.18.

Table C.6: Synopsis of the statistically significant analyte changes detected by the proteomic profiling of the developed *in vitro* simulation approaches to intracerebral haemorrhage.

Treatment	Analyte changes of $p<0.05$ significance detected (*versus* C_{48})		
O_{48}	ANGPT1; p=0.023; 17.5x	G-CSF; p=0.004; 1.7x	PTX3; p=0.004; 1.3x
	CCL19; p=0.009; 2.1x	IL-1α; p=0.050; 2.4x	RAGE; p=0.017; -0.7x (↑)
	CXCL16; p=0.004; 2.4x	IL-22; p=0.040; -0.2x (↓)	TNF-α; p=0.049; -0.5x (↑)
	CST3; p=0.000; 1.2x	OB; p=0.005; -13.3x (↑)	VEGF-A; p=0.008; 2.5x
	FGF-21; p=0.013; -18.5x (↑)	NGAL; p=0.013; 1.3x	
OH_{48}	ANGPT1; p=0.046; 27.7x	CXCL10; p=0.012; 0.6x	IL-12 p40; p=0.006; 4.2x
	CCL6; p=0.011; 5.7x	CXCL11; p=0.038; 20.9x	LDL-R; p=0.017; 2.6x
	CCL19; p=0.008; 3.9x	CXCL16; p=0.006; 3.5x	OB; p=0.039; -29.3x (↑)
	CCL22; p=0.026; 2.0x	Col18α1; p=0.050; 2.0x	LIF; p=0.025; 5.7x
	CD14; p=0.021; 5.6x	FGF-21; p=0.001; -56.7x (↑)	MMP-2; p=0.015; 5.7x
	CHI3L1; p=0.023; 0.8x	Flt3l; p=0.027; 3.7x	PDGF-BB; p=0.039; 2.3x
	TF; p=0.001; 7.1x	IGFBP-5; p=0.040; 28.9x	SAP; p=0.046; 4.1x
	C5; p=0.036; 5.0x	IL-1α; p=0.009; 3.9x	DLK-1; p=0.007; 5.8x
	CFD; p=0.044; -14.1x (↑)	IL-1ra; p=0.041; 2.8x	PCSK9; p=0.030; 3.6x
	CRP; p=0.040; -14.9x (↓)	IL-2; p=0.032; -2.2x (↓)	SERPINF1; p=0.001; 109.6x
	CX3CL1; p=0.050; 4.1x	IL-11; p=0.037; 14.7x	VCAM-1; p=0.003; 2.5x
OF_{48}	ANGPT2; p=0.010; -8.8x (↑)	DPP4; p=0.024; -3.4x (↑)	IL-3; p=0.002; -27.0x (↑)
	CD93; p=0.021; -22.2x (↑)	AHSG; p=0.026; 2.2x	IL-15; p=0.010; 5.4x
	CCL11; p=0.037; 4.7x	FGF-1; p=0.006; -9.8x (↑)	IL-23; p=0.031; -16.6x (↑)
	CCL21; p=0.023; -11.8x (↑)	Flt3l; p=0.021; 6.0x	MMP-2; p=0.022; 3.0x
	CD14; p=0.035; 8.7x	Gas6; p=0.010; 6.5x	POSTN; p=0.002; 4.0x
	CD160; p=0.026; 3.5x	G-CSF; p=0.008; 1.7x	DLK-1; p=0.038; 3.1x
	CHI3L1; p=0.005; 0.6x	GDF-15; p=0.050; 7.1x	RAGE; p=0.047; -2.0x (↑)
	C5; p=0.009; 11.2x	GM-CSF; p=0.029; 7.1x	ADSF; p=0.013; 3.1x
	CXCL9; p=0.003; -7.1x (↑)	HGF; p=0.014; -4.6x (↑)	CD62P; p=0.041; 9.9x
	CXCL10; p=0.003; 0.3x	IGFBP-6; p=0.037; 2.0x	SERPINE1; p=0.005; 0.8x
	CXCL11; p=0.020; 31.8x	IL-1α; p=0.017; 4.2x	SERPINF1; p=0.022; 4.7x
	CXCL13; p=0.003; 18.9x	IL-1β; p=0.020; 12.0x	WISP-1; p=0.003; 0.7x
	CXCL16; p=0.002; 6.1x	IL-1ra; p=0.020; 2.4x	
	CST3; p=0.034; 1.0x	IL-2; p=0.013; 9.3x	

Note: the table presents the analyte abbreviations followed by the p values of their difference compared to C_{48} and the untreated fold values; the latter are corrected (where necessary) by arrows in parenthesis (↑ or ↓), in order to indicate whether they reflect an increase or a decrease towards the C_{48} levels. Negative fold values derive from the fact that one of the compared treatment groups bears analyte levels below the negative control values; in other words, it is a methodological limitation that is better to be exposed rather than to be hidden under logarithmic transformations. Statistical analysis was performed with ANOVA, as specified for microarray data according to Cui and Churchill (2003).

analyte abbreviations are defined in Table C.5; ANOVA: analysis of variance; C_{48}: control (at 48 h); O_{48}: oligomycin (at 48 h); OF_{48}: oligomycin, ferrum (at 48 h); OH_{48}: oligomycin, haemin (at 48 h)

Figure C.8: Graphic summary of the assessed *in vitro* simulation approaches to intracerebral haemorrhage, based on the exposure of mHippoE-14 cells to FBS-deprivation and followed by exposure to oligomycin-A and, finally, to ferrum or haemin (at a concentration of 500 μM).

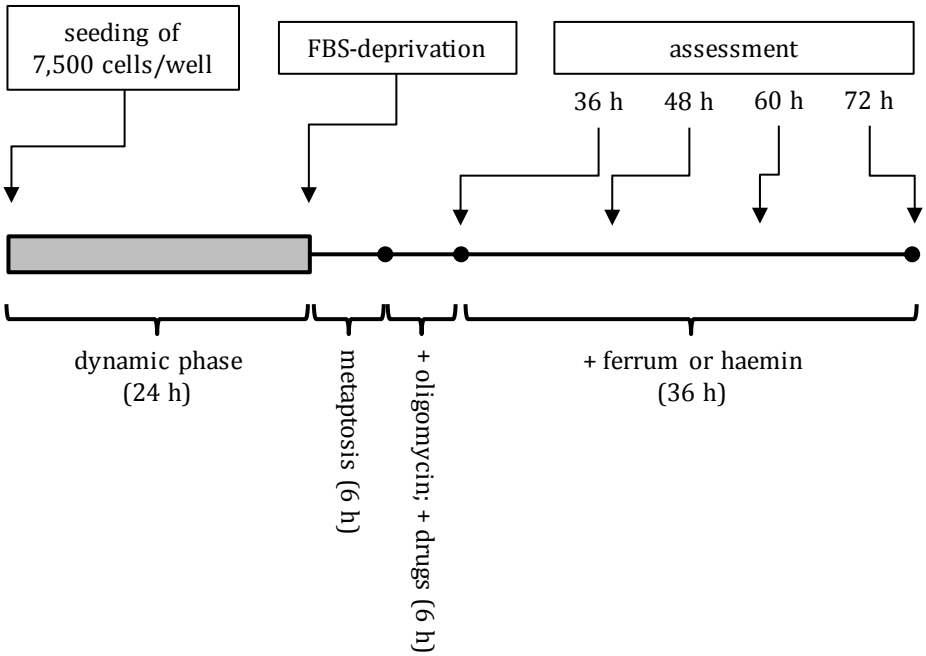

Note: the seeding density presented refers to a 96-well plate setting which is only relevant to the real-time cellular response analysis performed through the xCELLigence technology; a simulated density of 211,000 cells/dish was employed for the undertaking of all other assessments (phase-contrast microscopy, cell-lysate acquiring for the performance of Western blotting and neurochemical assessments, as well as media aspiration for the performance of proteomic profiling). The 4 indicated assessment time points have not been used for all assessment approaches, and the exposure to drugs (such as CDP-Ch or DFO) has only been performed in the case of the real-time cellular response analysis.

CDP-Ch: cytidine-5'-diphosphocholine; DFO: deferoxamine; FBS: foetal bovine serum

Figure C.9: Real-time cellular response profile of the developed *in vitro* simulation approaches to intracerebral haemorrhage.

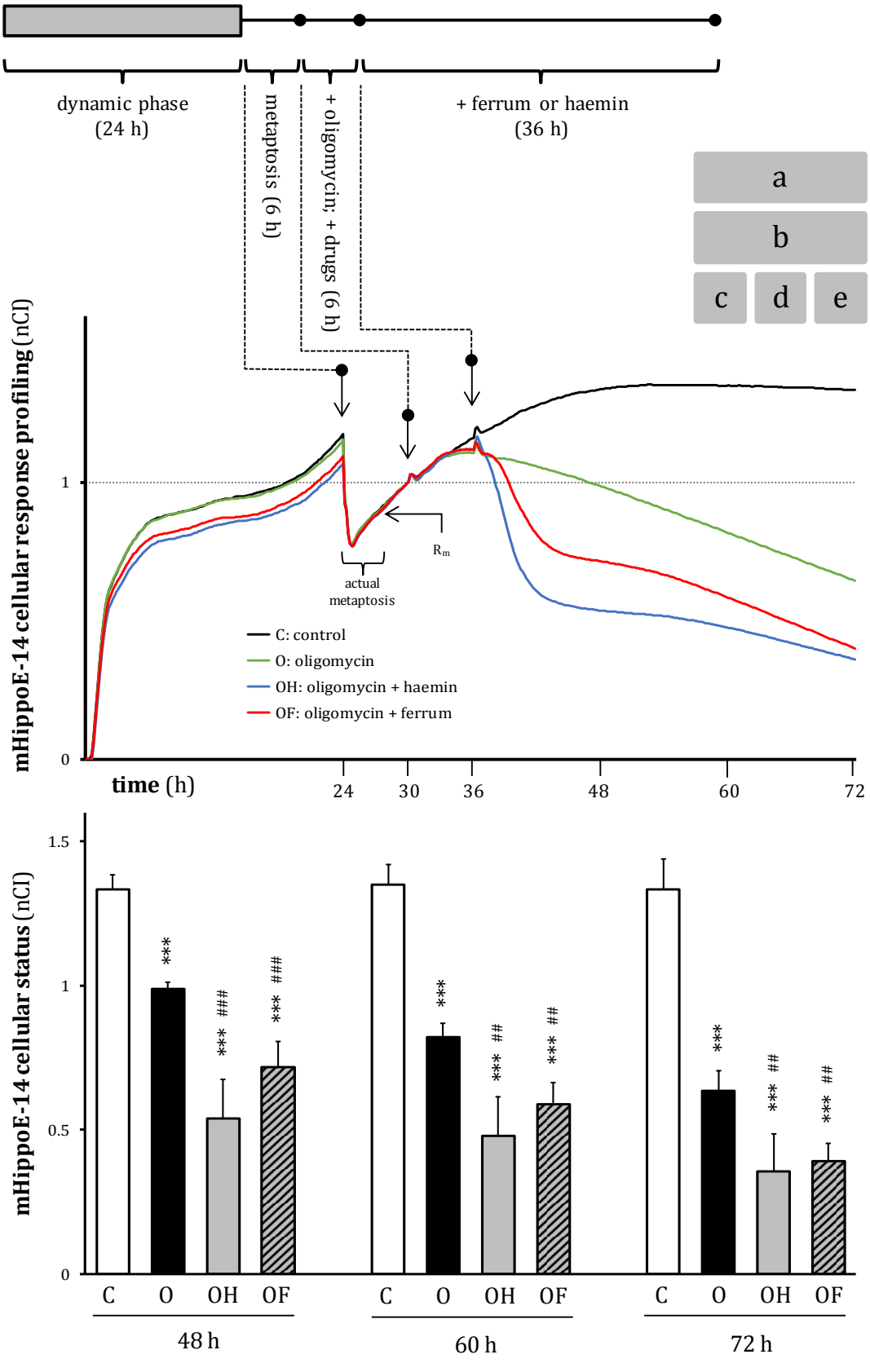

Note: arrows in Figure C.9.b indicate the induction of metaptosis, the addition of oligomycin and the addition of haemin or ferrum, at 24, 30 and 36 h, respectively. Data in Figures C.9.b to C.9.e are presented as mean (± standard deviation) of four independent experiments (n=4; IDs: 1410161436, 1410202228, 1410251044, 1410251218); normalization occurs at the R_m time point of each experiment (approximately 6 h after FBS-deprivation and 30 h after cells' seeding). Statistical analysis has been performed through the use of one-way ANOVA followed by *post hoc* Tukey's range test. Only statistically-significant differences (p<0.05) are annotated. For more details and further findings of these experiments, see Figures C.10 and C.11 as well as Table C.3.

***: p<0.001 (as compared to respective C values); ##: p<0.01 (as compared to respective O values); ###: p<0.001 (as compared to respective O values); ANOVA: analysis of variance; C: control; nCI: normalized cell index; O: oligomycin, OF: oligomycin, ferrum; OH: oligomycin, haemin; R_m: recovery point after metaptosis

Figure C.10: Real-time cellular response analysis of the effect of CDP-Ch (100 μM) on the developed *in vitro* simulation approaches to intracerebral haemorrhage.

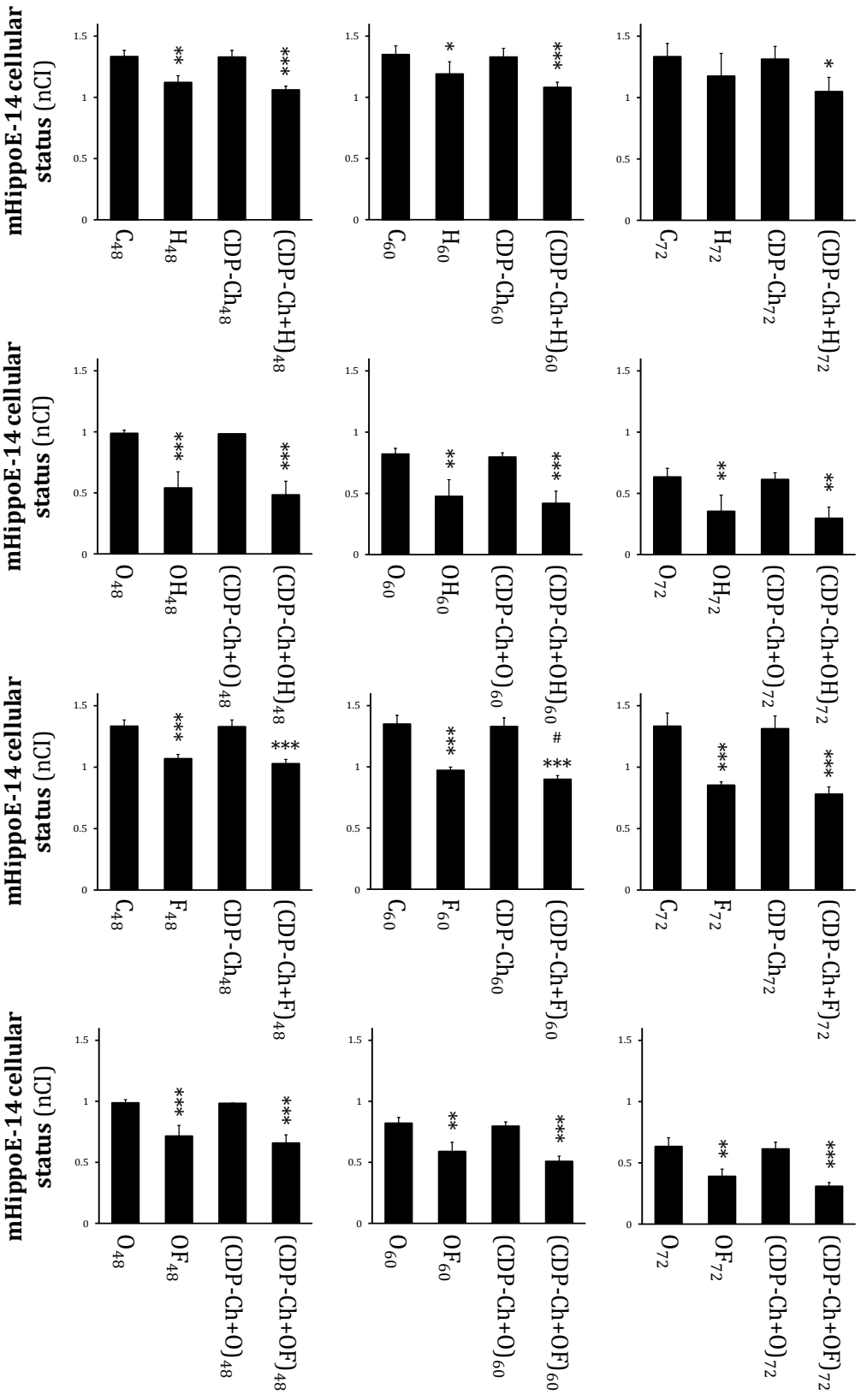

Note: data are presented as mean ± standard deviation of four independent experiments (n=4; IDs: 1410161436, 1410202228, 1410251044, 1410251218); normalization occurs at the R_m time point of each experiment (approximately 6 h after FBS-deprivation and 30 h after cells' seeding). Statistical analysis has been performed through the use of one-way ANOVA followed by *post hoc* Tukey's range test. Only statistically significant differences ($p<0.05$) are annotated. For more details and further findings of these experiments, see Figure C.9 and Table C.3.

*: $p<0.05$ (as compared to respective C or O values); **: $p<0.01$ (as compared to respective C or O values); ***: $p<0.001$ (as compared to respective C or O values); #: $p<0.05$ (as compared to F_{60} value); ANOVA: analysis of variance; C: control; CDP-Ch: cytidine-5'-diphosphocholine; nCI: normalized cell index; O: oligomycin, OF: oligomycin, ferrum; OH: oligomycin, haemin; R_m: recovery point after metaptosis

Figure C.11: Real-time cellular response analysis of the effect of DFO (100 μM) on the developed *in vitro* simulation approaches to intracerebral haemorrhage.

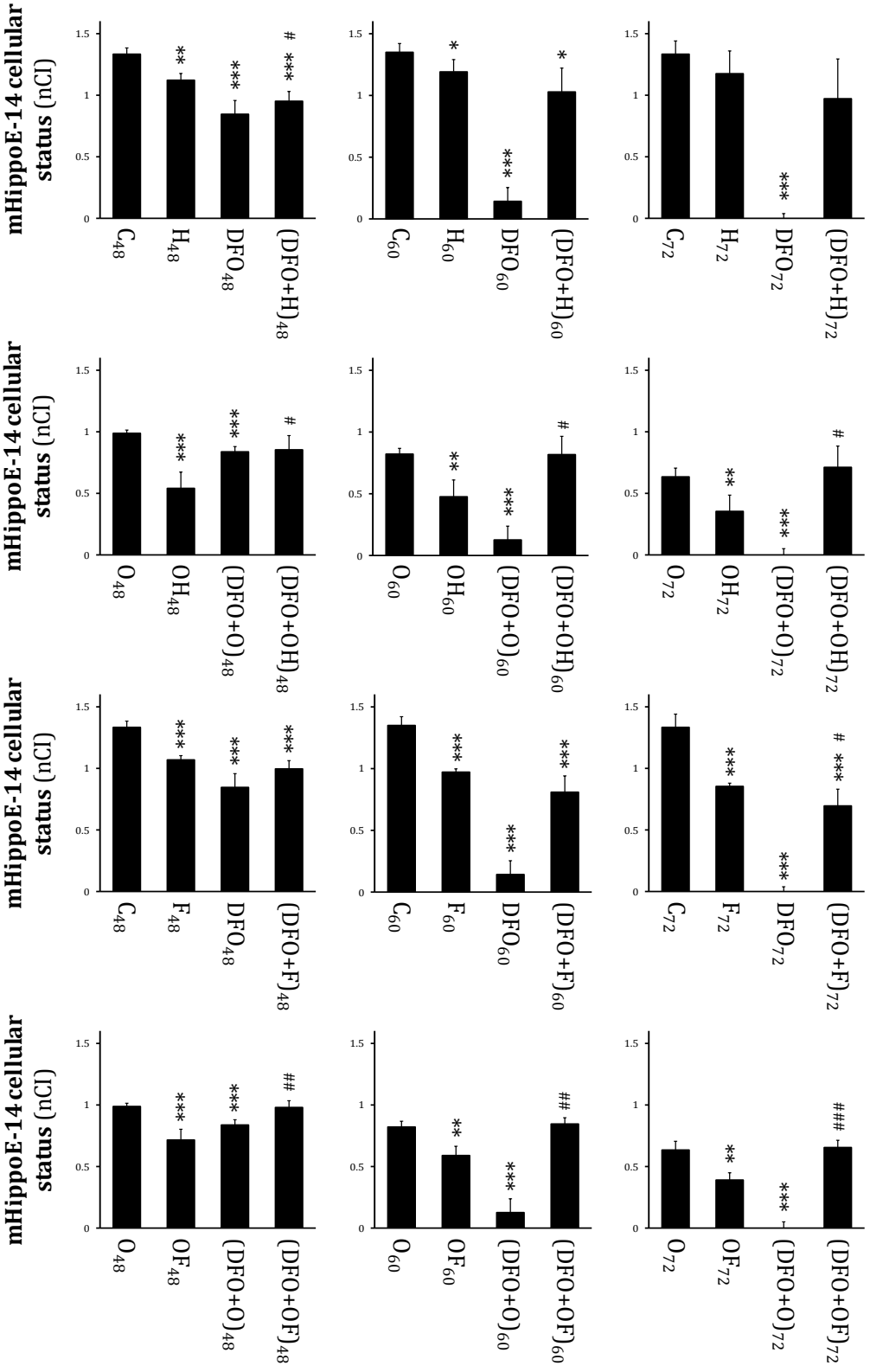

Note: data are presented as mean ± standard deviation of four independent experiments (n=4; IDs: 1410161436, 1410202228, 1410251044, 1410251218); normalization occurs at the R_m time point of each experiment (approximately 6 h after FBS-deprivation and 30 h after cells' seeding). Statistical analysis has been performed through the use of one-way ANOVA followed by *post hoc* Tukey's range test. Only statistically significant differences ($p<0.05$) are annotated. For more details and further findings of these experiments, see Figure C.9 and Table C.3.

*: $p<0.05$ (as compared to respective C or O values); **: $p<0.01$ (as compared to respective C or O values); ***: $p<0.001$ (as compared to respective C or O values); #: $p<0.05$ (as compared to respective H, OH or F values); ##: $p<0.01$ (as compared to respective OF values); ###: $p<0.001$ (as compared to OF_{72} value); ANOVA: analysis of variance; C: control; DFO: deferoxamine; nCI: normalized cell index; O: oligomycin, OF: oligomycin, ferrum; OH: oligomycin, haemin; R_m: recovery point after metaptosis

Figure C.12: Representative phase-contrast microscopy captions of live mHippoE-14 cells under the developed intracerebral haemorrhage-simulating conditions.

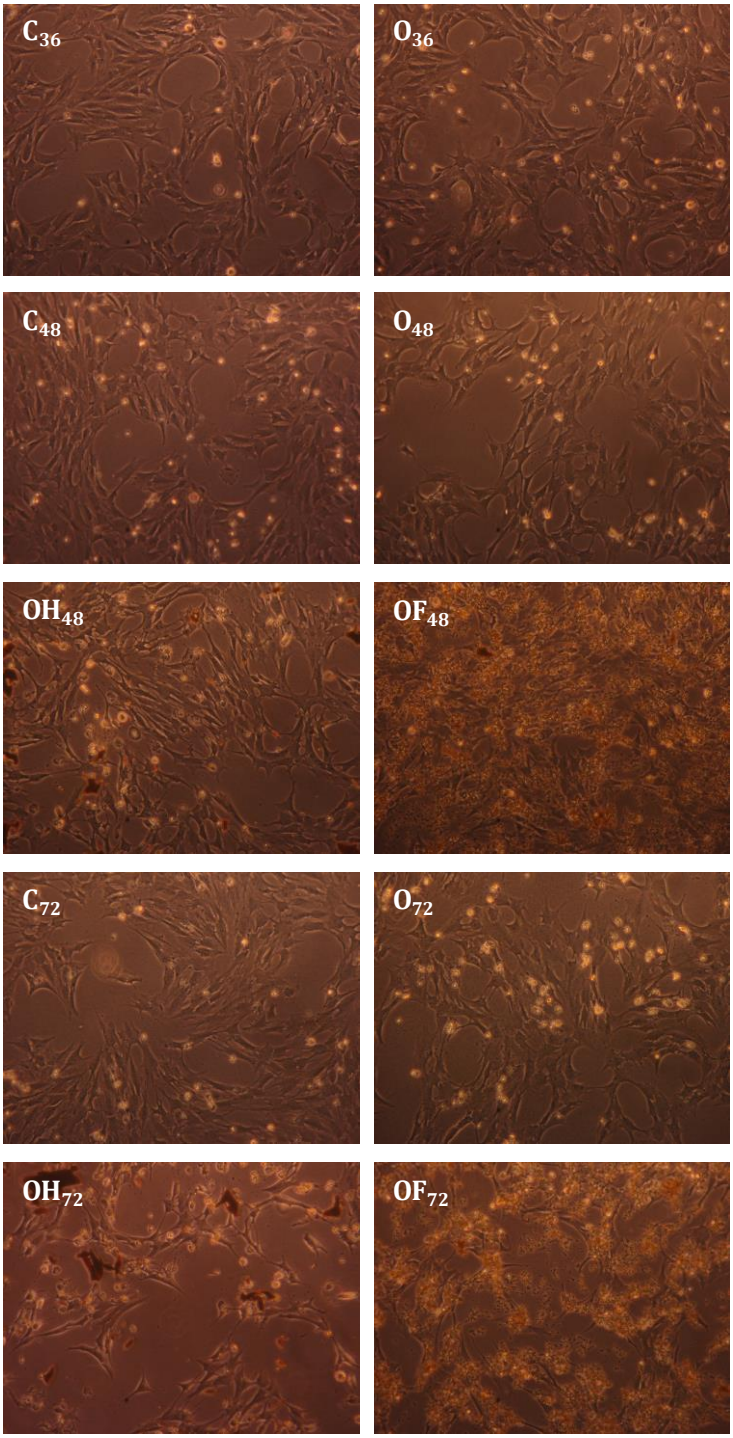

Note: the presented phase-contrast microscopy captions of the mHippoE-14 cell-line are representative captions from a series of three independent experiments (n=4) in which the cells were cultured in 35 mm Corning Dishes (at a density of 211,000 cells/dish) and their treatment followed the protocol of Figure C.8. In total, 210 captions were generated through a Carl Zeiss Axiovert 40 C inverted phase-contrast microscope (Ph1 condenser annulus; x10 magnification objective; blue filter) and an attached digital photo camera. For more details, see Figure C.13.

C_{36}: control (at 36 h); C_{48}: control (at 48 h); C_{72}: control (at 72 h); O_{36}: oligomycin (at 36 h); O_{48}: oligomycin (at 48 h); O_{72}: oligomycin (at 72 h); OF_{48}: oligomycin, ferrum (at 48 h); OF_{72}: oligomycin, ferrum (at 72 h); OH_{48}: oligomycin, haemin (at 48 h); OH_{72}: oligomycin, haemin (at 72 h)

Figure C.13: Cytomorphological analysis of the mHippoE-14 response to developed intracerebral haemorrhage-simulating conditions.

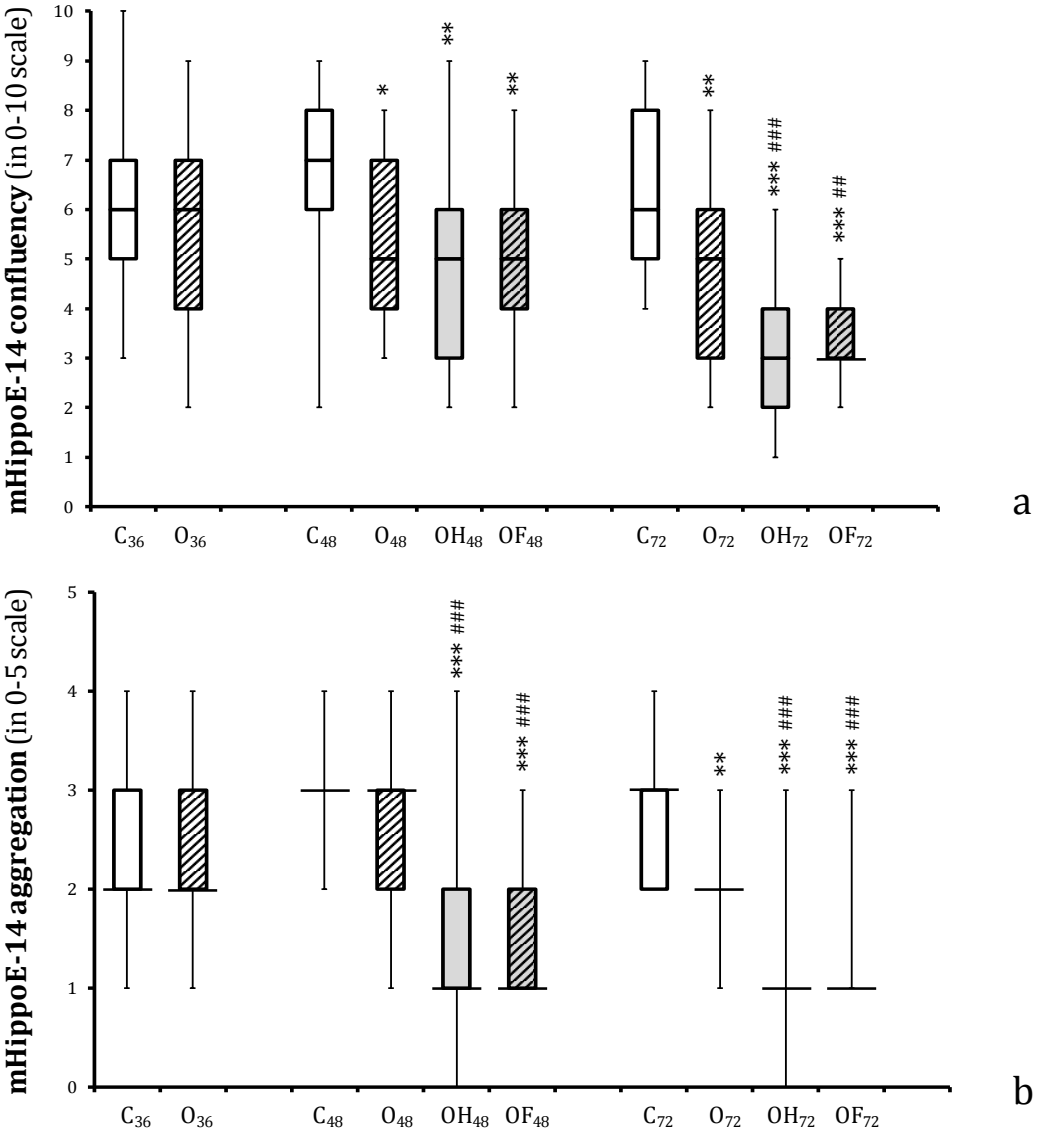

Note: data are presented as median and interquartile range (IQR) in a box-and-whisker plot (pooled caption scoring of three independent experiments; n=21), and statistical analysis has been performed through the use of a Mann-Whitney U test. Only statistically significant differences (p<0.05) are annotated. For more details on the parameters assessed and the experimental protocol followed, consult Table B.8 and the note of Figure C.12, respectively.

*: p<0.05 (as compared to the respective C score); **: p<0.01 (as compared to the respective C score); ***: p<0.001 (as compared to the respective C score); ##: p<0.01 (as compared to the O_{72} score); ###: p<0.001 (as compared to the respective O score); C_{36}: control (at 36 h); C_{48}: control (at 48 h); C_{72}: control (at 72 h); IQR: interquartile range; O_{36}: oligomycin (at 36 h); O_{48}: oligomycin (at 48 h); O_{72}: oligomycin (at 72 h); OF_{48}: oligomycin, ferrum (at 48 h); OF_{72}: oligomycin, ferrum (at 72 h); OH_{48}: oligomycin, haemin (at 48 h); OH_{72}: oligomycin, haemin (at 72 h)

Figure C.14: Profiling of neuronal markers' expression in mHippoE-14 cells: comparing the expression in the presence and absence of FBS.

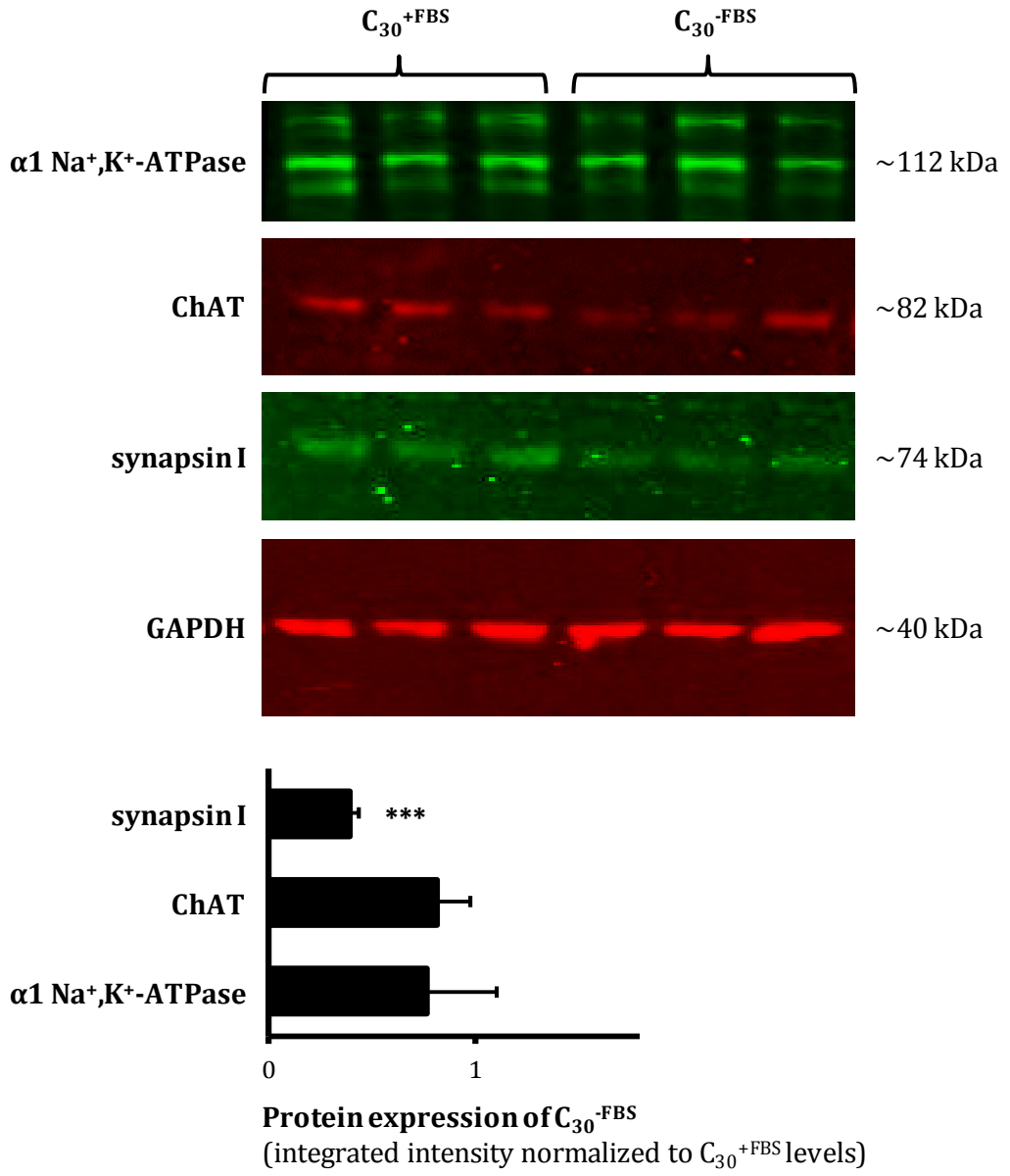

Note: data are presented as normalized mean ± standard error (n=3), and statistical analysis has been performed through the use of Student's *t*-test. Only statistically significant differences ($p<0.05$) are annotated. For more details on the hereby presented experimental conditions, see Figure C.8.

***: $p<0.001$ (as compared to C_{30}^{+FBS} levels); α1 Na^+,K^+-ATPase: alpha 1 subunit of sodium / potassium adenosine triphosphatase; C_{30}^{+FBS}: control in growing media (at 30 h); C_{30}^{-FBS}: control in FBS-deprived media (at 30 h); ChAT: choline acetyltransferase; FBS: foetal bovine serum; GAPDH: glyceraldehyde-3-phosphate dehydrogenase

Figure C.15: Profiling of neuronal markers' expression in mHippoE-14 cells: early effects of oligomycin's addition to FBS-deprived cultures.

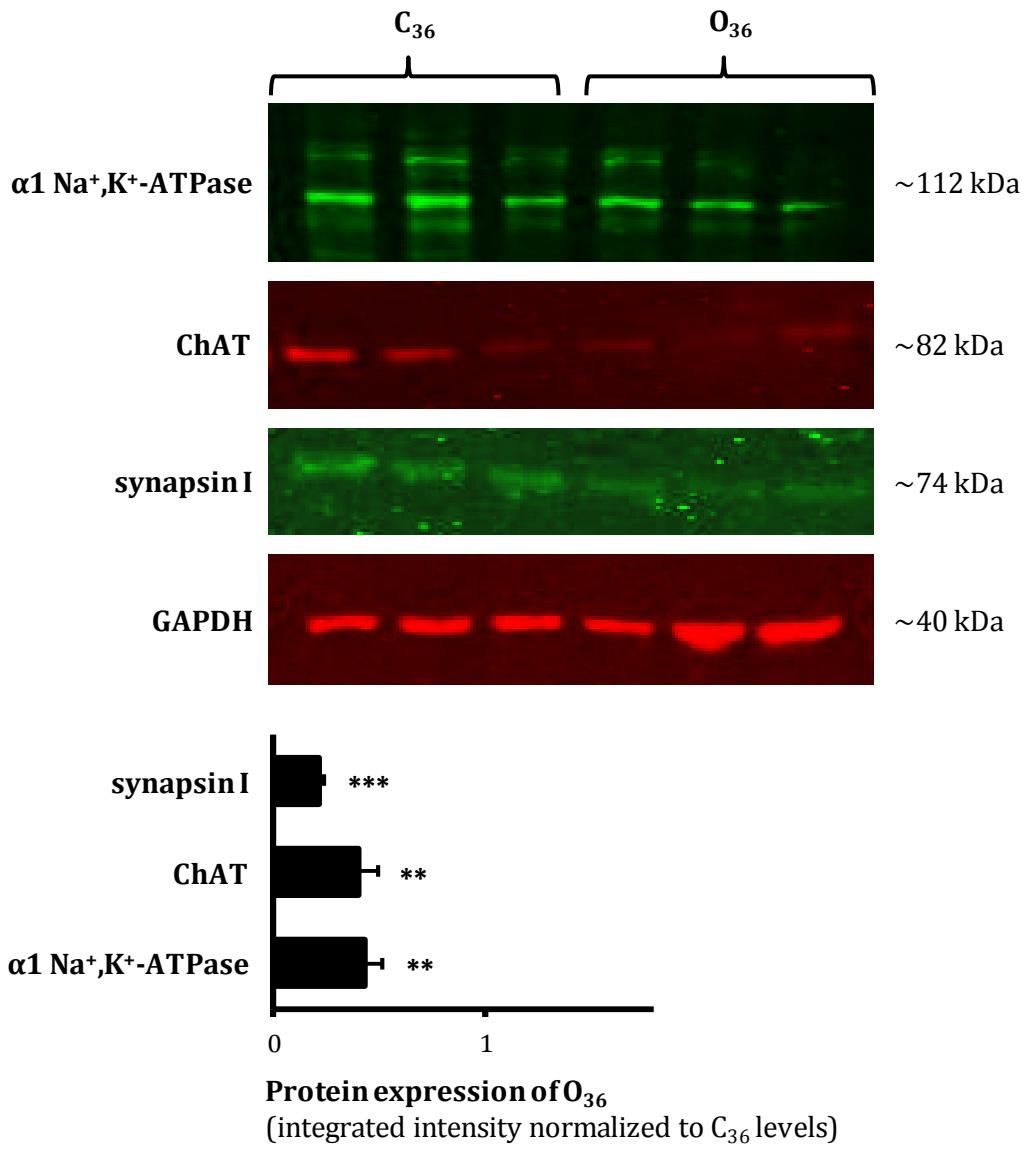

Note: data are presented as normalized mean ± standard error (n=3), and statistical analysis has been performed through the use of Student's *t*-test. Only statistically significant differences ($p<0.05$) are annotated. For more details on the hereby presented experimental conditions, see Figure C.8.

**: $p<0.01$ (as compared to C_{36} levels); ***: $p<0.001$ (as compared to C_{36} levels); α1 Na^+,K^+-ATPase: alpha 1 subunit of sodium / potassium adenosine triphosphatase; C_{36}: control (at 36 h); ChAT: choline acetyltransferase; FBS: foetal bovine serum; GAPDH: glyceraldehyde-3-phosphate dehydrogenase; O_{36}: oligomycin (at 36 h)

Figure C.16: Profiling of neuronal markers' expression in mHippoE-14 cells under the developed intracerebral haemorrhage-simulating *in vitro* conditions.

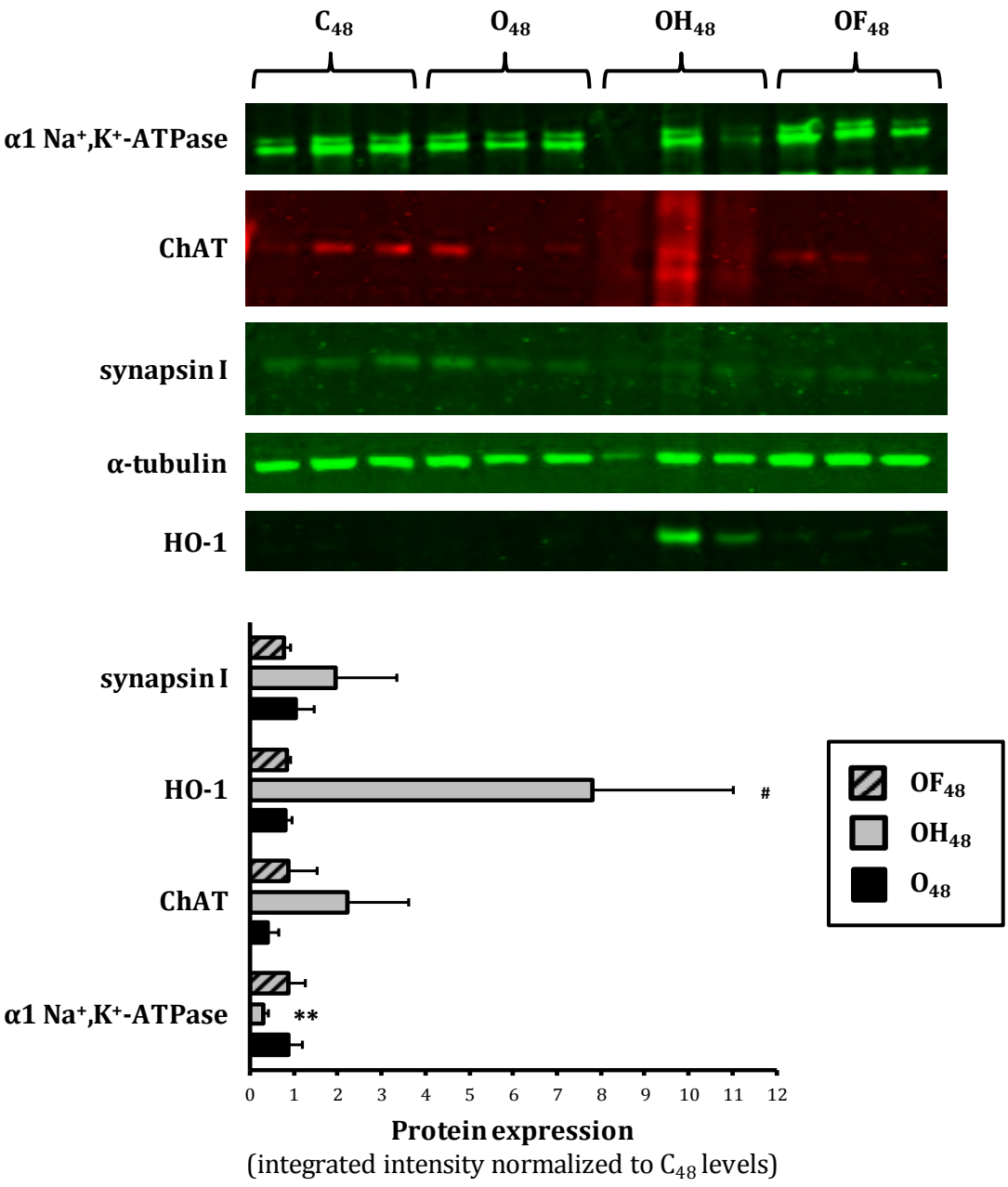

Note: data are presented as normalized mean ± standard error (n=3), and statistical analysis has been performed through the use of one-way ANOVA followed by *post hoc* Tukey's range test. Only statistically significant differences (p<0.05) are annotated. For more details on the hereby presented experimental conditions, see Figure C.8. The molecular weights of the a1 Na^+,K^+-ATPase, ChAT, synapsin I, α-tubulin and HO-1 bands are ~112, ~82, ~74, ~50 and ~32 kDa, respectively.

**: p<0.01 (as compared to C_{48} levels); #: p<0.05 (as compared to O_{48} levels); a-tubulin: alpha-tubulin; α1 Na^+,K^+-ATPase: alpha 1 subunit of sodium / potassium adenosine triphosphatase; ANOVA: analysis of variance; C_{48}: control (at 48 h); ChAT: choline acetyltransferase; HO-1: haeme oxygenase 1; O_{48}: oligomycin (at 48 h); OF_{48}: oligomycin, ferrum (at 48 h); OH_{48}: oligomycin, haemin (at 48 h)

Figure C.17: Activity of mHippoE-14 cells' AChE under the developed intracerebral haemorrhage-simulating *in vitro* conditions (a), and of *Electrophorus electricus* pure AChE following incubation with media deriving from mHippoE-14 cell cultures under the same intracerebral haemorrhage-simulating *in vitro* conditions (b).

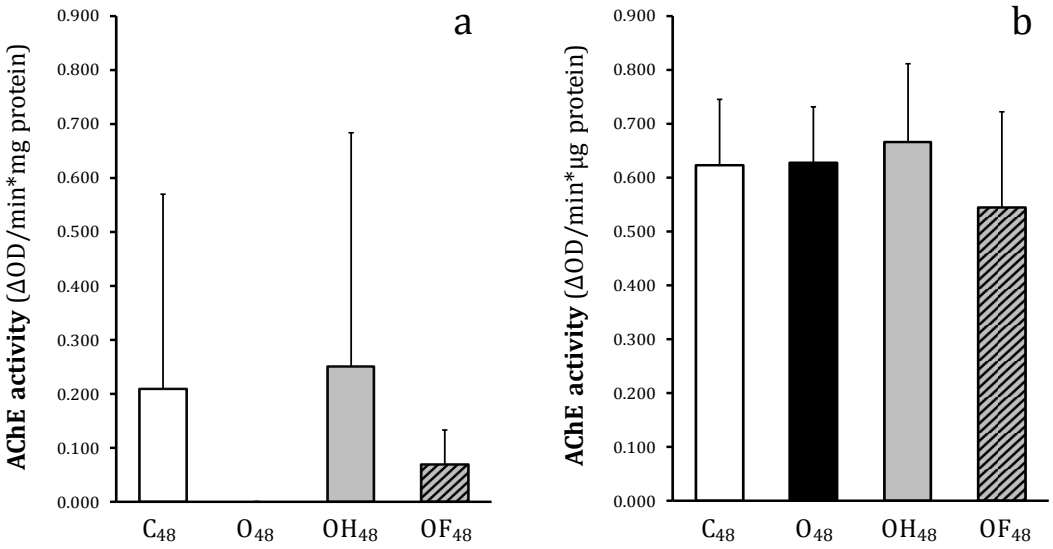

Note: data are presented as mean ± standard deviation (n=3), and statistical analysis has been performed through the use of one-way ANOVA followed by *post hoc* Tukey's range test. No statistically significant differences (p<0.05) were observed. For more details on the hereby presented experimental conditions, see Figure C.8.

AChE: acetylcholinesterase; ANOVA: analysis of variance; C_{48}: control (at 48 h); O_{48}: oligomycin (at 48 h); OF_{48}: oligomycin, ferrum (at 48 h); OH_{48}: oligomycin, haemin (at 48 h)

Figure C.18: Overview of the proteomic profiling methodology and the arrays produced.

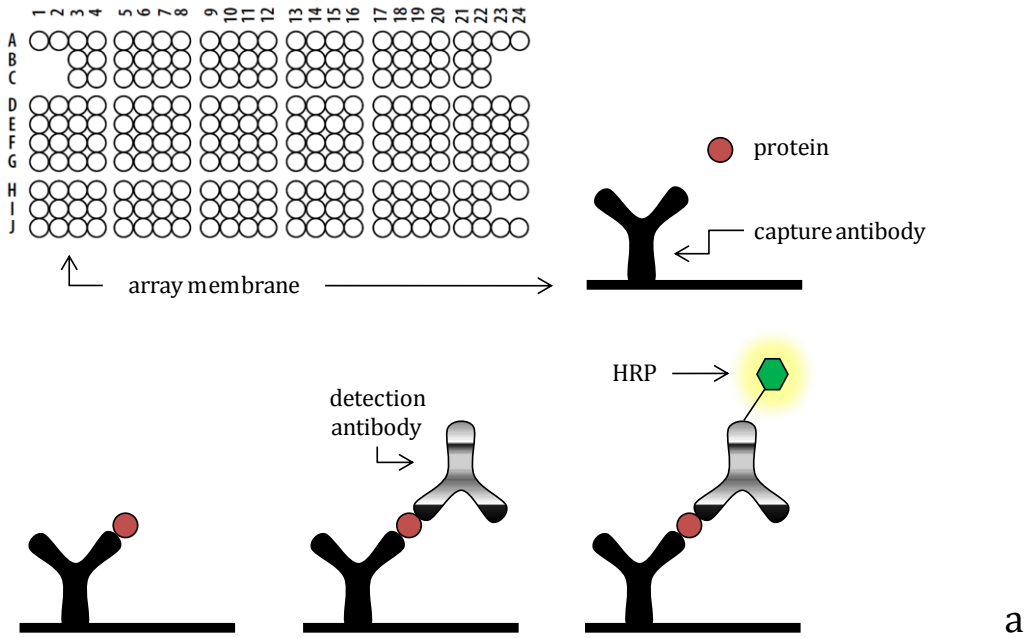

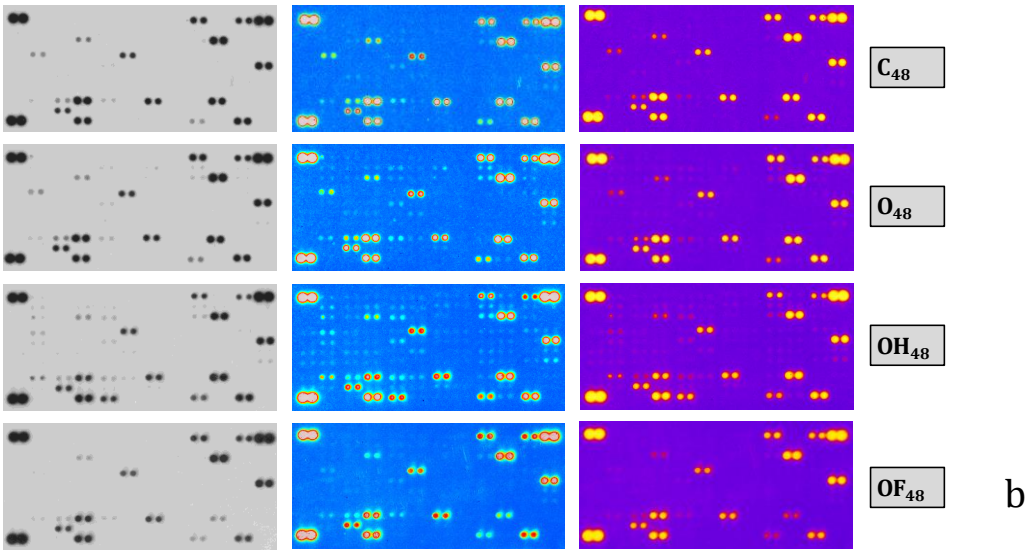

Note: in brief (Figure C.18.a), the array membranes are firstly activated, and then the sample (medium from cell-cultures, in our case) is incubated overnight on a rocking platform shaker, at 2 to 8°C. The following day, the sample is removed and the membranes are washed, and then exposed to a detection antibody cocktail and incubated for 1 h on a rocking platform shaker, at room temperature. The membranes are then washed, and exposed to streptavidin-HRP and incubated for 30 min on a rocking platform shaker, at room temperature. Finally, the membranes are washed and exposed to a mixture of stabilized hydrogen peroxide with preservative and stabilized luminol with preservative, that allows their visualization on an X-ray film (Figure C.18.b). For more details on the procedure and the particular reagents provided by the manufacturer, see the technical datasheet of the Proteome Profiler Mouse XL Cytokine Array Kit (R&D Systems, product number: ARY028) and consult Table C.5.

C_{48}: control (at 48 h); HRP: horseradish-peroxidase; O_{48}: oligomycin (at 48 h); OF_{48}: oligomycin, ferrum (at 48 h); OH_{48}: oligomycin, haemin (at 48 h)

Figure C.19: Volcano plot of the proteomic profiling of the O_{48} treatment group as compared to that of the control (C_{48}).

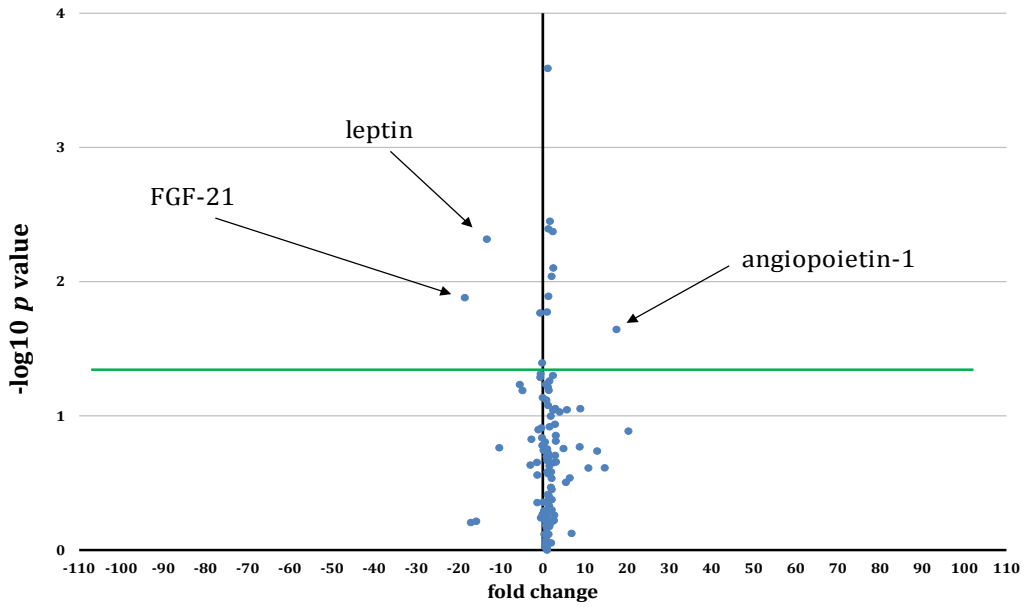

Note: for a synopsis of the protocol followed and the analytes measured, see Figure C.18 and Table C.5, respectively. For more details on the significant "hits" of this plot, see Table C.6.

analyte abbreviations are defined in Table C.5; C_{48}: control (at 48 h); O_{48}: oligomycin (at 48 h)

Figure C.20: Volcano plot of the proteomic profiling of the OH_{48} treatment group as compared to that of the control (C_{48}).

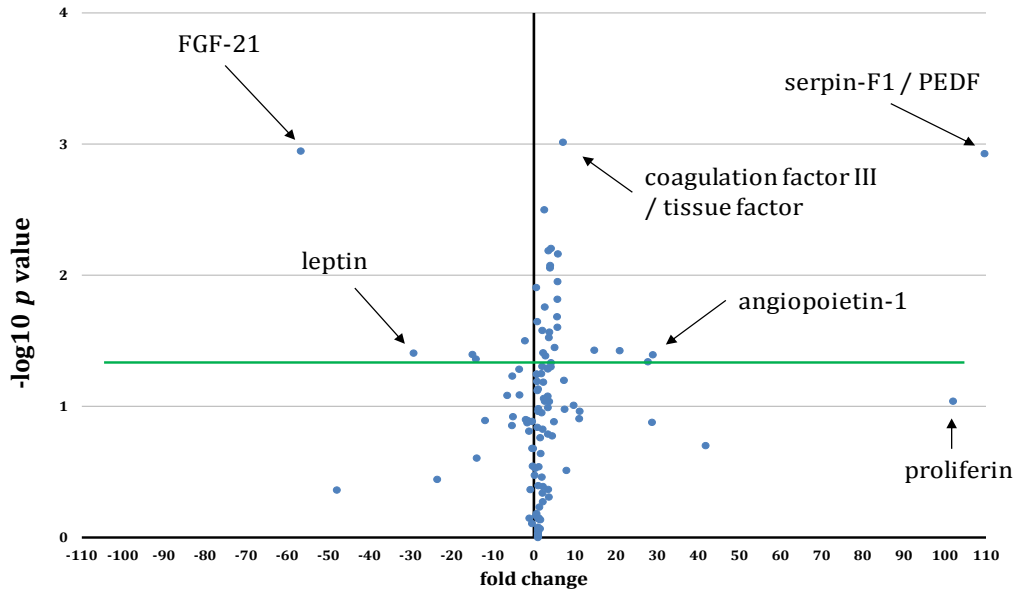

Note: for a synopsis of the protocol followed and the analytes measured, see Figure C.18 and Table C.5, respectively. For more details on the significant "hits" of this plot, see Table C.6.

analyte abbreviations are defined in Table C.5; C_{48}: control (at 48 h); OH_{48}: oligomycin, haemin (at 48 h); serpin-F1 / PEDF: serine (or cysteine) peptidase inhibitor, clade F, member 1 / pigment epithelium-derived factor

Figure C.21: Volcano plot of the proteomic profiling of the OF_{48} treatment group as compared to that of the control (C_{48}).

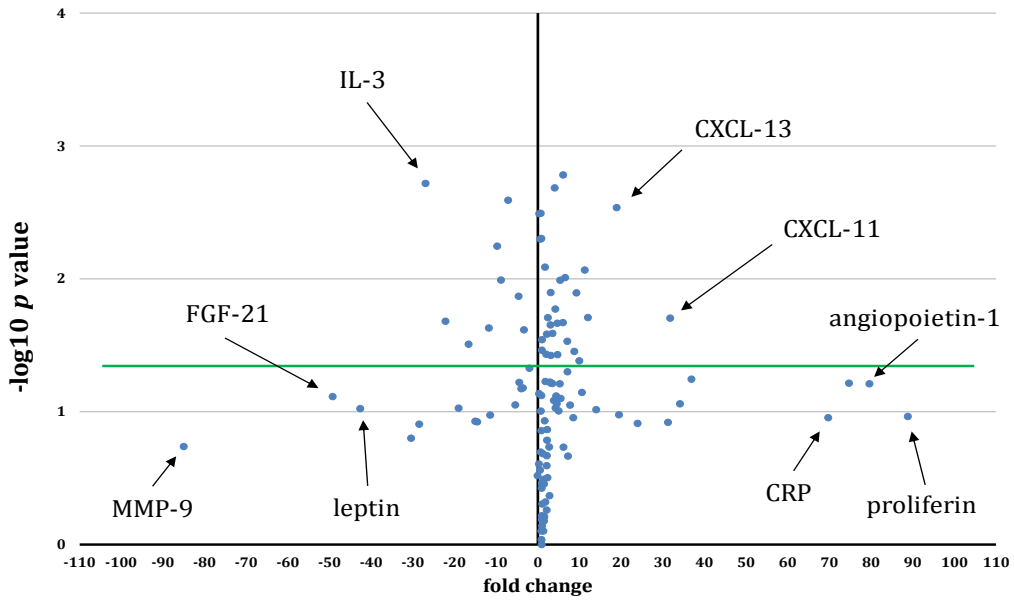

Note: for a synopsis of the protocol followed and the analytes measured, see Figure C.18 and Table C.5, respectively. For more details on the significant "hits" of this plot, see Table C.6.

analyte abbreviations are defined in Table C.5; C_{48}: control (at 48 h); OF_{48}: oligomycin, ferrum (at 48 h)

PART D

Critical appraisal

CHAPTER VIII

Utility, novelty and limitations of the developed *in vitro* simulation approaches

The term "model" is not adopted for the description of the developed or other *in vitro* simulation approaches to intracerebral haemorrhage in this PhD Thesis; at the heart of the choice to not do so, is my belief that this term should be reserved for refined simulation approaches or approaches that can be as close as possible to the *in vivo* reality, as justified by high standards and carefully-parametrised technical scrutiny[1]. The herein presented *in vitro* simulation approaches to intracerebral haemorrhage are far from being in place to be considered as "models" for this devastating disease of high pathophysiological complexity. They can, however, be extremely useful in ways that are discussed in this chapter, along with the novelty that their development has introduced. A selected overview of the limitations of the developed simulation approaches as well as of their assessment, is also provided.

VIII.1. Utility of the developed *in vitro* simulation approaches

We developed two novel *in vitro* simulation approaches to intracerebral haemorrhage, based on the use of a commercially-available immortalized embryonic murine hippocampal cell-line (mHippoE-14, available from CELLutions Biosystems Inc.) and its response to oligomycin-A and ferrum (as $FeCl_2$) or haemin under appropriately-selected conditions (Figure D.1). These two approaches: (a) are simulating aspects of both the primary and the secondary injury taking place in intracerebral haemorrhage, in an acceptable natural history-simulating manner (see Chapter I), (b) are utilizing acceptable (realistic) toxic compound concentrations (particularly with regards to ferrum and haemin; see Chapter VI), (c) are providing assessment (assay) windows of several hours in which injury is exerted in a constant manner (see Chapter VII), (d) are 3R-friendly (see Chapter III), and (e) can provide a good basis for the development of high-throughput *in vitro* drug-screening platforms toward the exploration of the neuroprotective potential of "candidate" compounds (see Chapter VII). A third *in vitro* simulation approach to intracerebral haemorrhage might also be claimed for the treatment group that is

[1] some ideas on how this technical scrutiny can come into reality within an universally-accepted (*erga omnes*) framework, are discussed in Chapter IX.

solely exposed to oligomycin; an approach that could be adopted in order to simulate parts of the brain that form the "metabolic" penumbra, but do not get to be exposed to the products of the lysis of the haematoma's erythrocytes (see Chapter VII).

To my opinion, the utility of the aforementioned *in vitro* simulation approaches to intracerebral haemorrhage is primarily condensed to the fact that they provide a well-designed basis for the development of more complex and sophisticated *in vitro* simulation approaches to this disease, based on the use of an immortalized cell-line that maintains a neuronal phenotype and can be well employed into a high-throughput assessment approach. In that respect, the possibility of developing a number of more complex experimental set-ups in which the FBS-deprived mHippoE-14 cell-line could: (a) be exposed to more / other intracerebral haemorrhage-related compounds / elements (such as thrombin, haemoglobin, TNF-α, IL-1β, *etc.*), (b) be subject to a modification of their gene expression, and / or (c) be co-cultured, either directly or indirectly (e.g. through well-inserts), along with glial or microglial cell-lines, is definitely worth exploring.

VIII.2. Novelty of the developed *in vitro* simulation approaches

Table D.1 summarizes the novelty of the developed *in vitro* simulation approaches to intracerebral haemorrhage, which arose both directly, from the simulation approaches' development (see Chapters VI and VII), as well as indirectly, from the work performed toward the characterization of the mHippoE-14 cell-line (see Chapters IV and V). The direct novelty elements are mainly highlighted by the fact that the developed *in vitro* simulation approaches are the first to combine the use of a commercially-available immortalized hippocampal cell-line (bearing neuronal characteristics) with a multi-level, synchronized simulation set-up that employs not 1, but 3 injurious factors related to the neuropathological cascade of intracerebral haemorrhage. Moreover, the careful employment of the xCELLigence real-time cellular response profiling technology in the development and assessment of these approaches, has not only transfused them with high-throughput applicability, but has generated important information with regards to their further improvement / exploitation. The credibility of the xCELLigence data has been confirmed by the performed cytomorphological assessment (see Chapters V and VII), while some aspects of the performed neuronal markers' expression profiling and proteomic profiling are highly-encouraging toward the consideration of these conditions as suitable and relevant to the neuropathological responses known to take place in intracerebral haemorrhage, *in vivo*.

The indirect novelty elements arose from the work performed for the purpose of the mHippoE-14 cell-line characterization (see Chapters IV and V); as already mentioned in the Preface, the latter is equally (if not more) important to the task of the actual development and

assessment of the *in vitro* simulation approaches that this PhD Thesis presents. This work had to be undertaken due to the limited data available for the mHippoE-14 cell-line (Gingerich *et al.*, 2010; Chapter III), and has provided us with valuable technical information with regards to: (a) their cellular responses to FBS-deprivation, (b) their interesting (but, concentration-dependent) dependency on iron, as well as (c) their own cytomorphology. Of particular and wider value is the proposed parametropoiesis of the real-time cellular response analysis that has been developed within the characterization of the mHippoE-14 cellular response profiling in response to FBS-deprivation (see Chapter IV); the latter can be very useful for the optimization of any *in vitro* assay reported in the literature that employs FBS-deprivation. Finally, the herein presented mHippoE-14 atlas and the cytomorphological parametropoiesis of the live (through phase-contrast microscopy) cell captioning of these cells, will be of paramount importance for the further characterization of these cell-lines[2], the optimization of the employed high-throughput approaches (Vistejnova *et al.*, 2009), and the undertaking of more accurate and detailed cytomorphological assessment of their response to toxic and / or neuroprotective conditions.

VIII.3. Limitations of the developed *in vitro* simulation approaches

Any *in vitro* simulation approach to a human disease - no matter how well-designed it is - is destined to bear serious limitations; the current project is no difference to this rule. One can easily recognise three types of limitations: (a) those that arise from the conceptual context of the development of these approaches, (b) those that arise from the technical limitations that they impose on the simulation of the disease, and (c) those that are related to the undertaken assessment. Table D.2 provides a synopsis of these limitations, which are also presented below:

- *characterization of the mHippoE-14 and associated cell-lines:* the available data with regards to the neurodynamic properties[3] of the mHippoE-14 cell-line are limited,
- *pathopoietic transformation of the mHippoE-14 cell-line:* unfortunately, the manual approach to FBS-deprivation introduces an additional variation factor to the consistency of the development and assessment of these *in vitro* simulation approaches to intracerebral haemorrhage,
- *atlas of the mHippoE-14 cellular morphology:* a study of the time-dependent patterns of the mHippoE-14 typology within the developed cytomorphological classification (as proposed in Chapter V) must be conducted in the future, along with a thorough im-

[2] I believe that the mHippoE-14 atlas and the cytomorphological parametropoiesis presented in Chapter V, could be applicable on all mHippoE cell-lines (-2, -5, -14 and -18; see Chapter III).
[3] particularly of the neurochemical and neurophysiological properties of these cells.

munocytochemical profiling of these cells; the latter must be comparatively assessed with the classification developed by Dotti *et al*. (1988),

- *parametropoiesis of the mHippoE-14 cellular morphology assessment:* the parametropoiesis developed was - to an extent - practically appropriate for the assessment of the developed *in vitro* simulation approaches to intracerebral haemorrhage, but could have been further upgraded through the adoption of assessment patterns present in the cytopathological assessment of cellular responses presented in Tables APP.1 and APP.2, and the use of more automated approaches toward its analysis (Kim *et al.*, 2011),
- *intra- and inter-rater reproducibility assessment of the introduced cytomorphological parameters:* the assessment of the reproducibility of the cytomorphological parameters presented in Table B.8 (not performed) might have provided useful information on the utility of the scoring system,
- *use of oligomycin-A as an approach to ischaemia-related phenomena:* although oligomycin was considered as a condition suitable for the *in vitro* simulation of the primary injury induced by intracerebral haemorrhage, one must not ignore data supporting the ability of this antibiotic to suppress TNF-α-induced apoptosis (Shchepina *et al.*, 2002) or prevent HIF-1α expression (Gong and Agani, 2005), in other experimental settings,
- *profiling of neuronal markers' expression:* further markers, aiming to characterize the mode(s) of neuronal death (see subchapter I.8) occurring, must be employed in order to fully-characterize the mechanisms through which oligomycin and haemin or ferrum exert their neurotoxicity on mHippoE-14 cells,
- *neurochemical assessment:* with regards to AChE activity in the mHippoE-14 cells under the developed intracerebral haemorrhage-simulating *in vitro* conditions, a reason for not obtaining statistically significant results might have been the fact that the buffer contained 50 mM Tris-HCl, pH 7.4, and 300 mM sucrose; the use of a high ionic strength buffer[4] was not adopted, and this might have had an effect on the effective solubilisation of the cells and the extraction of AChE,
- *proteomic profiling:* finally, as already underlined in subchapter VII.5, the proteomic profiling performed could further benefit from a validation of its hits *via* Western blotting.

>> Table D.1: page 157

>> Table D.2: page 158

>> Figure D.1: page 159

[4] consisting of 10 mM sodium phosphate ($NaHPO_4$), pH 7.0-8.0, 1 M NaCl, 10% Triton X-100 and 1 mM ethylenediaminetetraacetic acid (EDTA).

Table D.1: Synopsis of the novelty of the developed *in vitro* simulation approaches to intracerebral haemorrhage.

Novelty introduced by the developed *in vitro* simulation approaches
– the combination of the use of the mHippoE-14 cell-line in a multi-level, synchronized set-up that employs 3 injurious factors related to the neuropathology of intracerebral haemorrhage, with particular emphasis on the use of oligomycin as one of these factors
– the employment of the xCELLigence real-time cellular response profiling technology in the development and assessment of these approaches, generating important information with regards to their further improvement / exploitation
– the introduction of novel parametropoiesis of the real-time cellular response analysis that has been developed within the characterization of the mHippoE-14 cellular response profiling in response to FBS-deprivation
– the development of the mHippoE-14 atlas and the cytomorphological parametropoiesis of the live (through phase-contrast microscopy) cell captioning of these cells

FBS: foetal bovine serum

Table D.2: Synopsis of the limitations of the developed *in vitro* simulation approaches to intracerebral haemorrhage.

Limitations of the developed *in vitro* simulation approaches
– limited data exist with regards to the neurodynamic properties of the mHippoE-14 cells
– the manually-performed pathopoietic transformation of the mHippoE-14 cells (through FBS-deprivation), introduces concerns with regards to the approaches' repeatability
– the atlas of the mHippoE-14 cellular morphology requires further study and the undertaking of a thorough immunocytochemical profiling
– the developed parametropoiesis of the mHippoE-14 cytomorphological assessment could be further enriched, and benefit from the use of automated approaches toward its analysis
– the use of oligomycin-A as an approach to ischaemia-related phenomena produces biological phenomena that might prevent aspects of the *in vivo* intracerebral haemorrhage pathophysiology to be successfully simulated *in vitro*
– the profiling of neuronal markers' expression must be enriched with markers aiming to characterize the mode(s) of the occurring neuronal death under the developed conditions
– the performed neurochemical assessment might have failed due to technical reasons
– the performed proteomic profiling could benefit from a validation of its hits

FBS: foetal bovine serum

Figure D.1: Synopsis of the developed *in vitro* simulation approaches to intracerebral haemorrhage.

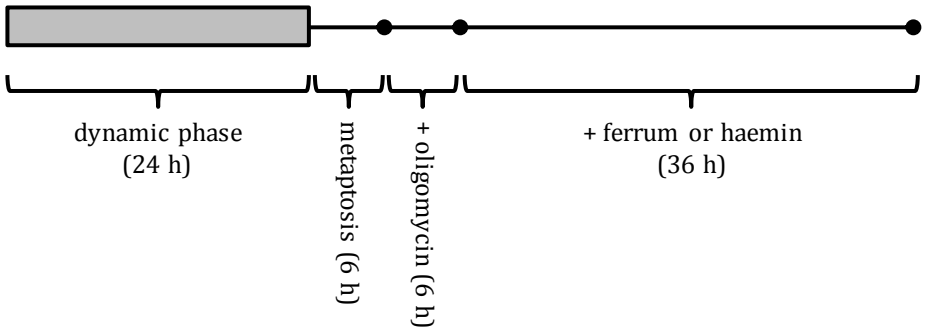

Note: the developed *in vitro* simulation approaches to intracerebral haemorrhage are based on the pathopoietic transformation of the mHippoE-14 cells through FBS-deprivation (induction of metaptosis), followed by exposure to oligomycin-A and, finally, to ferrum or haemin (at a concentration of 500 μM). For more details, see Chapters VI and VII.

FBS: foetal bovine serum

CHAPTER IX

The developed *in vitro* simulation approaches within the neuropathopoietic context

The work linked to the development and the characterization of the herein presented *in vitro* simulation approaches to intracerebral haemorrhage, is defined by a close association to the ideas presented along with the introduction of "neuropathopoiesis" (Zarros, 2014) and a recent evaluation of the nanoneurotoxicologic use of mHippoE-18 cells (Zarros *et al.*, 2015). This final chapter is an attempt to place these *in vitro* simulation approaches within the neuropathopoietic context; a task that requires a small introduction to what really is "neuropathopoiesis" (or, at least, what I perceive it to mean), and the ways I currently envisage its theoretical and technical parametropoiesis.

IX.1. Neuropathopoiesis

The term "neuropathopoiesis" was proposed by myself (Zarros, 2014) in reply to an insightful commentary written by Remco H.S. Westerink of the Utrecht University (Westerink, 2013) on the use of *in vitro* simulation approaches toward the development of high-throughput screening neurotoxicity tests; the commentary was actually focusing on how these tests could meet the screening requirement of the REACH (Registration, Evaluation and Authorization of CHemicals) framework and other similar legislative frameworks. The term "neuropathopoiesis" summarized - on that occasion - the need for the enforcement of a number of *"prerequisites as a means for a systematic and reliable introduction of neurotoxicity testing within the REACH legislative framework"* (Zarros, 2014), and has been ambitiously proposed as *"a new experimental subfield aiming to construct and establish theoretical principles and technical parameters which could be used as a basis for the development and assessment of in vitro simulation approaches to brain-representing entities and their diseases towards the delivery of more efficient and reliable drug-screening tools"* (Zarros, 2014).

Amongst these prerequisites, apart from the advancement of the 3R principles and the amendment of the REACH regulations, I underlined (Zarros, 2014) the need for: (a) a systematic designation of the usefulness of *in vitro* experimentation within an integrative approach to neurotoxicological assessment (Harry *et al.*, 1998), (b) the implementation and further de-

velopment of morphological[1] parametropoiesis of the *in vitro* testing endpoints (Bolon *et al.*, 1993; Marmiroli *et al.*, 2012), (c) the identification and abolishment of the technical misapplications and misinterpretations of currently employed *in vitro* approaches and their assessment endpoints (Westerink, 2013), and (d) the introduction and establishment of an *erga omnes* systematization / framework for the characterization of the reliability of each and every *in vitro* simulation approach to physiological processes or pathological nervous system-related entities (Zarros, 2014).

A few months later, the need for such an *erga omnes* framework was highlighted again (Zarros *et al.*, 2015). In the latter case, the reason was an experimental study by Janaszewska *et al*. (2013), in which mHippoE-18 cells were not deprived of FBS prior to their exposure to a novel nanoparticle; a modified polyamidoamine (PAMAM) dendrimer[2] of the fourth generation, with 4-carbomethoxypyrrolidone surface groups (PAMAM-pyrrolidone dendrimer).

IX.2. Suggested theoretical and technical parametropoiesis

My current understanding / vision on how such an *erga omnes* framework, a "Neuropathopoiesis Assessment Framework" (NAF), could be realized, is summarized in Figure D.2. I understand NAF to be a framework for the assessment of "simulation approach applications" (SAAs) prior to their designation as "drug-screening tools" (DSTs). At the core of this framework lies the "Neuropathopoiesis Assessment Scale" (NAS), the values of which are to be provided by the employment of two types of proposed assessment procedures[3]: the "technical pro-evaluation" (TPE) and the "technical meta-evaluation" (TME). The first procedure could provide a TPE index (TPE_i; see Table D.3) as a NAS metric of the assessment of an individual SAA, leading (hopefully) to its subsequent revision / improvement (function [1] of the NAF; Figure D.2). The second procedure could provide a TME score (TMES; see Table D.4) as a NAS metric of the assessment of an individual SAA as compared to multiple relevant (to each other) SAAs (function [2] of the NAF; Figure D.2). It is these NAS metrics that can potentially allow us to have a clear perspective on the reliability of each and every *in vitro* simulation approach (SAA) to *in vivo* physiological processes or pathological nervous system-related entities, and of their potential to eventually become DSTs (function [3] of the NAF; Figure D.2).

IX.3. Assessment and perspective of the developed *in vitro* simulation approaches

In view of the above parametropoiesis, the herein presented *in vitro* simulation approaches to intracerebral haemorrhage can only be assessed through the TPE_i (Table D.3) of function [1]

[1] neuropathological / cytopathological.
[2] dendrimers are repetitively-branched macromolecules with nanometer-scale dimensions.
[3] these two types of assessment procedures need to be to subject to editorial definition; they could become novel types of manuscripts for a number of academic journals.

of the NAF (Figure D.2). Considering that our SAAs (as summarized in Chapter VIII) employ a 3R-friendly monoculture that is relevant to the context of intracerebral haemorrhage, require a partial use of FBS, implement a partially-appropriate morphological and functional end-points' assessment, and qualify for a neuropathopoietic conditions' grading of BAB[4], they are eligible for a TPE_i of 20 (out of 120; see Table D.3). The interpretation of this TPE_i can only be meaningful within a TME, where it can be subject to a comparative assessment with other related SAAs that aim to simulate intracerebral haemorrhage. Until then, this TPE_i should be considered as a reference number that further experimental work should be designed to improve.

>> Table D.3: page 163
>> Table D.4: page 164
>> Figure D.2: page 165

[4] the conditions within our SAAs partially relate to reality (B), are highly timely-relevant (A), and can partially induce injury in a realistic manner (B); grade BAB (Table D.3).

Table D.3: The proposed NAS: an overview of the TPE_i and its calculation as part of the TPE assessment procedure.

Component of the TPE_i	**Component's specifics**	**Points**
nature of the SAA's cellular substrate	relevant polyculture; 3R-friendly	4
	relevant polyculture; non-3R-friendly	3
	relevant monoculture; 3R-friendly	2
	relevant monoculture; non-3R-friendly	1
	irrelevant polyculture or monoculture	0
use of FBS or other sera	no	2
	partial	1
	yes	0
morphological endpoints' assessment	yes	2
	partial	1
	no	0
functional endpoints' assessment	yes	2
	partial	1
	no	0
neuropathopoietic conditions' grading	grade AAA	x12
	grades AAB or ABA	x10
	grades AAC, ABB or ACA	x8
	grades ABC or ACB	x6
	grade BAA	x5
	grades ACC, BAB or BBA	x4
	grades BAC, BBB or BCA	x3
	grades BBC or BCB	x2
	grade BCC	x1
	grades CAA, CAB or CAC	x0
	grades CBA, CBB or CBC	x0
	grades CCA, CCB or CCC	x0

Note: the current method of calculating the TPE_i might not be final; further revisions of it might apply prior and / or after publication. The TPE_i is calculated as the sum of the points gathered from the first four components, multiplied by the point factor suggested from the fifth component (the neuropathopoietic conditions' grading); it can, thus, provide a final index between 0 and 120. The neuropathopoietic conditions' grading distinguishes whether the conditions mimicking the simulated neuropathopoietic context (normal or pathological nervous system entity; natural history of the disease, *etc*.) are relevant to (clinical) reality (first letter component; A: highly; B: partially; C: not at all), and whether they are applied in a timely-relevant to (clinical) reality manner (second letter component; A: highly; B: partially; C: not at all), and a realistic (function- or) injury-inducing manner (third letter component; A: highly; B: partially; C: not at all). The method should not be applied on cases of irrelevant polycultures or monocultures.

FBS: foetal bovine serum; NAS: Neuropathopoiesis Assessment Scale; TPE: technical pro-evaluation; TPE_i: TPE index; SAA: simulation approach application

Table D.4: The proposed NAS: an overview of the TMES and its calculation as part of the TME assessment procedure.

Component of the TMES	Component's specifics	Points
morphological endpoints' characterization	complete	2
	partially-complete	1
	inadequate	0
functional endpoints' characterization	complete	2
	partially-complete	1
	inadequate	0
classification of SAA's optimized TPE_i	top 10% of relevant SAAs	x5
	top 30% of relevant SAAs	x4
	top 50% of relevant SAAs	x3
	bottom 50% of relevant SAAs	x2
	bottom 30% of relevant SAAs	x1
	bottom 10% of relevant SAAs	x0
high-throughput applicability	yes	+
	no	-

Note: the current method of calculating the TMES might not be final; further revisions of it might apply prior and / or after publication. The TMES is calculated as the sum of the points gathered from the first two components, multiplied by the point factor suggested from the third component (the neuropathopoietic conditions' grading), and being given a "+" or "-" superscript depending on the fourth component; it can, thus, provide a final score between 0^- and 20^+. It is obvious that the TMES for a given SAA is highly dependent on the number of other relevant SAAs co-evaluated within the same TME; the power of the TME itself.

NAS: Neuropathopoiesis Assessment Scale; TME: technical meta-evaluation; TMES: TME score; TPE_i: technical pro-evaluation index; SAA: simulation approach application

Figure D.2: Temporary simplified schematic outline of the proposed NAF for *in vitro* simulation approaches to diseases, and its functions.

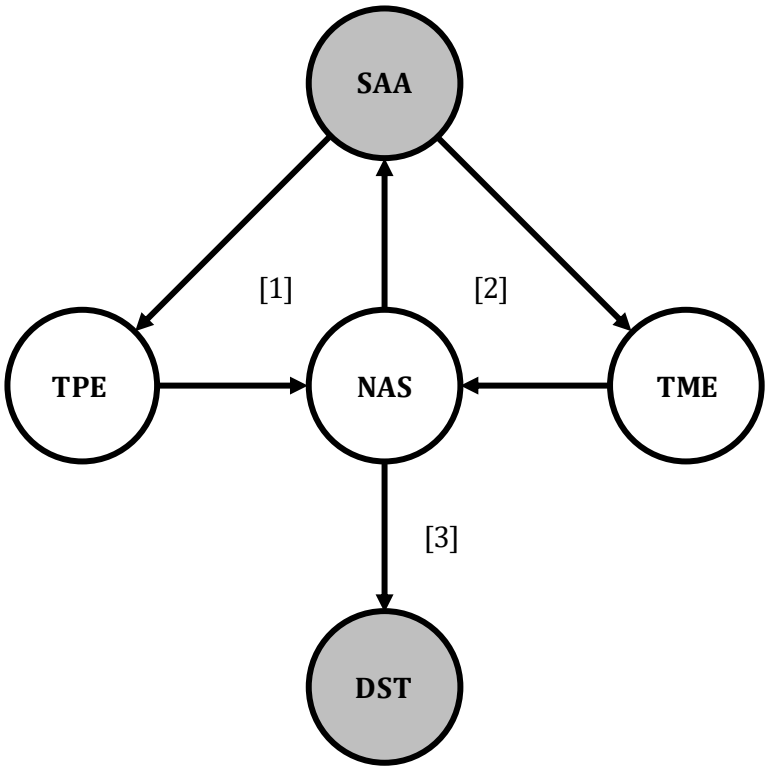

Note: the NAF should serve three functions ([1]-[3]): (a) the assessment of individual SAAs through TPEs, leading (hopefully) to a revision of future SAAs (function [1]), (b) the assessment of multiple SAAs through TMEs, leading to a critical appraisal of their neuropathopoietic capacity (function [2]), and (c) the comparative assessment of the suitability of certain SAAs to be adopted as DST (function [3]).

DST: drug-screening tool; NAF: Neuropathopoiesis Assessment Framework; NAS: Neuropathopoiesis Assessment Scale; TME: technical meta-evaluation; TPE: technical pro-evaluation; SAA: simulation approach application

REFERENCES

Development and Assessment of *In Vitro* Simulation Approaches to Intracerebral Haemorrhage

Abbed KM, Ogilvy CS. Intracerebral hematoma from aneurysm rupture. *Neurosurgical Focus* 2003; 15(4): E4.

Aggarwal SK, Williams V, Levine SR, Cassin BJ, Garcia JH. Cocaine-associated intracranial hemorrhage: absence of vasculitis in 14 cases. *Neurology* 1996; 46(6): 1741-1743.

Aguilar MI, Freeman WD. Spontaneous intracerebral hemorrhage. *Seminars in Neurology* 2010; 30(5): 555-564.

Aiyagari V, Testai FD. Correction of coagulopathy in warfarin associated cerebral hemorrhage. *Current Opinion in Critical Care* 2009; 15(2): 87-92.

Allen CM. Differential diagnosis of acute stroke: a review. *Journal of the Royal Society of Medicine* 1984; 77(10): 878-881.

Alluri H, Anasooya Shaji C, Davis ML, Tharakan B. Oxygen-glucose deprivation and reoxygenation as an in vitro ischemia-reperfusion injury model for studying blood-brain barrier dysfunction. *Journal of Visualized Experiments* 2015; (99): e52699.

Al-Shahi Salman R, Labovitz DL, Stapf C. Spontaneous intracerebral haemorrhage. *British Medical Journal* 2009; 339: b2586.

Andaluz N, Zuccarello M, Wagner KR. Experimental animal models of intracerebral hemorrhage. *Neurosurgery Clinics of North America* 2002; 13(3): 385-393.

Anderson CS. Medical management of acute intracerebral hemorrhage. *Current Opinion in Critical Care* 2009; 15(2): 93-98.

Anderson NL, Polanski M, Pieper R, Gatlin T, Tirumalai RS, Conrads TP, Veenstra TD, Adkins JN, Pounds JG, Fagan R, Lobley A. The human plasma proteome: a nonredundant list developed by combination of four separate sources. *Molecular & Cellular Proteomics* 2004; 3(4): 311-326.

Andres RH, Guzman R, Ducray AD, Mordasini P, Gera A, Barth A, Widmer HR, Steinberg GK. Cell replacement therapy for intracerebral hemorrhage. *Neurosurgical Focus* 2008; 24(3-4): E16.

Anzalone N, Scotti R, Riva R. Neuroradiologic differential diagnosis of cerebral intraparen-

chymal hemorrhage. *Neurological Sciences* 2004; 25(suppl.1): s3-s5.

Appelros P, Stegmayr B, Terént A. Sex differences in stroke epidemiology: a systematic review. *Stroke* 2009; 40(4): 1082-1090.

Arato-Oshima T, Matsui H, Wakizaka A, Homareda H. Mechanism responsible for oligomycin-induced occlusion of Na^+ within Na/K-ATPase. *Journal of Biological Chemistry* 1996; 271(41): 25604-25610.

Arboix A, Manzano C, García-Eroles L, Massons J, Oliveres M, Parra O, Targa C. Determinants of early outcome in spontaneous lobar cerebral hemorrhage. *Acta Neurologica Scandinavica* 2006; 114(3): 187-192.

Argyriou AA, Tsota I, Solomou E, Marangos M, Kalogeropoulou C, Petsas T, Dimopoulos PA, Chroni E. Intracerebral haemorrhage as a rare complication of HSV-1 meningoencephalitis: case report and review of the literature. *Scandinavian Journal of Infectious Diseases* 2006; 38(1): 63-66.

Ariesen MJ, Claus SP, Rinkel GJ, Algra A. Risk factors for intracerebral hemorrhage in the general population: a systematic review. *Stroke* 2003; 34(8): 2060-2065.

Aronowski J, Hall CE. New horizons for primary intracerebral hemorrhage treatment: experience from preclinical studies. *Neurological Research* 2005; 27(3): 268-279.

Aronowski J, Zhao X. Molecular pathophysiology of cerebral hemorrhage: secondary brain injury. *Stroke* 2011; 42(6): 1781-1786.

Asdaghi N, Manawadu D, Butcher K. Therapeutic management of acute intracerebral haemorrhage. *Expert Opinion on Pharmacotherapy* 2007; 8(18): 3097-3116.

Asgari S, Wanke I, Schoch B, Stolke D. Recurrent hemorrhage after initially complete occlusion of intracranial aneurysms. *Neurosurgical Review* 2003; 26(4): 269-274.

Askenase MH, Sansing LH. Stages of the inflammatory response in pathology and tissue repair after intracerebral hemorrhage. *Seminars in Neurology* 2016; 36(3): 288-297.

Athyros VG, Tziomalos K, Karagiannis A, Wierzbicki AS, Mikhailidis DP. Aggressive statin treatment, very low serum cholesterol levels and haemorrhagic stroke: is there an association? *Current Opinion in Cardiology* 2010; 25(4): 406-410.

Babikian VL, Kase CS, Pessin MS, Norrving B, Gorelick PB. Intracerebral hemorrhage in stroke patients anticoagulated with heparin. *Stroke* 1989; 20(11): 1500-1503.

Babu R, Bagley JH, Di C, Friedman AH, Adamson C. Thrombin and hemin as central factors in the mechanisms of intracerebral hemorrhage-induced secondary brain injury and as potential targets for intervention. *Neurosurgical Focus* 2012; 32(4): E8.

Badjatia N, Rosand J. Intracerebral hemorrhage. *Neurologist* 2005; 11(6): 311-324.

Balami JS, Buchan AM. Complications of intracerebral haemorrhage. *Lancet Neurology* 2012; 11(1): 101-118.

Ballesteros MA, López-Hoyos M, Muñoz P, Marin MJ, Miñambres E. Apoptosis of neuronal cells induced by serum of patients with acute brain injury: a new *in vitro* prognostic model. *Intensive Care Medicine* 2007; 33(1): 58-65.

Balucani C, Barlinn K. Medullary infarcts and hemorrhages. *Frontiers of Neurology and Neuroscience* 2012; 30: 166-170.

Bao L, Zhou S, Zhao H, Zu J, He Q, Ye X, Cui G. Neuroprotective effects of 17β-estradiol against thrombin-induced apoptosis in primary cultured cortical neurons. *Pharmacology* 2015; 96(5-6): 284-289.

Barald KF. Culture conditions affect the cholinergic development of an isolated subpopulation of chick mesencephalic neural crest cells. *Developmental Biology* 1989; 135(2): 349-366.

Barbacid M. The Trk family of neurotrophin receptors. *Journal of Neurobiology* 1994; 25(11): 1386-1403.

Bartlett WP, Banker GA. An electron microscopic study of the development of axons and dendrites by hippocampal neurons in culture. I. Cells which develop without intercellular contacts. *Journal of Neuroscience* 1984; 4(8): 1944-1953.

Barnes AP, Polleux F. Establishment of axon-dendrite polarity in developing neurons. *Annual Review of Neuroscience* 2009; 32: 347-381.

Barratt HE, Lanman TA, Carmichael ST. Mouse intracerebral hemorrhage models produce different degrees of initial and delayed damage, axonal sprouting, and recovery. *Journal of Cerebral Blood Flow & Metabolism* 2014; 34(9): 1463-1471.

Basset P, Zwiller J, Revel MO, Vincendon G. Growth promotion of transformed cells by iron in serum-free culture. *Carcinogenesis* 1985; 6(3): 355-359.

Beaudoin GM 3rd, Lee SH, Singh D, Yuan Y, Ng YG, Reichardt LF, Arikkath J. Culturing pyramidal neurons from the early postnatal mouse hippocampus and cortex. *Nature Protocols* 2012; 7(9): 1741-1754.

Belayev L, Saul I, Curbelo K, Busto R, Belayev A, Zhang Y, Riyamongkol P, Zhao W, Ginsberg MD. Experimental intracerebral hemorrhage in the mouse: histological, behavioral, and hemodynamic characterization of a double-injection model. *Stroke* 2003; 34(9): 2221-2227.

Belsham DD, Cai F, Cui H, Smukler SR, Salapatek AM, Shkreta L. Generation of a phenotypic array of hypothalamic neuronal cell models to study complex neuroendocrine disorders. *Endocrinology* 2004; 145(1): 393-400.

Bilmin K, Kopczyńska B, Grieb P. Influence of serum and albumin on the *in vitro* anandamide cytotoxicity toward C6 glioma cells assessed by the MTT cell viability assay: implications for the methodology of the MTT tests. *Folia Neuropathologica* 2013; 51(1): 44-50.

Bimpis A, Papalois A, Tsakiris S, Kalafatakis K, Zarros A, Gkanti V, Skandali N, Al-Humadi H, Kouzelis C, Liapi C. Modulation of crucial adenosinetriphosphatase activities due to U-74389G administration in a porcine model of intracerebral hemorrhage. *Metabolic Brain Disease* 2013; 28(3): 439-446.

Bimpis A, Papalois A, Tsakiris S, Zarros A, Kalafatakis K, Botis J, Stolakis V, Zissis KM, Liapi C. Activation of acetylcholinesterase after U-74389G administration in a porcine model of intracerebral hemorrhage. *Metabolic Brain Disease* 2012; 27(2): 221-225.

Bimpis A, Papalois A, Voumvourakis K, Oláh O, Tiszlavicz L, Liapi C. Neuronal tumour necrosis factor-α and interleukin-1β expression in a porcine model of intracerebral haemorrhage: modulation by U-74389G. *Brain Research* 2015; 1615: 98-105.

Bimpis A, Zarros A. Treatment of intracerebral hemorrhage: where do we stand? *Rhode Island Medical Journal* 2014; 97(7): 12.

Bolon B, Dorman DC, Bonnefoi MS, Randall HW, Morgan KT. Histopathologic approaches to chemical toxicity using primary cultures of dissociated neural cells grown in chamber slides. *Toxicologic Pathology* 1993; 21(5): 465-479.

Bornebroek M, Haan J, Maat-Schieman ML, Van Duinen SG, Roos RA. Hereditary cerebral hemorrhage with amyloidosis-Dutch type (HCHWA-D): I - a review of clinical, radiologic and genetic aspects. *Brain Pathology* 1996; 6(2): 111-114.

Bosch EP, Kennedy SS, Aschenbrener CA. Ocular bobbing: the myth of its localizing value. *Neurology* 1975; 25(10): 949-953.

Bradke F, Dotti CG. Establishment of neuronal polarity: lessons from cultured hippocampal neurons. *Current Opinion in Neurobiology* 2000; 10(5): 574-581.

Brand MD, Nicholls DG. Assessing mitochondrial dysfunction in cells. *Biochemical Journal* 2011; 435(2): 297-312.

Brass LM, Lichtman JH, Wang Y, Gurwitz JH, Radford MJ, Krumholz HM. Intracranial hemorrhage associated with thrombolytic therapy for elderly patients with acute myocardial infarction: results from the Cooperative Cardiovascular Project. *Stroke* 2000; 31(8): 1802-1811.

Braughler JM, Chase RL, Pregenzer JF. Stimulation and inhibition of iron-dependent lipid peroxidation by desferrioxamine. *Biochemical and Biophysical Research Communications* 1988; 153(3): 933-938.

Brenner S, Gülden M, Maser E, Seibert H. Lasting effect of preceding culture conditions on the susceptibility of C6 cells to peroxide-induced oxidative stress. *Toxicology In Vitro* 2010; 24(8): 2090-2096.

Brisman MH, Bederson JB, Sen CN, Germano IM, Moore F, Post KD. Intracerebral hemorrhage occurring remote from the craniotomy site. *Neurosurgery* 1996; 39(6): 1114-1121.

Broderick J, Brott T, Tomsick T, Tew J, Duldner J, Huster G. Management of intracerebral hemorrhage in a large metropolitan population. *Neurosurgery* 1994; 34(5): 882-887.

Brouwers HB, Chang Y, Falcone GJ, Cai X, Ayres AM, Battey TW, Vashkevich A, McNamara KA, Valant V, Schwab K, Orzell SC, Bresette LM, Feske SK, Rost NS, Romero JM, Viswanathan A, Chou SH, Greenberg SM, Rosand J, Goldstein JN. Predicting hematoma expansion after primary intracerebral hemorrhage. *Journal of the American Medical Association Neurology* 2014; 71(2): 158-164.

Brunner D, Frank J, Appl H, Schöffl H, Pfaller W, Gstraunthaler G. Serum-free cell culture: the serum-free media interactive online database. *ALTEX* 2010; 27(1): 53-62.

Buckner SB, England JM, Batheja N. General cytologic principles. In: Atkinson BF (ed). Atlas of Diagnostic Cytopathology. *W. B. Saunders Company*, Philadelphia, 1992; 1-48.

Bulger RE. Use of animals in experimental research: a scientist's perspective. *Anatomical Record* 1987; 219(3): 215-220.

Bullitt E. Expression of *c-fos*-like protein as a marker for neuronal activity following noxious stimulation in the rat. *Journal of Comparative Neurology* 1990; 296(4): 517-530.

Bullock R, Brock-Utne J, van Dellen J, Blake G. Intracerebral hemorrhage in a primate model: effect on regional cerebral blood flow. *Surgical Neurology* 1988; 29(2): 101-107.

Bullock R, Mendelow AD, Teasdale GM, Graham DI. Intracranial haemorrhage induced at arterial pressure in the rat. Part 1: Description of technique, ICP changes and neuropathological findings. *Neurological Research* 1984; 6(4): 184-188.

Butcher K, Davis SM. MRI of intracerebral hemorrhage. In: Carhuapoma JR, Mayer SA, Hanley DF (eds). Intracerebral Hemorrhage. *Cambridge University Press*, Cambridge, 2010; 125-138.

Cai Y, Cho GS, Ju C, Wang SL, Ryu JH, Shin CY, Kim HS, Nam KW, Jalin AM, Sun W, Choi IY, Kim WK. Activated microglia are less vulnerable to hemin toxicity due to nitric oxide-dependent inhibition of JNK and p38 MAPK activation. *Journal of Immunology* 2011; 187(3): 1314-1321.

Cameron R, Klein L, Shyjan AW, Rakic P, Levenson R. Neurons and astroglia express distinct subsets of Na,K-ATPase α and β subunits. *Brain Research - Molecular Brain Research* 1994; 21(3-4): 333-343.

Camós S, Mallolas J. Experimental models for assaying microvascular endothelial cell pathophysiology in stroke. *Molecules* 2010; 15(12): 9104-9134.

Caplan RL: Intracerebral hemorrhage. In: Caplan RL. Stroke: A Clinical Approach. Second edition. *Butterworth-Heinemann*, Stoneham, 1993; 425-467.

Cavallini A, Fanucchi S, Persico A. Warfarin-associated intracerebral hemorrhage. *Neurological Sciences* 2008; 29(suppl.2): s266-s268.

Cervera A, Amaro S, Chamorro A. Oral anticoagulant-associated intracerebral hemorrhage. *Journal of Neurology* 2012; 259(2): 212-224.

Cervoni L, Artico M, Salvati M, Bristot R, Franco C, Delfini R. Epileptic seizures in intracerebral hemorrhage: a clinical and prognostic study of 55 cases. *Neurosurgical Review* 1994; 17(3): 185-188.

Chan LL, Kuksin D, Laverty DJ, Saldi S, Qiu J. Morphological observation and analysis using automated image cytometry for the comparison of trypan blue and fluorescence-based viability detection method. *Cytotechnology* 2015; 67(3): 461-473.

Chandrasoma P, Taylor CR. Concise Pathology. Second edition. *Appleton & Lange*, Norwalk, 1995; 917-919.

Chang CF, Chen SF, Lee TS, Lee HF, Chen SF, Shyue SK. Caveolin-1 deletion reduces early brain injury after experimental intracerebral hemorrhage. *American Journal of Pathology* 2011; 178(4): 1749-1761.

Chatonnet A, Lockridge O. Comparison of butyrylcholinesterase and acetylcholinesterase. *Biochemical Journal* 1989; 260(3): 625-634.

Chaudhary V, Bano S, Yadav S, Garga UC, Singh SK. Cerebral amyloid angiopathy. In: Chaudhary V (ed). Intracerebral Hemorrhage. *InTech*, Rijeka, 2014; 41-50.

Chaudhuri C, Salahudeen AK. Massive intracerebral hemorrhage in an amphetamine addict. *American Journal of the Medical Sciences* 1999; 317(5): 350-352.

Chen M, Caplan LR. Laboratory and other ancillary testing in intracerebral hemorrhage: an algorithmic approach. In: Carhuapoma JR, Mayer SA, Hanley DF (eds). Intracerebral Hemorrhage. *Cambridge University Press*, Cambridge, 2010; 149-157.

Chen S, Zeng L, Hu Z. Progressing haemorrhagic stroke: categories, causes, mechanisms and managements. *Journal of Neurology* 2014; 261(11): 2061-2078.

Chen S, Zhao M, Wu G, Yao C, Zhang J. Recent advances in morphological cell image analysis. *Computational and Mathematical Methods in Medicine* 2012; 2012: 101536.

Cheng KM, Chan CM, Fu YT, Ho LC, Cheung FC, Law CK. Acute hemorrhage in late radiation necrosis of the temporal lobe: report of five cases and review of the literature. *Journal of Neuro-Oncology* 2001; 51(2): 143-150.

Chen-Roetling J, Chen L, Regan RF. Apotransferrin protects cortical neurons from hemoglobin toxicity. *Neuropharmacology* 2011; 60(2-3): 423-431.

Chen-Roetling J, Li Z, Regan RF. Hemoglobin neurotoxicity is attenuated by inhibitors of the protein kinase CK2 independent of heme oxygenase activity. *Current Neurovascular Research* 2008; 5(3): 193-198.

Chen-Roetling J, Song W, Schipper HM, Regan CS, Regan RF. Astrocyte overexpression of heme oxygenase-1 improves outcome after intracerebral hemorrhage. *Stroke* 2015;

46(4): 1093-1098.

Cheung RT, Zou LY. Use of the original, modified, or new intracerebral hemorrhage score to predict mortality and morbidity after intracerebral hemorrhage. *Stroke* 2003; 34(7): 1717-1722.

Chewning RH, Murphy KP. Cerebral angiography. In: Carhuapoma JR, Mayer SA, Hanley DF (eds). Intracerebral Hemorrhage. *Cambridge University Press*, Cambridge, 2010a; 139-148.

Chewning RH, Murphy KP. Computerized tomography and CT angiography in intracerebral hemorrhage. In: Carhuapoma JR, Mayer SA, Hanley DF (eds). Intracerebral Hemorrhage. *Cambridge University Press*, Cambridge, 2010b; 121-124.

Chiaretti A, Caresta E, Piastra M, Pulitanò S, Di Rocco C. Cerebral hemorrhage in Henoch-Schoenlein syndrome. *Child's Nervous System* 2002; 18(8): 365-367.

Chittiboina P, Ganta V, Monceaux CP, Scott LK, Nanda A, Alexander JS. Angiopoietins as promising biomarkers and potential therapeutic targets in brain injury. *Pathophysiology* 2013; 20(1): 15-21.

Cho DY, Chen CC, Lee WY, Lee HC, Ho LH. A new Modified Intracerebral Hemorrhage score for treatment decisions in basal ganglia hemorrhage - a randomized trial. *Critical Care Medicine* 2008; 36(7): 2151-2156.

Cho S, Wood A, Bowlby MR. Brain slices as models for neurodegenerative disease and screening platforms to identify novel therapeutics. *Current Neuropharmacology* 2007; 5(1): 19-33.

Choudhri TF, Hoh BL, Solomon RA, Connolly ES Jr, Pinsky DJ. Use of a spectrophotometric hemoglobin assay to objectively quantify intracerebral hemorrhage in mice. *Stroke* 1997; 28(11): 2296-2302.

Chow JM, Huang GC, Lin HY, Shen SC, Yang LY, Chen YC. Cytotoxic effects of metal protoporphyrins in glioblastoma cells: roles of albumin, reactive oxygen species, and heme oxygenase-1. *Toxicology Letters* 2008; 177(2): 97-107.

Christie R, Yamada M, Moskowitz M, Hyman B. Structural and functional disruption of vascular smooth muscle cells in a transgenic mouse model of amyloid angiopathy. *American Journal of Pathology* 2001; 158(3): 1065-1071.

Chuang YC, Chen YM, Peng SK, Peng SY. Risk stratification for predicting 30-day mortality of intracerebral hemorrhage. *International Journal for Quality in Health Care* 2009; 21(6): 441-447.

Chung CS, Caplan LR, Han W, Pessin MS, Lee KH, Kim JM. Thalamic haemorrhage. *Brain* 1996; 119(6): 1873-1886.

Ciuffi M, Tarlini L, Mugnai S, Franchi-Micheli S, Zilletti L. Hemoglobin affects lipid peroxida-

tion and prostaglandin E2 formation in rat corticocerebral tissues *in vitro*. *Biochemical Pharmacology* 1996; 52(1): 97-103.

Clark W, Gunion-Rinker L, Lessov N, Hazel K. Citicoline treatment for experimental intracerebral hemorrhage in mice. *Stroke* 1998; 29(10): 2136-2140.

Counsell C, Boonyakarnkul S, Dennis M, Sandercock P, Bamford J, Burn J, Warlow C. Primary intracerebral haemorrhage in the Oxfordshire Community Stroke Project: 2. prognosis. *Cerebrovascular Diseases* 1995; 5(1): 26-34.

Coyle DE. Adaptation of C6 glioma cells to serum-free conditions leads to the expression of a mixed astrocyte-oligodendrocyte phenotype and increased production of neurite-promoting activity. *Journal of Neuroscience Research* 1995; 41(3): 374-385.

Crassard I, Bousser MG. Cerebral venous thrombosis and intracerebral hemorrhage. In: Carhuapoma JR, Mayer SA, Hanley DF (eds). Intracerebral Hemorrhage. *Cambridge University Press*, Cambridge, 2010; 84-99.

Cruceru ML, Enciu AM, Popa AC, Albulescu R, Neagu M, Tanase CP, Constantinescu SN. Signal transduction molecule patterns indicating potential glioblastoma therapy approaches. *OncoTargets and Therapy* 2013; 6: 1737-1749.

Cui HJ, He HY, Yang AL, Zhou HJ, Wang C, Luo JK, Lin Y, Tang T. Efficacy of deferoxamine in animal models of intracerebral hemorrhage: a systematic review and stratified meta-analysis. *PLoS One* 2015; 10(5): e0127256.

Cui X, Churchill GA. Statistical tests for differential expression in cDNA microarray experiments. *Genome Biology* 2003; 4(4): 210.

Cui Z, Zhong Z, Yang Y, Wang B, Sun Y, Sun Q, Yang GY, Bian L. Ferrous iron induces Nrf2 expression in mouse brain astrocytes to prevent neurotoxicity. *Journal of Biochemical and Molecular Toxicology* 2016; 30(8): 396-403.

Culmsee C, Gerling N, Lehmann M, Nikolova-Karakashian M, Prehn JH, Mattson MP, Krieglstein J. Nerve growth factor survival signaling in cultured hippocampal neurons is mediated through TrkA and requires the common neurotrophin receptor p75. *Neuroscience* 2002; 115(4): 1089-1108.

Da Silva VF, Bormanis J. Intracerebral hemorrhage after combined anticoagulant-thrombolytic therapy for myocardial infarction: two case reports and a short review. *Neurosurgery* 1992; 30(6): 943-945.

Davis DA, Bortolato M, Godar SC, Sander TK, Iwata N, Pakbin P, Shih JC, Berhane K, McConnell R, Sioutas C, Finch CE, Morgan TE. Prenatal exposure to urban air nanoparticles in mice causes altered neuronal differentiation and depression-like responses. *PLoS One* 2013; 8(5): e64128.

Davis JB, Maher P. Protein kinase C activation inhibits glutamate-induced cytotoxicity in a

neuronal cell line. *Brain Research* 1994; 652(1): 169-173.

Dayan F, Bilton RL, Laferrière J, Trottier E, Roux D, Pouyssegur J, Mazure NM. Activation of HIF-1α in exponentially growing cells via hypoxic stimulation is independent of the Akt/mTOR pathway. *Journal of Cellular Physiology* 2009; 218(1): 167-174.

De Reuck J, Hemelsoet D, Van Maele G. Seizures and epilepsy in patients with a spontaneous intracerebral haematoma. *Clinical Neurology and Neurosurgery* 2007; 109(6): 501-504.

de San Pedro JR, Rodríguez FA, Níguez BF, Sánchez JF, López-Guerrero AL, Murcia MF, Vilar AM. Massive hemorrhage in hemangioblastomas: literature review. *Neurosurgical Review* 2010; 33(1): 11-26.

Deinsberger W, Vogel J, Kuschinsky W, Auer LM, Böker DK. Experimental intracerebral hemorrhage: description of a double injection model in rats. *Neurological Research* 1996; 18(5): 475-477.

Del Turco D, Deller T. Organotypic entorhino-hippocampal slice cultures - a tool to study the molecular and cellular regulation of axonal regeneration and collateral sprouting *in vitro*. *Methods in Molecular Biology* 2007; 399: 55-66.

Derex L, Nighoghossian N. Intracerebral haemorrhage after thrombolysis for acute ischaemic stroke: an update. *Journal of Neurology, Neurosurgery & Psychiatry* 2008; 79(10): 1093-1099.

Detwiler PW, Porter RW, Zabramski JM, Spetzler RF. *De novo* formation of a central nervous system cavernous malformation: implications for predicting risk of hemorrhage. Case report and review of the literature. *Journal of Neurosurgery* 1997; 87(4): 629-632.

Dey M, Jaffe J, Stadnik A, Awad IA. External ventricular drainage for intraventricular hemorrhage. *Current Neurology and Neuroscience Reports* 2012; 12(1): 24-33.

Diamond P, Gale S, Stewart K. Primary intracerebral haemorrhage - clinical and radiologic predictors of survival and functional outcome. *Disability and Rehabilitation* 2003; 25(13): 689-698.

Dibner MD, Insel PA. Growth of C6 glioma cells in serum-containing medium decreases β-adrenergic receptor number. *Journal of Cellular Physiology* 1981a; 109(2): 309-315.

Dibner MD, Insel PA. Serum catecholamines desensitize β-adrenergic receptors of cultured C6 glioma cells. *Journal of Biological Chemistry* 1981b; 256(14): 7343-7346.

Diemert S, Dolga AM, Tobaben S, Grohm J, Pfeifer S, Oexler E, Culmsee C. Impedance measurement for real time detection of neuronal cell death. *Journal of Neuroscience Methods* 2012; 203(1): 69-77.

Donnan GA, Davis SM. Surgery for intracerebral hemorrhage: an evidence-poor zone. *Stroke* 2003; 34(6): 1569-1570.

Dotti CG, Sullivan CA, Banker GA. The establishment of polarity by hippocampal neurons in

culture. *Journal of Neuroscience* 1988; 8(4): 1454-1468.

Duan X, Wen Z, Shen H, Shen M, Chen G. Intracerebral hemorrhage, oxidative stress, and antioxidant therapy. *Oxidative Medicine and Cellular Longevity* 2016; 2016: 1203285.

Dubinsky JM, Rothman SM. Intracellular calcium concentrations during "chemical hypoxia" and excitotoxic neuronal injury. *Journal of Neuroscience* 1991; 11(8): 2545-1551.

Ducruet AF, Zacharia BE, Hickman ZL, Grobelny BT, Yeh ML, Sosunov SA, Connolly ES Jr. The complement cascade as a therapeutic target in intracerebral hemorrhage. *Experimental Neurology* 2009; 219(2): 398-403.

Dye JA, Rees G, Yang I, Vespa PM, Martin NA, Vinters HV. Neuropathologic analysis of hematomas evacuated from patients with spontaneous intracerebral hemorrhage. *Neuropathology* 2014; 34(3): 253-260.

Elliott J, Smith M. The acute management of intracerebral hemorrhage: a clinical review. *Anesthesia and Analgesia* 2010; 110(5): 1419-1427.

Ellman GL, Courtney KD, Andres V Jr, Featherstone RM. A new and rapid colorimetric determination of acetylcholinesterase activity. *Biochemical Pharmacology* 1961; 7: 88-95.

Erecińska M, Silver IA. Ions and energy in mammalian brain. *Progress in Neurobiology* 1994; 43(1): 37-71.

Esiri MM. Oppenheimer's Diagnostic Neuropathology: A Practical Manual. Second edition. *Blackwell Science*, Oxford, 1996; 113-124.

Evans NJ, Bayliss AL, Reale V, Evans PD. Characterisation of signalling by the endogenous GPER1 (GPR30) receptor in an embryonic mouse hippocampal cell line (mHippoE-18). *PLoS One* 2016; 11(3): e0152138.

Eves EM, Tucker MS, Roback JD, Downen M, Rosner MR, Wainer BH. Immortal rat hippocampal cell lines exhibit neuronal and glial lineages and neurotrophin gene expression. *Proceedings of the National Academy of Sciences of the United States of America* 1992; 89(10): 4373-4377.

Fan K, Uzman BG. Rat glioma cells (C_6) cultured in serum-free defined medium. *Experimental Cell Research* 1977; 106(2): 397-401.

Fang X, Namba H, Akamine S, Sugiyama K. Methylenetetrahydrofolate reductase gene polymorphisms in patients with cerebral hemorrhage. *Neurological Research* 2005; 27(1): 73-76.

Feigin VL, Lawes CM, Bennett DA, Barker-Collo SL, Parag V. Worldwide stroke incidence and early case fatality reported in 56 population-based studies: a systematic review. *Lancet Neurology* 2009; 8(4): 355-369.

Feldman ZT, Reichenthal E, Zucker G, Greiff M. Haemangiopericytoma presenting with intracerebral haemorrhage. Case report and review of literature. *Acta Neurochirurgica* 1991;

112(3-4): 151-153.

Ferro JM. Update on intracerebral haemorrhage. *Journal of Neurology* 2006; 253(8): 985-999.

Finlay BL, Darlington RB. Linked regularities in the development and evolution of mammalian brains. *Science* 1995; 268(5217): 1578-1584.

Fiorella D, Zuckerman SL, Khan IS, Ganesh NK, Mocco J. Intracerebral hemorrhage: a common and devastating disease in need of better treatment. *World Neurosurgery* 2015; 84(4): 1136-1141.

Fisher CM. The pathologic and clinical aspects of thalamic hemorrhage. *Transactions of the American Neurological Association* 1959; 84: 56-59.

Flaherty ML, Woo D, Broderick JP. The epidemiology of intracerebral hemorrhage. In: Carhuapoma JR, Mayer SA, Hanley DF (eds). Intracerebral Hemorrhage. *Cambridge University Press*, Cambridge, 2010; 1-15.

Flaherty ML. Anticoagulant-associated intracerebral hemorrhage. *Seminars in Neurology* 2010; 30(5): 565-572.

Flower O, Smith M. The acute management of intracerebral hemorrhage. *Current Opinion in Critical Care* 2011; 17(2): 106-114.

Foerch C, Curdt I, Yan B, Dvorak F, Hermans M, Berkefeld J, Raabe A, Neumann-Haefelin T, Steinmetz H, Sitzer M. Serum glial fibrillary acidic protein as a biomarker for intracerebral haemorrhage in patients with acute stroke. *Journal of Neurology, Neurosurgery & Psychiatry* 2006; 77(2): 181-184.

Forman HP, Levin S, Stewart B, Patel M, Feinstein S. Cerebral vasculitis and hemorrhage in an adolescent taking diet pills containing phenylpropanolamine: case report and review of literature. *Pediatrics* 1989; 83(5): 737-741.

Friedman JA, Ecker RD, Piepgras DG, Duke DA. Cerebellar hemorrhage after spinal surgery: report of two cases and literature review. *Neurosurgery* 2002; 50(6): 1361-1363.

Fryer JD, Taylor JW, DeMattos RB, Bales KR, Paul SM, Parsadanian M, Holtzman DM. Apolipoprotein E markedly facilitates age-dependent cerebral amyloid angiopathy and spontaneous hemorrhage in amyloid precursor protein transgenic mice. *Journal of Neuroscience* 2003; 23(21): 7889-7896.

Funnell WR, Maysinger D, Cuello AC. Three-dimensional reconstruction and quantitative evaluation of devascularizing cortical lesions in the rat. *Journal of Neuroscience Methods* 1990; 35(2): 147-156.

Garofalo I (ed). Anonymi Medici: De Morbis Acutis et Chroniis. *Brill*, Leiden / New York, 1997.

Gass A. Is there a penumbra surrounding intracerebral hemorrhage? *Cerebrovascular Diseases* 2007; 23(1): 4-5.

Gebel JM, Sila CA, Sloan MA, Granger CB, Mahaffey KW, Weisenberger J, Green CL, White HD,

Gore JM, Weaver WD, Califf RM, Topol EJ. Thrombolysis-related intracranial hemorrhage: a radiographic analysis of 244 cases from the GUSTO-1 trial with clinical correlation. *Stroke* 1998; 29(3): 563-569.

Geddes JW, Pettigrew LC, Holtz ML, Craddock SD, Maines MD. Permanent focal and transient global cerebral ischemia increase glial and neuronal expression of heme oxygenase-1, but not heme oxygenase-2, protein in rat brain. *Neuroscience Letters* 1996; 210(3): 205-208.

Gerber CS. Stroke: historical perspectives. *Critical Care Nursing Quarterly* 2003; 26(4): 268-275.

Ghetti G. Putaminal hemorrhages. *Frontiers of Neurology and Neuroscience* 2012; 30: 141-144.

Gibbons KJ, Guterman LR, Hopkins LN. Iatrogenic intracerebral hemorrhage. *Neurosurgery Clinics of North America* 1992; 3(3): 667-683.

Gingerich S, Kim GL, Chalmers JA, Koletar MM, Wang X, Wang Y, Belsham DD. Estrogen receptor α and G-protein coupled receptor 30 mediate the neuroprotective effects of 17β-estradiol in novel murine hippocampal cell models. *Neuroscience* 2010; 170(1): 54-66.

Gironell A, Domingo P, Mancebo J, Coll P, Martí-Vilalta JL. Hemorrhagic stroke as a complication of bacterial meningitis in adults: report of three cases and review. *Clinical Infectious Diseases* 1995; 21(6): 1488-1491.

Giroud M, Gras P, Chadan N, Beuriat P, Milan C, Arveux P, Dumas R. Cerebral haemorrhage in a French prospective population study. *Journal of Neurology, Neurosurgery & Psychiatry* 1991; 54(7): 595-598.

Godoy DA, Piñero G, Di Napoli M. Predicting mortality in spontaneous intracerebral hemorrhage: can modification to original score improve the prediction? *Stroke* 2006; 37(4): 1038-1044.

Goldstein JN, Rosand J, Schwamm LH. Warfarin reversal in anticoagulant-associated intracerebral hemorrhage. *Neurocritical Care* 2008; 9(2): 277-283.

Goldstein LB, Adams R, Becker K, Furberg CD, Gorelick PB, Hademenos G, Hill M, Howard G, Howard VJ, Jacobs B, Levine SR, Mosca L, Sacco RL, Sherman DG, Wolf PA, del Zoppo GJ. Primary prevention of ischemic stroke: A statement for healthcare professionals from the Stroke Council of the American Heart Association. *Stroke* 2001; 32(1): 280-299.

Gomes AR, Correia SS, Esteban JA, Duarte CB, Carvalho AL. PKC anchoring to GluR4 AMPA receptor subunit modulates PKC-driven receptor phosphorylation and surface expression. *Traffic* 2007; 8(3): 259-269.

Gong Y, Agani FH. Oligomycin inhibits HIF-1α expression in hypoxic tumor cells. *American Journal of Physiology - Cell Physiology* 2005; 288(5): C1023-C1029.

Gonzalez A, Moya-Alvarado G, Gonzalez-Billaut C, Bronfman FC. Cellular and molecular mech-

anisms regulating neuronal growth by brain-derived neurotrophic factor (BDNF). *Cytoskeleton (Hoboken)* 2016; in press.

Gorelick PB, Weisman SM. Risk of hemorrhagic stroke with aspirin use: an update. *Stroke* 2005; 36(8): 1801-1807.

Govaert P, Staelens V, Vanhaesebrouch P. Perinatal intracranial hemorrhage due to maternal salicylate ingestion. *Clinical Pediatrics* 1995; 34(3): 174-175.

Govan ADT, Macfarlane PS, Callander R. Pathology Illustrated. Fourth edition. *Churchill Livingstone*, Edinburgh, 1995; 708-709.

Greenberg SM, Rebeck GW, Vonsattel JP, Gomez-Isla T, Hyman BT. Apolipoprotein E epsilon 4 and cerebral hemorrhage associated with amyloid angiopathy. *Annals of Neurology* 1995; 38(2): 254-259.

Greenberg SM. Cerebral amyloid angiopathy. In: Carhuapoma JR, Mayer SA, Hanley DF (eds). Intracerebral Hemorrhage. *Cambridge University Press*, Cambridge, 2010; 41-57.

Greenhalgh AD, Brough D, Robinson EM, Girard S, Rothwell NJ, Allan SM. Interleukin-1 receptor antagonist is beneficial after subarachnoid haemorrhage in rat by blocking haem-driven inflammatory pathology. *Disease Models & Mechanisms* 2012; 5(6): 823-833.

Gstraunthaler G. Alternatives to the use of fetal bovine serum: serum-free cell culture. *ALTEX* 2003; 20(4): 275-281.

Gstraunthaler G, Lindl T, van der Valk J. A plea to reduce or replace fetal bovine serum in cell culture media. *Cytotechnology* 2013; 65(5): 791-793.

Guan J, Zhang B, Zhang J, Ding W, Xiao Z, Zhu Z, Han Q, Wu C, Sun Y, Tong W, Dai J, Wang R. Nerve regeneration and functional recovery by collagen-binding brain-derived neurotrophic factor in an intracerebral hemorrhage model. *Tissue Engineering Part A* 2015; 21(1-2): 62-74.

Guan J, Zhang S, Zhou Q, Yuan Z, Lu Z. Effect of thrombin preconditioning on migration of subventricular zone-derived cells after intracerebral hemorrhage in rats. *Neurological Research* 2016; in press.

Guan N, Deng J, Li T, Xu X, Irelan JT, Wang MW. Label-free monitoring of T cell activation by the impedance-based xCELLigence system. *Molecular BioSystems* 2013; 9(5): 1035-1043.

Gurwitz JH, Gore JM, Goldberg RJ, Barron HV, Breen T, Rundle AC, Sloan MA, French W, Rogers WJ. Risk for intracranial hemorrhage after tissue plasminogen activator treatment for acute myocardial infarction. *Annals of Internal Medicine* 1998; 129(8): 597-604.

Hahl P, Davis T, Washburn C, Rogers JT, Smith A. Mechanisms of neuroprotection by hemopexin: modeling the control of heme and iron homeostasis in brain neurons in inflammatory states. *Journal of Neurochemistry* 2013; 125(1): 89-101.

Halliday J, Joseph JA, Gurusinghe NT. Fatal intracerebral haemorrhage secondary to Aspergillus arteritis following aneurysm clipping. *British Journal of Neurosurgery* 2014; 28(6): 791-792.

Hamann GF, del Zoppo GJ, von Kummer R. Hemorrhagic transformation of cerebral infarction--possible mechanisms. *Thrombosis and Haemostasis* 1999; 82(suppl.1): 92-94.

Hanel RA, Xavier AR, Mohammad Y, Kirmani JF, Yahia AM, Qureshi AI. Outcome following intracerebral hemorrhage and subarachnoid hemorrhage. *Neurological Research* 2002; 24(suppl.1): s58-s62.

Hänggi D, Steiger HJ. Spontaneous intracerebral haemorrhage in adults: a literature overview. *Acta Neurochirurgica* 2008; 150(4): 371-379.

Hankey GJ. Evacuation of intracerebral hematoma is likely to be beneficial - against. *Stroke* 2003; 34(6): 1568-1569.

Harry GJ, Billingsley M, Bruinink A, Campbell IL, Classen W, Dorman DC, Galli C, Ray D, Smith RA, Tilson HA. *In vitro* techniques for the assessment of neurotoxicity. *Environmental Health Perspectives* 1998; 106(suppl.1): 131-158.

Hart RG, Boop BS, Anderson DC. Oral anticoagulants and intracranial hemorrhage. Facts and hypotheses. *Stroke* 1995; 26(8): 1471-1477.

Hasan N, McColgan P, Bentley P, Edwards RJ, Sharma P. Towards the identification of blood biomarkers for acute stroke in humans: a comprehensive systematic review. *British Journal of Clinical Pharmacology* 2012; 74(2): 230-240.

Hassan AE, Zacharatos H, Qureshi AI. Acute hypertensive response in intracerebral hemorrhage. In: Carhuapoma JR, Mayer SA, Hanley DF (eds). Intracerebral Hemorrhage. *Cambridge University Press*, Cambridge, 2010; 17-30.

Hassler W, Hejazi N. Complications of angioma surgery - personal experience in 191 patients with cerebral angiomas. *Neurologia Medico-Chirurgica* 1998; 38(suppl.): 238-244.

He Y, Hua Y, Song S, Liu W, Keep RF, Xi G. Induction of autophagy in rat hippocampus and cultured neurons by iron. *Acta Neurochirurgica Supplement* 2008a; 105: 29-32.

He Y, Wan S, Hua Y, Keep RF, Xi G. Autophagy after experimental intracerebral hemorrhage. *Journal of Cerebral Blood Flow & Metabolism* 2008b; 28(5): 897-905.

Hemphill JC 3rd, Bonovich DC, Besmertis L, Manley GT, Johnston SC. The ICH score: a simple, reliable grading scale for intracerebral hemorrhage. *Stroke* 2001; 32(4): 891-897.

Heros RC, Morcos JJ. Cerebrovascular surgery: past, present, and future. *Neurosurgery* 2000; 47(5): 1007-1033.

Heros RC. Cerebellar hemorrhage and infarction. *Stroke* 1982; 13(1): 106-109.

Herweh C, Jüttler E, Schellinger PD, Klotz E, Jenetzky E, Orakcioglu B, Sartor K, Schramm P. Evidence against a perihemorrhagic penumbra provided by perfusion computed to-

mography. *Stroke* 2007; 38(11): 2941-2947.

Herzig MC, Winkler DT, Burgermeister P, Pfeifer M, Kohler E, Schmidt SD, Danner S, Abramowski D, Stürchler-Pierrat C, Bürki K, van Duinen SG, Maat-Schieman ML, Staufenbiel M, Mathews PM, Jucker M. Aβ is targeted to the vasculature in a mouse model of hereditary cerebral hemorrhage with amyloidosis. *Nature Neuroscience* 2004; 7(9): 954-960.

Hier DB, Davis KR, Richardson EP Jr, Mohr JP. Hypertensive putaminal hemorrhage. *Annals of Neurology* 1977; 1(2): 152-159.

Ho TC, Chen SL, Yang YC, Liao CL, Cheng HC, Tsao YP. PEDF induces p53-mediated apoptosis through PPAR gamma signaling in human umbilical vein endothelial cells. *Cardiovascular Research* 2007; 76(2): 213-223.

Honegger P, Schilter B. The use of serum-free aggregating brain cell cultures in Neurotoxicology. In: Chang LW, Slikker W Jr (eds). Neurotoxicology: Approaches and Methods. *Academic Press*, San Diego, 1995; 507-516.

Hook EW, Luttrell CN, Slaten K, Wagner RR. Hemorrhagic encephalopathy in chicken embryos infected with influenza virus. IV. Endothelial localization of viral antigens determined by immunofluorescence. *American Journal of Pathology* 1962; 41: 593-602.

Hornsby AK, Redhead YT, Rees DJ, Ratcliff MS, Reichenbach A, Wells T, Francis L, Amstalden K, Andrews ZB, Davies JS. Short-term calorie restriction enhances adult hippocampal neurogenesis and remote fear memory in a Ghsr-dependent manner. P*sychoneuroendocrinology* 2016; 63: 198-207.

Hoshimaru M, Ray J, Sah DW, Gage FH. Differentiation of the immortalized adult neuronal progenitor cell line HC2S2 into neurons by regulatable suppression of the v-myc oncogene. *Proceedings of the National Academy of Sciences of the United States of America* 1996; 93(4): 1518-1523.

Hottinger AF, DeAngelis LM. Etiology of tumor-related intracranial hemorrhage. In: Carhuapoma JR, Mayer SA, Hanley DF (eds). Intracerebral Hemorrhage. *Cambridge University Press*, Cambridge, 2010; 31-40.

Hou XQ, Yan R, Yang C, Zhang L, Su RY, Liu SJ, Zhang SJ, He WQ, Fang SH, Cheng SY, Su ZR, Chen YB, Wang Q. A novel assay for high-throughput screening of anti-Alzheimer's disease drugs to determine their efficacy by real-time monitoring of changes in PC12 cell proliferation. *International Journal of Molecular Medicine* 2014; 33(3): 543-549.

Hu S, Xi G, Jin H, He Y, Keep RF, Hua Y. Thrombin-induced autophagy: a potential role in intracerebral hemorrhage. *Brain Research* 2011; 1424: 60-66.

Hua Y, Keep RF, Hoff JT, Xi G. Brain injury after intracerebral hemorrhage: the role of thrombin and iron. *Stroke* 2007; 38(2): 759-762.

Hua Y, Keep RF, Hoff JT, Xi G. Deferoxamine therapy for intracerebral hemorrhage. *Acta Neurochirurgica Supplement* 2008; 105: 3-6.

Huang FP, Xi G, Keep RF, Hua Y, Nemoianu A, Hoff JT. Brain edema after experimental intracerebral hemorrhage: role of hemoglobin degradation products. *Journal of Neurosurgery* 2002; 96(2): 287-293.

Humpel C. Organotypic brain slice cultures: a review. *Neuroscience* 2015; 305: 86-98.

Hurtado O, Moro MA, Cárdenas A, Sánchez V, Fernández-Tomé P, Leza JC, Lorenzo P, Secades JJ, Lozano R, Dávalos A, Castillo J, Lizasoain I. Neuroprotection afforded by prior citicoline administration in experimental brain ischemia: effects on glutamate transport. *Neurobiology of Disease* 2005; 18(2): 336-345.

Huttner HB, Steiner T. Coagulopathy-related intracerebral hemorrhage. In: Carhuapoma JR, Mayer SA, Hanley DF (eds). Intracerebral Hemorrhage. *Cambridge University Press*, Cambridge, 2010; 58-70.

Hwang BY, Appelboom G, Ayer A, Kellner CP, Kotchetkov IS, Gigante PR, Haque R, Kellner M, Connolly ES. Advances in neuroprotective strategies: potential therapies for intracerebral hemorrhage. *Cerebrovascular Diseases* 2011; 31(3): 211-222.

Hwang BY, Appelboom G, Kellner CP, Carpenter AM, Kellner MA, Gigante PR, Sander Connolly E. Clinical grading scales in intracerebral hemorrhage. *Neurocritical Care* 2010; 13(1): 141-151.

Iida S, Baumbach GL, Lavoie JL, Faraci FM, Sigmund CD, Heistad DD. Spontaneous stroke in a genetic model of hypertension in mice. *Stroke* 2005; 36(6): 1253-1258.

Iranmanesh F, Vakilian A. Efficiency of citicoline in increasing muscular strength of patients with nontraumatic cerebral hemorrhage: a double-blind randomized clinical trial. *Journal of Stroke & Cerebrovascular Diseases* 2008; 17(3): 153-155.

James M, Gokhale S. Gender differences in incidence, pathophysiology, and outcome of primary intracerebral hemorrhage. In: Chaudhary V (ed). Intracerebral Hemorrhage. *InTech*, Rijeka, 2014; 11-24.

James ML, Warner DS, Laskowitz DT. Preclinical models of intracerebral hemorrhage: a translational perspective. *Neurocritical Care* 2008; 9(1): 139-152.

Janaszewska A, Ciolkowski M, Wróbel D, Petersen JF, Ficker M, Christensen JB, Bryszewska M, Klajnert B. Modified PAMAM dendrimer with 4-carbomethoxypyrrolidone surface groups reveals negligible toxicity against three rodent cell-lines. *Nanomedicine: Nanotechnology, Biology, and Medicine* 2013; 9(4): 461-464.

Janaszewska A, Studzian M, Petersen JF, Ficker M, Christensen JB, Klajnert-Maculewicz B. PAMAM dendrimer with 4-carbomethoxypyrrolidone: *in vitro* assessment of neurotoxicity. *Nanomedicine: Nanotechnology, Biology, and Medicine* 2015; 11(2): 409-411.

Jayme DW, Gruber DF. Development of serum-free media: optimization of nutrient composition and delivery format. In: Celis JE (ed). Cell Biology: A Laboratory Handbook. Volume 1. *Elsevier - Academic Press*, Burlington, 2006; 33-41.

Jensen L, Heath KJ, Scott G, Byard RW. Sudden death and the forensic evaluation of neurocutaneous syndromes. *Journal of Forensic and Legal Medicine* 2009; 16(7): 369-374.

Jensson O, Palsdottir A, Thorsteinsson L, Arnason A. The saga of cystatin C gene mutation causing amyloid angiopathy and brain hemorrhage - clinical genetics in Iceland. *Clinical Genetics* 1989; 36(5): 368-377.

Johnson RT, Narayan O. Experimental neurological diseases of animals caused by viruses. In: Klawans HL Jr (ed). Models of Human Neurological Diseases. *Excerpta Medica*, Amsterdam, 1974; 39-82.

Josephson CB, Frantzias J, Samarasekera N, Al-Shahi Salman R. The persisting burden of intracerebral haemorrhage: can effective treatments be found? *PLoS Medicine* 2010; 7(10): e1000353.

Jovanovic JN, Czernik AJ, Fienberg AA, Greengard P, Sihra TS. Synapsins as mediators of BDNF-enhanced neurotransmitter release. *Nature Neuroscience* 2000; 3(4): 323-329.

Jung KH, Chu K, Jeong SW, Han SY, Lee ST, Kim JY, Kim M, Roh JK. HMG-CoA reductase inhibitor, atorvastatin, promotes sensorimotor recovery, suppressing acute inflammatory reaction after experimental intracerebral hemorrhage. *Stroke* 2004; 35(7): 1744-1749.

Jung KH, Chu K, Lee ST, Shin YW, Lee KJ, Park DK, Yoo JS, Kim S, Kim M, Lee SK, Roh JK. Experimental induction of cerebral aneurysms by developmental low copper diet. *Journal of Neuropathology & Experimental Neurology* 2016; 75(5): 455-463.

Kaech S, Banker G. Culturing hippocampal neurons. *Nature Protocols* 2006; 1(5): 2406-2415.

Kalita J, Bansal V, Misra UK, Jain SK. Intracerebral haemorrhage due to cerebral venous sinus thrombosis. *QJM* 2008; 101(3): 247-249.

Kalita J, Ranjan P, Misra UK. Current status of osmotherapy in intracerebral hemorrhage. *Neurology India* 2003; 51(1): 104-109.

Kane PJ, Cook S, Chambers IR, Mendelow AD. Cerebral oedema following intracerebral haemorrhage: the effect of the NMDA receptor antagonists MK-801 and D-CPPene. *Acta Neurochirurgica Supplementum* 1994; 60: 561-563.

Karki K, Knight RA, Han Y, Yang D, Zhang J, Ledbetter KA, Chopp M, Seyfried DM. Simvastatin and atorvastatin improve neurological outcome after experimental intracerebral hemorrhage. *Stroke* 2009; 40(10): 3384-3389.

Karwacki Z, Kowiański P, Witkowska M, Karwacka M, Dziewiatkowski J, Moryś J. The pathophysiology of intracerebral haemorrhage. *Folia Morphologica* 2006; 65(4): 295-300.

Kase CS. Clinical presentation of intracerebral hemorrhage. In: Carhuapoma JR, Mayer SA,

Hanley DF (eds). Intracerebral Hemorrhage. *Cambridge University Press*, Cambridge, 2010; 101-120.

Kathirvelu B, Carmichael ST. Intracerebral hemorrhage in mouse models: therapeutic interventions and functional recovery. *Metabolic Brain Disease* 2015; 30(2): 449-459.

Katsu M, Niizuma K, Yoshioka H, Okami N, Sakata H, Chan PH. Hemoglobin-induced oxidative stress contributes to matrix metalloproteinase activation and blood-brain barrier dysfunction *in vivo*. *Journal of Cerebral Blood Flow & Metabolism* 2010; 30(12): 1939-1950.

Katsuki H. Exploring neuroprotective drug therapies for intracerebral hemorrhage. *Journal of Pharmacological Sciences* 2010; 114(4): 366-378.

Kaufman HH, Pruessner JL, Bernstein DP, Borit A, Ostrow PT, Cahall DL. A rabbit model of intracerebral hematoma. *Acta Neuropathologica* 1985; 65(3-4): 318-321.

Ke N, Nguyen K, Irelan J, Abassi YA. Multidimensional GPCR profiling and screening using impedance-based label-free and real-time assay. *Methods in Molecular Biology* 2015; 1272: 215-226.

Ke N, Wang X, Xu X, Abassi YA. The xCELLigence system for real-time and label-free monitoring of cell viability. *Methods in Molecular Biology* 2011; 740: 33-43.

Keep RF, Xiang J, Ennis SR, Andjelkovic A, Hua Y, Xi G, Hoff JT. Blood-brain barrier function in intracerebral hemorrhage. *Acta Neurochirurgica Supplement* 2008; 105: 73-77.

Kellner CP, Connolly ES Jr. Neuroprotective strategies for intracerebral hemorrhage: trials and translation. *Stroke* 2010; 41(10 suppl.1): s99-s102.

Kensler TW, Wakabayashi N, Biswal S. Cell survival responses to environmental stresses *via* the Keap1-Nrf2-ARE pathway. *Annual Review of Pharmacology and Toxicology* 2007; 47: 89-116.

Kern A, Mavrikaki M, Ullrich C, Albarran-Zeckler R, Brantley AF, Smith RG. Hippocampal dopamine/DRD1 signaling dependent on the ghrelin receptor. *Cell* 2015; 163(5): 1176-1190.

Kernagis DN, Laskowitz DT. Evolving role of biomarkers in acute cerebrovascular disease. *Annals of Neurology* 2012; 71(3): 289-303.

Khama-Murad AKh, Mokrushin AA, Pavlinova LI. Development of edema in nervous tissue in the model of hemorrhagic stroke *in vitro*. *Zhurnal Nevrologii i Psikhiatrii Imeni S.S. Korsakova* 2009; 109(10 suppl.2): 47-51.

Khama-Murad AKh, Mokrushin AA, Pavlinova LI. Modeling of hemorrhage stroke *in vitro*. *Zhurnal Nevrologii i Psikhiatrii Imeni S.S. Korsakova* 2008; (suppl.22): 66-70.

Khama-Murad AKh, Mokrushin AA, Pavlinova LI. Neuroprotective properties of L-carnosine in the brain slices exposed to autoblood in the hemorrhagic stroke model *in vitro*. *Regulatory Peptides* 2011; 167(1): 65-69.

Khama-Murad AKh. Edema in nervous tissue studied on model of hemorrhagic stroke *in vitro*. *Eksperimental'naia i Klinicheskaia Farmakologiia* 2011a; 74(4): 6-9.

Khama-Murad AKh. Effect of heparin on the neuron bioelectric activity in a hemorrhagic stroke model *in vitro*. *Eksperimental'naia i Klinicheskaia Farmakologiia* 2011b; 74(1): 36-38.

Khama-Murad AKh. Protective and antiedema effect of heat shock HSP70 protein in hemorrhagic stroke model *in vitro*. *Eksperimental'naia i Klinicheskaia Farmakologiia* 2011c; 74(2): 19-22.

Khama-Murad AKh. Protective properties of L-carnosine studied *in vitro* on a hemorrhagic stroke model. *Eksperimental'naia i Klinicheskaia Farmakologiia* 2009; 72(6): 46-48.

Kho D, MacDonald C, Johnson R, Unsworth CP, O'Carroll SJ, du Mez E, Angel CE, Graham ES. Application of xCELLigence RTCA biosensor technology for revealing the profile and window of drug responsiveness in real time. *Biosensors* 2015; 5(2): 199-222.

Kim CK, Ryu WS, Choi IY, Kim YJ, Rim D, Kim BJ, Jang H, Yoon BW, Lee SH. Detrimental effects of leptin on intracerebral hemorrhage via the STAT3 signal pathway. *Journal of Cerebral Blood Flow & Metabolism* 2013; 33(6): 944-953.

Kim DW, Im SH, Kim JY, Kim DE, Oh GT, Jeong SW. Decreased brain edema after collagenase-induced intracerebral hemorrhage in mice lacking the inducible nitric oxide synthase gene. Laboratory investigation. *Journal of Neurosurgery* 2009; 111(5): 995-1000.

Kim GS, Yang L, Zhang G, Zhao H, Selim M, McCullough LD, Kluk MJ, Sanchez T. Critical role of sphingosine-1-phosphate receptor-2 in the disruption of cerebrovascular integrity in experimental stroke. *Nature Communications* 2015; 6: 7893.

Kim KM, Kim SY, Minxha J, Palmore GT. A novel method for analyzing images of live nerve cells. *Journal of Neuroscience Methods* 2011; 201(1): 98-105.

Kirkman MA, Allan SM, Parry-Jones AR. Experimental intracerebral hemorrhage: avoiding pitfalls in translational research. *Journal of Cerebral Blood Flow & Metabolism* 2011a; 31(11): 2135-2151.

Kirkman MA, Greenwood N, Singh N, Tyrrell PJ, King AT, Patel HC. Difficulties with recruiting into neurosurgical clinical trials: the Surgical Trial in IntraCerebral Haemorrhage II as an example. *British Journal of Neurosurgery* 2011b; 25(2): 231-234.

Kirkman MA. Debate - does a reversible penumbra exist in intracerebral haemorrhage? *British Journal of Neurosurgery* 2011; 25(4): 523-525.

Kobayashi E, Saeki N, Oishi H, Hirai S, Yamaura A. Long-term natural history of hemorrhagic moyamoya disease in 42 patients. *Journal of Neurosurgery* 2000; 93(6): 976-980.

Koeppen AH, Dickson AC, McEvoy JA. The cellular reactions to experimental intracerebral hemorrhage. *Journal of the Neurological Sciences* 1995; 134(suppl.): 102-112.

Kondziolka D, Bernstein M, Resch L, Tator CH, Fleming JF, Vanderlinden RG, Schutz H. Significance of hemorrhage into brain tumors: clinicopathological study. *Journal of Neurosurgery* 1987; 67(6): 852-857.

Koutroulis I, Zarros A, Theocharis S. The role of matrix metalloproteinases in the pathophysiology and progression of human nervous system malignancies: a chance for the development of targeted therapeutic approaches? *Expert Opinion on Therapeutic Targets* 2008; 12(12): 1577-1586.

Krafft PR, Bailey EL, Lekic T, Rolland WB, Altay O, Tang J, Wardlaw JM, Zhang JH, Sudlow CL. Etiology of stroke and choice of models. *International Journal of Stroke* 2012a; 7(5): 398-406.

Krafft PR, Rolland WB, Duris K, Lekic T, Campbell A, Tang J, Zhang JH. Modeling intracerebral hemorrhage in mice: injection of autologous blood or bacterial collagenase. *Journal of Visualized Experiments* 2012b; (67): e4289.

Kramer AH, Joos-Vandewalle J, Edkins AL, Frost CL, Prinsloo E. Real-time monitoring of 3T3-L1 preadipocyte differentiation using a commercially available electric cell-substrate impedance sensor system. *Biochemical and Biophysical Research Communications* 2014; 443(4): 1245-1250.

Küker W, Thiex R, Rohde I, Rohde V, Thron A. Experimental acute intracerebral hemorrhage. Value of MR sequences for a safe diagnosis at 1.5 and 0.5 T. *Acta Radiologica* 2000; 41(6): 544-552.

Kumar R, Prakash O, Sharma BS. Intracranial hemorrhage in dengue fever: management and outcome: a series of 5 cases and review of literature. *Surgical Neurology* 2009; 72(4): 429-433.

Kurland D, Hong C, Aarabi B, Gerzanich V, Simard JM. Hemorrhagic progression of a contusion after traumatic brain injury: a review. *Journal of Neurotrauma* 2012; 29(1): 19-31.

Kuroda S, Houkin K. Moyamoya disease: current concepts and future perspectives. *Lancet Neurology* 2008; 7(11): 1056-1066.

Kustermann S, Boess F, Buness A, Schmitz M, Watzele M, Weiser T, Singer T, Suter L, Roth A. A label-free, impedance-based real time assay to identify drug-induced toxicities and differentiate cytostatic from cytotoxic effects. *Toxicology In Vitro* 2013; 27(5): 1589-1595.

Kwon HJ, Hwang IK, An HJ, Han SH, Yang JI, Shin HS, Yoo ID, Kang TC, Won MH. Changes of glial Na^+-K^+ ATPase (α1 subunit) immunoreactivity in the gerbil hippocampus after transient forebrain ischemia. *Brain Research* 2003; 987(2): 233-239.

Kwon KJ, Kim JN, Kim MK, Kim SY, Cho KS, Jeon SJ, Kim HY, Ryu JH, Han SY, Cheong JH, Ignarro LJ, Han SH, Shin CY. Neuroprotective effects of valproic acid against hemin toxicity: possible involvement of the down-regulation of heme oxygenase-1 by regulating ubiq-

uitin-proteasomal pathway. *Neurochemistry International* 2013; 62(3): 240-250.

Lakovic K, Ai J, D'Abbondanza J, Tariq A, Sabri M, Alarfaj AK, Vasdev P, Macdonald RL. Bilirubin and its oxidation products damage brain white matter. *Journal of Cerebral Blood Flow & Metabolism* 2014; 34(11): 1837-1847.

Lazniewska J, Janaszewska A, Miłowska K, Caminade AM, Mignani S, Katir N, El Kadib A, Bryszewska M, Majoral JP, Gabryelak T, Klajnert-Maculewicz B. Promising low-toxicity of viologen-phosphorus dendrimers against embryonic mouse hippocampal cells. *Molecules* 2013a; 18(10): 12222-12240.

Lazniewska J, Milowska K, Zablocka M, Mignani S, Caminade AM, Majoral JP, Bryszewska M, Gabryelak T. Mechanism of cationic phosphorus dendrimer toxicity against murine neural cell lines. *Molecular Pharmaceutics* 2013b; 10(9): 3484-3496.

Leach MK, Naim YI, Feng ZQ, Gertz CC, Corey JM. Stages of neuronal morphological development *in vitro* - an automated assay. *Journal of Neuroscience Methods* 2011; 199(2): 192-198.

Lee EJ, Hung YC, Lee MY. Anemic hypoxia in moderate intracerebral hemorrhage: the alterations of cerebral hemodynamics and brain metabolism. *Journal of the Neurological Sciences* 1999; 164(2): 117-123.

Lee HJ, Hammond DN, Large TH, Roback JD, Sim JA, Brown DA, Otten UH, Wainer BH. Neuronal properties and trophic activities of immortalized hippocampal cells from embryonic and young adult mice. *Journal of Neuroscience* 1990; 10(6): 1779-1787.

Lee HJ, Kim KS, Park IH, Kim SU. Human neural stem cells over-expressing VEGF provide neuroprotection, angiogenesis and functional recovery in mouse stroke model. *PLoS One* 2007; 2(1): e156.

Lee HS, Kim KS, Lim HS, Choi M, Kim HK, Ahn HY, Shin JC, Joe YA. Priming Wharton's jelly-derived mesenchymal stromal/stem cells with ROCK inhibitor improves recovery in an intracerebral hemorrhage model. *Journal of Cellular Biochemistry* 2015; 116(2): 310-319.

Lee KR, Kawai N, Kim S, Sagher O, Hoff JT. Mechanisms of edema formation after intracerebral hemorrhage: effects of thrombin on cerebral blood flow, blood-brain barrier permeability, and cell survival in a rat model. *Journal of Neurosurgery* 1997; 86(2): 272-278.

Lee ST, Chu K, Jung KH, Kang KM, Kim JH, Bahn JJ, Jeon D, Kim M, Lee SK, Roh JK. Cholinergic anti-inflammatory pathway in intracerebral hemorrhage. *Brain Research* 2010; 1309: 164-171.

Lendahl U, McKay RD. The use of cell lines in neurobiology. *Trends in Neurosciences* 1990; 13(4): 132-137.

Leng Y, Wang Z, Tsai LK, Leeds P, Fessler EB, Wang J, Chuang DM. FGF-21, a novel metabolic

regulator, has a robust neuroprotective role and is markedly elevated in neurons by mood stabilizers. *Molecular Psychiatry* 2015; 20(2): 215-223.

Leonardo CC, Robbins S, Doré S. Translating basic science research to clinical application: models and strategies for intracerebral hemorrhage. *Frontiers in Neurology* 2012; 3: 85.

Levy YS, Streifler JY, Panet H, Melamed E, Offen D. Hemin-induced apoptosis in PC12 and neuroblastoma cells: implications for local neuronal death associated with intracerebral hemorrhage. *Neurotoxicity Research* 2002; 4(7-8): 609-616.

Liliang PC, Liang CL, Lu CH, Chang HW, Cheng CH, Lee TC, Chen HJ. Hypertensive caudate hemorrhage prognostic predictor, outcome, and role of external ventricular drainage. *Stroke* 2001; 32(5): 1195-1200.

Lilleyman JS. Intracranial hemorrhage in chronic childhood ITP. *Pediatric Hematology and Oncology* 1997; 14(5): iii-v.

Limame R, Wouters A, Pauwels B, Fransen E, Peeters M, Lardon F, De Wever O, Pauwels P. Comparative analysis of dynamic cell viability, migration and invasion assessments by novel real-time technology and classic endpoint assays. *PLoS One* 2012; 7(10): e46536.

Linn J, Brückmann H. Differential diagnosis of nontraumatic intracerebral hemorrhage. *Clinical Neuroradiology* 2009; 19(1): 45-61.

Liu B, Zhang L, Yang Q. Genetics of intracerebral hemorrhage: insights from candidate gene approaches. *Neurology India* 2012; 60(1): 3-8.

Liu CM, Shi BZ, Zhou JS. Effects of thrombin on the secondary cerebral injury of perihematomal tissues of rats after intracerebral hemorrhage. *Genetics and Molecular Research* 2014; 13(2): 4617-4626.

Liu L, Wang S, Xu R, Zheng J, Tang J, Tang X, Zhang D. Experimental intracerebral haemorrhage: description of a semi-coagulated autologous blood model in rats. *Neurological Research* 2015; 37(10): 874-879.

Lo EH, Moskowitz MA, Jacobs TP. Exciting, radical, suicidal: how brain cells die after stroke. *Stroke* 2005; 36(2): 189-192.

Lopez Valdes E, Hernandez Lain A, Calandre L, Grau M, Cabello A, Gomez-Escalonilla C. Time window for clinical effectiveness of mass evacuation in a rat balloon model mimicking an intraparenchymatous hematoma. *Journal of the Neurological Sciences* 2000; 174(1): 40-46.

Lou M, Lieb K, Selim M. The relationship between hematoma iron content and perihematoma edema: an MRI study. *Cerebrovascular Diseases* 2009; 27(3): 266-271.

Lovelock CE, Cordonnier C, Naka H, Al-Shahi Salman R, Sudlow CL, Edinburgh Stroke Study Group, Sorimachi T, Werring DJ, Gregoire SM, Imaizumi T, Lee SH, Briley D, Rothwell

PM. Antithrombotic drug use, cerebral microbleeds, and intracerebral hemorrhage: a systematic review of published and unpublished studies. *Stroke* 2010; 41(6): 1222-1228.

Lowry OH, Rosebrough NJ, Farr AL, Randall RJ. Protein measurement with the Folin phenol reagent. *Journal of Biological Chemistry* 1951; 193(1): 265-275.

Lu A, Tang Y, Ran R, Ardizzone TL, Wagner KR, Sharp FR. Brain genomics of intracerebral hemorrhage. *Journal of Cerebral Blood Flow & Metabolism* 2006; 26(2): 230-252.

Lunardi P. Lobar hemorrhages. *Frontiers of Neurology and Neuroscience* 2012; 30: 145-148.

Ma Q, Khatibi NH, Chen H, Tang J, Zhang JH. History of preclinical models of intracerebral hemorrhage. *Acta Neurochirurgica Supplement* 2011; 111: 3-8.

Ma X, Qin J, Song B, Shi C, Zhang R, Liu X, Ji Y, Ji W, Gong G, Xu Y. Stem cell-based therapies for intracerebral hemorrhage in animal model: a meta-analysis. *Neurological Sciences* 2015; 36(8): 1311-1317.

Maat-Schieman ML, van Duinen SG, Bornebroek M, Haan J, Roos RA. Hereditary cerebral hemorrhage with amyloidosis-Dutch type (HCHWA-D): II - a review of histopathological aspects. *Brain Pathology* 1996; 6(2): 115-120.

Mackenzie JM, Clayton JA. Early cellular events in the penumbra of human spontaneous intracerebral hemorrhage. *Journal of Stroke & Cerebrovascular Diseases* 1999; 8(1): 1-8.

MacLellan CL, Silasi G, Auriat AM, Colbourne F. Rodent models of intracerebral hemorrhage. *Stroke* 2010; 41(suppl.1): S95-S98.

Maines MD. The heme oxygenase system and its functions in the brain. *Cellular and Molecular Biology (Noisy-le-Grand)* 2000; 46(3): 573-585.

Majd S, Zarifkar A, Rastegar K, Takhshid MA. Culturing adult rat hippocampal neurons with long-interval changing media. *Iranian Biomedical Journal* 2008; 12(2): 101-107.

Manaenko A, Chen H, Zhang JH, Tang J. Comparison of different preclinical models of intracerebral hemorrhage. *Acta Neurochirurgica Supplement* 2011; 111: 9-14.

Manno EM. Update on intracerebral hemorrhage. *Continuum* 2012; 18(3): 598-610.

Mansoor GA, White WB, Grunnet M, Ruby ST. Intracerebral hemorrhage after carotid endarterectomy associated with ipsilateral fibrinoid necrosis: a consequence of the hyperperfusion syndrome? *Journal of Vascular Surgery* 1996; 23(1): 147-151.

Marietta M, Pedrazzi P, Girardis M, Torelli G. Intracerebral haemorrhage: an often neglected medical emergency. *Internal and Emergency Medicine* 2007; 2(1): 38-45.

Marinkovic I, Strbian D, Mattila OS, Abo-Ramadan U, Tatlisumak T. A novel combined model of intracerebral and intraventricular hemorrhage using autologous blood-injection in rats. *Neuroscience* 2014; 272: 286-294.

Marinova Z, Walitza S, Grünblatt E. 5-HT_{2A} serotonin receptor agonist DOI alleviates cytotoxi-

city in neuroblastoma cells: role of the ERK pathway. *Progress in Neuro-Psychopharmacology & Biological Psychiatry* 2013; 44: 64-72.

Marlin MC, Li G. Biogenesis and function of the NGF/TrkA signaling endosome. *International Review of Cell and Molecular Biology* 2015; 314: 239-257.

Marmiroli P, Nicolini G, Miloso M, Scuteri A, Cavaletti G. The fundamental role of morphology in experimental neurotoxicology: the example of chemotherapy-induced peripheral neurotoxicity. *Italian Journal of Anatomy and Embryology* 2012; 117(2): 75-97.

Martínez-González NA, Sudlow CL. Effects of apolipoprotein E genotype on outcome after ischaemic stroke, intracerebral haemorrhage and subarachnoid haemorrhage. *Journal of Neurology, Neurosurgery & Psychiatry* 2006; 77(12): 1329-1335.

Masotti L, Di Napoli M, Godoy DA, Rafanelli D, Liumbruno G, Koumpouros N, Landini G, Pampana A, Cappelli R, Poli D, Prisco D. The practical management of intracerebral hemorrhage associated with oral anticoagulant therapy. *International Journal of Stroke* 2011; 6(3): 228-240.

Massaro AR, Sacco RL, Mohr JP, Foulkes MA, Tatemichi TK, Price TR, Hier DB, Wolf PA. Clinical discriminators of lobar and deep hemorrhages: the Stroke Data Bank. *Neurology* 1991; 41(12): 1881-1885.

Matsuoka Y, Kitamura Y, Okazaki M, Sakata M, Tsukahara T, Taniguchi T. Induction of heme oxygenase-1 and major histocompatibility complex antigens in transient forebrain ischemia. *Journal of Cerebral Blood Flow & Metabolism* 1998; 18(8): 824-832.

Matyja E, Taraszewska A, Nagańska E, Grieb P, Rafałowska J. CDP-choline protects motor neurons against apoptotic changes in a model of chronic glutamate excitotoxicity *in vitro*. *Folia Neuropathologica* 2008; 46(2): 139-148.

Maxwell SS, Jackson CA, Paternoster L, Cordonnier C, Thijs V, Al-Shahi Salman R, Sudlow CL. Genetic associations with brain microbleeds: Systematic review and meta-analyses. *Neurology* 2011; 77(2): 158-167.

Mayer SA, Rincon F. Treatment of intracerebral haemorrhage. *Lancet Neurology* 2005; 4(10): 662-672.

McCarron MO, Nicoll JA, Stewart J, Ironside JW, Mann DM, Love S, Graham DI, Dewar D. The apolipoprotein E ε2 allele and the pathological features in cerebral amyloid angiopathy-related hemorrhage. *Journal of Neuropathology and Experimental Neurology* 1999; 58(7): 711-718.

McCourt R, Gould B, Gioia L, Kate M, Coutts SB, Dowlatshahi D, Asdaghi N, Jeerakathil T, Hill MD, Demchuk AM, Buck B, Emery D, Butcher K; ICH ADAPT Investigators. Cerebral perfusion and blood pressure do not affect perihematoma edema growth in acute intracerebral hemorrhage. *Stroke* 2014; 45(5): 1292-1298.

McDonald P, Guha A, Provias J. Primary intracranial fibrosarcoma with intratumoral hemorrhage: neuropathological diagnosis with review of the literature. *Journal of Neuro-Oncology* 1997; 35(2): 133-139.

McGee SM, McGee DN, McGee MB. Spontaneous intracerebral hemorrhage related to methamphetamine abuse: autopsy findings and clinical correlation. *American Journal of Forensic Medicine and Pathology* 2004; 25(4): 334-337.

Mead GE, Wardlaw JM, Dennis MS, Lewis SC. Extensive haemorrhagic transformation of infarct: might it be an important cause of primary intracerebral haemorrhage? *Age and Ageing* 2002; 31(6): 429-433.

Meindl C, Absenger M, Roblegg E, Fröhlich E. Suitability of cell-based label-free detection for cytotoxicity screening of carbon nanotubes. *BioMed Research International* 2013; 2013: 564804.

Mena H, Cadavid D, Rushing EJ. Human cerebral infarct: a proposed histopathologic classification based on 137 cases. *Acta Neuropathologica* 2004; 108(6): 524-530.

Mencacci NE, Bersano A, Cinnante CM, Ciammola A, Corti S, Meroni PL, Silani V. Intracerebral haemorrhage, a possible presentation in Churg-Strauss syndrome: case report and review of the literature. *Journal of the Neurological Sciences* 2011; 301(1-2): 107-111.

Mendelow AD, Gregson BA, Fernandes HM, Murray GD, Teasdale GM, Hope DT, Karimi A, Shaw MD, Barer DH; STICH investigators. Early surgery versus initial conservative treatment in patients with spontaneous supratentorial intracerebral haematomas in the International Surgical Trial in Intracerebral Haemorrhage (STICH): a randomised trial. *Lancet* 2005; 365(9457): 387-397.

Mendelow AD, Gregson BA, Rowan EN, Murray GD, Gholkar A, Mitchell PM; STICH II Investigators. Early surgery versus initial conservative treatment in patients with spontaneous supratentorial lobar intracerebral haematomas (STICH II): a randomised trial. *Lancet* 2013; 382(9890): 397-408.

Mendelow AD, Unterberg A. Surgical treatment of intracerebral haemorrhage. *Current Opinion in Critical Care* 2007; 13(2): 169-174.

Mendelow AD. Surgical management of intracerebral hemorrhage. In: Carhuapoma JR, Mayer SA, Hanley DF (eds). Intracerebral Hemorrhage. *Cambridge University Press*, Cambridge, 2010; 165-175.

Michler-Stuke A, Bottenstein JE. Proliferation of glial-derived cells in defined media. *Journal of Neuroscience Research* 1982; 7(2): 215-228.

Migliore M, Shepherd GM. An integrated approach to classifying neuronal phenotypes. *Nature Reviews Neuroscience* 2005; 6(10): 810-818.

Milowska K, Szwed A, Mutrynowska M, Gomez-Ramirez R, de la Mata FJ, Gabryelak T,

Bryszewska M. Carbosilane dendrimers inhibit α-synuclein fibrillation and prevent cells from rotenone-induced damage. *International Journal of Pharmaceutics* 2015; 484(1-2): 268-275.

Milowska K, Szwed A, Zablocka M, Caminade AM, Majoral JP, Mignani S, Gabryelak T, Bryszewska M. *In vitro* PAMAM, phosphorus and viologen-phosphorus dendrimers prevent rotenone-induced cell damage. *International Journal of Pharmaceutics* 2014; 474(1-2): 42-49.

Minematsu K. Evacuation of intracerebral hematoma is likely to be beneficial. *Stroke* 2003; 34(6): 1567-1568.

Missori P, Salvati M, Polli FM, Conserva V, Delfini R. Intraparenchymal haemorrhage after evacuation of chronic subdural haematoma. Report of three cases and review of the literature. *British Journal of Neurosurgery* 2002; 16(1): 63-66.

Mitchell P, Gregson B. Comment on "Debate - does a reversible penumbra exist in intracerebral haemorrhage?". *British Journal of Neurosurgery* 2011; 25(4): 526.

Mocco J, Rose JC, Komotar RJ, Mayer SA. Blood pressure management in patients with intracerebral and subarachnoid hemorrhage. *Neurosurgery Clinics of North America* 2006; 17(suppl.1): 25-40.

Mokrushin AA, Khama-Murad AX, Pavlinova LI. Effects of long-term exposure of nerve cells to autoblood in *in vitro* model of hemorrhagic stroke. *Bulletin of Experimental Biology and Medicine* 2008; 146(3): 379-381.

Mokrushin AA, Pavlinova LI. Effects of heparin on synaptic activity in the hemorrhagic stroke model *in vitro*. *Bulletin of Experimental Biology and Medicine* 2012; 152(6): 684-687.

Mokrushin AA, Pavlinova LI. Effects of the blood components on the AMPA and NMDA synaptic responses in brain slices in the onset of hemorrhagic stroke. *General Physiology and Biophysics* 2013; 32(4): 489-504.

Moncayo J. Midbrain infarcts and hemorrhages. *Frontiers of Neurology and Neuroscience* 2012a; 30: 158-161.

Moncayo J. Pontine infarcts and hemorrhages. *Frontiers of Neurology and Neuroscience* 2012b; 30: 162-165.

Moodley K, Angel CE, Glass M, Graham ES. Real-time profiling of NK cell killing of human astrocytes using xCELLigence technology. *Journal of Neuroscience Methods* 2011; 200(2): 173-180.

Morgenstern LB, Zahuranec DB, Sánchez BN, Becker KJ, Geraghty M, Hughes R, Norris G, Hemphill JC 3rd. Full medical support for intracerebral hemorrhage. *Neurology* 2015; 84(17): 1739-1744.

Morimoto BH, Koshland DE Jr. Excitatory amino acid uptake and *N*-methyl-D-aspartate-

mediated secretion in a neural cell line. *Proceedings of the National Academy of Sciences of the United States of America* 1990a; 87(9): 3518-3521.

Morimoto BH, Koshland DE Jr. Induction and expression of long- and short-term neurosecretory potentiation in a neural cell line. *Neuron* 1990b; 5(6): 875-880.

Morita K, Lee MS, Her S. Possible relation of hemin-induced HO-1 expression to the upregulation of VEGF and BDNF mRNA levels in rat C6 glioma cells. *Journal of Molecular Neuroscience* 2009; 38(1): 31-40.

Mosquera A, Idrovo LA, Tafur A, Del Brutto OH. Stroke following *Bothrops spp.* snakebite. *Neurology* 2003; 60(10): 1577-1580.

Mun-Bryce S, Wilkerson AC, Papuashvili N, Okada YC. Recurring episodes of spreading depression are spontaneously elicited by an intracerebral hemorrhage in the swine. *Brain Research* 2001; 888(2): 248-255.

Nabika T, Cui Z, Masuda J. The stroke-prone spontaneously hypertensive rat: how good is it as a model for cerebrovascular diseases? *Cellular and Molecular Neurobiology* 2004; 24(5): 639-646.

Nakamura T, Keep RF, Hua Y, Schallert T, Hoff JT, Xi G. Deferoxamine-induced attenuation of brain edema and neurological deficits in a rat model of intracerebral hemorrhage. *Journal of Neurosurgery* 2004a; 100(4): 672-678.

Nakamura T, Xi G, Hua Y, Schallert T, Hoff JT, Keep RF. Intracerebral hemorrhage in mice: model characterization and application for genetically modified mice. *Journal of Cerebral Blood Flow & Metabolism* 2004b; 24(5): 487-494.

Naval NS, Nyquist PA, Carhuapoma JR. Medical management of intracerebral hemorrhage. In: Carhuapoma JR, Mayer SA, Hanley DF (eds). Intracerebral Hemorrhage. *Cambridge University Press*, Cambridge, 2010; 159-164.

Nawrotek K, Tylman M, Decherchi P, Marqueste T, Rudnicka K, Gatkowska J, Wieczorek M. Assessment of degradation and biocompatibility of electrodeposited chitosan and chitosan-carbon nanotube tubular implants. *Journal of Biomedical Materials Research - Part A* 2016a; in press.

Nawrotek K, Tylman M, Rudnicka K, Gatkowska J, Balcerzak J. Tubular electrodeposition of chitosan-carbon nanotube implants enriched with calcium ions. *Journal of the Mechanical Behavior of Biomedical Materials* 2016b; 60: 256-266.

Neuhaus W, Gaiser F, Mahringer A, Franz J, Riethmüller C, Förster C. The pivotal role of astrocytes in an *in vitro* stroke model of the blood-brain barrier. *Frontiers in Cellular Neuroscience* 2014; 8: 352.

Ni H, Shen J, Song Y, Cao M, Liu X, Huang J, Zhang W, Xie L, Ning X, Ke K. EP3, Prostaglandin E2 receptor subtype 3, associated with neuronal apoptosis following intracerebral hemor-

rhage. *Cellular and Molecular Neurobiology* 2016; 36(6): 971-980.

Ni W, Okauchi M, Hatakeyama T, Gu Y, Keep RF, Xi G, Hua Y. Deferoxamine reduces intracerebral hemorrhage-induced white matter damage in aged rats. *Experimental Neurology* 2015; 272: 128-134.

Nimura T, Weinstein PR, Massa SM, Panter S, Sharp FR. Heme oxygenase-1 (HO-1) protein induction in rat brain following focal ischemia. *Brain Research - Molecular Brain Research* 1996; 37(1-2): 201-208.

NINDS ICH Workshop Participants. Priorities for clinical research in intracerebral hemorrhage: report from a National Institute of Neurological Disorders and Stroke workshop. *Stroke* 2005; 36(3): e23-e41.

Nutt SH, Patchell RA. Intracranial hemorrhage associated with primary and secondary tumors. *Neurosurgery Clinics of North America* 1992; 3(3): 591-599.

Nutton V. Anonymi medici: De morbis acutis et chroniis. *Medical History* 1998; 42(3): 414-415.

Nyquist P. Management of acute intracranial and intraventricular hemorrhage. *Critical Care Medicine* 2010; 38(3): 946-953.

Nyquist PA, Naval NS, Carhuapoma JR. Future therapy in intracerebral hemorrhage and intraventricular hemorrhage: aspiration and thrombolysis. In: Carhuapoma JR, Mayer SA, Hanley DF (eds). Intracerebral Hemorrhage. *Cambridge University Press*, Cambridge, 2010; 176-186.

O'Donnell HC, Rosand J, Knudsen KA, Furie KL, Segal AZ, Chiu RI, Ikeda D, Greenberg SM. Apolipoprotein E genotype and the risk of recurrent lobar intracerebral hemorrhage. *New England Journal of Medicine* 2000; 342(4): 240-245.

Obach V, Revilla M, Vila N, Cervera AA, Chamorro AA. α_1-Antichymotrypsin polymorphism: a risk factor for hemorrhagic stroke in normotensive subjects. *Stroke* 2001; 32(11): 2588-2591.

Ohtani R, Kazui S, Tomimoto H, Minematsu K, Naritomi H. Clinical and radiographic features of lobar cerebral hemorrhage: hypertensive versus non-hypertensive cases. *Internal Medicine* 2003; 42(7): 576-580.

Okabe S, Vicario-Abejón C, Segal M, McKay RD. Survival and synaptogenesis of hippocampal neurons without NMDA receptor function in culture. *European Journal of Neuroscience* 1998; 10(6): 2192-2198.

Okamoto K, Hazama F, Yamori Y, Haebara H, Nagaoka A. Pathogenesis and prevention of stroke in spontaneously hypertensive rats. *Clinical Science and Molecular Medicine Supplement* 1975; 2: 161s-163s.

Okauchi M, Hua Y, Keep RF, Morgenstern LB, Xi G. Effects of deferoxamine on intracerebral

hemorrhage-induced brain injury in aged rats. *Stroke* 2009; 40(5): 1858-1863.

Osborne NN, Larsen A, Barnett NL. Influence of excitatory amino acids and ischemia on rat retinal choline acetyltransferase-containing cells. *Investigative Ophthalmology & Visual Science* 1995; 36(8): 1692-1700.

Ott KH, Kase CS, Ojemann RG, Mohr JP. Cerebellar hemorrhage: diagnosis and treatment. A review of 56 cases. *Archives of Neurology* 1974; 31(3): 160-167.

Ozgun B, Castillo M. Basal ganglia hemorrhage related to lightning strike. *American Journal of Neuroradiology* 1995; 16(6): 1370-1371.

Pamenter ME, Perkins GA, McGinness AK, Gu XQ, Ellisman MH, Haddad GG. Autophagy and apoptosis are differentially induced in neurons and astrocytes treated with an *in vitro* mimic of the ischemic penumbra. *PLoS One* 2012; 7(12): e51469.

Pan T, Huang B, Zhang W, Gabos S, Huang DY, Devendran V. Cytotoxicity assessment based on the AUC_{50} using multi-concentration time-dependent cellular response curves. *Analytica Chimica Acta* 2013a; 764: 44-52.

Pan T, Khare S, Ackah F, Huang B, Zhang W, Gabos S, Jin C, Stampfl M. *In vitro* cytotoxicity assessment based on KC_{50} with real-time cell analyzer (RTCA) assay. Computational Biology and Chemistry 2013b; 47: 113-120.

Parizel PM, Makkat S, Van Miert E, Van Goethem JW, van den Hauwe L, De Schepper AM. Intracranial hemorrhage: principles of CT and MRI interpretation. *European Radiology* 2001; 11(9): 1770-1783.

Park HK, Lee SH, Chu K, Roh JK. Effects of celecoxib on volumes of hematoma and edema in patients with primary intracerebral hemorrhage. *Journal of the Neurological Sciences* 2009; 279(1-2): 43-46.

Park SK, Yi HJ, Paik SS, Kim YJ, Ko Y, Oh SJ. Metastasizing malignant peripheral nerve sheath tumor initially presenting as intracerebral hemorrhage. Case report and review of the literature. *Surgical Neurology* 2007; 68(1): 79-84.

Passero S, Rocchi R, Rossi S, Ulivelli M, Vatti G. Seizures after spontaneous supratentorial intracerebral hemorrhage. *Epilepsia* 2002; 43(10): 1175-1180.

Patel B. Differential activation of microglia in an *in vitro* model of intracerebral hemorrhage. Syracuse University Honors Program Capstone Projects. *Syracuse University*, Syracuse NY, 2015; paper 826.

Peacock JH, Rush DF, Mathers LH. Morphology of dissociated hippocampal cultures from fetal mice. *Brain Research* 1979; 169(2): 231-246.

Pellizzaro Venti M, Paciaroni M, Caso V. Caudate infarcts and hemorrhages. *Frontiers of Neurology and Neuroscience* 2012; 30: 137-140.

Pezzini A, Padovani A. Cerebral amyloid angiopathy-related hemorrhages. *Neurological Sci-*

ences 2008; 29(suppl.2): s260-s263.

Pietrini G, Matteoli M, Banker G, Caplan MJ. Isoforms of the Na,K-ATPase are present in both axons and dendrites of hippocampal neurons in culture. *Proceedings of the National Academy of Sciences of the United States of America* 1992; 89(18): 8414-8418.

Pinho FM, Burdmann EA. Fatal cerebral hemorrhage and acute renal failure after young *Bothrops jararacussu* snake bite. *Renal Failure* 2001; 23(2): 269-277.

Ploughman M, Granter-Button S, Chernenko G, Tucker BA, Mearow KM, Corbett D. Endurance exercise regimens induce differential effects on brain-derived neurotrophic factor, synapsin-I and insulin-like growth factor I after focal ischemia. *Neuroscience* 2005; 136(4): 991-1001.

Power C, Henry S, Del Bigio MR, Larsen PH, Corbett D, Imai Y, Yong VW, Peeling J. Intracerebral hemorrhage induces macrophage activation and matrix metalloproteinases. *Annals of Neurology* 2003; 53(6): 731-742.

Pozzi M, Roccatagliata D, Sterzi R. Drug abuse and intracranial hemorrhage. *Neurological Sciences* 2008; 29(suppl.2): s269-s270.

Prabhakaran S, Naidech AM. Ischemic brain injury after intracerebral hemorrhage: a critical review. *Stroke* 2012; 43(8): 2258-2263.

Psychogios N, Hau DD, Peng J, Guo AC, Mandal R, Bouatra S, Sinelnikov I, Krishnamurthy R, Eisner R, Gautam B, Young N, Xia J, Knox C, Dong E, Huang P, Hollander Z, Pedersen TL, Smith SR, Bamforth F, Greiner R, McManus B, Newman JW, Goodfriend T, Wishart DS. The human serum metabolome. *PLoS One* 2011; 6(2): e16957.

Quinones-Hinojosa A, Gulati M, Singh V, Lawton MT. Spontaneous intracerebral hemorrhage due to coagulation disorders. *Neurosurgical Focus* 2003; 15(4): E3.

Qureshi AI, Ali Z, Suri MF, Shuaib A, Baker G, Todd K, Guterman LR, Hopkins LN. Extracellular glutamate and other amino acids in experimental intracerebral hemorrhage: an *in vivo* microdialysis study. *Critical Care Medicine* 2003a; 31(5): 1482-1489.

Qureshi AI, Ling GS, Khan J, Suri MF, Miskolczi L, Guterman LR, Hopkins LN. Quantitative analysis of injured, necrotic, and apoptotic cells in a new experimental model of intracerebral hemorrhage. *Critical Care Medicine* 2001a; 29(1): 152-157.

Qureshi AI, Mendelow AD, Hanley DF. Intracerebral haemorrhage. *Lancet* 2009; 373(9675): 1632-1644.

Qureshi AI, Suri MF, Ostrow PT, Kim SH, Ali Z, Shatla AA, Guterman LR, Hopkins LN. Apoptosis as a form of cell death in intracerebral hemorrhage. *Neurosurgery* 2003b; 52(5): 1041-1047.

Qureshi AI, Tuhrim S, Broderick JP, Batjer HH, Hondo H, Hanley DF. Spontaneous intracerebral hemorrhage. *New England Journal of Medicine* 2001b; 344(19): 1450-1460.

Qureshi AI, Wilson DA, Hanley DF, Traystman RJ. No evidence for an ischemic penumbra in massive experimental intracerebral hemorrhage. *Neurology* 1999; 52(2): 266-272.

Ralston JS, Rush RS, Doctor BP, Wolfe AD. Acetylcholinesterase from fetal bovine serum. Purification and characterization of soluble G_4 enzyme. *Journal of Biological Chemistry* 1985; 260(7): 4312-4318.

Ramis G, Martínez-Alarcón L, Quereda JJ, Mendonça L, Majado MJ, Gomez-Coelho K, Mrowiec A, Herrero-Medrano JM, Abellaneda JM, Pallares FJ, Ríos A, Ramírez P, Muñoz A. Optimization of cytotoxicity assay by real-time, impedance-based cell analysis. *Biomedical Microdevices* 2013; 15(6): 985-995.

Randell A, Daneshtalab N. Adjuvant-induced mono-arthritis potentiates cerebral hemorrhage in the spontaneously hypertensive rats. *Life Sciences* 2016; 151: 15-22.

Rapanà A, Lamaida E, Pizza V. Multiple postoperative intracerebral haematomas remote from the site of craniotomy. *British Journal of Neurosurgery* 1998; 12(4): 364-368.

Reddy P, Najundaswamy S, Mehta R, Petrova A, Hegyi T. Tin-mesoporphyrin in the treatment of severe hyperbilirubinemia in a very-low-birth-weight infant. *Journal of Perinatology* 2003; 23(6): 507-508.

Regan RF, Panter SS. Neurotoxicity of hemoglobin in cortical cell culture. *Neuroscience Letters* 1993; 153(2): 219-222.

Remes-Troche JM, Téllez-Zenteno JF, Rojas-Serrano J, Senties-Madrid H, Vega-Boada F, García-Ramos G. Thalamic and mesencephalic hemorrhages after multiple honeybee stings: a life-threatening apitherapy complication. *European Neurology* 2003; 49(3): 188-189.

Renfranz PJ, Cunningham MG, McKay RD. Region-specific differentiation of the hippocampal stem cell line HiB5 upon implantation into the developing mammalian brain. *Cell* 1991; 66(4): 713-729.

Repetto G, del Peso A, Zurita JL. Neutral red uptake assay for the estimation of cell viability/cytotoxicity. *Nature Protocols* 2008; 3(7): 1125-1131.

Richmond J. Refinement, reduction, and replacement of animal use for regulatory testing: future improvements and implementation within the regulatory framework. *Institute of Laboratory Animal Resources Journal* 2002; 43(suppl.): s63-s68.

Riela AR, Roach ES. Etiology of stroke in children. *Journal of Child Neurology* 1993; 8(3): 201-220.

Rincon F, Friedman DP, Bell R, Mayer SA, Bray PF. Targeted temperature management after intracerebral hemorrhage (TTM-ICH): methodology of a prospective randomized clinical trial. *International Journal of Stroke* 2014; 9(5): 646-651.

Rincon F, Mayer SA. Clinical review: Critical care management of spontaneous intracerebral

hemorrhage. *Critical Care* 2008; 12(6): 237.

Rincon F, Mayer SA. Novel therapies for intracerebral hemorrhage. *Current Opinion in Critical Care* 2004; 10(2): 94-100.

Rincon F, Mayer SA. The epidemiology of intracerebral hemorrhage in the United States from 1979 to 2008. *Neurocritical Care* 2013; 19(1): 95-102.

Riss TL, Moravec RA. Cell proliferation assays: improved homogeneous methods used to measure the number of cells in culture. In: Celis JE (ed). Cell Biology: A Laboratory Handbook. Volume 1. *Elsevier - Academic Press*, Burlington, 2006; 25-31.

Rivera S, Guillot S, Agassandian C, Ben Ari Y, Khrestchatisky M. Serum deprivation-induced apoptosis in cultured hippocampi is prevented by kainate. *NeuroReport* 1998; 9(17): 3949-3953.

Robinson SR, Dang TN, Dringen R, Bishop GM. Hemin toxicity: a preventable source of brain damage following hemorrhagic stroke. *Redox Report* 2009; 14(6): 228-235.

Rodríguez-Yáñez M, Castellanos M, Freijo MM, López Fernández JC, Martí-Fàbregas J, Nombela F, Simal P, Castillo J; Comitéad hoc del Grupo de Estudio de Enfermedades Cerebrovasculares de la SEN, Díez-Tejedor E, Fuentes B, Alonso de Leciñana M, Alvarez-Sabin J, Arenillas J, Calleja S, Casado I, Dávalos A, Díaz-Otero F, Egido JA, Gállego J, García Pastor A, Gil-Núñez A, Gilo F, Irimia P, Lago A, Maestre J, Masjuan J, Martínez-Sánchez P, Martínez-Vila E, Molina C, Morales A, Purroy F, Ribó M, Roquer J, Rubio F, Segura T, Serena J, Tejada J, Vivancos J. Clinical practice guidelines in intracerebral haemorrhage. *Neurologia* 2013; 28(4): 236-249.

Rodríguez-Yáñez M, Dávalos A, Castillo J. Natural history of perihaematomal brain edema. In: Carhuapoma JR, Mayer SA, Hanley DF (eds). Intracerebral Hemorrhage. *Cambridge University Press*, Cambridge, 2010; 229-237.

Roger VL, Go AS, Lloyd-Jones DM, Benjamin EJ, Berry JD, Borden WB, Bravata DM, Dai S, Ford ES, Fox CS, Fullerton HJ, Gillespie C, Hailpern SM, Heit JA, Howard VJ, Kissela BM, Kittner SJ, Lackland DT, Lichtman JH, Lisabeth LD, Makuc DM, Marcus GM, Marelli A, Matchar DB, Moy CS, Mozaffarian D, Mussolino ME, Nichol G, Paynter NP, Soliman EZ, Sorlie PD, Sotoodehnia N, Turan TN, Virani SS, Wong ND, Woo D, Turner MB; American Heart Association Statistics Committee and Stroke Statistics Subcommittee. Heart disease and stroke statistics - 2012 update: a report from the American Heart Association. *Circulation* 2012; 125(1): e2-e220.

Ropper AH, Davis KR. Lobar cerebral hemorrhages: acute clinical syndromes in 26 cases. *Annals of Neurology* 1980; 8(2): 141-147.

Ropper AH, Zervas NT. Cerebral blood flow after experimental basal ganglia hemorrhage. *Annals of Neurology* 1982; 11(3): 266-271.

Rosell A, Foerch C, Murata Y, Lo EH. Mechanisms and markers for haemorrhagic transformation after stroke. *Acta Neurochirurgica Supplement* 2008; 105: 173-178.

Rosenberg GA, Mun-Bryce S, Wesley M, Kornfeld M. Collagenase-induced intracerebral hemorrhage in rats. *Stroke* 1990; 21(5): 801-807.

Roshan Moniri M, Young A, Reinheimer K, Rayat J, Dai LJ, Warnock GL. Dynamic assessment of cell viability, proliferation and migration using real time cell analyzer system (RTCA). *Cytotechnology* 2015; 67(2): 379-386.

Rost NS, Smith EE, Chang Y, Snider RW, Chanderraj R, Schwab K, FitzMaurice E, Wendell L, Goldstein JN, Greenberg SM, Rosand J. Prediction of functional outcome in patients with primary intracerebral hemorrhage: the FUNC score. *Stroke* 2008; 39(8): 2304-2309.

Ruiz-Sandoval JL, Chiquete E, Romero-Vargas S, Padilla-Martínez JJ, González-Cornejo S. Grading scale for prediction of outcome in primary intracerebral hemorrhages. *Stroke* 2007; 38(5): 1641-1644.

Russell DA, Gough MJ. Intracerebral haemorrhage following carotid endarterectomy. *European Journal of Vascular and Endovascular Surgery* 2004; 28(2): 115-123.

Ryder EF, Snyder EY, Cepko CL. Establishment and characterization of multipotent neural cell lines using retrovirus vector-mediated oncogene transfer. *Journal of Neurobiology* 1990; 21(2): 356-375.

Rynkowski MA, Kim GH, Komotar RJ, Otten ML, Ducruet AF, Zacharia BE, Kellner CP, Hahn DK, Merkow MB, Garrett MC, Starke RM, Cho BM, Sosunov SA, Connolly ES. A mouse model of intracerebral hemorrhage using autologous blood infusion. *Nature Protocols* 2008; 3(1): 122-128.

Sacco S, Marini C, Carolei A. Medical treatment of intracerebral hemorrhage. *Neurological Sciences* 2004; 25(suppl.1): s6-s9.

Salmaggi A, Erbetta A, Silvani A, Maderna E, Pollo B. Intracerebral haemorrhage in primary and metastatic brain tumours. *Neurological Sciences* 2008; 29(suppl.2): s264-s265.

Samadani U, Rohde V. A review of stereotaxy and lysis for intracranial hemorrhage. *Neurosurgical Review* 2009; 32(1): 15-21.

Samarasekera N, Smith C, Al-Shahi Salman R. The association between cerebral amyloid angiopathy and intracerebral haemorrhage: systematic review and meta-analysis. *Journal of Neurology, Neurosurgery & Psychiatry* 2012; 83(3): 275-281.

Sandin JA 3rd, Salamat MS, Baskaya M, Dempsey RJ. Intracerebral hemorrhage caused by the rupture of a nontraumatic middle meningeal artery aneurysm. Case report and review of the literature. *Journal of Neurosurgery* 1999; 90(5): 951-954.

Santana R, McGarry LM, Bielza C, Larrañaga P, Yuste R. Classification of neocortical interneu-

rons using affinity propagation. *Frontiers in Neural Circuits* 2013; 7: 185.

Sastry BS, Phillis JW. Antagonism of biogenic amine-induced depression of cerebral cortical neurones by Na^+,K^+-ATPase in inhibitors. *Canadian Journal of Physiology and Pharmacology* 1977; 55(2): 170-179.

Schellinger PD, Fiebach JB. Intracranial hemorrhage: the role of magnetic resonance imaging. *Neurocritical Care* 2004; 1(1): 31-45.

Schiff L, Hadker N, Weiser S, Rausch C. A literature review of the feasibility of glial fibrillary acidic protein as a biomarker for stroke and traumatic brain injury. *Molecular Diagnosis & Therapy* 2012; 16(2): 79-92.

Schiller F. Concepts of stroke before and after Virchow. *Medical History* 1970; 14(2): 115-131.

Schlichter LC, Kaushal V, Moxon-Emre I, Sivagnanam V, Vincent C. The Ca^{2+} activated SK3 channel is expressed in microglia in the rat striatum and contributes to microglia-mediated neurotoxicity *in vitro*. *Journal of Neuroinflammation* 2010; 7: 4.

Scrace S, O'Neill E, Hammond EM, Pires IM. Use of the xCELLigence system for real-time analysis of changes in cellular motility and adhesion in physiological conditions. *Methods in Molecular Biology* 2013; 1046: 295-306.

Seifman MA, Lewis PM, Rosenfeld JV, Hwang PY. Postoperative intracranial haemorrhage: a review. *Neurosurgical Review* 2011; 34(4): 393-407.

Selim M. Deferoxamine mesylate - a new hope for intracerebral hemorrhage: from bench to clinical trials. *Stroke* 2009; 40(3 suppl.1): s90-s91.

Senanayake N, Román GC. Neurological complications of malaria. *Southeast Asian Journal of Tropical Medicine and Public Health* 1992; 23(4): 672-680.

Sessa M. Intracerebral hemorrhage and hypertension. *Neurological Sciences* 2008; 29(suppl.2): s258-s259.

Seyfried D, Han Y, Lu D, Chen J, Bydon A, Chopp M. Improvement in neurological outcome after administration of atorvastatin following experimental intracerebral hemorrhage in rats. *Journal of Neurosurgery* 2004; 101(1): 104-107.

Sharp BM. Conversion of the U937 monocyte into “macrophage-like” populations exhibiting M1 or M2 characteristics. MS Thesis (Microbiology and Immunology Graduate Program). *Wright State University*, Dayton OH, 2013.

Sharp FR. Stress proteins are sensitive indicators of injury in the brain produced by ischemia and toxins. *Journal of Toxicological Sciences* 1995; 20(4): 450-453.

Shchepina LA, Pletjushkina OY, Avetisyan AV, Bakeeva LE, Fetisova EK, Izyumov DS, Sapronova VB, Vyssokikh MY, Chernyak BV, Skulachev VP. Oligomycin, inhibitor of the F_0 part of H^+-ATP-synthase, suppresses the TNF-induced apoptosis. *Oncogene* 2002; 21(53): 8149-8157.

Shen X, Ma L, Dong W, Wu Q, Gao Y, Luo C, Zhang M, Chen X, Tao L. Autophagy regulates intracerebral hemorrhage induced neural damage via apoptosis and NF-κB pathway. *Neurochemistry International* 2016; 96: 100-112.

Shi J, Li H, Jin G, Zhu P, Tian M, Qin J, Tan X, Zhao S, Wang F, Hua Y, Xiao Y. Lhx8 promote differentiation of hippocampal neural stem/progenitor cells into cholinergic neurons *in vitro*. *In Vitro Cellular & Developmental Biology - Animal* 2012; 48(10): 603-609.

Shi Y, Li Z, Zhang S, Xie M, Meng X, Xu J, Liu N, Tang Z. Establishing a model of supratentorial hemorrhage in the piglet. *Tohoku Journal of Experimental Medicine* 2010; 220(1): 33-40.

Silver B. Advances in stroke over the past decade. *Rhode Island Medical Journal* 2014; 97(5): 27-30.

Silwedel C, Förster C. Differential susceptibility of cerebral and cerebellar murine brain microvascular endothelial cells to loss of barrier properties in response to inflammatory stimuli. *Journal of Neuroimmunology* 2006; 179(1-2): 37-45.

Sinar EJ, Mendelow AD, Graham DI, Teasdale GM. Experimental intracerebral hemorrhage: effects of a temporary mass lesion. *Journal of Neurosurgery* 1987; 66(4): 568-576.

Singh G, Siddiqui MA, Khanna VK, Kashyap MP, Yadav S, Gupta YK, Pant KK, Pant AB. Oxygen glucose deprivation model of cerebral stroke in PC-12 cells: glucose as a limiting factor. *Toxicology Mechanisms and Methods* 2009; 19(2): 154-160.

Sinn DI, Lee ST, Chu K, Jung KH, Song EC, Kim JM, Park DK, Kim M, Roh JK. Combined neuroprotective effects of celecoxib and memantine in experimental intracerebral hemorrhage. *Neuroscience Letters* 2007; 411(3): 238-242.

Själander A, Engström G, Berntorp E, Svensson P. Risk of haemorrhagic stroke in patients with oral anticoagulation compared with the general population. *Journal of Internal Medicine* 2003; 254(5): 434-438.

Slowik A, Turaj W, Dziedzic T, Haefele A, Pera J, Malecki MT, Glodzik-Sobanska L, Szermer P, Figlewicz DA, Szczudlik A. DD genotype of ACE gene is a risk factor for intracerebral hemorrhage. *Neurology* 2004; 63(2): 359-361.

Squier W. The "Shaken Baby" syndrome: pathology and mechanisms. *Acta Neuropathologica* 2011; 122(5): 519-542.

Squinto SP, Stitt TN, Aldrich TH, Davis S, Bianco SM, Radziejewski C, Glass DJ, Masiakowski P, Furth ME, Valenzuela DM, DiStefano PS, Yancopoulos GD. *trkB* encodes a functional receptor for brain-derived neurotrophic factor and neurotrophin-3 but not nerve growth factor. *Cell* 1991; 65(5): 885-893.

Stapf C, Mohr JP. Vascular malformations of the brain. In: Carhuapoma JR, Mayer SA, Hanley DF (eds). Intracerebral Hemorrhage. *Cambridge University Press*, Cambridge, 2010; 71-

83.

Starke RM, Komotar RJ, Connolly ES. A randomized clinical trial and meta-analysis of early surgery vs. initial conservative treatment in patients with spontaneous lobar intracerebral hemorrhage. *Neurosurgery* 2014; 74(2): N11-N12.

Staykov D, Huttner HB, Köhrmann M, Bardutzky J, Schellinger PD. Novel approaches to the treatment of intracerebral haemorrhage. *International Journal of Stroke* 2010; 5(6): 457-465.

Stein RW, Caplan LR, Hier DB. Intracerebral hemorrhage: role of blood pressure and location and size of lesions. *Annals of Neurology* 1983; 14(1): 132-133.

Stein RW, Kase CS, Hier DB, Caplan LR, Mohr JP, Hemmati M, Henderson K. Caudate hemorrhage. *Neurology* 1984; 34(12): 1549-1554.

Steiner T, Al-Shahi Salman R, Beer R, Christensen H, Cordonnier C, Csiba L, Forsting M, Harnof S, Klijn CJ, Krieger D, Mendelow AD, Molina C, Montaner J, Overgaard K, Petersson J, Roine RO, Schmutzhard E, Schwerdtfeger K, Stapf C, Tatlisumak T, Thomas BM, Toni D, Unterberg A, Wagner M; European Stroke Organisation. European Stroke Organisation (ESO) guidelines for the management of spontaneous intracerebral hemorrhage. *International Journal of Stroke* 2014; 9(7): 840-855.

Steiner T, Petersson J, Al-Shahi Salman R, Christensen H, Cordonnier C, Csiba L, Harnof S, Krieger D, Mendelow D, Molina C, Montaner J, Overgaard K, Roine RO, Schmutzhard E, Tatlisumak T, Toni D, Stapf C; European Research Network on Intracerebral Haemorrhage. European research priorities for intracerebral haemorrhage. *Cerebrovascular Diseases* 2011; 32(5): 409-419.

Steiner T, Rosand J, Diringer M. Intracerebral hemorrhage associated with oral anticoagulant therapy: current practices and unresolved questions. *Stroke* 2006; 37(1): 256-262.

Storey CE, Pols H. A history of cerebrovascular disease. In: Finger S, Boller F, Tyler KL (eds). Handbook of Clinical Neurology - History of Neurology. *Elsevier*, Edinburgh, 2010; 95: 401-415.

Strbian D, Durukan A, Tatlisumak T. Rodent models of hemorrhagic stroke. *Current Pharmaceutical Design* 2008; 14(4): 352-358.

Sun H, Li L, Zhou F, Zhu L, Ke K, Tan X, Xu W, Rui Y, Zheng H, Zhou Z, Yang H. The member of high temperature requirement family HtrA2 participates in neuronal apoptosis after intracerebral hemorrhage in adult rats. *Journal of Molecular Histology* 2013; 44(4): 369-379.

Sundström C, Nilsson K. Establishment and characterization of a human histiocytic lymphoma cell line (U-937). *International Journal of Cancer* 1976; 17(5): 565-577.

Sutherland GR, Auer RN. Primary intracerebral hemorrhage. *Journal of Clinical Neuroscience*

2006; 13(5): 511-517.

Suttner DM, Dennery PA. Reversal of HO-1 related cytoprotection with increased expression is due to reactive iron. *FASEB Journal* 1999; 13(13): 1800-1809.

Takasugi S, Ueda S, Matsumoto K. Chronological changes in spontaneous intracerebral hematoma - an experimental and clinical study. *Stroke* 1985; 16(4): 651-658.

Takeda A, Kimpara T, Onodera H, Itoyama Y, Shibahara S, Kogure K. Regional difference in induction of heme oxygenase-1 protein following rat transient forebrain ischemia. *Neuroscience Letters* 1996; 205(3): 169-172.

Taoufik E, Probert L. Ischemic neuronal damage. *Current Pharmaceutical Design* 2008; 14(33): 3565-3573.

Tasca CI, Dal-Cim T, Cimarosti H. *In vitro* oxygen-glucose deprivation to study ischemic cell death. *Methods in Molecular Biology* 2015; 1254: 197-210.

Terro F, Esclaire F, Yardin C, Hugon J. *N*-Methyl-D-aspartate receptor blockade enhances neuronal apoptosis induced by serum deprivation. *Neuroscience Letters* 2000; 278(3): 149-152.

Thanvi BR, Sprigg N, Munshi SK. Advances in spontaneous intracerebral haemorrhage. *International Journal of Clinical Practice* 2012; 66(6): 556-564.

Thiex R, Tsirka SE. Brain edema after intracerebral hemorrhage: mechanisms, treatment options, management strategies, and operative indications. *Neurosurgical Focus* 2007; 22(5): E6.

Thiex R, Weis J, Krings T, Barreiro S, Yakisikli-Alemi F, Gilsbach JM, Rohde V. Addition of intravenous N-methyl-D-aspartate receptor antagonists to local fibrinolytic therapy for the optimal treatment of experimental intracerebral hemorrhages. *Journal of Neurosurgery* 2007; 106(2): 314-320.

Thiex R. Future perspectives on the fibrinolytic therapy of intracerebral hemorrhages. *Central Nervous System Agents in Medicinal Chemistry* 2011; 11(2): 150-156.

Thompson BB, Béjot Y, Caso V, Castillo J, Christensen H, Flaherty ML, Foerch C, Ghandehari K, Giroud M, Greenberg SM, Hallevi H, Hemphill JC 3rd, Heuschmann P, Juvela S, Kimura K, Myint PK, Nagakane Y, Naritomi H, Passero S, Rodríguez-Yáñez MR, Roquer J, Rosand J, Rost NS, Saloheimo P, Salomaa V, Sivenius J, Sorimachi T, Togha M, Toyoda K, Turaj W, Vemmos KN, Wolfe CD, Woo D, Smith EE. Prior antiplatelet therapy and outcome following intracerebral hemorrhage: a systematic review. *Neurology* 2010; 75(15): 1333-1342.

Thoonsen H, Richard E, Bentham P, Gray R, van Geloven N, De Haan RJ, Van Gool WA, Nederkoorn PJ. Aspirin in Alzheimer's disease: increased risk of intracerebral hemorrhage: cause for concern? *Stroke* 2010; 41(11): 2690-2692.

Thrift AG, Donnan GA, McNeil JJ. Epidemiology of intracerebral hemorrhage. *Epidemiologic Reviews* 1995; 17(2): 361-381.

Thrift AG, Donnan GA, McNeil JJ. Heavy drinking, but not moderate or intermediate drinking, increases the risk of intracerebral hemorrhage. *Epidemiology* 1999a; 10(3): 307-312.

Thrift AG, Evans RG, Donnan GA. Hypertension and the risk of intracerebral haemorrhage: special considerations in patients with renal disease. *Nephrology, Dialysis, Transplantation* 1999b; 14(10): 2291-2292.

Thrift AG, McNeil JJ, Forbes A, Donnan GA. Risk of primary intracerebral haemorrhage associated with aspirin and non-steroidal anti-inflammatory drugs: case-control study. *British Medical Journal* 1999c; 318(7186): 759-764.

Tombran-Tink J, Barnstable CJ. PEDF: a multifaceted neurotrophic factor. *Nature Reviews Neuroscience* 2003; 4(8): 628-636.

Tsakiris S. Effects of L-phenylalanine on acetylcholinesterase and Na^+,K^+-ATPase activities in adult and aged rat brain. *Mechanisms of Ageing and Development* 2001; 122(5): 491-501.

Tseng HC, Ruegg SJ, Maronski M, Messam CA, Grinspan JB, Dichter MA. Injuring neurons induces neuronal differentiation in a population of hippocampal precursor cells in culture. *Neurobiology of Disease* 2006; 22(1): 88-97.

Tuhrim S. Mathematical models of intracerebral hemorrhage and intraventricular hemorrhage outcomes prediction: their comparison, advantages, and limitations. In: Carhuapoma JR, Mayer SA, Hanley DF (eds). Intracerebral Hemorrhage. *Cambridge University Press*, Cambridge, 2010; 187-191.

Uyama O, Okamura N, Yanase M, Narita M, Kawabata K, Sugita M. Quantitative evaluation of vascular permeability in the gerbil brain after transient ischemia using Evans blue fluorescence. *Journal of Cerebral Blood Flow & Metabolism* 1988; 8(2): 282-284.

van Asch CJ, Luitse MJ, Rinkel GJ, van der Tweel I, Algra A, Klijn CJ. Incidence, case fatality, and functional outcome of intracerebral haemorrhage over time, according to age, sex, and ethnic origin: a systematic review and meta-analysis. *Lancet Neurology* 2010; 9(2): 167-176.

van der Valk J, Brunner D, De Smet K, Fex Svenningsen A, Honegger P, Knudsen LE, Lindl T, Noraberg J, Price A, Scarino ML, Gstraunthaler G. Optimization of chemically defined cell culture media - replacing fetal bovine serum in mammalian *in vitro* methods. *Toxicology In Vitro* 2010; 24(4): 1053-1063.

van Kralingen C, Kho DT, Costa J, Angel CE, Graham ES. Exposure to inflammatory cytokines IL-1β and TNFα induces compromise and death of astrocytes; implications for chronic neuroinflammation. *PLoS One* 2013; 8(12): e84269.

Vespa PM. Metabolic penumbra in intracerebral hemorrhage. *Stroke* 2009; 40(5): 1547-1548.

Viola GM, White AC Jr, Serpa JA. Hemorrhagic cerebrovascular events and neurocysticercosis: a case report and review of the literature. *American Journal of Tropical Medicine and Hygiene* 2011; 84(3): 402-405.

Vistejnova L, Dvorakova J, Hasova M, Muthny T, Velebny V, Soucek K, Kubala L. The comparison of impedance-based method of cell proliferation monitoring with commonly used metabolic-based techniques. *Neuroendocrinology Letters* 2009; 30(suppl.1): 121-127.

Wagner KR, Hua Y, de Courten-Myers GM, Broderick JP, Nishimura RN, Lu SY, Dwyer BE. Tin-mesoporphyrin, a potent heme oxygenase inhibitor, for treatment of intracerebral hemorrhage: *in vivo* and *in vitro* studies. *Cellular and Molecular Biology (Noisy-le-Grand)* 2000; 46(3): 597-608.

Wagner KR, Sharp FR, Ardizzone TD, Lu A, Clark JF. Heme and iron metabolism: role in cerebral hemorrhage. *Journal of Cerebral Blood Flow & Metabolism* 2003; 23(6): 629-652.

Wagner KR, Xi G, Hua Y, Kleinholz M, de Courten-Myers GM, Myers RE, Broderick JP, Brott TG. Lobar intracerebral hemorrhage model in pigs: rapid edema development in perihematomal white matter. *Stroke* 1996; 27(3): 490-497.

Wagner KR, Zuccarello M. Animal models and experimental treatments of intracerebral hemorrhage. In: Carhuapoma JR, Mayer SA, Hanley DF (eds). Intracerebral Hemorrhage. *Cambridge University Press*, Cambridge, 2010; 193-205.

Wagner KR. Modeling intracerebral hemorrhage: glutamate, nuclear factor-κB signaling and cytokines. *Stroke* 2007; 38(2): 753-758.

Wang DZ, Talkad AV. Treatment of intracerebral hemorrhage: what should we do now? *Current Neurology and Neuroscience Reports* 2009; 9(1): 13-18.

Wang G. The pathogenesis of edema and secondary insults after ICH. In: Chaudhary V (ed). Intracerebral Hemorrhage. *InTech*, Rijeka, 2014; 25-40.

Wang J, Doré S. Heme oxygenase 2 deficiency increases brain swelling and inflammation after intracerebral hemorrhage. *Neuroscience* 2008; 155(4): 1133-1141.

Wang J, Doré S. Inflammation after intracerebral hemorrhage. *Journal of Cerebral Blood Flow & Metabolism* 2007; 27(5): 894-908.

Wang J, Zhuang H, Doré S. Heme oxygenase 2 is neuroprotective against intracerebral hemorrhage. *Neurobiology of Disease* 2006; 22(3): 473-476.

Wang J. Preclinical and clinical research on inflammation after intracerebral hemorrhage. *Progress in Neurobiology* 2010; 92(4): 463-477.

Wang Q, Wang D, Liu M, Fang Y, You C, Dong W, Chang X, Lei C, Zhang J, Chen Y. Is diabetes a predictor of worse outcome for spontaneous intracerebral hemorrhage? *Clinical Neurology and Neurosurgery* 2015; 134: 67-71.

Wang XQ, Xiao AY, Sheline C, Hyrc K, Yang A, Goldberg MP, Choi DW, Yu SP. Apoptotic insults impair Na^+,K^+-ATPase activity as a mechanism of neuronal death mediated by concurrent ATP deficiency and oxidant stress. *Journal of Cell Science* 2003; 116(10): 2099-2110.

Wasserman JK, Schlichter LC. Minocycline protects the blood-brain barrier and reduces edema following intracerebral hemorrhage in the rat. *Experimental Neurology* 2007a; 207(2): 227-237.

Wasserman JK, Schlichter LC. Neuron death and inflammation in a rat model of intracerebral hemorrhage: effects of delayed minocycline treatment. *Brain Research* 2007b; 1136(1): 208-218.

Weimar C, Roth M, Willig V, Kostopoulos P, Benemann J, Diener HC. Development and validation of a prognostic model to predict recovery following intracerebral hemorrhage. *Journal of Neurology* 2006; 253(6): 788-793.

Weisberg LA, Stazio A, Elliott D, Shamsnia M. Putaminal hemorrhage: clinical-computed tomographic correlations. *Neuroradiology* 1990; 32(3): 200-206.

Wessels T, Möller-Hartmann W, Noth J, Klötzsch C. CT findings and clinical features as markers for patient outcome in primary pontine hemorrhage. *American Journal of Neuroradiology* 2004; 25(2): 257-260.

Westerink RH. Do we really want to REACH out to *in vitro*? *NeuroToxicology* 2013; 39: 169-172.

Whittemore SR, Holets VR, Keane RW, Levy DJ, McKay RD. Transplantation of a temperature-sensitive, nerve growth factor-secreting, neuroblastoma cell line into adult rats with fimbria-fornix lesions rescues cholinergic septal neurons. *Journal of Neuroscience Research* 1991; 28(2): 156-170.

Witzel F, Fritsche-Guenther R, Lehmann N, Sieber A, Blüthgen N. Analysis of impedance-based cellular growth assays. *Bioinformatics* 2015; 31(16): 2705-2712.

Wong GK, Siu DY, Abrigo JM, Ahuja AT, Poon WS. Computed tomographic angiography for patients with acute spontaneous intracerebral hemorrhage. *Journal of Clinical Neuroscience* 2012; 19(4): 498-500.

Woo D, Kaushal R, Chakraborty R, Woo J, Haverbusch M, Sekar P, Kissela B, Pancioli A, Jauch E, Kleindorfer D, Flaherty M, Schneider A, Khatri P, Sauerbeck L, Khoury J, Deka R, Broderick J. Association of apolipoprotein E4 and haplotypes of the apolipoprotein E gene with lobar intracerebral hemorrhage. *Stroke* 2005; 36(9): 1874-1879.

Woo D, Sauerbeck LR, Kissela BM, Khoury JC, Szaflarski JP, Gebel J, Shukla R, Pancioli AM, Jauch EC, Menon AG, Deka R, Carrozzella JA, Moomaw CJ, Fontaine RN, Broderick JP. Genetic and environmental risk factors for intracerebral hemorrhage: preliminary re-

sults of a population-based study. *Stroke* 2002; 33(5): 1190-1195.

Woodruff TM, Thundyil J, Tang SC, Sobey CG, Taylor SM, Arumugam TV. Pathophysiology, treatment, and animal and cellular models of human ischemic stroke. *Molecular Neurodegeneration* 2011; 6(1): 11.

Worster A, Keim SM, Carpenter CR, Adeoye O; Best Evidence in Emergency Medicine (BEEM) Group. Does early intensive lowering of blood pressure reduce hematoma volume and improve clinical outcome after acute cerebral hemorrhage? *Journal of Emergency Medicine* 2009; 37(4): 433-438.

Wu CH, Ding XY, Wang HY, Ye XB, Huang SY, Huang AM, Li HZ, Wu SY, Yu J, Yan XH. Neural apoptosis and apoptosis-related genes in intracerebral hemorrhage patients. *Zhonghua Yi Xue Za Zhi* 2006; 86(43): 3073-3076.

Wu G, Bao X, Xi G, Keep RF, Thompson BG, Hua Y. Brain injury after intracerebral hemorrhage in spontaneously hypertensive rats. *Journal of Neurosurgery* 2011; 114(6): 1805-1811.

Wu G, Wu J, Jiao Y, Wang L, Wang F, Zhang Y. Rosiglitazone infusion therapy following minimally invasive surgery for intracerebral hemorrhage evacuation decreases matrix metalloproteinase-9 and blood-brain barrier disruption in rabbits. *BMC Neurology* 2015; 15: 37.

Wu J, Yang S, Hua Y, Liu W, Keep RF, Xi G. Minocycline attenuates brain edema, brain atrophy and neurological deficits after intracerebral hemorrhage. *Acta Neurochirurgica Supplement* 2010; 106: 147-150.

Wu J, Yang S, Xi G, Song S, Fu G, Keep RF, Hua Y. Microglial activation and brain injury after intracerebral hemorrhage. *Acta Neurochirurgica Supplement* 2008; 105: 59-65.

Xavier AR, Qureshi AI, Kirmani JF, Yahia AM, Bakshi R. Neuroimaging of stroke: a review. *Southern Medical Journal* 2003; 96(4): 367-379.

Xi G, Keep RF, Hoff JT. Mechanisms of brain injury after intracerebral haemorrhage. *Lancet Neurology* 2006; 5(1): 53-63.

Xi G, Keep RF, Hoff JT. Thrombin and secondary brain damage following intracerebral hemorrhage. In: Carhuapoma JR, Mayer SA, Hanley DF (eds). Intracerebral Hemorrhage. *Cambridge University Press*, Cambridge, 2010; 206-216.

Xi G, Strahle J, Hua Y, Keep RF. Progress in translational research on intracerebral hemorrhage: is there an end in sight? *Progress in Neurobiology* 2014; 115: 45-63.

Xie C, Markesbery WR, Lovell MA. Survival of hippocampal and cortical neurons in a mixture of MEM+ and B27-supplemented neurobasal medium. *Free Radical Biology and Medicine* 2000; 28(5): 665-672.

Xue M, Del Bigio MR. Comparison of brain cell death and inflammatory reaction in three models of intracerebral hemorrhage in adult rats. *Journal of Stroke & Cerebrovascular Dis-*

eases 2003; 12(3): 152-159.

Xue M, Yong VW. Matrix metalloproteinases in intracerebral hemorrhage. *Neurological Research* 2008; 30(8): 775-782.

Yamada K, Nabeshima T. Brain-derived neurotrophic factor/TrkB signaling in memory processes. *Journal of Pharmacological Sciences* 2003; 91(4): 267-270.

Yan T, Chopp M, Chen J. Experimental animal models and inflammatory cellular changes in cerebral ischemic and hemorrhagic stroke. *Neuroscience Bulletin* 2015; 31(6): 717-734.

Yang GY, Betz AL, Chenevert TL, Brunberg JA, Hoff JT. Experimental intracerebral hemorrhage: relationship between brain edema, blood flow, and blood-brain barrier permeability in rats. *Journal of Neurosurgery* 1994; 81(1): 93-102.

Yenari MA, Xu L, Tang XN, Qiao Y, Giffard RG. Microglia potentiate damage to blood-brain barrier constituents: improvement by minocycline *in vivo* and *in vitro*. *Stroke* 2006; 37(4): 1087-1093.

Zahari M, Mohd Ali AK, Chandrasekharan S. Delayed intracranial haemorrhage in head injury. *Singapore Medical Journal* 1996; 37(3): 285-287.

Zarros A, Bimpis A, Papalois A, Baillie GS. Perihaematomal cytokine expression is a crucial component of intracerebral haemorrhage pathophysiology. *Neurological Sciences* 2014; 35(9): 1471-1473.

Zarros A, Johnson SA, Mackenzie-Gray Scott CA, Baillie GS. Cytodynamics and endpoint selection for a reliable *in vitro* assessment of nanoneurotoxicity. *Nanomedicine: Nanotechnology, Biology, and Medicine* 2015; 11(2): 407-408.

Zarros A. Prerequisites for a reliable introduction of *in vitro* neurotoxicity testing within the REACH framework. *NeuroToxicology* 2014; 44: 365.

Zazulia AR, Diringer MN, Videen TO, Adams RE, Yundt K, Aiyagari V, Grubb RL Jr, Powers WJ. Hypoperfusion without ischemia surrounding acute intracerebral hemorrhage. *Journal of Cerebral Blood Flow & Metabolism* 2001; 21(7): 804-810.

Zhang J, Zhang CH, Lin XL, Zhang Q, Wang J, Shi SL. Serum glial fibrillary acidic protein as a biomarker for differentiating intracerebral hemorrhage and ischemic stroke in patients with symptoms of acute stroke: a systematic review and meta-analysis. *Neurological Sciences* 2013; 34(11): 1887-1892.

Zhang JH, Chung TD, Oldenburg KR. A simple statistical parameter for use in evaluation and validation of high throughput screening assays. *Journal of Biomolecular Screening* 1999; 4(2): 67-73.

Zhao X, Song S, Sun G, Strong R, Zhang J, Grotta JC, Aronowski J. Neuroprotective role of haptoglobin after intracerebral hemorrhage. *Journal of Neuroscience* 2009; 29(50): 15819-

15827.

Zhao X, Sun G, Zhang J, Strong R, Song W, Gonzales N, Grotta JC, Aronowski J. Hematoma resolution as a target for intracerebral hemorrhage treatment: role for peroxisome proliferator-activated receptor gamma in microglia/macrophages. *Annals of Neurology* 2007a; 61(4): 352-362.

Zhao X, Zhang Y, Strong R, Grotta JC, Aronowski J. 15d-Prostaglandin J_2 activates peroxisome proliferator-activated receptor-γ, promotes expression of catalase, and reduces inflammation, behavioral dysfunction, and neuronal loss after intracerebral hemorrhage in rats. *Journal of Cerebral Blood Flow & Metabolism* 2006; 26(6): 811-820.

Zhao X, Zhang Y, Strong R, Zhang J, Grotta JC, Aronowski J. Distinct patterns of intracerebral hemorrhage-induced alterations in NF-κB subunit, iNOS, and COX-2 expression. *Journal of Neurochemistry* 2007b; 101(3): 652-663.

Zhou X, Xie Q, Xi G, Keep RF, Hua Y. Brain CD47 expression in a swine model of intracerebral hemorrhage. *Brain Research* 2014; 1574: 70-76.

Zhou Y, Wang Y, Wang J, Anne Stetler R, Yang QW. Inflammation in intracerebral hemorrhage: from mechanisms to clinical translation. *Progress in Neurobiology* 2014; 115: 25-44.

APPENDIX A

List of biomedical abbreviations and symbolography used

The following list of abbreviations and symbolography includes the majority of the abbreviations and symbols defined and used within the main corpus of the current PhD Thesis (Parts A, B, C and D). This list does not include (a) the abbreviations / symbols of many of the standard scientific units, (b) most abbreviations of the herein presented *in vitro* treatment groups, or (c) some of the well-established abbreviations of everyday use and brand names that are found within the current PhD Thesis (as this was considered unnecessary). The abbreviations of the analytes of the proteomic profiling described in subchapter VII.5 are provided in Table C.5. Moreover, none of the abbreviations that are defined and used for the first time (in this PhD Thesis) in Appendix B are included in this list. However, every effort has been made in order to make sure that the readers will not find it difficult to cope with the use of abbreviations and symbols at certain crucial points of this PhD Thesis (such as at the Tables and the Figures used).

*	$p<0.05$; #
**	$p<0.01$; ##
***	$p<0.001$; ###
Δ	difference (operator)
ΔOD	difference (change / increase) of absorbance
μ_i	index of metaptotic adaptability
$[Ca^{2+}]_i$	intracellular calcium concentration
α1 Na^+,K^+-ATPase	alpha 1 subunit of sodium / potassium adenosine triphosphatase
Aβ	amyloid beta
ACE	angiotensin-converting enzyme
ACh	acetylcholine
AChE	acetylcholinesterase
ANGPT1	angiopoietin 1
ANGPT2	angiopoietin 2
ApoE	apolipoprotein E

APOE	apolipoprotein E gene
AR	androgen receptor
ATP	adenosine triphosphate
Bax	B cell lymphoma-2-associated X (protein)
BBB	blood-brain barrier
Bcl-2	B cell lymphoma-2 (protein)
BDNF	brain-derived neurotrophic factor
BOXes	bilirubin oxidative products
C5	haemolytic complement
CAL2	calretinin
CB	calbindin
CDP-Ch	cytidine-5'-diphosphocholine
ChAT	choline acetyltransferase
CI	cell index
CO	carbon monoxide
CO_2	carbon dioxide
COX-2	cyclooxygenase 2
CR	cellular response
CSF	cerebrospinal fluid
CT	computed tomography
CV	coefficient of variation
CXCL11	chemokine (C-X-C motif) ligand 11
DCX	doublecortin
DFO	deferoxamine
DMEM	Dulbecco's modified Eagle's medium
DST	drug-screening tool; plural: DSTs
DTNB	5,5'-dithionitrobenzoic acid
E_{24}	evaluation endpoint at 24 h
E_{36}	evaluation endpoint at 36 h
E_{48}	evaluation endpoint at 48 h
E_{60}	evaluation endpoint at 60 h
E14	embryonic day 14
E16	embryonic day 16
E18	embryonic day 18
E_d	endpoint within the dynamic phase
EDTA	ethylenediaminetetraacetic acid

E_e	end of the experiment (endpoint)
ECG	electrocardiogram
E_p	endpoint within the pathopoietic phase
EP3	prostaglandin E2 receptor subtype 3
ERα	oestrogen receptor alpha
ERβ	oestrogen receptor beta
E_t	endpoint after a treatment intervention
E_x	evaluation endpoint at a time point of choice (x: number / letter)
Ex	embryonic day x (x: day number)
FBS	foetal bovine serum
Fe^{2+}	ferrous iron
Fe^{3+}	ferric iron
FGF-21	fibroblast growth factor 21
Flt3l	FMS-like tyrosine kinase 3 ligand
G418	geneticin
GCS	Glasgow Coma Scale
GFAP	glial fibrillary acidic protein
GHSR	growth hormone secretagogue receptor
GluR3	glutamate receptor subtype 3
GluR4	glutamate receptor subtype 4
GPR30	G protein-coupled receptor 30
HIF-1α	hypoxia inducible factor 1 alpha
HO	haeme oxygenase; plural: HOs
HO-1	haeme oxygenase 1
HO-2	haeme oxygenase 2
HRP	horseradish-peroxidase
ICH	intracerebral haemorrhage (note: not in use throughout this PhD Thesis)
ICP	intracranial pressure
I_e	experiment's initiation point
IFN-γ	interferon gamma
IL-1α	interleukin 1 alpha
IL-1β	interleukin 1 beta
IL-1ra	interleukin 1 receptor antagonist
IL-6	interleukin 6
I_m	metaptosis' initiation point
iNOS	inducible nitric oxide synthase

I_o	recording's initiation point
IQR	interquartile range
IR	insulin receptor
I_t	treatment's initiation point
KCN	potassium cyanide
LC3	microtubule-associated protein light chain-3
LDH	lactate dehydrogenase
LPS	lipopolysaccharide
MAP2	microtubule-associated protein 2
m_i	metaptotic index
MMP	matrix metalloproteinase; plural: MMPs
MMP-2	matrix metallopeptidase 2
MMP-9	matrix metalloproteinase 9
MMP-12	matrix metalloproteinase 12
MRI	magnetic resonance imaging
MTT	3-(4,5-dimethylthiazol-2-yl)-2,5-diphenyltetrazolium bromide
n/a	not applicable
Na^+	sodium ion
Na^+,K^+-ATPase	sodium / potassium adenosine triphosphatase
NaCl	sodium chloride
NaCN	sodium cyanide
NAF	Neuropathopoiesis Assessment Framework
$NaHPO_4$	sodium phosphate
NaOH	sodium hydroxide
NAS	Neuropathopoiesis Assessment Scale
nCI	normalized cell index
nCR	normalized cellular response
NeuN	neuronal nuclei antigen
NF-κB	nuclear factor kappa B (kappa-light-chain-enhancer of activated B cells)
NGF	nerve growth factor
NIHSS	National Institute of Health Stroke Scale
N_m	metaptosis' nadir point
N_t	nadir point after treatment
NMDA	*N*-methyl-D-aspartate
NMDA-R1	*N*-methyl-D-aspartate receptor 1
NPY	neuropeptide Y

Nrf2	nuclear factor (erythroid-derived 2)-like 2
NSE	neuron specific enolase
OB	leptin
OB-R	leptin receptor
OGD	oxygen / glucose deprivation
P21	postnatal day 21
PAMAM	polyamidoamine
PBS	phosphate-buffered saline
PEDF	pigment epithelium-derived factor; SERPINF1
PG	proglucagon
PhD	Doctor of Philosophy
PPAR-γ	peroxisome proliferator-activated receptor gamma
PV	parvalbumin
REACH	Registration, Evaluation and Authorization of CHemicals (framework)
R_m	metaptosis' recovery point
R_t	recovery point after a treatment intervention
ROS	reactive oxygen species
RT-PCR	reverse transcriptase polymerase chain reaction
S1PR2	sphingosine-1-phosphate receptor 2
SAA	simulation approach application; plural: SAAs
SDS-PAGE	sodium dodecyl sulfate polyacrylamide gel electrophoresis
S_e	stabilization point (point of transition from initial to dynamic phase)
SERPINF1	serine (or cysteine) peptidase inhibitor, clade F, member 1; PEDF
SMI-310	200 kDa + 160 kDa neurofilament
SnMP	tin-mesoporphyrin
SSTY1	spermiogenesis specific transcript on the Y 1
STICH	Surgical Trial of IntraCerebral Haemorrhage
t	time
TBS-T	Tris-buffered saline - Tween 20
TME	technical meta-evaluation
TMES	technical meta-evaluation score; TME score
TNF-α	tumour necrosis factor alpha
TPE	technical pro-evaluation
TPE_i	technical pro-evaluation index; TPE index
Tris	tris(hydroxymethyl)aminomethane
Tris-HCl	tris(hydroxymethyl)aminomethane-hydrochloride; Tris-hydrochloride

TrkA	tropomyosin receptor kinase A
TrkB	tropomyosin receptor kinase B
UCL	University College London
VEGF	vascular endothelial growth factor
Z-factor	measure of statistical effect size; screening assays' quality indicator
Z_m	metaptosis' zenith point
Z_t	zenith point after treatment

APPENDIX B

Notes related to the current PhD Thesis

The readers of the current PhD Thesis should consider the following notes concerning certain points within the text:

- Note 1: within this PhD Thesis, the reaction for the estimation of AChE activity was followed spectrophotometrically by the ΔOD at 412 nm, where ΔOD accounts for the mean of the difference in the optical density measured.
- Note 2: all chemicals used for the experiments described in this PhD Thesis were of the highest analytical grade available and were purchased from Sigma-Aldrich, unless differently stated.

>> Table APP.1: page 216
>> Table APP.2: page 217
>> Table APP.3: page 218
>> Table APP.4: page 219
>> Figure APP.1: page 220
>> Figure APP.2: page 221

Table APP.1: Cellular responses to inflammation, cell injury and malignant transformation: an interpretation of the cytopathological perspective (based on Buckner *et al.*, 1992).

Cellular feature	inflammatory cell reaction	reversible cell injury	irreversible cell injury	malignant transformation
NUCLEUS (N)				
– location	ND	ND	ND	ND or EL
– shape	ND	ND	ND	ND or irregular
– size	ND or ↑	↑	↓	varied
– number	ND	ND	ND	ND
– membrane	ND or wavy	ND	ND or wrinkled	ND or irregular
– nucleoli (n)	ND	hazy, indistinct	NWD	varied
– n/N ratio	ND	↑	[---]	varied
– other	anisonucleosis	karyolysis	karyorrhexis	anisonucleosis
CYTOPLASM (C)				
– shape	ND	ND or round	ND	ND or irregular
– borders	ND	NWD	NWD	ND or NWD
– size	varied	↑ or ↓	↓	varied
– N/C ratio	ND or ↑	ND or ↑	↑ or ↓	varied or ↑
– other	vacuolization	vacuolization	[---]	[---]
ARRANGEMENTS				
– single cells	ND	ND	ND	ND
– aggregates	↑	ND	ND	ND
– sheets	↑	NWD borders	NWD borders	ND
– pseudosyncytia	ND	ND	ND	↑
– background	inflammatory	ND	ND	diathesis

Note: all herein presented cellular features are compared to the benign cell equivalents considered by cytopathologists, where the nuclear location is "central", the nuclear shape is "round to oval", the nuclear size is "variable by cell-type", the nuclear number is "single or multiple", the nuclear membrane is "smooth", the nucleoli are "present or absent, single or multiple, small in size", the cytoplasmic shape is "retained or rounded (in a fluid environment)", the cytoplasmic borders are "well-defined", the N/C ratio is "low in mature and high in immature cells", single cells are "present", aggregates are "present with maintained cell borders", sheets of cells might be "present with defined cell borders and maintained polarity", pseudosyncytia of cells are "absent or rare, with loss of cell borders and of polarity", and the background is "clean and clear". Data summarizing those provided by Buckner *et al.* (1992), with extensive modifications considering the utility of the observations for the assessment of cellular responses in a cell-line growing as a monolayer in an *in vitro* environment.

↑: increased; ↓: decreased; [---]: no data; EL: eccentrically-located; ND: no difference; NWD: not well-defined; PG: polygonal;

Table APP.2: Cellular responses to therapy and typical or atypical repair: an interpretation of the cytopathological perspective (based on Buckner *et al.*, 1992).

Cellular feature	**cellular response to typical repair**	**cellular response to atypical repair**	**therapy-induced cellular response**
NUCLEUS (N)			
– location	ND	ND	ND
– shape	ND	ND	ND
– size	↑	varied	↑
– number	ND	ND	ND
– membrane	ND	ND	ND or undulating
– nucleoli (n)	ND	varied	ND
– n/N ratio	[---]	[---]	[---]
– other	[---]	anisonucleosis	[---]
CYTOPLASM (C)			
– shape	round to PG	round to PG	ND
– borders	ND	NWD	ND or NWD
– size	ND or ↑	ND or ↑	ND or ↑
– N/C ratio	↑	↑	ND or ↑
– other	[---]	[---]	[---]
ARRANGEMENTS			
– single cells	absent	ND	ND
– aggregates	absent	ND	ND
– sheets	ND	NWD borders	ND
– pseudosyncytia	ND	↑	ND
– background	inflammatory	inflammatory	inflammatory

Note: all herein presented cellular features are compared to the benign cell equivalents considered by cytopathologists, where the nuclear location is "central", the nuclear shape is "round to oval", the nuclear size is "variable by cell-type", the nuclear number is "single or multiple", the nuclear membrane is "smooth", the nucleoli are "present or absent, single or multiple, small in size", the cytoplasmic shape is "retained or rounded (in a fluid environment)", the cytoplasmic borders are "well-defined", the N/C ratio is "low in mature and high in immature cells", single cells are "present", aggregates are "present with maintained cell borders", sheets of cells might be "present with defined cell borders and maintained polarity", pseudosyncytia of cells are "absent or rare, with loss of cell borders and of polarity", and the background is "clean and clear". Data summarizing those provided by Buckner *et al.* (1992), with extensive modifications considering the utility of the observations for the assessment of cellular responses in a cell-line growing as a monolayer in an *in vitro* environment.

↑: increased; ↓: decreased; [---]: no data; ND: no difference; NWD: not well-defined; PG: polygonal

Table APP.3: Inter- and intra-variance of independent experiments conducted for the cyto-morphological analysis of the mHippoE-14 cells' confluency in response to FBS-deprivation.

		Conducted experiments (number)				
Treatment group	**Parameter**	**1**	**2**	**3**	**4**	**CV**
FBS(+) at 6 h	median	2	2	2	2	0.000
	IQR	1	1.5	1	0.5	0.408
	IQR/median	0.500	0.750	0.500	0.250	---
FBS(+) at 12 h	median	2	2	3	2	0.222
	IQR	1	2	2	1	0.385
	IQR/median	0.500	1.000	0.667	0.500	---
FBS(+) at 18 h	median	3	2	4	4	0.295
	IQR	1	2	0.5	2	0.545
	IQR/median	0.333	1.000	0.125	0.500	---
FBS(+) at 24 h	median	4	4	6	6	0.231
	IQR	1	3	0	2.5	0.847
	IQR/median	0.250	0.750	0.000	0.417	---
FBS(+) at 30 h	median	6	5	7	6	0.136
	IQR	2	3.5	1	3.5	0.490
	IQR/median	0.333	0.700	0.143	0.583	---
FBS(+) at 36 h	median	6	6	8	7	0.142
	IQR	0	2.5	1.5	1.5	0.750
	IQR/median	0.000	0.417	0.188	0.214	---
FBS(+) at 48 h	median	8	9	9	7	0.116
	IQR	1	1	0.5	2	0.559
	IQR/median	0.125	0.111	0.056	0.286	---
FBS(+/-) at 30 h	median	4	4	6	5	0.202
	IQR	1	3.5	1.5	1.5	0.591
	IQR/median	0.250	0.875	0.250	0.300	---
FBS(+/-) at 36 h	median	5	5	6	5	0.095
	IQR	1.5	2	1	1.5	0.272
	IQR/median	0.300	0.400	0.167	0.300	---
FBS(+/-) at 48 h	median	3	5	5	5	0.222
	IQR	1	1.5	2	2	0.295
	IQR/median	0.333	0.300	0.400	0.400	---

Note: data refer to median and IQR values of confluency assessments (scale 0-10; n=7 captions assessed per condition, see Table B.8) of each of the four independent experiments conducted. For more details and the findings of these experiments, see Figure B.10.a. The IQR/median ratio is an indicator of the variance within each experiment, while the coefficient of variation (CV) is herein used as an indicator of the variance of the median across the experiments for any given condition. Values of CV that are lower than 1, are considered as indicators of low variance.

CV: coefficient of variation; FBS: foetal bovine serum; IQR: interquartile range

Table APP.4: Z-factors for the mHippoE-14 cellular status under the major conditions chosen for the developed *in vitro* simulation approaches to intracerebral haemorrhage.

	Z-factor in each of the conducted experiments (number)				
Treatment group	**1**	**2**	**3**	**4**	**mean**
O_{48}	0.370	0.475	0.345	0.563	0.438
OH_{48}	0.791	0.724	0.763	0.678	0.739
OF_{48}	0.121	0.838	0.516	0.673	0.537
O_{60}	0.627	0.696	0.572	0.751	0.662
OH_{60}	0.722	0.836	0.780	0.800	0.784
OF_{60}	0.250	0.903	0.716	0.733	0.650
O_{72}	0.692	0.761	0.715	0.735	0.726
OH_{72}	0.698	0.886	0.771	0.758	0.778
OF_{72}	0.405	0.914	0.791	0.702	0.703

Note: data refer to Z-factors of triplicate assessments from each of the four independent experiments conducted (n=4; IDs: 1410161436, 1410202228, 1410251044, 1410251218) and their mean. For more details and further findings of these experiments, see Figures C.9, C.10 and C.11 as well as Table C.3. The Z-factor is calculated by the following equation:

$$\text{Z-factor} = 1 - (3*(\text{standard deviation}_{(\text{positive})} + \text{standard deviation}_{(\text{negative})}) / (\text{mean}_{(\text{positive})} - \text{mean}_{(\text{negative})}))$$

where "positive" and "negative" refer to the respective "controls" of the assay. For more details on the calculation and meaning of the Z-factor, see Zhang *et al*. (1999).

C_{48}: control (at 48 h); C_{60}: control (at 60 h); C_{72}: control (at 72 h); O_{48}: oligomycin (at 48 h); O_{60}: oligomycin (at 60 h); O_{72}: oligomycin (at 72 h); OF_{48}: oligomycin, ferrum (at 48 h); OF_{60}: oligomycin, ferrum (at 60 h); OF_{72}: oligomycin, ferrum (at 72 h); OH_{48}: oligomycin, haemin (at 48 h); OH_{60}: oligomycin, haemin (at 60 h); OH_{72}: oligomycin, haemin (at 72 h)

Figure APP.1: Real-time cellular response of the mHippoE-14 cells after exposure to oligomycin and / or haemin or ferrum (at various concentrations), within metaptosis.

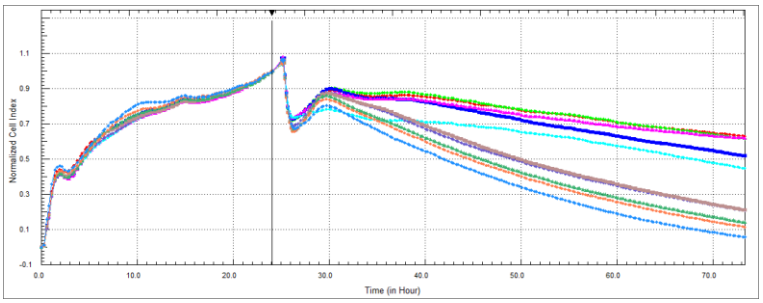

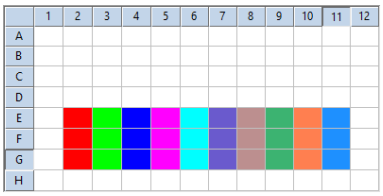

setting A: average nCI per group
(normalization at 24:08:06)
(10 well groups included)

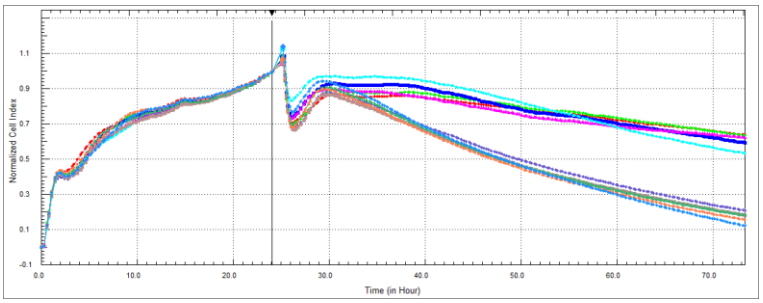

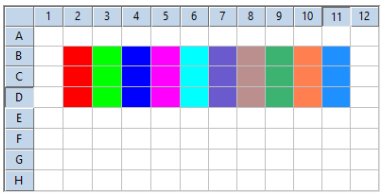

setting B: average nCI per group
(normalization at 24:08:06)
(10 well groups included)

Note: representative screen captions from the xCELLigence RTCA SP analysis software (plots and well selection maps); experiment's ID: 1210071923. All compounds were added to the wells right after FBS-deprivation (induction of metaptosis). Setting A demonstrates the average nCI values of the following treatment groups: control (E2, F2, G2), haemin [5 μM] (E3, F3, G3), haemin [50 μM] (E4, F4, G4), haemin [100 μM] (E5, F5, G5), haemin [500 μM] (E6, F6, G6), oligomycin (E7, F7, G7), oligomycin + haemin [5 μM] (E8, F8, G8), oligomycin + haemin [50 μM] (E9, F9, G9), oligomycin + haemin [100 μM] (E10, F10, G10), oligomycin + haemin [500 μM] (E11, F11, G11). Setting B demonstrates the average nCI values of the following treatment groups: control (B2, C2, D2), ferrum [5 μM] (B3, C3, D3), ferrum [50 μM] (B4, C4, D4), ferrum [100 μM] (B5, C5, D5), ferrum [500 μM] (B6, C6, D6), oligomycin (B7, C7, D7), oligomycin + ferrum [5 μM] (B8, C8, D8), oligomycin + ferrum [50 μM] (B9, C9, D9), oligomycin + ferrum [100 μM] (B10, C10, D10), oligomycin + ferrum [500 μM] (B11, C11, D11). Oligomycin was used at a concentration of 1 μg/mL. The experiment has been conducted in triplicate (IDs: 1210011536, 1210041518, 1210071923; n=3) and has consistently shown that: (a) oligomycin is the leading cause for the reduction of nCI in mHippoE-14 cells, (b) ferrum or haemin exert their highest toxicity at 500 μM (irrespectively of oligomycin's presence), and (c) the addition of these compounds within the phase of metaptosis modifies the mHippoE-14 metaptotic response and, thus, should be avoided.

FBS: foetal bovine serum; nCI: normalized cell index

Figure APP.2: Representative captions of mHippoE-14 cells after attempts to remove haemin- or ferrum-induced debris through washing with PBS.

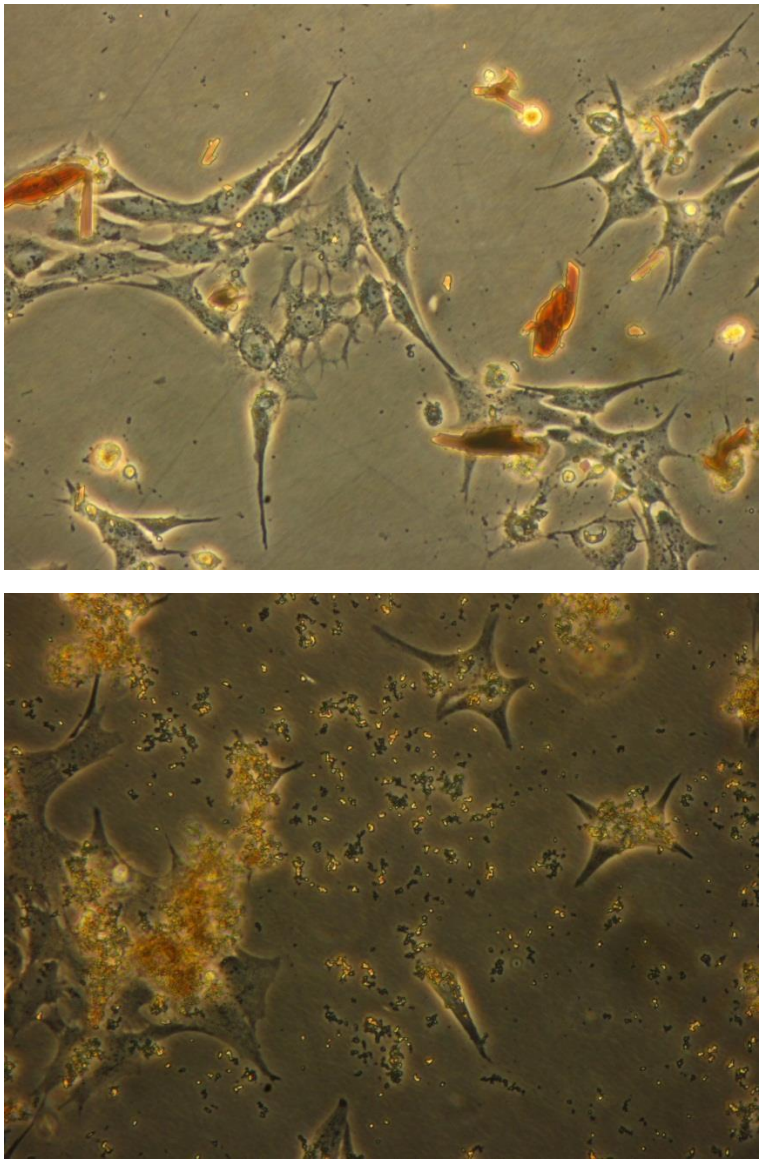

Note: in the OH treatment groups, optical field can be shadowed by unsolved haemin crystals, while in the case of the OF treatment groups, the assessment of the floating debris and the undertaking of analytical cytomorphology is practically impossible; neither of these problems could be solved by removing the media and undertaking 3 gentle washes with pre-warmed PBS.

OF_{72}: oligomycin, ferrum (at 72 h); OH_{72}: oligomycin, haemin (at 72 h); PBS: phosphate-buffered saline

_____

(unique number of PhD Thesis' copy)

_____

(owner of the copy)

_____

_____

_____

_____

_____

_____

_____

_____

_____

_____

(Notes)

--- END OF THE THESIS ---